UNIVERSITÉ DE STRASBOURG

ÉCOLE DOCTORALE PHYSIQUE ET DE CHIMIE-PHYSIQUE

ICPEES – UMR 7515

THÈSE présentée par :

Khantutta-Kim TREMBLAY-PARRADO

soutenue le : **3 mars 2020**

pour obtenir le grade de : **Docteur de l'Université de Strasbourg**

Discipline/ Spécialité : Chimie des Polymères

Synthèse par chimie click de réseaux polyuréthanes biosourcées aux propriétés avancées

THÈSE dirigée par :
M. AVEROUS Luc Professeur, Université de Strasbourg

RAPPORTEURS :
Mme. ECEIZA Arantxa Professeure, Université du Pays Basque
M. ZINCK Philippe Professeur, Université de Lille

AUTRES MEMBRES DU JURY :
M. JIERRY Loic Professeur, Université de Strasbourg

MEMBRE INVITE :
M. PERRIN Rémi Directeur R&D, SOPREMA

ICPEES (Institut de chimie et procédés pour l'énergie, l'environnement et la santé) – UMR 7515

25 rue Becquerel – 67087 Strasbourg Cedex 2

UNIVERSITÉ DE STRASBOURG

ÉCOLE DOCTORALE PHYSIQUE ET DE CHIMIE-PHYSIQUE

ICPEES – UMR 7515

THESIS presented by:

Khantutta-Kim TREMBLAY-PARRADO

defended: **March 3rd, 2020**

to obtain the degree : **Doctor of the University of Strasbourg**

Discipline / Speciality: Polymer Chemistry

Synthesis by click chemistry of biobased polyurethane networks with advanced properties

THESIS directed by:
M. AVEROUS Luc Professor, University of Strasbourg

JURY:
Mme. ECEIZA Arantxa Professor, University of Basque Country
M. ZINCK Philippe Professor, University of Lille

OTHER MEMEBER OF THE JURY:
M. JIERRY Loic Professor University of Strasbourg

INVITED MEMBER:
M. PERRIN Rémi R&D Director, SOPREMA

ICPEES (Institut de chimie et procédés pour l'énergie, l'environnement et la santé) – UMR 7515

25 rue Becquerel – 67087 Strasbourg Cedex 2

This doctoral thesis was drafted using, for each chapter, the format commonly used for the redaction of scientific articles appearing in peer-reviewed journals. For this reason, the indulgence of the reader is solicited for the inherent repetitions this chosen form of redaction may cause.

The present memoir is written in English, in agreement with the authorization given by the Professor Dinia Aziz, University Professor at the Institute of Physics and Chemistry of Materials of Strasbourg and Director of the doctoral school of Physics and Chemistry-Physics.

Communications related to thesis work

Published articles

Tremblay-Parrado K., Avérous L., Renewable Responsive Systems Based on Original Click and Polyurethane Cross-linked Architectures with Advanced Properties. *ChemSusChem* 2020, *13*, 238. DOI:10.1002/cssc.201901991

Submitted articles

Tremblay-Parrado K., Avérous L. (2020), Synthesis and Behavior of Responsive Biobased Polyurethane Networks Cross-linked by Click Chemistry: Effect of the Cross-Linkers and Backbone Structures. Submitted in Journal of Materials Chemistry A.

Articles to be submitted

Tremblay-Parrado K.-K., Bordin C., Nicholls S., Avérous L. Renewable and Responsive Cross-linked Systems Based on Polyurethane Backbones; from Clickable Biobased Bismaleimide Architecture. Will be submitted in European Polymer Journal.

Tremblay-Parrado K.-K., Garcia-Astrain C., Avérous L. Click Green Chemistry for the Synthesis of Biobased Polymers and Network derived from Vegetable Oils.

Posters

Tremblay-Parrado K.-K., Avérous L. (2017) «Development of New Biobased Stimulable Thermoplastic Polymers, Derived from Vegetable Oils», *Groupe Français des Polymères (GFP) Grand Est – 15ème Journée Scientifique - Polymères et Chimie Durable*, June 28th, 2017, Strasbourg (France)

Oral communications

Tremblay-Parrado K.-K., Avérous L. (2019) «Development of New Biobased Innovative and Responsive Materials based on Fatty Acid Derivatives», *10th Workshop on Fats and Oils as Renewable Feedstock for the Chemical Industry*, March 17th – 19th, 2019, Karlsruhe (Germany)

Tremblay-Parrado K.-K., Avérous L. (2019) «From Vegetable Oil to Innovative and Responsive Materials», *7th International Conference on Bio-based and Biodegradable Polymers (BIOPOL),* June 17th – 19th, 2019, Stockholm (Sweden)

Tremblay-Parrado K.-K., Avérous L. (2019) «Stimulable Materials from Biobased Polyurethanes», Institut de Chimie et Procédés pour L'Energie, l'Environnement et la Santé (ICPEES) *Journée Scientifique et Technique*, July 5th, 2019, Strasbourg (France)

List of abbreviations

%NCO	Isocyanate content
6-MHA	6-maleimidohexanoic acid
6-MHC	6-maleimidohexanoyl chloride
ATR	Attenuated total refection
AV	Acid value
BDO	1,4-Butanediol
BMI	Bismaleimide
CAN	Covalent adaptable network
$CHCl_3$	Chloroform
Cl-TDP	2-chloro-4,4,5,5-tetramethyl-1,3,2-dioxaphospholane
CuAAC	Copper catalyzed azide-alkyne cycloaddition
DA	Diels-Alder
DCC	*N,N*-dicyclohexylcarboiimide
DCM	Dichloromethane
DCU	Dicyclohexylurea
DHB	2,5-dihydroxybenzoic acid
DMAP	4-dimethylaminopyridine
DMF	Dimethylformamide
DMPA	2,2-Dimethoxy-2-phenylacetophenone
DMSO	Dimethyl sulfoxide
DP	Degree of polymerization
DSC	Differential scanning calorimetry
FA	Fatty acid
FAME	Fatty acid methyl ester
FDM	Furan-2,5-diyl-dimethanol
FM	Furan-2-ylmethanol
FMO	Furan-2-ylmethyl-octadec-9-enoate
FMOO	Furan-2-ylmethlyl 8-(3-octyloxiran-2-yl)octonoate
FO	Furan Oligomer
FTIR	Fourier-transform infrared spectroscopy
G'	Storage modulus
G''	Loss modulus
HDI	Hexamethylene diisocyanate
HS	Hard Segment
HV	Hydroxyl Value
IF	Insoluble fraction
IV	Iodine value
MALDI TOF	Matrix assisted laser desorption ionisation - time of flight

MDI	4,4'-Methylene diisocyanate
ME	Mercaptoethanol
Mn	Number average molecular weight
MO	Methyl oleate
MOBMI	Methyl oleate bismaleimide
MO Diol	Methyl 10-hydroxy-9-(4-hydroxybutoxy)octadecanoate
MOO	Methyl 8-(3-octyloxiran-2-yl)octanoate
MPBMI	1,1'-(Methylene di-4,1-phenylene)bismaleimide
MUDO	Methyl undecenoate
Mw	Weight average molecular weight
NIPU	Non-isocyanate polyurethane
NMR	Nuclear magnetic resonance
OA	octadec-9-enoice acid / oleic acid
PA	Polyamide
PFB	Pentafluorobenzaldehyde
PHU	Polyhydroxyurethane
PPOBMI	Polypropylene oxide bismaleimide
PPOPEOBMI	Poylpropylene oxide-polyethylene oxide bismaleimide
PU	Polyurethane
r-DA	retro-Diels-Alder
ROP	Ring-opening polymerization
SEC	Size exclusion chromatography
SRs	Swelling ratio
$T_{5\%}$	Initial degradation temperature
TAD	Triazolinedione
TEC	Thiol-ene coupling
T_g	Glass transition temperature
TGA	Thermogravimetric analysis
THF	Tetrahydrofuran
TPU	Thermoplastic polyurethanes
TYC	Thiol-yne coupling
UDA	Undecyclenic acid
UDC	10-undecenol
UV	Ultra-violet
ε	Elongation at break
$\tilde{\nu}$	Wavenumber (cm^{-1})
δ	Chemical shift (ppm)
σ	Tensile strength

Table of contents

Table of contents

List of illustrations

Schemes

Chapter 1

Chapter 2

Chapter 3

Chapter 4

Figures

Introduction

Chapter 1

Chapter 2

Chapter 3

Chapter 4

General Conclusions & Perspectives

Tables

Chapter 1

Chapter 2

Chapter 3

Chapter 4

General Introduction

This work took place within the BioTeam group directed by Pr. Luc Avérous, at the Institut of Chemistry and Processes for Energy, Environment and Health (Institut de Chimie et Procédés pour l'Energie, l'Environnement et la Santé, ICPEES), a joint research unit (UMR 7515) between University of Strasbourg and CNRS, located at the European School of Chemistry, Polymers and Materials (Ecole Européenne de Chimie, Polymères et Matériaux, ECPM). The main research thematic of the BioTeam is focused on biobased and/or biodegradable polymers for environmental and biomedical applications.

This research work is part of the Trans'alg project financed by BPI France. This project aimed to produce biosourced molecules for biobased chemistry and bioenergy markets. The target markets of the Trans'alg project are bioplasticizers, biolubricants, waterproof membranes, insulation, biofuels. The consortium consists of several industrial partners such as Pierre Geurin, Fermentalg, Seppic, Soprema and research entities such as CEA, ITERG and ICPEES. Concerning this work, Fermentalg (France) is the lipid supplier (vegetable oils and fatty acids), Soprema is one of the main industrial partners and a worldwide leader in the field of insulation for the construction industry. This project is also involved in the frame of Mutaxio, a joint research lab between the BioTeam and the R&D of Soprema-France (2017-present). In the context of this project, Soprema did not impose materials specifications or specific objectives. This PhD had the liberty of creative freedom in context of research and innovations for the development of new adaptive biobased PUs derived from vegetable oils.

Since two decades, the BioTeam has developed biobased polyurethanes from diverse biomass with innovative renewable macromolecular architectures in the frame of different projects (Hablot et al. 2008; Bueno-Ferrer et al. 2012; Reulier et al. 2017; Tremblay-Parrado and Avérous 2019). This work is then fully integrated in this historical research line. However, nowadays "biobased is not enough", thus the main idea of this work is to develop PU-based materials with added values to develop systems with innovative and advanced properties to fulfill several societal and industrial requirements.

Oils and fats of vegetable and animal origin remain historically and currently the most abundantly used renewable resource of the chemical industry (Ursula et al. 2011). Classically, in industry,

vegetable oils have been found in several compounds to replace fossil-based systems. Combining the impacts of the consumption of non-renewable resources and greenhouse gases has led to growing pressures to substitute the use of fossil-based polymer.

Vegetable oils are prime candidates to replace fossil-based derivatives in polymer materials for a multitude of reasons. Generally, their universal availability, low toxicity, and low price have rendered them of primary interest. Furthermore, it is their inherent structure that is of the highest interest for the synthesis of new monomers and polymers. Vegetable oils mainly consist of triglycerides (Figure I.1), defined as esters of glycerol where the three long-chain fatty acids (R_1, R_2, R_3) composition varying according to the plant species, crop type, season and growing conditions (Meier, Metzger, and Schubert 2007). The chemical and physical properties of triglycerides are defined by the structures of the fatty acid chains in terms of (i) length, (ii) degree of unsaturations and (iii) stereochemistry of the double bonds (Zlatanic et al. 2004). Typically, the length of fatty acid chains varies between 14-22 carbons (mostly consisting of 16 or 18 carbons) with the unsaturations number ranging between 0-3. Over 1000 fatty acids have been discovered but only 20 present substantial quantities in triglycerides (Wool and Sun 2005). Thus, vegetable oils are suitable for the synthesis of hydrophobic polymers and their structure is similar to petroleum-based monomers.

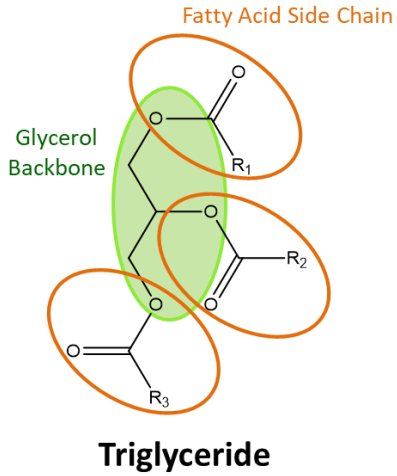

Figure I.1 – General structure of a natural triglyceride component of vegetable oils in which R_1, R_2 and R_3 are fatty-acid side chains.

Within around 80 years, polyurethanes (PUs) have become one of the major polymer family due to their versatile properties that can be tuned for a wide range of applications e.g.; foams, elastomers, adhesives, sealants, fibers, thermoplastics and thermosets for the construction, automotive and medical industry. Consequently, PUs were ranked 6th worldwide in terms of polymer production in 2016 (Cornille et al. 2017) and had a planned production of approximately 23 million tons in 2019 (Akindoyo et al. 2016). Classically, PUs are obtained by the polyaddition reaction between polyols and polyisocyanates (Figure I.2). As most of these raw materials are derived from fossil resources and given the current climate of the chemical industry, the biobased PU market is expanding with a particular emphasis on the use of vegetable oils. Vegetable oils consist of adequate architectures for the development of polyols for thermosets (Lligadas 2013) or thermoplastic PU applications (Palaskar et al. 2012), controlling the corresponding functionality. Nevertheless, utilizing renewable feedstocks and synthesizing biobased polymers does not suffice. The synthesis of biobased polymers should also include the use of sustainable chemistry as well as incorporate advanced properties to extend lifetimes and ensure a controlled end-of-life.

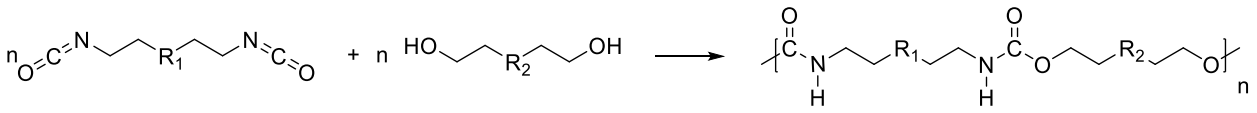

Figure I.2 – Polyurethane synthesis from a diol and a diisocyanate.

The concept of sustainable in chemistry is guided by the “12 Principles of Green Chemistry” published by Anastas and Warner in 1998, which include the following concepts: (i) minimizing waste, (ii) the use of renewable feedstocks and energy, (iii) the use of safe and environment benign substances and (iv) atom economy (Anastas and Warner 1998). More recently, the use of click chemistry for the controlled synthesis of different macromolecular architectures has gained prevalence and these reactions are following the principles of green chemistry. Click chemistry was introduced by Sharpless and co-workers in 2001 and consists of a wide range of reactions that are required to be modular, wide in scope, give high yields, generate only inoffensive by-products and be stereospecific. Moreover, characteristic of the process should include simple reaction conditions, readily available starting materials and reagents, the use of no solvents or a

solvents that are benign and simple product isolation. It is the high thermodynamic driving force of click reactions that allow them to achieve these characteristics. (Kolb, Finn, and Sharpless 2001)

When it comes to the synthesis of monomers and polymers from vegetable oils by click chemistry, the literature reports the use of different reactions, such as (i) thiol-ene addition (ii) thiol-yne addition, (iii) Cu(I)-catalyzed azide-alkyne cycloaddition (CuAAC), (iv) Diels–Alder (DA) cycloadditions and (iv) triazolinedione (TAD) chemistry. Although the thiol-ene addition reaction dominates the use of click chemistry in oleochemistry, the efficient application of the DA reaction to oleochemistry has recently been brought forth (Gandini et al. 2018). The DA reaction is a [4+2] cycloaddition between a conjugated diene and dienophile (a substituted alkene-bearing electron-withdrawing group) leading to the formation of a substituted cyclohexene adduct (Figure I. 3-a). Moreover, the DA adduct can be reversed by the retro-DA reaction under certain conditions. In the context of oleochemistry, Gandini and coworkers have highlighted the use of the furan (diene) / maleimide (dienophile) DA reaction that occurs at low temperatures (below 90 °C), whereas the retro-DA (r-DA) reaction, occurs between 110 and 130 °C (Figure I. 3-b) (Lacerda, Carvalho, and Gandini 2016). The attractive feature of the reversible reaction has been exploited in polymer chemistry for the development of architectures containing dynamic covalent bonds to yield advanced properties such as self-healing and recyclability (particularly of thermosets).

Practically in parallel with the emergence of click chemistry, the DA reaction, and most specifically the DA reaction between a furan and maleimide moiety was also being exploited for the development of macromolecular networks containing the reversible cross-linking of covalent bonds (Chen et al. 2002). As such, in the decade that followed, the use of exploiting different types of reversible covalent bonds (also known as dynamic covalent bonds) proliferated. Consequently, the emergence of polymer networks with dynamic cross-links has blurred the line between thermoplastics and thermosets. In 2010, Kloxin and coworkers defined this new class of materials as Covalent Adaptable Networks (CANs) (Kloxin et al. 2010). With the innovations that followed in this field, Du Prez and coworkers further defined the ways by which CANs assembled and disassembled by two distinct processes, either by “dissociative” or “associative” means when exposed to an external stimuli (often thermal) or autonomously (Denissen, Winne, and Du Prez 2016). Dissociative CANs exhibit chemical bond exchanges where bonds are first broken and

reformed again (Figure I. 3-c). Examples of such bonds include, the DA cycloaddition, hindered urea exchange (Ying, Zhang, and Cheng 2014) and 1,2,3-trazolium salts (Obadia et al. 2017). Nevertheless, the thermoreversible furan-maleimide [4+2] cycloaddition DA reaction is the most prominently studied reversible chemistry used to synthesize dissociative CANs. Alternatively, associative CANs consists of bond exchanges between polymer chains, with a preserved cross-linking density as a new covalent bond can only be formed if another has been broken (Figure I. 3-c). A prominent example of such systems is vitrimers, coined by Leibler and coworkers (Montarnal et al. 2011). Irrespective of the reversible chemistry or dynamic cross-links used, designing materials with a preconceived notion of recyclability and a controlled end-of-life further allows scientists to have a holistic approach to sustainable material design.

Several biobased CANs have been synthesized derived from lignins (Buono et al. 2017), tannins (Duval et al. 2017), alginate (García-Astrain and Avérous 2018), chitosan (Guaresti et al. 2018), starch (González et al. 2018), vegetable oils (Gandini et al. 2018) and fructose (Dhers, Vantomme, and Avérous 2019). Nevertheless, according to the literature, the development of dynamic biobased PU architectures is largely limited (Zhang, Michel Jr, and Co 2019; Hu, Chen, and Torkelson 2019), regardless of its eminent need to be explored. It is for this reason that this experimental work is centered on the development of reversibly cross-linked PUs based on vegetable oils using the thermally reversible furan-maleimide DA reaction.

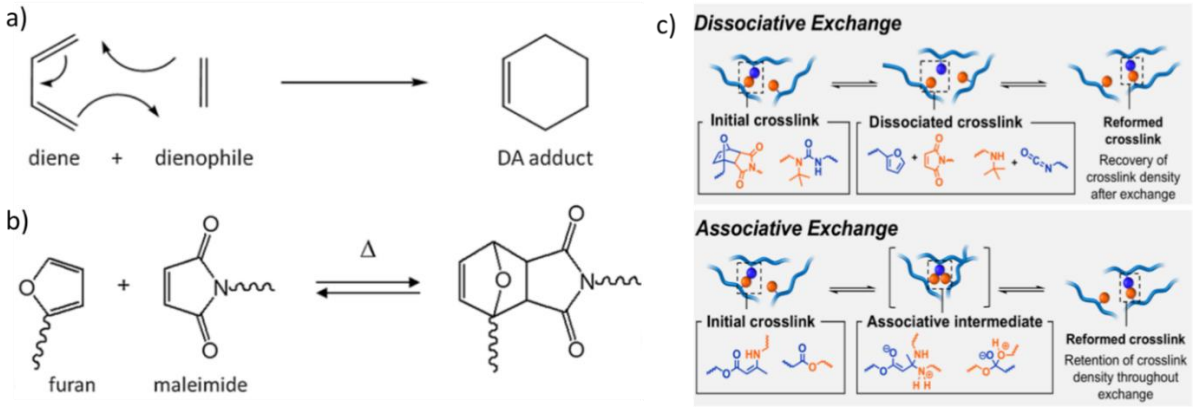

Figure I. 3 – (a) Diels-Alder mechanism between diene and dienophile and (b) Diels-Alder reaction between furan and maleimide moiety (Kwart and Burchuk 1952), and (c) schematic of Covalent Adaptable Networks (Scheutz et al. 2019).

The architecture of this manuscript is focused on different chapters and each chapter is centered on a scientific article. To ease the transition between chapters for the reader, a short introduction and conclusion are presented before and after the scientific article, respectively. The body of the manuscript consists of a bibliographic chapter followed by three experimental chapters (Figure I. 4).

The first chapter of this manuscript develops the context of sustainable polymer chemistry, the use of click chemistry as a powerful tool in the context of a bibliographic review on the synthesis of monomers and polymers from vegetable oils by click chemistry. This chapter emphasizes the latest innovations in this field, with particular attention to the synthesis of materials with advanced properties and polymer synthesis. The main conclusion of this bibliographic chapter has largely directed the research lines of the following experimental chapters.

The second chapter starts the experimental part of this memoir on the synthesis and characterization of new biobased building block, derived from oleic acid, consisting of diol structures and pendant furan rings. This building block, alongside a bismaleimide cross-linker, is used in the synthesis of PUs to introduce a cross-linked architecture. The chapter goes on to establish a proof of concept that these PU architectures using these building blocks are indeed dissociative responsive architectures, leading to advanced properties such as recyclability and self-healing.

The third chapter is an extensive study of the experimental results of chapter two. In chapter two, the new biobased building block and one specific bismaleimide were used to form the cross-links of PU architectures. The experimental results of chapter three explored the effect of varying the length and structure of bismaleimides used as well as studying the introduction of hard segments, on PU polymer properties, thermal recyclability, and self-healing

Lastly, the **fourth chapter** puts forth the synthesis and characterization of fatty acid based bismaleimide and its use as a cross-linking agent in PU architectures. Contrarily to chapter two or three, where the dynamic cross-links are studied in a simple system (without hard segments) or in the soft segments of PU architectures, chapter four explores the use dynamic cross-links in the

hard segments of biobased PU architectures on polymer properties and advanced properties. The use of varying the type of bismaleimide was also studied.

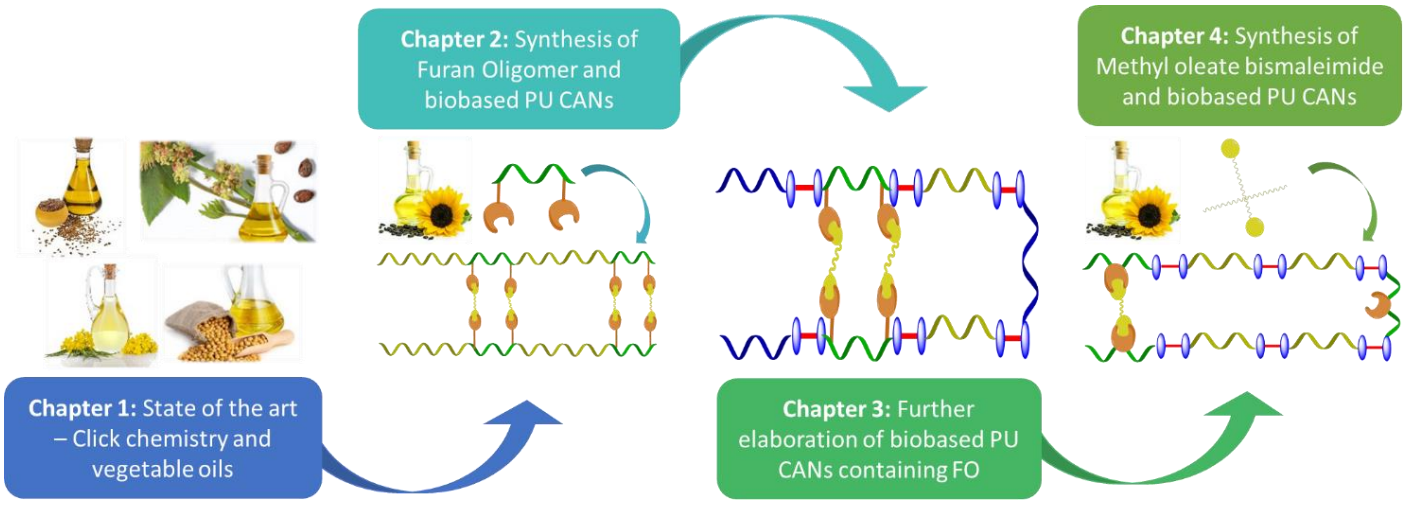

Figure I. 4 – Diagram summarizing the organization of the manuscript.

References:

Akindoyo, John, Mohammad Beg, Suriati Ghazali, Muhammad Islam, Nitthiyah Jeyaratnam, and Yuvaraj Ar. 2016. 'Polyurethane types, synthesis and applications-a review', *RSC Advances*, 6: 114453-82.

Anastas, Paul T., and John Charles Warner. 1998. *Green chemistry : theory and practice* (Oxford University Press: Oxford [England]; New York).

Bueno-Ferrer, Carmen, Elodie Hablot, María del Carmen Garrigós, Sergio Bocchini, Luc Averous, and Alfonso Jiménez. 2012. 'Relationship between morphology, properties and degradation parameters of novative biobased thermoplastic polyurethanes obtained from dimer fatty acids', *Polymer Degradation and Stability*, 97: 1964-69.

Buono, Pietro, Antoine Duval, Luc Averous, and Youssef Habibi. 2017. 'Thermally healable and remendable lignin-based materials through Diels – Alder click polymerization', *Polymer*, 133: 78-88.

Chen, Xiangxu, Matheus A. Dam, Kanji Ono, Ajit Mal, Hongbin Shen, Steven R. Nutt, Kevin Sheran, and Fred Wudl. 2002. 'A Thermally Re-mendable Cross-Linked Polymeric Material', *Science*, 295: 1698-702.

Cornille, Adrien, Rémi Auvergne, Oleg Figovsky, Bernard Boutevin, and Sylvain Caillol. 2017. 'A perspective approach to sustainable routes for non-isocyanate polyurethanes', *European Polymer Journal*, 87: 535-52.

Denissen, Wim, Johan M. Winne, and Filip E. Du Prez. 2016. 'Vitrimers: permanent organic networks with glass-like fluidity', *Chemical Science*, 7: 30-38.

Dhers, Sébastien, Ghislaine Vantomme, and Luc Avérous. 2019. 'A fully bio-based polyimine vitrimer derived from fructose', *Green Chemistry*, 21: 1596-601.

Duval, A., G. Couture, S. Caillol, and L. Averous. 2017. 'Biobased and Aromatic Reversible Thermoset Networks from Condensed Tannins via the Diels-Alder Reaction', *ACS Sustainable Chemistry & Engineering*, 5: 1199-207.

Gandini, Alessandro, Antonio J. F. Carvalho, Eliane Trovatti, Ricardo K. Kramer, and Talita M. Lacerda. 2018. 'Macromolecular materials based on the application of the Diels–Alder reaction to natural polymers and plant oils', *European Journal of Lipid Science and Technology*, 120: 1700091.

García-Astrain, Clara, and Luc Avérous. 2018. 'Synthesis and evaluation of functional alginate hydrogels based on click chemistry for drug delivery applications', *Carbohydrate Polymers*, 190: 271-80.

González, Kizkitza, Clara García-Astrain, Arantzazu Santamaria-Echart, Lorena Ugarte, Luc Avérous, Arantxa Eceiza, and Nagore Gabilondo. 2018. 'Starch/graphene hydrogels via click chemistry with relevant electrical and antibacterial properties', *Carbohydrate Polymers*, 202: 372-81.

Guaresti, O., C. García–Astrain, R. H. Aguirresarobe, A. Eceiza, and N. Gabilondo. 2018. 'Synthesis of stimuli–responsive chitosan–based hydrogels by Diels–Alder cross–linking `click´ reaction as potential carriers for drug administration', *Carbohydrate Polymers*, 183: 278-86.

Hablot, Elodie, Dan Zheng, Michel Bouquey, and Luc Avérous. 2008. 'Polyurethanes Based on Castor Oil: Kinetics, Chemical, Mechanical and Thermal Properties', *Macromolecular Materials and Engineering*, 293: 922-29.

Hu, Sumeng, Xi Chen, and John M. Torkelson. 2019. 'Biobased Reprocessable Polyhydroxyurethane Networks: Full Recovery of Crosslink Density with Three Concurrent Dynamic Chemistries', *ACS Sustainable Chemistry & Engineering*, 7: 10025-34.

Kloxin, Christopher J., Timothy F. Scott, Brian J. Adzima, and Christopher N. Bowman. 2010. 'Covalent Adaptable Networks (CANs): A Unique Paradigm in Cross-Linked Polymers', *Macromolecules*, 43: 2643-53.

Kolb, Hartmuth C., M. G. Finn, and K. Barry Sharpless. 2001. 'Click Chemistry: Diverse Chemical Function from a Few Good Reactions', *Angewandte Chemie International Edition*, 40: 2004-21.

Kwart, Harold, and Isabel Burchuk. 1952. 'Isomerism and Adduct Stability in the Diels—Alder Reaction.1a I. The Adducts of Furan and Maleimide', *Journal of the American Chemical Society*, 74: 3094-97.

Lacerda, Talita M., Antonio J. F. Carvalho, and Alessandro Gandini. 2016. 'A minimalist furan–maleimide AB-type monomer and its thermally reversible Diels–Alder polymerization', *RSC Advances*, 6: 45696-700.

Lligadas, G. 2013. 'Renewable Polyols for Polyurethane Synthesis via Thiol-ene/yne Couplings of Plant Oils', *Macromolecular Chemistry and Physics*, 214: 415-22.

Meier, Michael A. R., Jurgen O. Metzger, and Ulrich S. Schubert. 2007. 'Plant oil renewable resources as green alternatives in polymer science', *Chemical Society Reviews*, 36: 1788-802.

Montarnal, D., M. Capelot, F. Tournilhac, and L. Leibler. 2011. 'Silica-Like Malleable Materials from Permanent Organic Networks', *Science*, 334: 965-68.

Obadia, Mona M., Antoine Jourdain, Philippe Cassagnau, Damien Montarnal, and Eric Drockenmuller. 2017. 'Tuning the Viscosity Profile of Ionic Vitrimers Incorporating 1,2,3-Triazolium Cross-Links', *Advanced Functional Materials*, 27: 1703258.

Palaskar, Dnyaneshwar V., Aurélie Boyer, Eric Cloutet, Jean-François Le Meins, Benoit Gadenne, Carine Alfos, Céline Farcet, and Henri Cramail. 2012. 'Original diols from sunflower and ricin oils: Synthesis, characterization, and use as polyurethane building blocks', *Journal of Polymer Science Part A: Polymer Chemistry*, 50: 1766-82.

Reulier, M., R. Matadi Boumbimba, Z. Walsh Korb, R. Vaudemont, and L. Avérous. 2017. 'Thermomechanical and cyclic behavior of biocomposites based on renewable thermoplastics from dimer fatty acids', *Journal of Applied Polymer Science*, 134: 44610.

Scheutz, Georg M., Jacob J. Lessard, Michael B. Sims, and Brent S. Sumerlin. 2019. 'Adaptable Crosslinks in Polymeric Materials: Resolving the Intersection of Thermoplastics and Thermosets', *Journal of the American Chemical Society*, 141: 16181-96.

Tremblay-Parrado, Khantutta-Kim, and Luc Avérous. 2019. 'Renewable Responsive Systems Based on Original Click and Polyurethane Cross-Linked Architectures with Advanced Properties', *Chemsuschem*, 13: 238.

Ursula, Biermann, Bornscheuer Uwe, Meier Michael A. R., Metzger Jürgen O., and Schäfer Hans J. 2011. 'Oils and Fats as Renewable Raw Materials in Chemistry', *Angewandte Chemie International Edition*, 50: 3854-71.

Wool, R. P., and X. Sun. 2005. *Bio-Based Polymers and Composites* (Elsevier).

Ying, Hanze, Yanfeng Zhang, and Jianjun Cheng. 2014. 'Dynamic urea bond for the design of reversible and self-healing polymers', *Nature Communications*, 5: 3218.

Zhang, Lu, Frederick C. Michel Jr, and Anne C. Co. 2019. 'Nonisocyanate route to 2,5-bis(hydroxymethyl)furan-based polyurethanes crosslinked by reversible diels–alder reactions', *Journal of Polymer Science Part A: Polymer Chemistry*, 57: 1495-99.

Zlatanic, Alisa, Charlene Lava, Wei Zhang, and Zoran Petrović. 2004. 'Effect of Structure on Properties of Polyols and Polyurethanes Based on Different Vegetable Oils', *Journal of Polymer Science Part B: Polymer Physics*, 42: 809-19.

Chapter 1. Click green chemistry for the synthesis of biobased polymers and networks derived from vegetable oils – A literature review

Chapter 1: State of the art – Click chemistry and vegetable oils

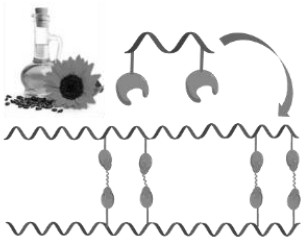

Chapter 2: Synthesis of Furan Oligomer and biobased PU CANs

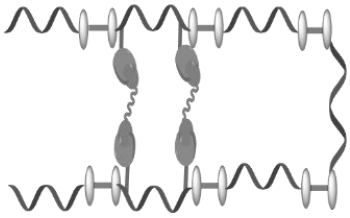

Chapter 3: Further elaboration of biobased PU CANs containing FO

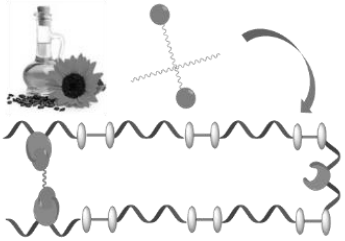

Chapter 4: Synthesis of Methyl oleate bismaleimide and biobased PU CANs

Introduction of Chapter 1

The literature review presented in this chapter describes the use of click and green chemistry for the synthesis of polymers and networks derived from vegetable oils. First, this state of art gives the general context of oleochemistry towards polymer-based systems and the properties of vegetable oils-based materials. The most commonly accessible and prevalent glycerides and the common chemistry performed on the main moieties of vegetable oils are described. This is followed by a section that describes the principles of click chemistry, the main reactions and the mechanisms used on vegetable oils-based systems. Lastly, the most recently published works involving the synthesis of adequate (macro)monomers and polymers using click chemistry reactions are analyzed. This part of the article pays particular attention to the use of click chemistry to develop biobased macromolecular architectures with advanced properties. Since the literature is abundant on this field, this work puts a particular emphasis on the most recent works, published during the last decade.

Click green chemistry for the synthesis of biobased polymers and networks derived from vegetable oils – A review

Khantutta-Kim Tremblay-Parrado, Clara García-Astrain, Luc Avérous

1. Abstract

Living in the time of the most heighten environmental issues, material science is required to prepare sustainable polymers by means that are in line with green chemistry ideals. For over a century, vegetable oils and their fatty acid derivatives have been largely regarded for their uses in polymer chemistry for a large range of applications. Recently, the development of the click chemistry has drastically effected the synthesis of vegetable oil-derived polymers.

This review covers the most recent and relevant developments in click chemistry as a functionalization and polymerization method of vegetable oils and their derivatives. First a quick overview is provided of the main properties of the most commonly accessible vegetable oils and their most prevalent chemical modifications. This is followed by an introduction of the click chemistry reactions frequently excerised on vegetable oils. The focus of the manuscript is the utilization of this efficient chemistry for the synthesis of polymers derived from vegetable oils.

Keywords: Biobased polymers, Monomers, Renewable Resources, Thermoplastics, Thermosets

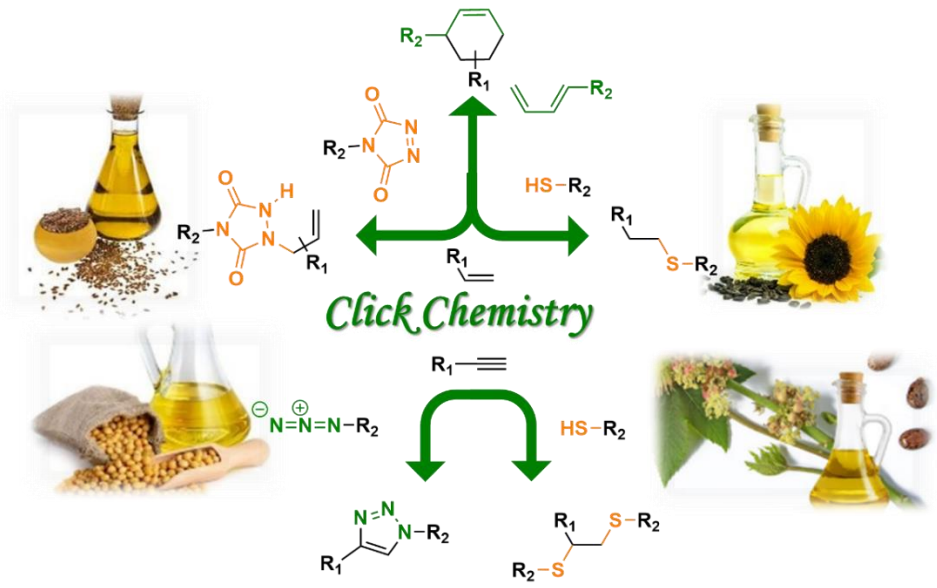

2. Introduction

Living in these mediatized times, citizens are aware more than ever of how individuals and industrials contribute to the preservation of the environment. As such, the topics of sustainability, recyclability, developing and utilizing renewable resources, waste management and eco-friendly products are widespread due to rising environmental concerns. Consequently, a major responsibility lies on academics and industrials to develop solutions that address this global problematic. In the field of chemistry, Anastas and Warner conceptualized the ideals of sustainable chemistry by developing the "12 Principles of Green Chemistry". Generally, the ideals of green chemistry are centered around: (i) minimizing waste, (ii) the use of renewable feedstock and energy, (iii) the use of safe and environment benign substances and (iv) atom economy (Anastas and Warner 1998). According to a 2019 European Bioplastics report, biobased polymers represent less than 1% of the over 359 million tons produced annually. Consequently, the polymer industry has considerable progress to achieve in order to adhere to the green chemistry principle of using renewable feedstock.

Historically and presently, oils and fats of vegetable and animal origin remain the most abundantly used renewable resource of the chemical industry (Ursula et al. 2011). Vegetable oils are prime candidates to replace fossil-based derivatives in polymer materials for a multitude of reasons such as: (i) their universal availabilities, (ii) low toxicities (iii) low prices and, (iv) their inherent chemical structures (de Espinosa and Meier 2011; Ursula et al. 2011; Ronda et al. 2011). Generally, their chemical structure provides linear carbon chains with different active groups such as hydroxyls, oxiranes, and double bonds along them, with carboxylic acid ends, which provides a huge potential to perform a rich amount of chemistries. The use of vegetable oils has been studied and explored in several different types of polymer syntheses, notably epoxy resins, polyamides (PA) (Miao et al. 2014; Hablot et al. 2008), polyesters (Xia and Larock 2010), or polyurethanes (PUs) (Desroches et al. 2012; Hablot et al. 2008; Bueno-Ferrer, Hablot, Perrin-Sarazin, et al. 2012; Bueno-Ferrer, Hablot, Garrigós, et al. 2012; Laurichesse and Avérous 2014). Consequently, vegetable oils are attractive building blocks for the synthesis of biobased polymers which can compete with petroleum-based equivalents. Besides, some new macromolecular architectures

linked to original biobased building blocks can be obtained, for instance polymers from fatty acids dimers (Bueno-Ferrer, Hablot, Perrin-Sarazin, et al. 2012; Bueno-Ferrer, Hablot, Garrigós, et al. 2012; Reulier and Avérous 2015; Reulier et al. 2016; Reulier, Perrin, and Avérous 2016; Reulier et al. 2017; Charlon et al. 2014).

Approximately ten years after the establishment of the principles of green chemistry, the concept of click chemistry was introduced by Sharpless and co-workers in 2001. The use of click chemistry for the controlled synthesis of different macromolecular architectures gained substantial interest as these reactions adhere to the principles of green chemistry. Click chemistry consists of a wide range of reactions that are required to be modular, wide in scope, give high yields, generate only inoffensive by-products and be stereospecific. It is the high thermodynamic driving force of click reactions that allow them to achieve these characteristics (Kolb, Finn, and Sharpless 2001). With regards to the synthesis of monomers and polymers from vegetable oils by click chemistry, the literature reports the use of different reactions, such as (i) triazolinedione (TAD) chemistry, (ii) Diels–Alder (DA) cycloadditions, (iii) thiol-ene addition (iv) thiol-yne addition, and (v) Cu(I)-catalyzed azide-alkyne reaction. Although the thiol-ene addition reaction dominates in use of click chemistry in oleochemistry, the efficient application of the DA reaction (Gandini et al. 2018) and TAD click chemistry (De Bruycker et al. 2016) to oleochemistry has recently been brought forth.

In this review article, the most recent strategies for the modifications of oleochemicals into networks and polymers via click chemistry reactions are analyzed and highlighted. This state of art gives the general context of the oleochemistry towards polymer-based systems and the properties of vegetable oils-based materials. The most commonly accessible and prevalent glycerides and the common chemistry performed on the main moieties from vegetable oils are described. This part is followed by a section that describes the main click chemistry reactions used on vegetable oils. The article will focus particular attention on the recent uses of click chemistry to develop biobased macromolecular architectures with advanced properties.

3. Fatty acids

3.1. Properties

Vegetable oils mainly consist of triglycerides which are depicted in Figure 1.1. They can be defined as esters of glycerol, consisting of three long-chain fatty acids (FAs). They are mainly obtained from vegetable oils, animal fats or micro-algae. Three main structural elements tend to dictate the physical and chemical properties of triglycerides: (i) chain length, which usually varies up to 24 carbons, (ii) degree of unsaturation, often between 0-3 and lastly, (iii) the stereochemistry of the double bonds (Zlatanic et al. 2004). Figure 1.2, illustrates the chemical structure of the most common FAs found. The FA composition of vegetable oils can vary according to the plant species (Table 1.1), crop type, season and growing conditions (Meier, Metzger, and Schubert 2007). Table 1.1 presents the main industrial vegetable oils, their composition and their average number of double bonds per triglyceride. It is also evidenced in Table 1.1 that palmitic, stearic, oleic, linoleic and linoleic acids consist of the majority of the composition of common vegetable oils.

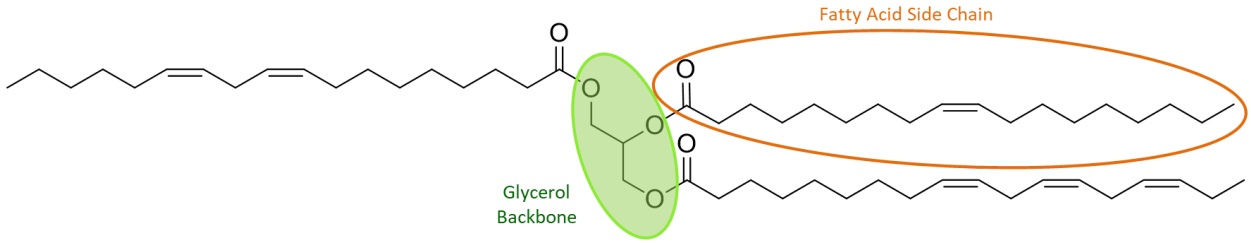

Figure 1.1 – General chemical structure of triglycerides.

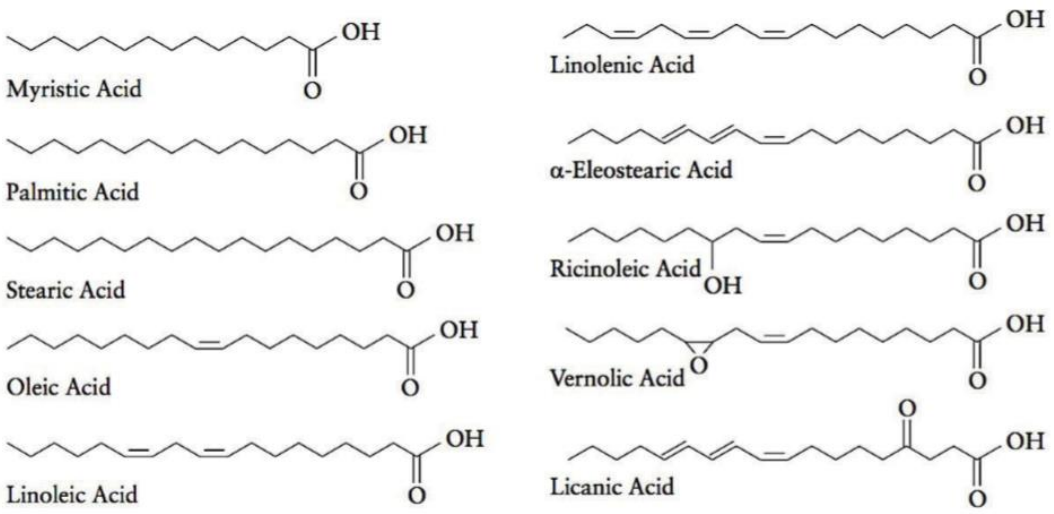

Figure 1.2 – Structure of most common fatty acids.

Table 1.1 – Fatty acid composition and properties of the most industrially viable vegetable oils. (Meier, Metzger, and Schubert 2007; Lu and Larock 2009; Gandini and Lacerda 2018).

Fatty Acid	Systematic name	Structure [C:DB] [a]	Formula	Canola	Corn	Cottonseed	Linseed	Olive	Palm	Rapseed	Soybean	High Oleic [b]
Myristic	Tetradecanoic acid	14:0	$C_{14}H_{28}O_2$	0.1	0.1	0.7	0.0	0.0	1.0	0.1	0.1	0.0
Myristoleic	Tetradecenoic acid	14:1	$C_{14}H_{26}O_2$	0.0	0.0	0.0	0.0	0.0	0.0	0.0	0.0	0.0
Palmitic	Hexadecanoic acid	16:0	$C_{16}H_{32}O_2$	4.1	10.9	21.6	5.5	13.7	44.4	3.0	11.0	6.4
Palmitoleic	Hexadecenoic acid	16:1	$C_{16}H_{30}O_2$	0.3	0.2	0.6	0.0	1.2	0.2	0.2	0.1	0.1
Margaric	Heptadecanoic acid	17:0	$C_{17}H_{34}O_2$	0.1	0.1	0.1	0.0	0.0	0.1	0.0	0.0	0.0
Margaroleic	Heptadecenoic acid	17:1	$C_{17}H_{32}O_2$	0.0	0.0	0.1	0.0	0.0	0.0	0.0	0.0	0.0
Stearic	Octadecanoic acid	18:0	$C_{18}H_{36}O_2$	1.8	2.0	2.6	3.5	2.5	4.1	1.0	4.0	3.1
Oleic	*Cis*-9-octadecenoic acid	18:1	$C_{18}H_{34}O_2$	60.9	25.4	18.6	19.1	71.1	39.3	13.2	23.4	82.6
Linoleic	*Cis*,*cis*-9,12-octodecdienoic acid	18:2	$C_{18}H_{32}O_2$	21.0	59.6	54.4	15.3	10.0	10.0	13.2	53.2	2.3
Linolenic	*Cis*,*cis*,*cis*-9,12,15-octadecatrienoic acid	18:3	$C_{18}H_{30}O_2$	8.8	1.2	0.7	56.6	0.6	0.4	9.0	7.8	3.7
Arachidic	Eicosanoic acid	20:0	$C_{20}H_{40}O_2$	0.7	0.4	0.3	0.0	0.9	0.3	0.5	0.3	0.2
Gadoleic	*Cis*-9-eicosenoic acid	20:1	$C_{20}H_{38}O_2$	1.0	0.0	0.0	0.0	0.0	0.0	9.0	0.0	0.4
Eicosadienoic	*Cis*,*cis*-11,14-eicosadienoic acid	20:2	$C_{20}H_{36}O_2$	0.0	0.0	0.0	0.0	0.0	0.0	0.7	0.0	0.0
Behenic	Docosanoic acid	22:0	$C_{22}H_{42}O_2$	0.3	0.1	0.2	0.0	0.0	0.1	0.5	0.1	0.3
Erucic	*Cis*-13-docosenoic acid	22:1	$C_{22}H_{40}O_2$	0.7	0.0	0.0	0.0	0.0	0.0	49.2	0.0	0.1
Lignoceric	Tetracosanoic acid	24:0	$C_{22}H_{44}O_2$	0.2	0.0	0.0	0.0	0.0	0.0	1.2	0.0	0.0
	Average : #DB/triglyceride			3.9	4.5	3.9	6.6	2.8	1.8	3.8	4.6	3.0

[a] C represents the number of carbon atom and DB the number of double bonds in the fatty-acid chain [b] Gentically engineered high oleic acid content soybean oil (DuPont).

3.2. Modification of fatty acids

Various chemical reactions can be used to modify the reactive chemical groups of FAs. In fact, oleochemistry is the term used to define the rich chemistry that can be performed on glycerides,

resulting in physico-chemical modifications and transformations of FAs. As the most common structures of triglycerides contain carbonyls and double bonds, the sites most likely to undergo reactions or chemical modifications include: (i) double bonds, (ii) methylene moieties α to double bonds (allylic carbons), (iii) ester groups, and (iv) methylene sites α to esters. To show the richness of the oleochemistry, a simplified list of different reactions based on FAs is found in

Table 1.2. During the two last decades, the most important reactions related the ester and double-bond moieties have been thoroughly and largely reviewed (Biermann et al. 2000; Corma, Iborra, and Velty 2007; Meier, Metzger, and Schubert 2007; Behr, Westfechtel, and Pérez Gomes 2008; Ursula et al. 2011; Miao et al. 2014) .

Table 1.2 – Overview of main chemical modifications performed on fatty acids. Selection from (Desroches et al. 2012).

Reaction Site	Reaction Name	Reaction Schematic
Main reactions on the carbonyl group	(Trans)esterification	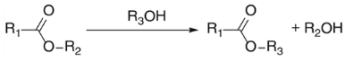
	Amidification	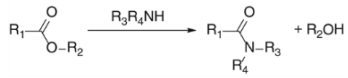
	Reduction	
Main reactions on the carbon-carbon double bond	Epoxidation	
	Epoxide ring opening	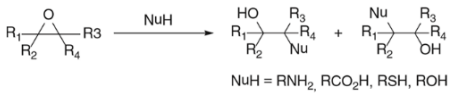 NuH = RNH_2, RCO_2H, RSH, ROH
	Hydroformylation	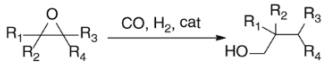
	Ozonolysis-Hydrogenation	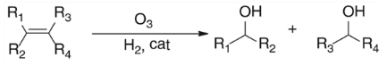
	Metathesis	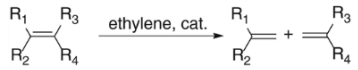
	Thiol-ene coupling	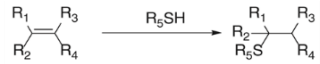
	Diels-Alder cyclo-addition	

3.2.1. Modification on carbonyl group

As previously mentioned FAs and FA esters can easily be obtained by transesterification (hydrolysis or alcoholysis) of triglycerides. Esterification and transesterification (ester interchange reaction) are equilibrium reactions, often requiring the excess of one reagent (often alcohol or water) to shift the equilibrium. Commonly, acid (sulfuric acid) and basic (sodium or potassium hydroxide) catalysts are used. In this way, biodiesel production is mainly based on transesterification reactions of triglycerides and methanol to yield glycerol and FA methyl esters (FAMEs) (Gerpen 2005). FAMEs can also be used as green solvents (Salehpour and Dubé 2008). Moreover, glycerol can be used as a precursor for industrial commodities such as 1, 3-propanediol and ethylene glycol (Corma, Iborra, and Velty 2007) to replace fossil-based derivatives. The FAs

and FAMEs that yield from the saponification or alcoholysis process are often modified by esterification and transesterification reaction to obtain architectures of interest for several chemical reactions. Furthermore, a convenient way to achieve reactive hydroxyl groups from carboxylic acids is their reduction using lithium aluminum hydride ($LiAlH_4$). This reaction is commonly used for the synthesis of polyols (Ligthelm, von Rudloff, and Sutton 1950).

3.2.2. Modifications on unsaturations of FAs and FAMEs

As shown in Table 1.2, different reactions on the double bonds can occur such as epoxidation, hydroformylation, ozonolysis, thiol-ene coupling, oxidation, Diels-Alder, and metathesis of unsaturated oils. Based on FAs and FAMEs, they yield powerful modifications for the synthesis of biobased polymers (Biermann et al. 2000; Corma, Iborra, and Velty 2007; Behr, Westfechtel, and Pérez Gomes 2008; Belgacem and Gandini 2008)

The epoxidation of unsaturated FAs can be attained by direct means by reacting FAs with hydrogen peroxide, oxygen and chemo-enzymatic reactions (Biermann et al. 2000). Industrially, the epoxidation of vegetable oils is carried out by the use of peroxoacetic and peroxoformic acids (Petrović et al. 2002). Epoxy groups can be opened by different reagents (amines, carboxylic acids, thiols, alcohols, water and hydrogen halides) or hydrogenation to yield secondary hydroxyl groups (Peyrton, Chambaretaud, and Avérous 2019). These modifications can for instance yield diverse polyols for the synthesis of PUs (Desroches et al. 2012).

Hydroformylation can be used to convert an unsaturation to an aldehyde group. The reaction entails the conversion of the unsaturation to a carbonyl moiety using carbon monoxide and hydrogen (syngas). Then, the aldehyde can further be converted to an alcohol moiety by the presence of a Raney nickel under H_2 pressure at high temperatures (Petrovic 2008).

Ozonolysis is another powerful reaction can yield primary hydroxyl groups (Petrović, Zhang, and Javni 2005). Oxidative scission on triglycerides yields FA chains to contain terminal primary hydroxyls groups, and depending on the work-up conditions can also yield the formation of carboxylic acids and aldehyde group. A prominent example includes the ozonolysis reaction of oleic acid with use of hydrogen peroxide to yield azaleic and perlargonic acids (Meier, Metzger, and Schubert 2007).

The use of olefin metathesis allows the possibility to obtain valuable building blocks from FAs. Generally, metathesis allows for the re-allotting of olefin moiety, by the scission and the renewal of an unsaturation. The metallic catalyst play a crucial role in success of the reaction and ruthenium based- catalyst have been found to be the most efficient and selective (Rybak, Fokou, and Meier 2008). A prominent example of the metathesis reaction is the cross metathesis of methyl oleate with ethene to produce the bifunctional entity, methyl 9-decenoate.

Castor oil is a non-edible vegetable oil with the particularity of containing a high content of ricinoleic acid (as high as 90 % FA content) (Mubofu 2016). Pyrolysis, a thermal treatment in the absence of air, decomposes organic biomass into lower molar mass (MW) compounds. As show in Scheme 1.1, the pyrolysis of methylricinoleate cleaves the molecule to produce methyl undecenoate and heptaldehyde (Jeppesen, Devaux, and Dubois 2015). Such a reaction is industrially used in the production of PA 11 (Arkema, France). Methyl undecenoate (MUDO) and its carboxylic acid counterpart, undecylenic acid (UDA), are molecules of high interest and often use in the synthesis of monomers and polymers by click- chemistry, particularly in thiol-ene chemistry.

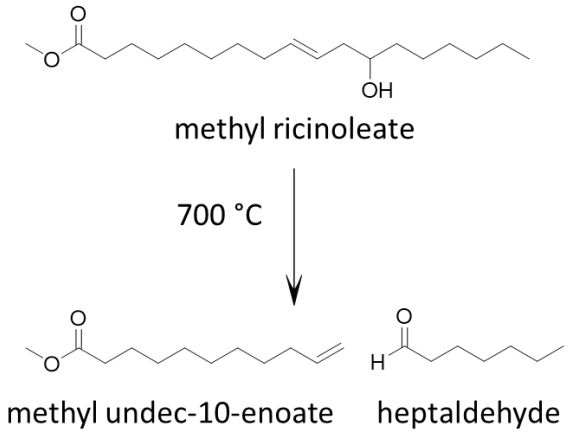

Scheme 1.1 – Schematic of pyrolysis reaction of methyl ricinoleate.

4. Click Chemistry

Click chemistry was introduced by Sharpless and co-workers in 2001 and consists of a wide range of reactions that are required to be modular, wide in scope, give high yields, generate only inoffensive by-products and be stereospecific. Moreover, characteristics of the process should

include simple reaction conditions, readily available starting materials and reagents, the use of no solvents or a benign solvent and simple product isolation. Some common click chemistry reactions used on vegetable oils and their derivatives are highlighted in Scheme 1.2. For a deeper mechanistic view, the recent literature presents several state of arts (Hoyle and Bowman 2010; Hoogenboom 2010; Moses and Moorhouse 2007; Qin, Lam, and Tang 2010; De Bruycker et al. 2016).

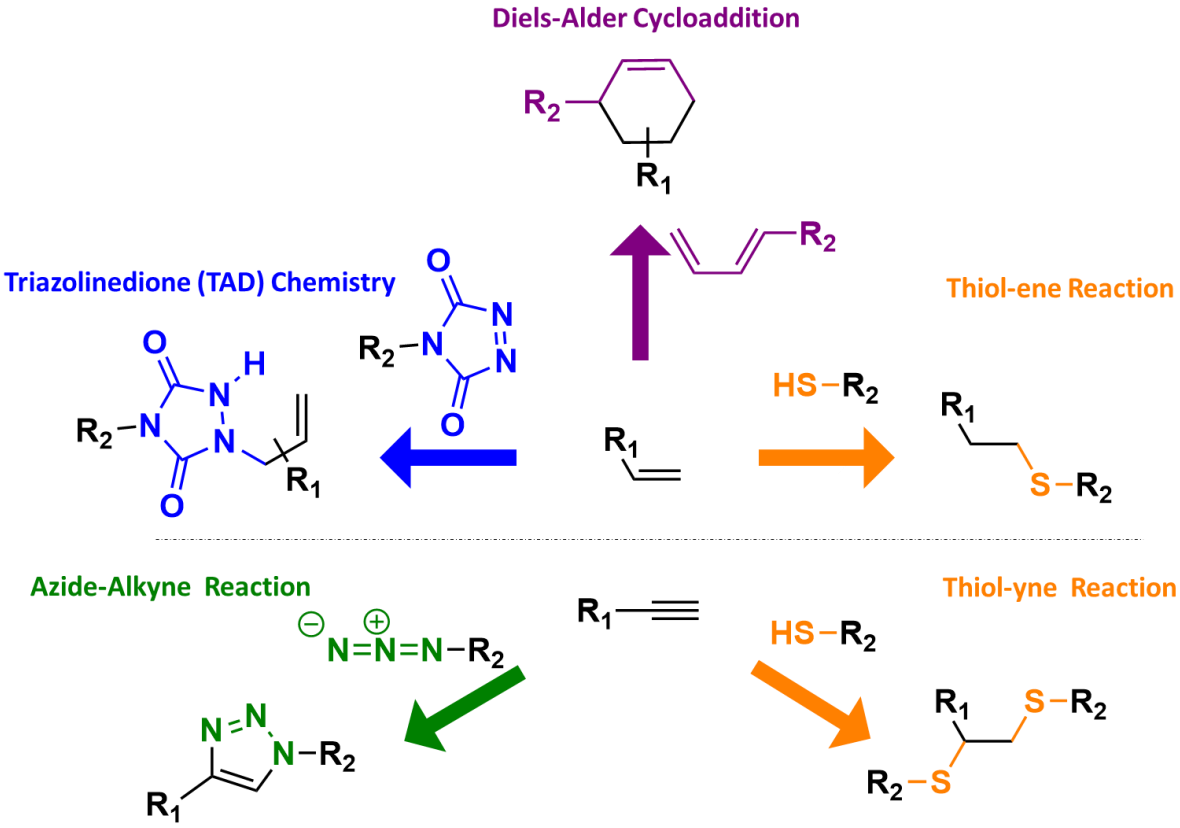

Scheme 1.2 – Schematic representation of click chemistry reactions applied to plant oil triglycerides and derivatives.

4.1. Diels-Alder cycloaddition

The Diels-Alder (DA) reaction consists of the [4+2] cycloaddition between a diene and a dienophile to form an adduct (Scheme 1.2). This reaction was first reported by Otto Diels and Kurt Alder in 1931 (Diels and Alder 1931). It is extensively used in organic chemistry to produce six-membered unsaturated rings with good control over regio- and stereochemical properties (Buono et al. 2018). This reaction has been widely used in the last decades in oleochemistry and polymer chemistry (Dumont 2016). This reaction takes place through a concerted mechanism and is

particularly interesting due to its thermal reversibility (retro DA reaction or r-DA) which varies depending on the diene/dienophile couple (Gandini 2013). The thermal reversibility is highly appealing in polymer chemistry for applications such as recyclable or self-healing materials.

4.1.1. Furan-Maleimide coupling

One of the most well-known diene/dienophile couple used in polymer chemistry is the furan/maleimide system (Scheme 1.3). One of the main characteristics of this coupling is that the r-DA can be achieved at relatively low temperature (Gandini 2013). Typically, the DA reaction takes place around 65 °C whereas the r-DA leading to uncoupling of the adduct is predominant at around 110 °C. Another interesting particularity of the furan/maleimide couple is based on the renewable character of the furan derivatives, leading to greener chemistry alternatives. Moreover, the strong dienic character of the furan ring renders it interesting in terms of reaction yield and kinetics.

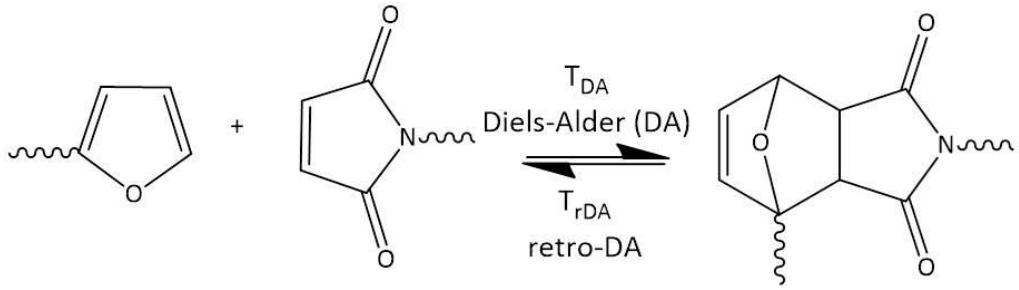

Scheme 1.3 – Schematic of the DA reaction and r-DA between furan and maleimide moiety, adapted from reference (Kwart and Burchuk 1952).

4.1.2. Other diene/dienophile

Although the furan/maleimide couple is the most popular couple for DA reaction, other diene/dienophile couples can also be used for the preparation polymers and derivatives from vegetable oils. The double bonds of vegetable oils can be used as dienes and reacted with anhydrides such as maleic anhydride, acrylic acids or methacrylates (Huang, Zhang, et al. 2013; Huang et al. 2014, 2015; Liu et al. 2015; Huang, Pang, et al. 2013; Bétron, Cassagnau, and Bounor-Legaré 2018; Gallart-Sirvent et al. 2017; Ma et al. 2013; Liu et al. 2013; Mangeon et al. 2017; Yang et al. 2017; Nalawade et al. 2014; Yang et al. 2015). Moreover, the dimerization of mono-

unsaturated FAs by DA addition at high temperatures to yield linoleic derivatives has been exploited to obtain monomers for the synthesis of polyesters, PA, polyethers and PUs (Corma, Iborra, and Velty 2007). In this review, we will focus only on the examples of the DA reaction fulfilling the criteria of click chemistry reactions such as mild reaction conditions (T < 100 ºC) and simple purification processes, amongst others.

4.2. Triazolinediones chemistry

Recently, another example of click chemistry based on the reactivity of 1,2,4-triazoline-3,5-dione (TAD) has been added to the toolbox of chemists for polymer science. TADs are heterocyclic molecules with an azo group and two carbonyl functionalities, highly resembling maleimide dienophiles (De Bruycker et al. 2016). Within this electronic configuration, the azo group is stabilized and the electron-withdrawing carbonyls coupled with the molecule conformation make them highly reactive (Billiet et al. 2014). The high reactivity of azodicarbonyl derivatives was first reported by Diels and co-workers in 1925 (Diels, Blom, and Koll 1925), but the use of the more reactive TAD versions for the DA reaction was not reported until the 60s (Cookson, Gilani, and Stevens 1962, 1967). Indeed, TADs can take part in DA and ene-type reactions fulfilling the requirements of click chemistry reactions such as orthogonality and reversibility as well as high yields under mild reaction conditions (Scheme 1.4-a) (Billiet et al. 2014). When compared to maleimides, TADs show higher reactivity, reacting with dienes almost instantaneously and at low temperatures, and, in most cases, produce irreversible products (De Bruycker et al. 2016). The group of Du Prez and co-workers have intensively worked with these types of reactions in the last years and also introduced the term of “transclick” reactions (Scheme 1.4–b) (Billiet et al. 2014). These reactions have been defined as covalent linking processes that can be triggered to form a new bond with other available orthogonal partners, releasing one of the initially involved counterparts. Thus, this strategy could be applied for the formation of dynamic bonds or the thermal exchange between clickable groups.

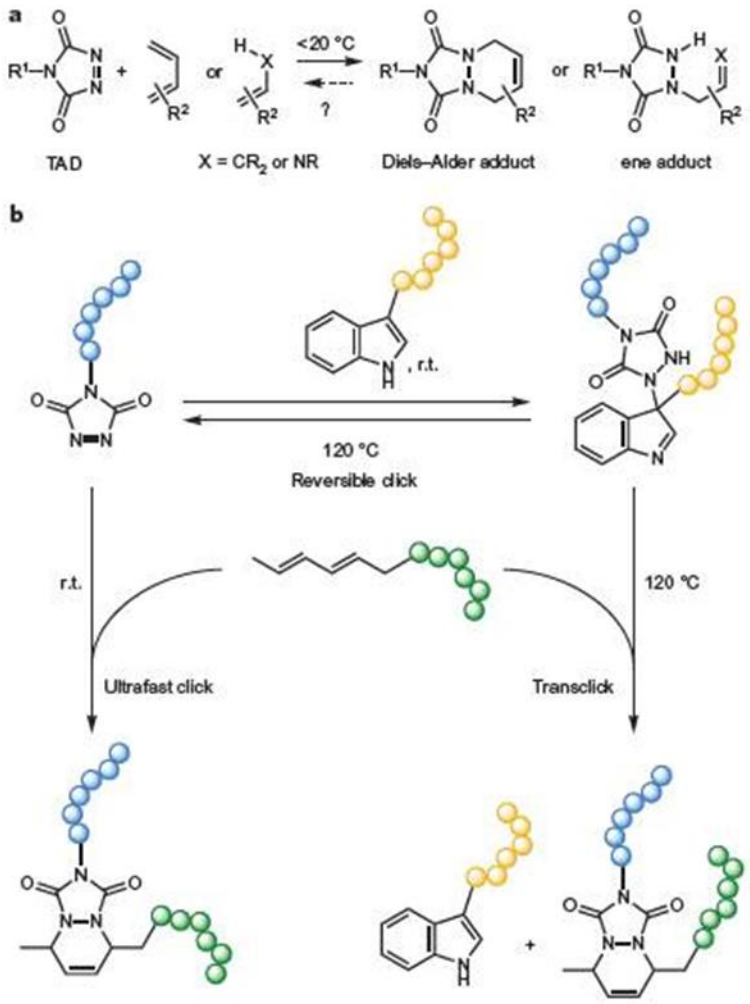

Scheme 1.4 – TAD chemistry for click and transclick reactions (a) TAD-based DA and ene click reactions and, (b) example of a transclick reaction, adapted from reference (Billiet et al. 2014).

4.3. Thiol-ene reaction

Thiol-ene reaction (otherwise defined as thiol-ene coupling (TEC)) takes place between double bonds (enes), that can be either terminal monosubstituted or internal disubstituted enes, and thiol groups (Scheme 1.2). The reaction takes advantage of the labile sulfur-hydrogen bond (Kade, Burke, and Hawker 2010). Two reactions between thiols and double bonds have gained prevalence and possess many characteristics of click reactions: (i) the free-radical addition of thiyl radicals (generated from thiols initiated by light, heat or radical initiators) to electron rich or poor double bonds and (ii) the catalyzed (by a base or nucleophile) thiol-Michael addition to electron deficient double bonds. With respect to the free-radical thiol-ene reaction, the reaction rate depends strongly on the structure of the thiol and the ene. Thiyl radicals tend to add faster to

electron-rich enes (terminal double bonds), than electron-poor enes (acrylates) (Claudino 2011). Thiol-ene click reaction has been vastly applied to unsaturated oils and FAs (Lligadas et al. 2013; Türünç and Meier 2013).

4.4. Thiol -yne reaction

The thiol-yne reaction (otherwise defined as thiol-yne coupling (TYC)) was re-introduced as a powerful tool for polymerization by Bowan and co-workers in 2009 (Fairbanks et al. 2009). Their work demonstrated how thiol-ene reactions could be complemented by readily accessible azide-alkyne building blocks. Essentially by the thiol-yne reaction, two thiyl radicals can react with alkynes to form thio-ether linkages, consequently saturating the alkyne bond (Scheme 1.2) (Konkolewicz, Gray-Weale, and Perrier 2009). Similar to the free-radical thiol-ene addition, a radical source or UV irradiation can be used and thus there is no need for potential toxic catalyst use in the azide-alkyne cycloaddition. There has been limited use the thiol-yne reaction in oleochemistry as acetylenic FAs rarely occur in nature. Nevertheless, as it will be described in the next sections, modifications can be brought on to FAs to yield interesting architectures containing alkyne bonds. For example, UDA can be converted to 10-undecynoic acid by successive bromination and debromination. Unfortunately, this procedure does not respect all the ideals of green chemistry (Lligadas et al. 2007; Silbert 1984).

4.5. Huisgen 1,3-dipolar cycloaddition

One of the most appealing examples of click chemistry is the Huisgen [3 + 2] dipolar cycloaddition of alkynes and azides to yield 1,2,3-triazoles (Scheme 1.2) (Buono et al. 2018; Hong et al. 2012). Molecules can be easily functionalized with alkyne and azide moieties under mild conditions. Moreover, their tolerance to a wide variety of functional groups and reaction conditions turns these coupling agents into attractive alternatives for polymer chemistry (Buono et al. 2018; Hu et al. 2016).

The copper catalyzed version of the azide-alkyne cycloaddition (CuAAC) was reported by Sharpless and Meldal (Rostovtsev et al. 2002; Tornøe, Christensen, and Meldal 2002). This reaction between azides and alkynes is high yielding and shows higher regioselectivity, resulting

solely in 1,4-regioisomer, increasing the reaction rate up to 10^7 times, and avoiding the use of high temperatures (Buono et al. 2018; Hong et al. 2012; Hu et al. 2016). Furthermore, the use of water as a solvent proved to induce a beneficial kinetic effect on the reaction. The CuAAC reaction has been widely used in polymer chemistry to produce polymers with different macromolecular structures such as linear or block copolymers, or dendrimers, circumventing some common problems such as steric hindrance of reactive sites in a growing polymer chain (Hong et al. 2012; Hu et al. 2016). As a greener alternative to the use of copper as catalyst in the Huisgen 1,3-dipolar cycloaddition, the thermally driven version of this reaction has also been employed in polymer chemistry (Hong et al. 2015). The thermal Huisgen 1,3-dipolar cycloaddition offers some advantages over the CuAAC, particularly in polymer chemistry where the removal of the catalyst entrapped within the polymer matrix becomes difficult. However, this version is non-stereoselective and forms both 1,4- and 1,5-disubstituted triazole rings (Hong et al. 2015).

5. Synthesis of derivates and polymers through click reactions

5.1. Diels Alder cycloaddition

5.1.1. Furan-Maleimide coupling

The use of the DA reaction for derivatives and polymer synthesis has bloomed over the last two decades and is now an established strategy for the synthesis of macromolecular architectures. Several reviews have been published by Gandini in the last decade, summarizing the most relevant results regarding the use of the DA reaction in polymer chemistry (Gandini 2013; Gandini et al. 2016; Lacerda and Gandini 2014). The purpose of the present review is also to complement those works with the latest results regarding vegetable oils in this very active field. This section focuses on the combination of furans and vegetable oils both for monomer modification, to widen the reactivity of triglycerides after the modification with furan groups, and for polymers design via the DA reaction with maleimides.

Even if vegetable oils contain reactive groups, such as double bonds or epoxy groups, they found limited reactivity in polymerization reactions and, often, require the incorporation of more reactive functionalities. In this sense, first generation furan compounds, such as furfural and 5-

hydroxymethylfurfural, that can be readily obtained from sugars or polysaccharides, can be associated on to glycerides, opening the way to different monomers derived from renewable resources (Lacerda and Gandini 2014).

Two approaches can be mainly applied for the preparation of macromolecular materials from the DA reaction (Gandini et al. 2018). One way deals with the synthesis of thermally-reversible linear, branched and cross-linked polymers based on the polycondensation of building blocks incorporating both DA complementary moieties such as furan and maleimide groups. On the other hand, the thermally reversible cross-linking of linear polymers bearing pendant furan or maleimide moieties and using complementary maleimide or furan bifunctional cross-linkers has also been widely explored. One of the most interesting features of this reaction is the temperature control for the forward and r-DA reactions that allows for the decoupling of the DA reaction groups resulting in recyclable or self-healing cross-linked materials.

Gandini and co-workers have extensively worked on the use of DA reaction for monomer modification and polymer synthesis (Gandini 2013; Gandini, Coelho, and Silvestre 2008; Gandini, Silvestre, and Coelho 2011; Gandini, Silvestre, and Coelho 2010; Vilela, Silvestre, and Gandini 2013; Gheneim, Perez-Berumen, and Gandini 2002; García-Astrain et al. 2013; Gousse, Gandini, and Hodge 1998; Vilela et al. 2011). The first report for the preparation of vegetable oils-based monomers was reported by these authors using UDA, derived from castor oil, that possess two terminal reactive sites available for the insertion of furan and/or maleimide moieties (Vilela et al. 2011, 2012). In these works, two difuran monomers were prepared using esterification and thiol-ene reactions (Figure 1.3 – a & b). Another bifunctional monomer, bearing both furan and maleimide groups was also prepared from 10-undecenol (UDC) using protective chemistry (Figure 1.3 - c). These monomers were polymerized by DA reaction at 65 °C in 1,1,2,2-tetrachloroethane (TCE) using 1,6-bismaleimidohexane with the first two whereas the bifunctional monomer was self-polymerized after deprotection (Figure 1.4). Raising the temperature to 110 °C allowed for the recovery of the monomers through r-DA depolymerizations. The reported polymers obtained using difuran and bismaleimide (BMI) monomers had a MW of 7-9 kDa and a T_g of about -30 °C. In the case of the self-polymerized polymer, the resulting MW was 17 kDa with a T_g of -2 °C due to a stiffer macromolecular architecture.

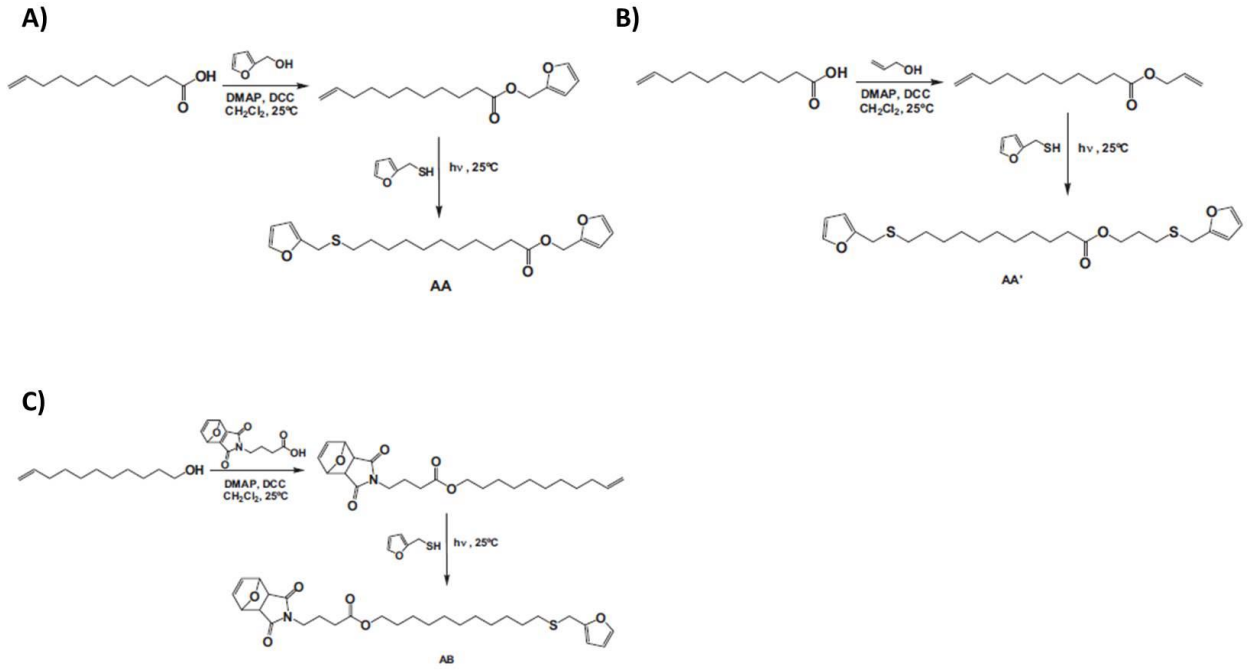

Figure 1.3 – (a) Synthesis of difuran monomer from 10-undecenoic acid, (b) synthesis of a second difuran monomer from 10-undecenoic acid and, (c) synthesis of protected AB macromonomer. Reproduced with permission of Wiley (Vilela et al. 2011).

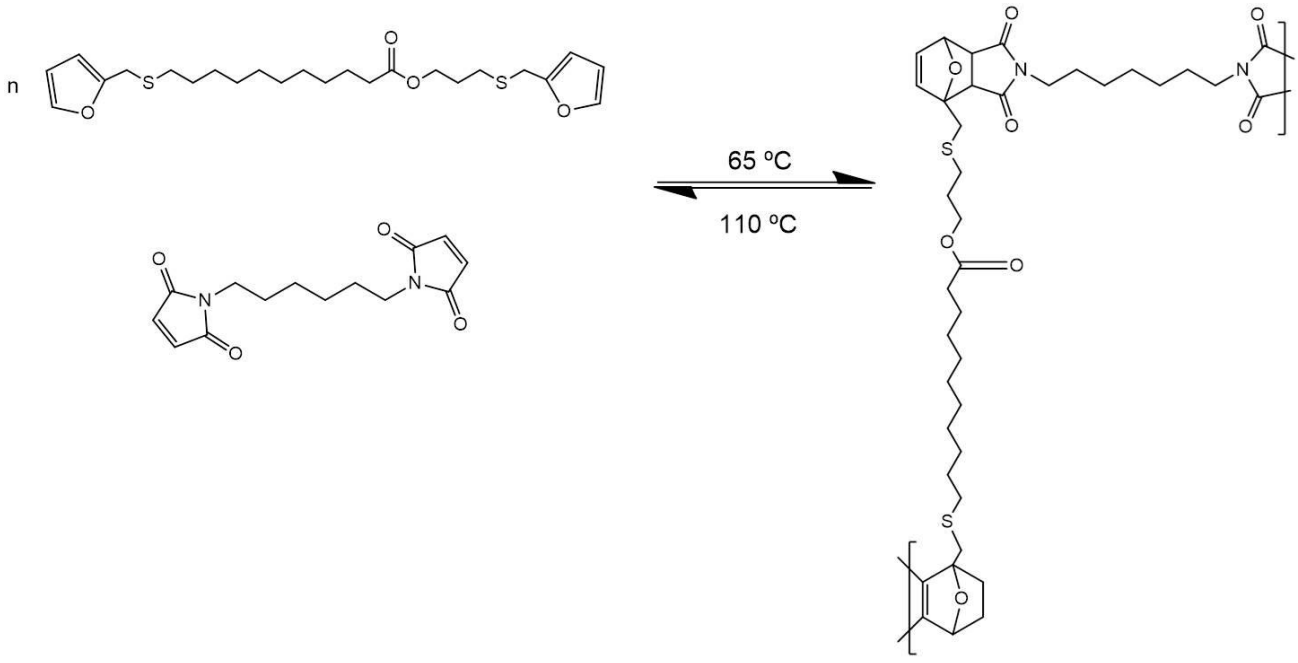

Figure 1.4 – Reversible DA polycondensation of difuran monomer with an aliphatic BMI adapted from reference (Gandini et al. 2018).

In a more recent work by the same authors, non-linear polymers were prepared employing trifuran, difuran or bismaleimide monomers (Figure 1.5) (Vilela, Silvestre, and Gandini 2013). The trifuran monomer was polymerized with an aliphatic bismaleimide whereas the difuran monomer was polymerized with a trimaleimide, leading to the same types of macromolecular architectures (Figure 1.6). Both macromolecular structures showed MW between 35 and 50 kDa and a T_g around 0 °C when using a 0.5 trifunctional/bifunctional molar ratio. The authors reported that stoichiometric monomer conditions produced gels with T_g values of about 15 °C. On the other hand, the DA self-polymerization resulted in hyperbranched macromolecules with a MW between 50 and 70 kDa and T_g around 5 °C.

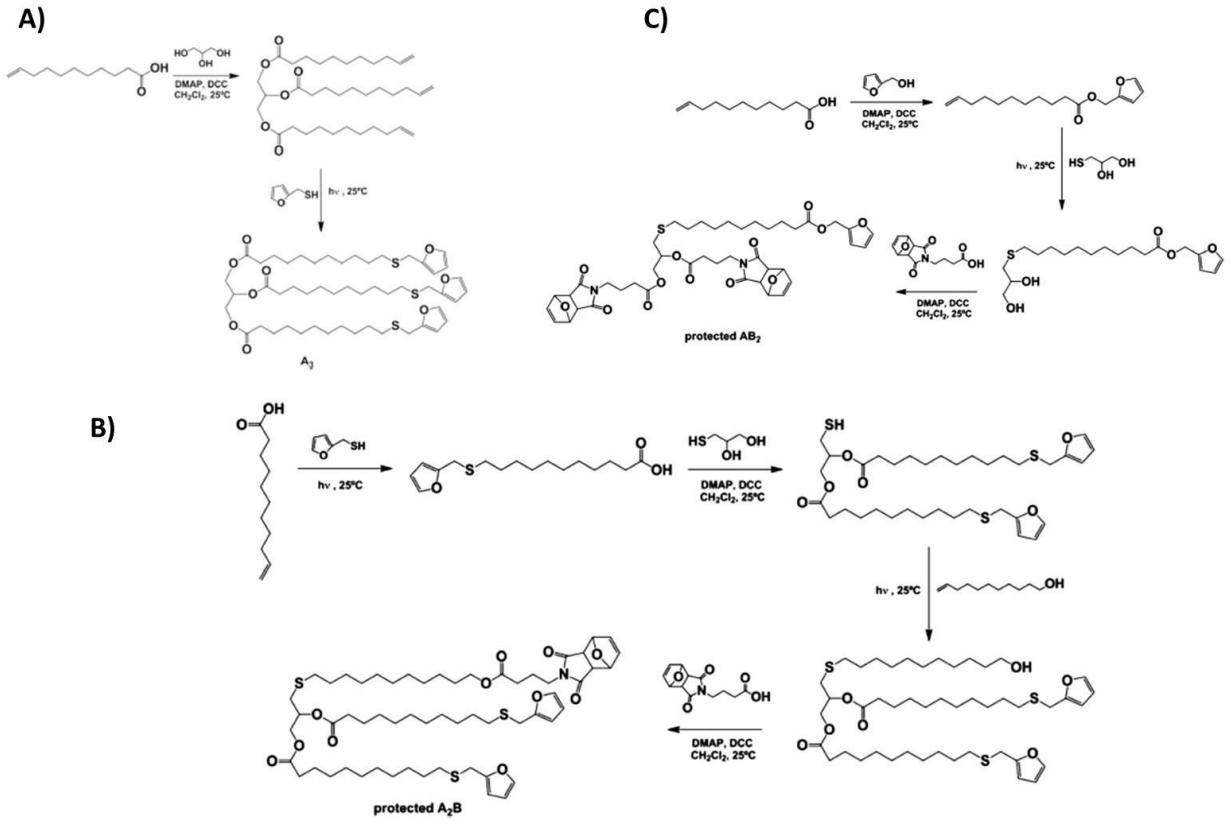

Figure 1.5 – (a) Synthesis of trifuran monomer based on 10-undecenoic acid, (b) synthesis of a difuran monomer bearing a protected maleimide moiety and (c) synthesis of a monofuran monomer bearing two protected maleimide moieties. Reproduced with permission of Wiley (Vilela, Silvestre, and Gandini 2013).

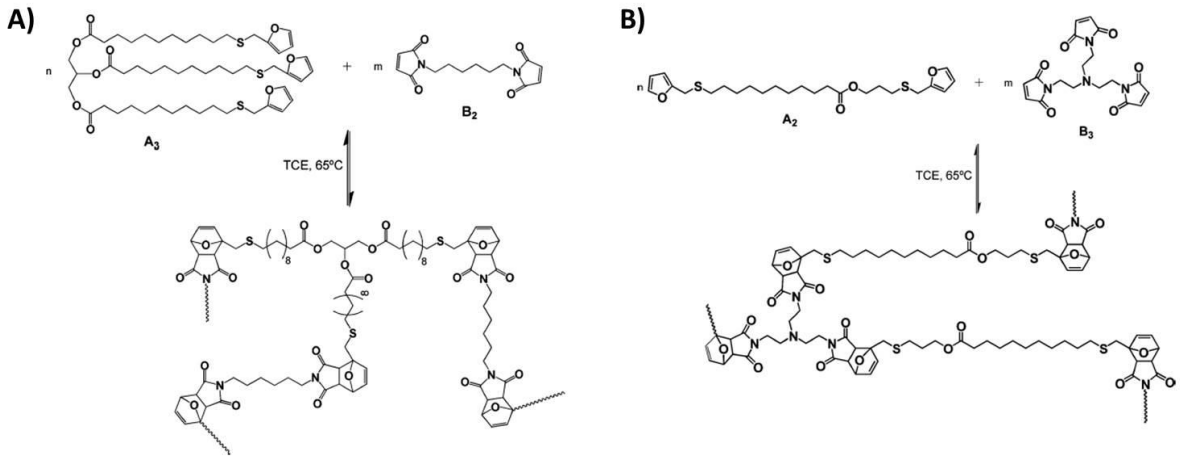

Figure 1.6 – (a) Non-linear thermally reversible DA polycondensation using a trifuran and a bismaleimide monomer, and (b) non-linear thermally reversible DA polycondensation of a difuran and trimaleimide monomer, reproduced with permission of Wiley (Vilela, Silvestre, and Gandini 2013).

In an effort to shift to greener synthetic routes for the preparation of plant-oil derived furan monomers, the same authors explored a simpler catalyst and solvent-free route. Commercial epoxidized linseed oil was submitted to a reaction with furfuryl amine, resulting in the transamination of the three ester groups and the epoxy ring opening induced by the primary amine under a solvent-free and catalyst-free reaction (Figure 1.7) (Gandini, Lacerda, and Carvalho 2013). Moreover, this reaction allowed the complete recovery of both the product and the excess reagent, fulfilling the principles of green chemistry. The resulting products incorporated available furan groups for DA polymerizations with bismaleimides. The DA polycondensation resulted in a mixture of linear and branched polymers with a MW between 35 and 40 kDa and T_g around 80-100 °C. However, in this case, the DA reaction was not solvent-free and was conducted in TCE. The same strategy was applied to commercial epoxidized soybean oil and similar results were obtained.

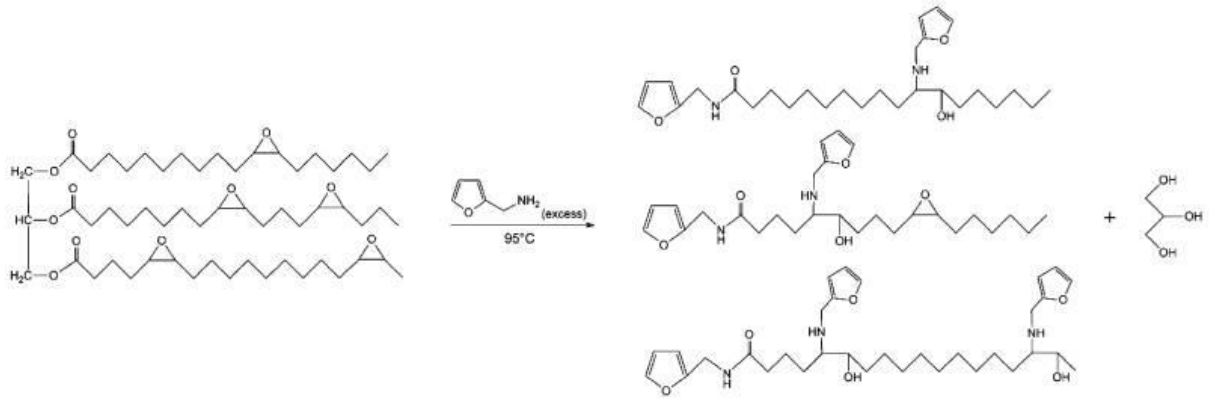

Figure 1.7 – Transamidation and epoxy coupling of epoxidized linseed oil induced by furfuryl amine, reference adapted by (Gandini, Lacerda, and Carvalho 2013).

On their continued efforts to develop greener processes, the reaction of commercial tung oil (TO) with maleimides under solvent-free conditions was also explored. (Lacerda, Carvalho, and Gandini 2014). This oil contains three conjugated unsaturations that can behave as dienes for the DA reaction. The authors explored the reaction of this glyceride with methylmaleimide at 65 °C resulting in a stable adduct not able to undergo the retro DA reaction. When combined with different bismaleimides of varying flexibility, the DA crosslinking of TO resulted in gels with T_g values between -10 and 75 °C (Figure 1.8). Again, the stability of these adducts was high and did not offer the reversibility of the previously reported systems.

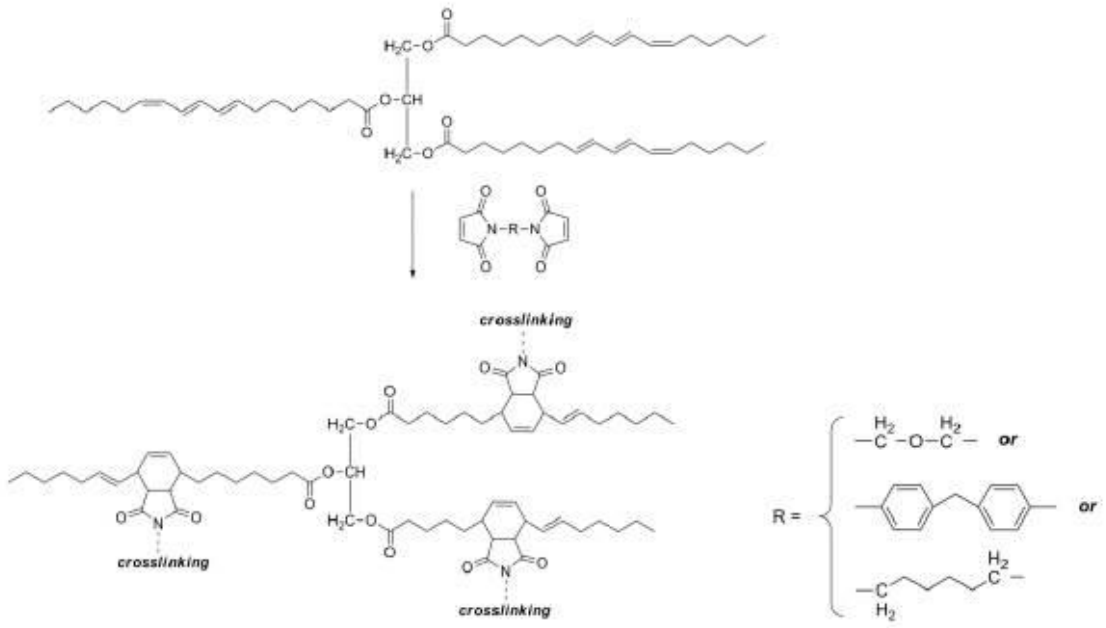

Figure 1.8 – The DA cross-linking reaction of tung oil with bismaleimides, adapted from reference (Gandini et al. 2018)

In a second approach, the same transamination reaction reported for epoxidized plant oils was performed and the resulting furan/triene difunctional DA dienes were cross-linked with the same bismaleimides (Figure 1.9). In this case, the resulting polymers had one thermally labile furan/maleimide adduct in each monomer unit and a thermally stable one formed by a maleimide group with the α-eleostearic triene moiety, thus, the depolymerisation was successfully achieved for the furan/maleimide adducts around 110 °C. The reported T_gs were higher than in the previous system due to the amide-based hydrogen bonds, responsible of the stiffening of the polymer.

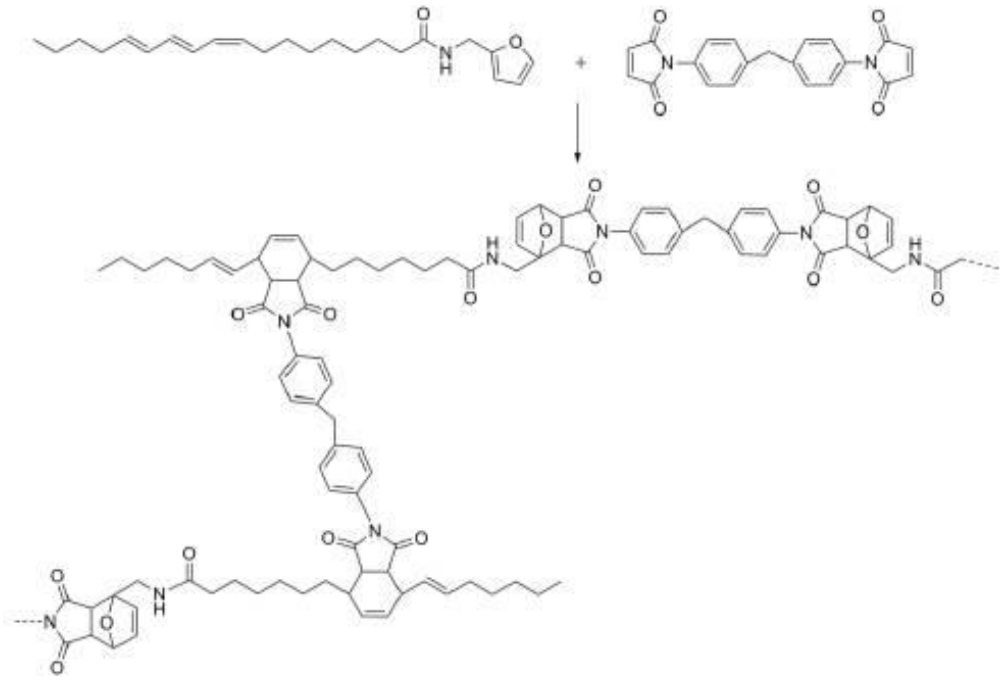

Figure 1.9 – Linear DA polycondensation of α-eleostearic furfurylamide with an aromatic bismaleimide, adapted from reference (Lacerda, Carvalho, and Gandini 2014)

Recently, some authors also prepared self-healing PUs based on soy oil polyol modified with furfuryl alcohol via the DA reaction with 1,5-bis(maleimido)-2-methylpenthane (Zheng et al. 2018). The recycling ability of PU was studied using a solubility test. The material dissolved in DMSO after heating at 180 °C from 6 to 9 min due to the thermoreversibility of the DA reaction. The authors reported that when the PU film was cut into pieces, heated at 130 °C for 10 min, hot-press under 10 MPa for 10 min and post-cured, a new film was successfully achieved (Figure 1.10). The shape-memory properties of the obtained films were also evaluated. The film was heated at 40 °C for 10 min, rolled up and immersed into ice water for 10 min to fix the shape. After introducing it into warm water, the original shape was recovered. The films showed a shape recovery around 90%, higher than that of traditional soy oil-based PU. This increase in the shape recovery was attributed to a more regular cross-linked network of the DA cross-linked PU due to one-to-one correspondence between furan and maleimide. Finally, the self-healing ability of the PU was investigated by cut, scratch and tensile testing. Preliminary healing was achieved at 70 °C whereas deep self-healing occurs at temperatures above 120 °C.

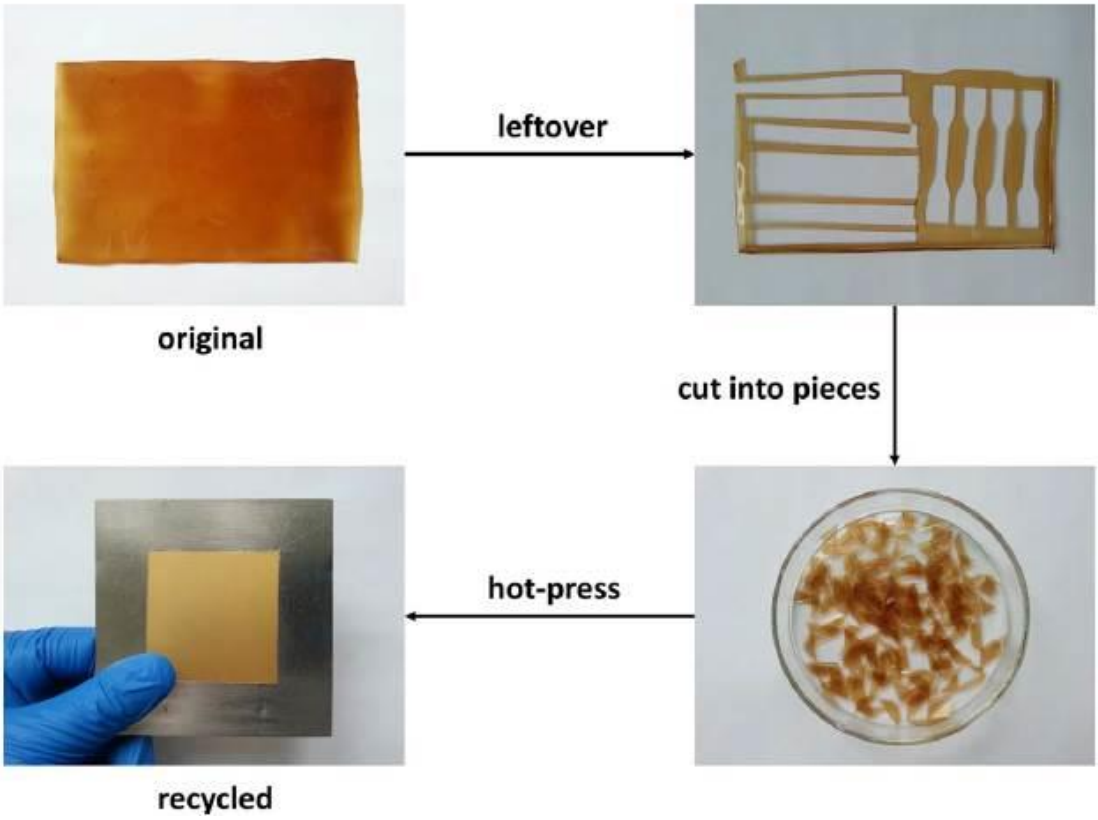

Figure 1.10 – Preparation process of recycled soy oil-based PU, reproduced with permission of Wiley (Zheng et al. 2018)

The DA reaction has also been used for the cross-linking of acrylated soybean oil (AESO), an easily polymerizable monomer used for different applications such as coatings or flame retardant products (Frias et al. 2015). Frias and co-workers reported the use of the DA reaction between furfuryl functionalized AESO with a monofunctional N-phenylmaleimide and a bismaleimide, 1,1-(methylenedi-4,1-phenylene) (Frias et al. 2015). The prepared materials showed one endothermic transition at temperatures between 103 and 134 °C, indicating that both the endo and exo adducts can be reverted at similar temperatures. The formation of the adduct resulted in more rigid materials with an increased T_g.

Furan-functionalized fatty esters have been also prepared by Iqbal and co-workers for their use as oligomers for network formation (Iqbal et al. 2018). Methyl oleate, methyl linoleate and jatropha oil were epoxidized using in situ generated performic acid. Then, the epoxidized compounds were reacted with furfurylamine and cross-linked with bismaleimides through DA reaction. Furfuryl-amine functionalized jatropha oil was reacted with 1-1'-(methylenedi-4,1-

phenylene) bismaleimide and the thermoreversibility was analyzed by DSC. An increase in the heat flow was observed around 125 °C confirming the r-DA reaction. The authors observed that the thermo-recovering degree for each cycle decreased when compared to previous cycles. This behavior was attributed to short time for bond reconstitution and formation of the most stable adduct isomer. Moreover, the high degree of cross-linking results in brittle materials. Finally, the authors explored the use of furan-functionalized jatropha oil for partial substitution of (1,4)-polyketone reacted with furfurylamine to improve the polymer properties and add a renewable character to the material. The addition of 10% of furan-functionalized linoleate resulted in an increase of the thermal stability and the temperature to achieve the reversible cross-linking of the network.

5.1.2. Other diene/dienophile coupling

Some others examples of the DA reaction, involving different diene/dienophile couples,for the modification or cross-linking of vegetable oils have been also reported in the literature. Huang and co-workers reported the use of the DA reaction to cross-link a biobased epoxy monomer with conjugated double bonds, glycidyl ester of eleostearic acid, synthesized from TO (Huang et al. 2014). The DA reaction resulted to be more active than the ring-opening of epoxy and anhydride. The monomer was cured by using both maleic anhydride, nadic methyl anhydride and 1,1'-(methylenedi-4,1-phenylene)-bismaleimide (Figure 1.11). The structures and cross-linking densities of the prepared thermosetting polymers can be tuned by varying the anhydrides and dienophiles structure.

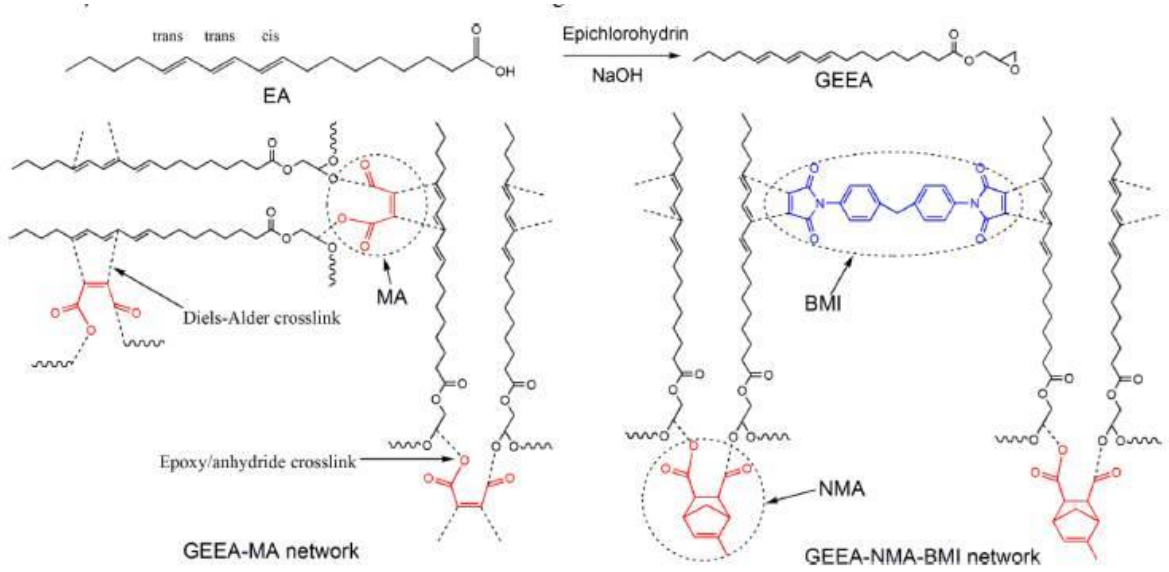

Figure 1.11 – Preparation of thermosetting networks using glycidyl ester of eleostearic acid and DA reaction, adapted from reference (Huang et al. 2014). Reprinted with permission from (Huang et al. 2014).

Liu and co-workers reported the green microwave-assisted maleation of TO and investigated the mechanisms involved in the reaction, namely DA reaction and free radical copolymerization (Liu et al. 2015). This work points out another example of solvent and catalyst-free reaction, with low reaction time and high yields. The obtained product was reacted with epoxidized glycidyl ester, epoxidized soybean oil and epoxidized octyl soyate to produce fully oil-based epoxy resins. The authors reported that when using low maleic anhydride: TO contents ratios, the dominant mechanism for the maleation was the DA reaction.

As another example of green chemistry, sunflower oil can also be used for the DA reaction with terpenes. Mangeon and co-workers reported the DA reaction in the presence of oxygen between β-myrcene or β-farnesene and sunflower oil to design novel biobased networks (Mangeon et al. 2017). The DA reaction is considered as the main reaction mechanism for the preparation of the materials. However, secondary reactions such as oxidation are also present and proved to be necessary for the cohesion of the film prepared. Sunflower oil not only takes part in the DA reaction but also increases the flexibility of the system. The resulting materials showed different T_g, varying from 20 to 92 °C.

5.2. Triazolinediones chemistry

As mentioned earlier, TADs have become interesting compounds in organic synthesis and, more recently, in polymer chemistry. A recent review from Du Prez and co-workers reported the versatility of TADs as an alternative click chemistry option in polymer chemistry (De Bruycker et al. 2016).

Biswas and co-workers were the first to report the reaction of TADs with soybean oil (Biswas et al. 2014). The authors reported the modification of a triglyceride oil through the reaction with 4-phenyl-1,2-3-triazoline-3,5-dione. The increase in viscosity confirmed the formation of ene and DA reaction products between the TAD and the oil, giving an example of self-curing vegetable oils that could be used as additives in lubricants or as thickeners in a variety of formulations.

As mentioned, Du Prez and co-workers explored the use of TADs for the click cross-linking of vegetable oils at room temperature and without catalysts (Türünç et al. 2015). First, the reaction was studied with natural FAs and monofunctional TAD moieties. Oleyl alcohol, elaidyl alcohol, methyl ricinoleate, 10-undecenoic acid, methyl linoleate and methyl linolenate were used as model FAs and reacted with phenyl-TAD. The same studies were also conducted with polyunsaturated FAs such as methyl linoleate and methyl linolenate. This strategy was then applied for the cross-linking of vegetable oils such as olive, sunflower, colza, corn, groundnut, pumpkinseed, soybean and castor oils using a bifunctional TAD. Gelation took place within minutes but the red color of the TAD compounds was observed for longer reaction times. The differences in the gelation time observed for the different oils were attributed to the reaction kinetics of the different FAs and the ene: TAD ratio. The T_gs of the resulting materials ranged from 60 to 124 °C revealing the rigidity imparted by the aromatic TAD cross-linker.

The same research group went on to report the first time use of TAD-based chemistry for the preparation of nanoparticles using vegetable oils as the starting compound. (Figure 1.12) (Chattopadhyay and Du Prez 2016). The preparation of nanoparticles was performed with a simple water-based one-step procedure without surfactants being an example of greener chemistry for nanoparticle synthesis. The nanoparticle size was controlled by varying the solvent ratio and the plant oil/TAD ratio. The strategy was applied to different oils such as castor, olive,

pumpkin, sunflower and hazelnut oils. The size of the resulting nanoparticles varied from 140 to 260 nm depending on the reaction conditions. When reducing the amount of TAD-based cross-linker the size of the nanoparticle increased indicating that lower degrees of cross-linking resulted in higher swelling ratios.

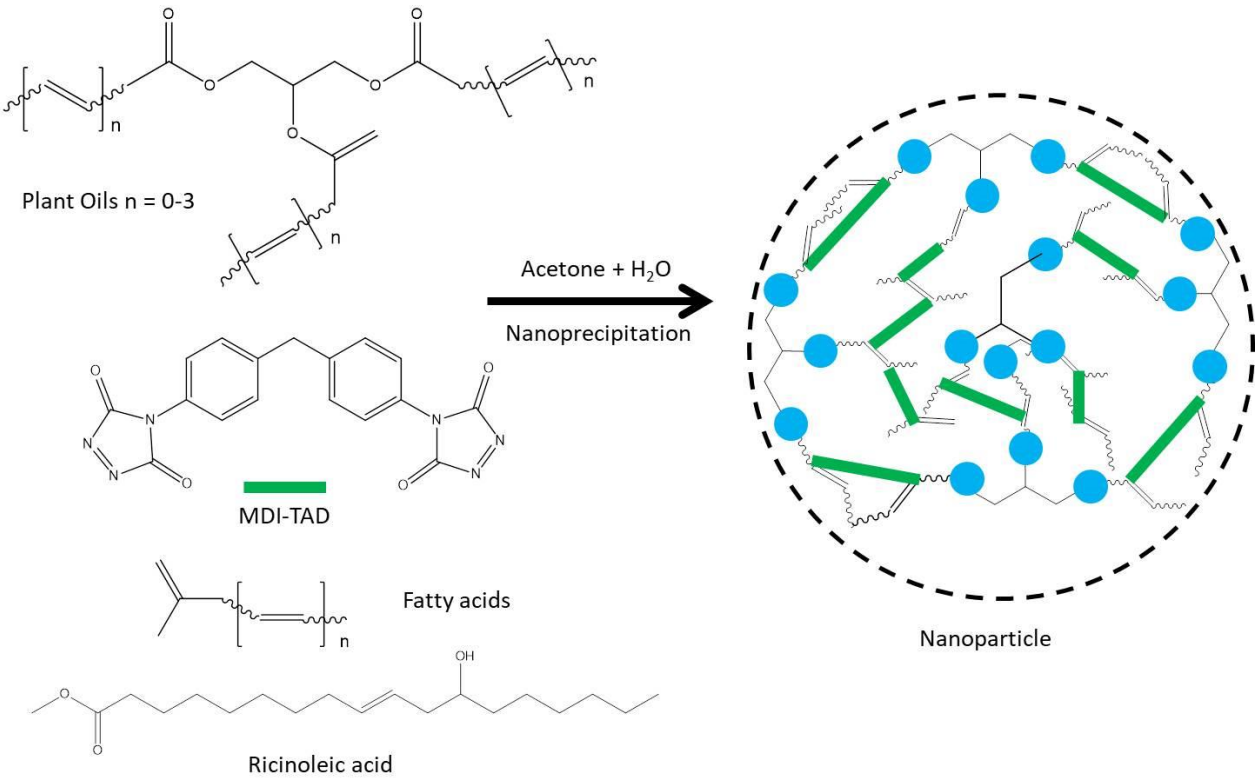

Figure 1.12 – Reaction scheme and illustration for the cross-linking of vegetable oil-based nanoparticles using TAD-based cross-linkers, adapted from reference (Chattopadhyay and Du Prez 2016).

Multishape-memory materials have been also developed combining high oleic soybean oil and TAD click chemistry (Wang et al. 2016). In this study, the double bonds of plant oil-derived polymers grafted cellulose nanocrystals were cross-linked using TAD chemistry. The matrix is prepared by surface-initiated atom transfer radical polymerization of soybean amide methacrylate. Consequently, two types of cross-links were achieved. On one hand, permanent TAD cross-links were produced. On the other hand, dynamic physically cross-links were also achieved by the hydrogen bonds from the plant oil and the TAD groups. Therefore, TAD cross-linking produces a permanent shape while the physical network ensures multiresponsive and multishape-memory properties. Heating of the samples results in the deformation of the material

due to decomplexation of hydrogen bonds. Upon cooling, the temporary shape is blocked. The hydrogen bonds can be eliminated by further heating and the material recovers its permanent shape.

5.3. Thiol – ene reaction

The first systematic study of the use of TEC on unsaturated fats and oils was brought forth by Koenig and co-workers in the 1950s (Koenig and Swern 1957). Since then, the use of TEC for synthesis of monomer, polymers and post-polymerization modifications has grown considerably (Lligadas et al. 2013; Türünç and Meier 2013; Gandini and Lacerda 2018). This section describes the latest works based on TEC in three sub-sections: (i) monomer synthesis, (ii) polymer synthesis and (iii) post-polymerization modifications.

5.3.1. Monomer synthesis

The use of TEC for monomer synthesis has been used for a wide range of polymers. The use of synthesized AA and AB type monomers for polycondensation or polyaddition to obtain polyesters, PA and non-isocyanate polyurethanes (NIPUs) has been of recent interest. Moreover, the modifications of triglycerides and their derivatives by TEC to yield highly functional molecules has also been studied for applications such as polyols for PU synthesis, epoxy resin curing agents, monomers for coating applications and plasticizers for PVC. This section presents the AA and AB type monomers for polyester, PA and NIPUs, and then, the polyfunctional architectures used in PUs, epoxy resins, coatings and plasticizers.

The use of synthesizing AB type monomers for the synthesis of polyesters has been recently explored by Cadiz and co-workers. In a recent study, the authors used the enone derivative of methyl oleate (EMO) (methyl-9-oxo-10-octadecenoate and methyl-10-oxo-8-octadecenoate) (Montero de Espinosa et al. 2008)) to obtain a hydroxyester containing a ketone via TEC (Moreno et al. 2014). TEC was used to functionalize the EMO with primary hydroxyl groups using mercaptoethanol (ME) and octanethiol. The highest functionalization conditions for both reagents was achieved by the use of a basic/nucleophilic catalyst, at room temperature with stoichiometric equivalents. This respects several ideals of green chemistry, most notably such as atom economy and energy efficiency. As depicted in Figure 1.13-a, hydroxyester functionalized

by ME was then used for polyesterification synthesis via enzymatic polymerization (with Novozyme 435 -lipase CalB- as a biocatalyst) to exploit the use of safer catalyst rather than toxic organometallic catalysts. The ketone moiety found on the polymer backbone could be further modified via oxyamines (at room temperature) to yield oximes moieties as a functionalization strategy for ligands to be covalently immobilized. In a subsequent study, the authors synthesized AA and AB monomers for polycondensation using heptanal from the pyrolysis of ricinoleic acid (Scheme 1.1) (Ruiz et al. 2019). Heptanal was modified by one pot sequential modifications via Horner-Wadsworth-Emmons and thiol-Michael reactions to yield a branched diester (AA monomer) and a branched hydroxyester (AB monomer) (Figure 1.13-b). Although these monomers require purification by column chromatography, they can be used for polycondensation via enzymatic-catalyzed means to yield MW of 15000 g mol^{-1} with the use of polyethylene glycol as co-monomer. These monomers underwent polycondensation via enzymatic-catalyzed means to yield MW of 15000 g mol^{-1} with the use of polyethylene glycol as co-monomer. The copolymers containing pendant moieties self-assembled into micelles in aqueous solution, exhibiting potential behavior for drug delivery applications. Yu and co-workers also contributed to the development of AB monomers via TEC for the synthesis of polyesters. As depicted in Figure 1.13-c, authors reported the use of UDC to synthesize methyl 3-((11-hydroxyundecyl-thio-propanoate) (MHUTP), a hydroxyester (Wu et al. 2019). MHUTP was obtained via TEC by previously reported method (Pang et al. 2014), where UDC was reacted with 3-mercaptopropionate, 2,2-Dimethoxy-2-phenylacetophenone (DMPA) (photoinitiator) under UV in just minutes. MHUTP was used for polyesterification by lipase catalyzed means and the influence of reaction time and temperature on the MW was studied. Methyl ricinoleate was also investigated as a co-monomer in polyesterification reactions. The monomers reported in this section synthesized by TEC were all further used for polycondensation via enzymatic catalyzed further promoted and developing the use of CalB as alternative to organometallic catalyst for the synthesis of polyesters.

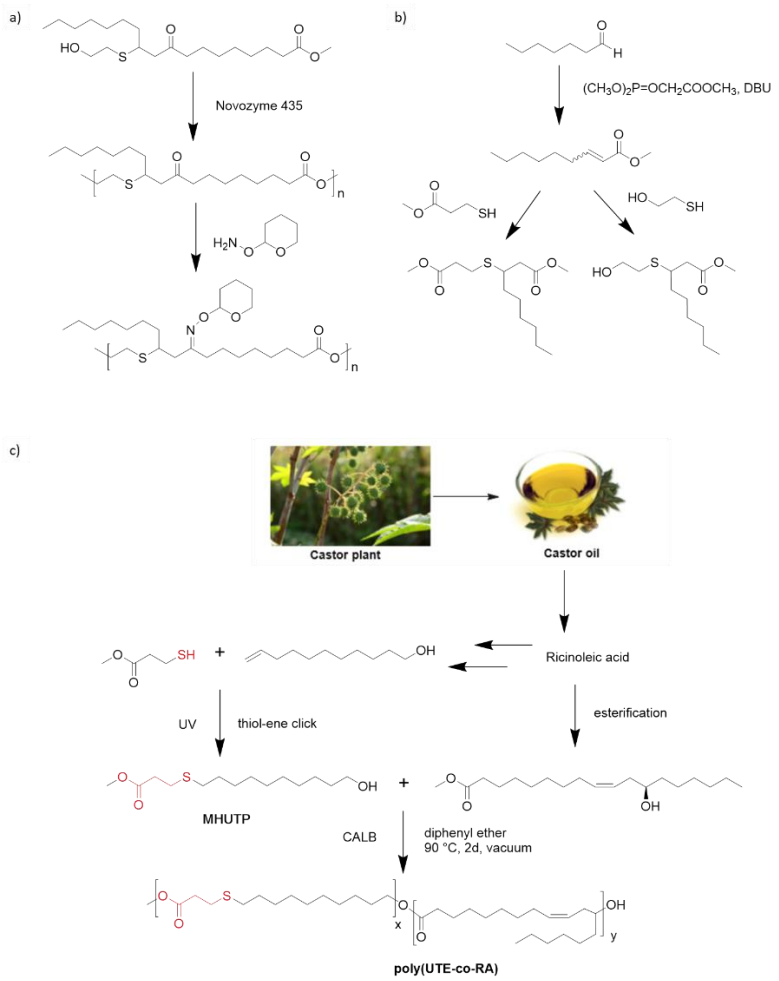

Figure 1.13 – (a) Synthesis of polyketoesters using Novozyme 435 (Lipase CalB) followed by modification by oxyamine, adapted from reference (Moreno et al. 2014), (b) functionalization of heptanal for the synthesis of poly(β-thioether ester)s, adapted from reference (Ruiz et al. 2019), and (c) synthesis of poly(β-thioether ester) and poly(β-thioether ester-co-ricinoleic acid by enzyme catalyzed transesterication, adapted from reference (Wu et al. 2019).

Developing AA and AB monomers using TEC has also been used for the synthesis of PA. Meier and co-workers develop a dimer FA to be used in PA and PUs (Unverferth and Meier 2016). The dimer FA was synthesized using methyl oleate, ethane-1,2-dithiol in a 1.9 : 1 ratio, DMPA and UV radiation at room temperature. Alternatively to industrial established procedure of obtaining dimmer fatty acids, the reported procedure does not required further purification, respects atom economy and reduced use of solvents. The authors observed the dimerization of OA by TEC was much slower than methyl oleate. The developed dimer FA was used in collaboration with hexamethylenediamine and dimethyl adipate to synthesize PA with varying ratios of dimethyl adipate and dimer FA in copolymerization. PA synthesized using the novel dimer FA exhibited

superior hydrophobic properties such as lower water intake compared to similar commercial alternatives. Similarly, Seppala and co-workers synthesized di-acids containing sulphur units within the backbone for the synthesis of PA (Nguyen, Spoljaric, and Seppälä 2018). The di-acids were synthesized using UDA and different length aliphatic dithiols via TEC using DMPA under UV radiation with the slight use of solvent. These diacids were used in the synthesis of PA with MW approaching 55, 0000 g mol^{-1} with higher dispersities, as well as superior material properties such as higher impact, chemical resistance, increased ductility and lower water adsorptions. Furthermore, used a melt condensation for polymerization without the use of dangerous catalysis. Mostly recently, some authors synthesized PA via enzyme catalyzed synthesis using AB-type functional monomer derived from methyl oleate (Finnveden et al. 2019). It was found the using lipase CalB was as effective as the previously used toxic catalyst using less mole equivalents.

As of late, two different strategies were investigated for the synthesis of monomers using TEC to obtain NIPUs. Cadiz and co-workers obtained NIPUs and non-isocyanate polyurea by synthesizing AB monomers capable of transurethanization (Calle et al. 2016). As depicted in Figure 1.14-a, from castor oil, more specifically UDA derivatives were used to synthesize two monomers with a carbamate and either a hydroxyl or amine final group. The authors reported the synthesis of a cysteamine methyl carbamate (MMC) that was reacted with two UDA derivatives, UDC and 10-undecenylamine via TEC. The reaction was performed in bulk, using DMPA under UV irradiation. NIPUs were synthesized by polycondensation using a conventional organometallic catalyst. Although this work circumvents the use of isocyanates for PU synthesis, the use dangerous reagents are indeed used for the synthesis of MMC and the polymerization process. In contrast, Cramail and co-workers synthesized various biscyclic carbonates to be reacted with diamines to obtain NIPUs by polyaddition. In an initial study, two different (bis) 6-membered cyclic carbonates (bis6CC) were synthesized using MUDO by a four step synthesis (Maisonneuve et al. 2014). As depicted in Figure 1.14-b, the last step for the synthesis of the bis6CC, UndS b6CC, was accomplished via TEC using Und-6CC, 1,4-butanethiol under UV radiation. Although the synthesis of UndS-b6CC used TEC in its final synthesis step, previous reaction steps for both bis6CCs obtained required purification by chromatography, contradicting some aspects of green chemistry. The two bis6CC were reacted with dodecane-1,12-diamine. Unexpectedly, networks

were obtained by the side reaction of carbonate opening via hydroxyl functions. In a continued work, the authors reported the design of (bis) 5-membered cyclic carbonates (bis5CC) from thioglycerol, FAs and sugar derivatives using TEC (Lamarzelle et al. 2017). A panel of different bis5CC were obtained from derivatives of castor oil (UDC, 1-bromo-10-undecene and UDA) and sunflower oil (oleyl alcohol) by following the same general procedure (Figure 1.14-c); (i) terminal di-ene structures were obtained using the appropriate chemistry, (ii) TEC coupling of terminal ene with thioglycerol under UV radiation with the use of DMPA, and lastly, (iii) carbonation of synthesized FA tetraols using dimethyl carbonate. Although some of the synthesis did required the use of some dangerous solvents such as DCM, in comparison to their previous work on the topic, the bis5CCs were obtained by rather direct pathways without laborious purifications irrespective of green chemistry principles. The bis5CCs were successfully polymerized with the use of diamines to yield NIPU with MW up to 14900 g mol^{-1}. Depending on the bis5CC used, PHU properties could be tuned. Moreover, two PHUs underwent post-functionalization by sulfonation of the thioethers found on the polymer backbone and showed an increase in T_g and melting temperature. In complement to this section, our group has recently published a review on synthesis of biobased cyclic carbonates for the synthesis of PHUs (Carré et al. 2019).

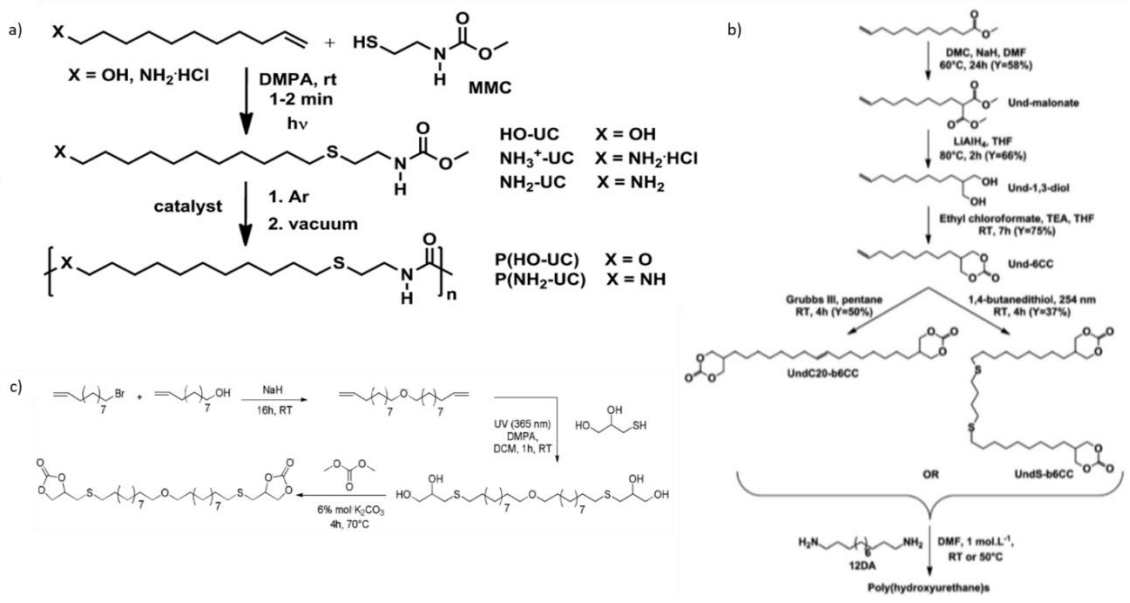

Figure 1.14 – (a) Thiol-ene addition of MMC to UDC and 10-undecen-1-amine chlorhydrate followed by the PU synthesis by polycondensation, adapted from reference (Calle et al. 2016), (b) synthetic route to bis6CC and PHUs syntheses, adapted from reference (Maisonneuve et al. 2014), and (c) synthetic route to bis5CC from FAs, adapted from reference (Lamarzelle et al. 2017).

As PUs are a major polymer family, researchers have invested in the development of building blocks from triglycerides and FAs via TEC in order to introduce reactive groups for synthesis of PUs by classic polyaddition of hydroxyl and isocyanates groups. Thus required the synthesis of or use of reagents containing isocyanate moieties a dangerous allergen for humans. Given its unique structure, castor oil and derivatives (most notably UDA) have been reported for the synthesis of monomers via TEC but as well as di-isocyanates. Shen and co-workers have been particularly active developing derivatives for polyurethane synthesis using TEC for the development of biobased waterborne PUs for coating applications (Fu, Zheng, et al. 2014). As shown in Figure 1.5-a, TEC was used to introduce carboxylic acid groups on to UDA and castor oil triglycerides. The modified UDA was then transformed from a di-carboxylic acid structure to a diisocyanate by Curtis rearrangement and the modified castor oil was used as hydrophilic chain-extender. The same authors went on to develop silanized castor oil via TEC to be used as a functionalized polyol (Fu, Yang, et al. 2014) to be reacted with diisocyanates. As depicted in Figure 1.5-b, the functionalized silane PU then underwent silane moiety hydrolysis through a sol-gel process by utilizing the methoxysilane groups. The introduction of silane groups in the PU exhibited water-repellent surfaces and the cross-linking nature of the PU with Si-O-Si units increased thermal stability and mechanical properties. Other than the use of isocyanates, the general synthesis respected several ideals of green chemistry most predominately atom economy. In their most recent work on the topic, the research group modified cardanol to achieve polyols for PU synthesis (Fu et al. 2015). Cardanol is a byproduct from the cashew processing industry and is extracted from cashew net shell liquid. Cardanol is a phenolic compound with 15-carbon side chain in the Meta position with varying degrees of unsaturation. The authors used ME to functionalize the cardanol fatty side chain with hydroxyl groups via TEC (Figure 1.5-c). Similar to their previously mentioned work (Fu et al. 2015), they used a radical initiator, UV light irradiation to react the unsaturations with the reagents , with however with use of the hazardous solvent such as DCM. In this particular work, degrees of functionalization were varied according to reaction time. The polyols were then reacted with HDI to yield PUs with good thermal and hydrophobic properties. Cardonal has also been solicited more recently by other research groups for the synthesis of polyols for PU synthesis. Upshaw and co-workers similarly functionalized the C=C bonds of the fatty side chains

by TEC, but also went on the protect the phenolic group by propoxylation to improve TEC reaction conditions (Shrestha et al. 2018) and Zhou and co-workers went on to generate a panel of polyols from variety of chemical reactions (epoxide ring opening and TEC using ME) demonstrating varying PU properties with respect to their hydroxyl content (Wang and Zhou 2018). The similar method of functionalizing ME onto soybean oil via TEC were also exploited to the obtain polyols for PU synthesis (Alagi et al. 2016; Feng et al. 2017) and also without use of hazardous solvents in line with the ideals of green chemistry (Feng et al. 2017).

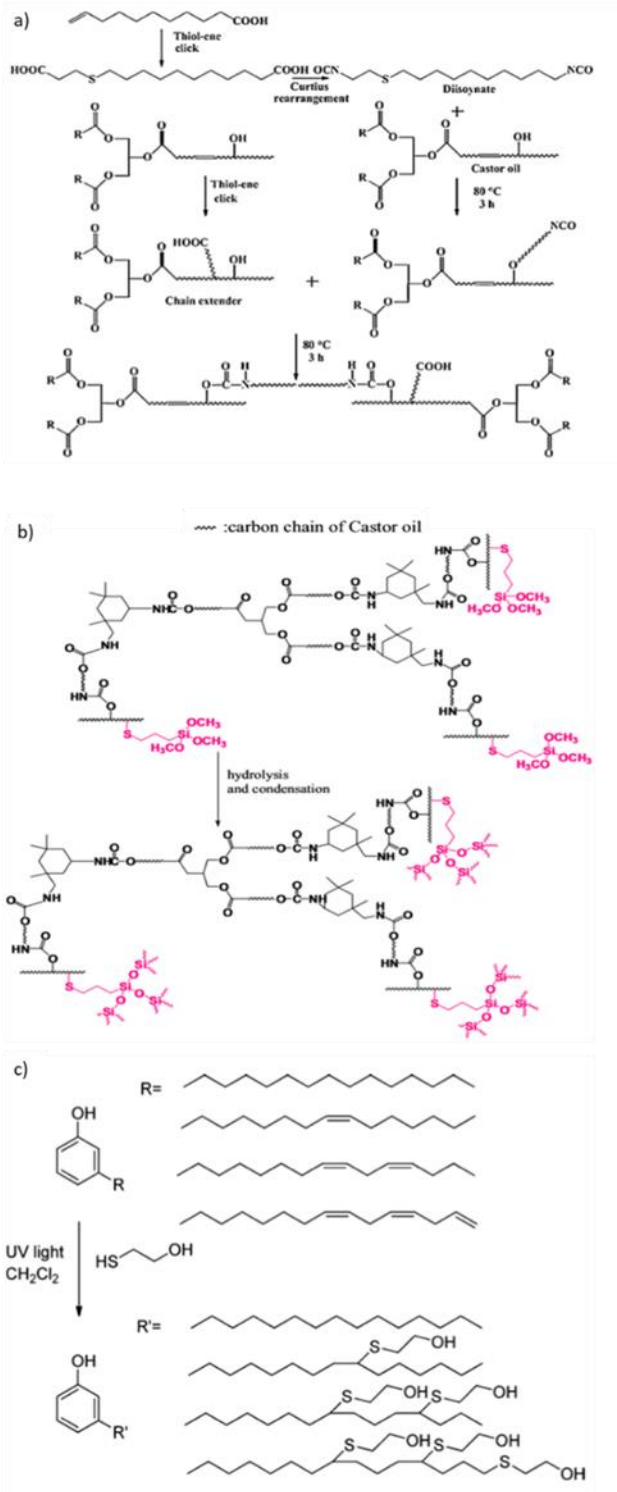

Figure 1.15 – (a) Synthesis of UDA based diisocyanate and modified castor oil with carboxylic acid groups via TEC, adapted from reference (Fu, Zheng, et al. 2014), (b) synthesis of silicon cross-linked PUs, adapted from reference (Fu, Yang, et al. 2014), and (c) synthesis of polyols of cardanol via TEC, adapted from reference (Fu et al. 2015).

TEC can be used on triglycerides and FAs for the direct functionalization of reactive moieties in high functionality. Based on TEC, different architectures with high functionality have be used as curing agents for epoxy resins in the synthesis of coating and as plasticizers. Hardeners for the curing of epoxy resins have been recently synthesized such as polyamines from FAs of rapeseed oil (Cornille et al. 2014), or grapeseed oil (Stemmelen et al. 2015) and polyacids (Espinosa et al. 2020). For coating applications, polyfunctional acrylates from soybean oil have been achieved (He et al. 2014), as well as acetoacetate-modified castor oil for the synthesis of ambient curable films when reacted with amines (Zuo et al. 2019), aldehydes or acrylates (Xu et al. 2019). Furthermore, Upshaw and co-workers successfully functionalized soybean oil with hydroxyl, amine, isocyanate, isothiocyanate, epoxy and silane terminal groups by TEC for applications such as foams, adhesives, coatings sealants and elastomers (Ionescu et al. 2015). In the field of plasticizers some interesting works have been published. For instance, some authors used alkyl thiols to be substituted on the double bonds of technical OA and rapeseed oil by TEC (Montero de Espinosa et al. 2014). The sulfur containing compounds where then oxidized to yield sulfoxide and sulfone groups to be used as odorless, stable plasticizers. Alternatively, polyfunctional terminal epoxy architectures are synthesized from TO via TEC as a substitute for dioctyl phthalate (Jia et al. 2018).

5.3.2. Polymer synthesis

The recent literature consisting of TEC based on polymerization can be subdivided in two main areas: linear polymerization using AA or AB type monomers, or polyfunctional architectures for the synthesis of thermosets. AA monomers consists of diene or dithiols, whereas AB monomers contain one diene and one sulfur reactive moiety. Given the particular structure of castor oil and its derivatives, they are abundantly utilized. UDA is classically used in the synthesis of α,ω-dienes, whereas castor oil triglycerides for the synthesis of polyfunctional molecules.

Developing AA monomers from (most notably) UDA for TEC polymerization has led to obtaining polymer backbones containing amides, ethers and esters in addition the thio(ether) bonds. Recently, Tang and co-workers developed very interesting sustainable ultra-strong elastomers by TEC of a diamide diene monomers, derived from UDA, reacted with a di-thiol (3,6-dioxa-1,8-octanedithiol) (Song et al. 2019). A first diamide diene was developed by amidation of MUDO with

1,3-diamino-2-propanol to yield N,N'(2-hydroxypropane-1,3-diyl)bis(undec-10-enamide) (UDA-1). UDA-1 can be further reacted with butyric anhydride via the pendant hydroxyl group to yield 1,3-di (undec-10-enamido)propane-2-yl butyrate (BUDA), introducing a longer pendant group that can inhibit crystallization (Figure 1.16). Polymerization took place by thio-Michael addition with varying amounts of UDA-1, BUDA, dithiol, azobisisobutyronitrile (AIBN) (radical initiator) at 70 °C for 12 h. The pendant polar hydroxyl and non-polar butyrate groups allowed for control structuring of hydrogen bonding and tuning of crystallization, whereas thioether bonds induced metal-ligand coordination. Unidirectional step-cycle deformation was applied to these materials and enhanced to tensile strengths to over 210 MPa, while maintaining elasticity, mainly due to rearrangement and alignment of crystalline microstructures. Furthermore, these materials exhibited aggregation-induced emission when observed with strong luminescence due to the formation of amide clusters with restrictive molecular motions. Other research groups obtained α,ω-dienes via similar means. Such structures can be obtained by transesterification of MUDO or 9-decenoate (obtained from the ethenolysis of methyl oleate) and diol (1,3-propanediol), or diacids such as diethyl adipate were esterified by UDC (Dannecker et al. 2019). The esters of these diene monomers were reduced via catalytic reduction to obtain ethers in the final polymer backbone when these dienes were polymerized with dithiols. On the other hand, diene structure have been obtained by the transesterification of 9-decenoic acid by ethylene glycol or UDC to then undergo photo-polymerization with various dithiols (Moser, Doll, and Peterson 2019).

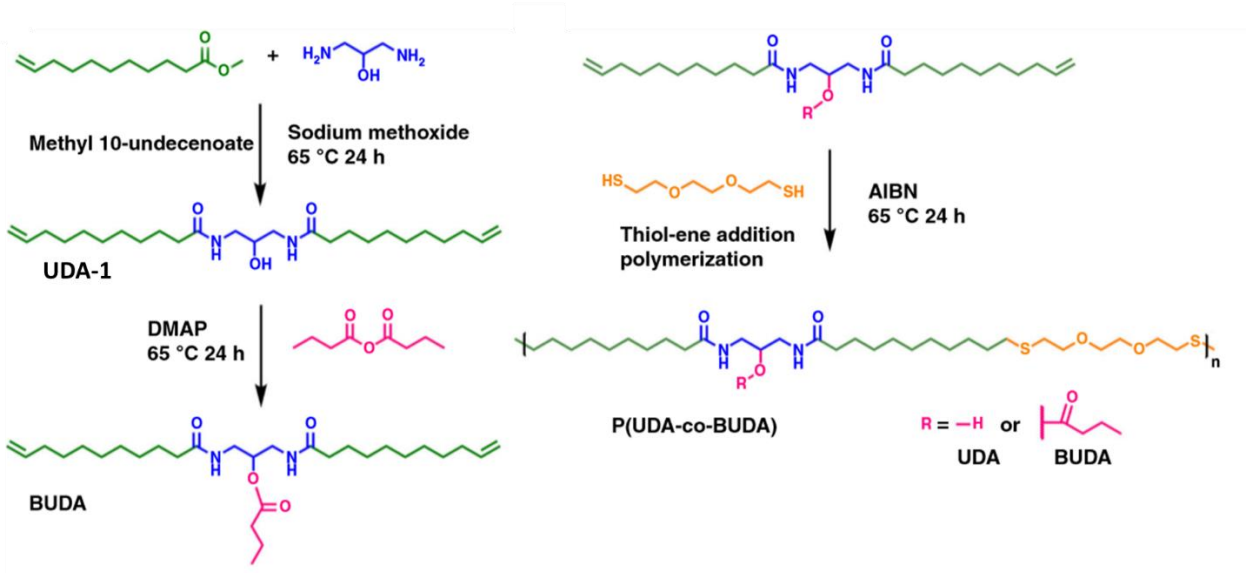

Figure 1.16 – Design of monomers UDA-1 and BUDA and functional PA via thiol-ene addition, adapted reference (Song et al. 2019).

UDA based AA monomers with diene structures coupled with dithiols for TEC polymerization have been particularly exploited for the synthesis of nanoparticles in miniemulsion. Araújo and co-workers obtained a diester diene monomer denoted DGU by the esterification of isosorbide and UDA (Machado et al. 2017) (Figure 1.17-a). DGU was copolymerized by 1,4-butanethiol by thiol-ene miniemulsion polymerization. The organic phased consisted of DGU and an organic-soluble initiator (if used), whereas the aqueous phase contained distilled water and surfactants and was added to the organic phase to form an emulsion under vigorous stirring. This was followed by the addition of stoichiometric amounts of the dithiol followed by vigorous stirring to yield the final emulsion at 60-90 °C for 4 to 8 h. This resulted in (poly(thioether-ester) nanoparticles in water. Furthermore, coumarin 6 was encapsulated in polymer particles at efficiency of up to 98%. The same authors continued their work on thiol-ene miniemulsion polymerization by synthesis a different diester diene utilizing UDA but this time using 1,3-propanediol as the diol for transesterification (Cardoso et al. 2018). Thiol-ene miniemulsion procedure proceeded as previously described. The developed nanoparticles exhibited the potential to be used for controlled release drug delivery vector for intravenous administration (Figure 1.17-b). The authors most recent work on the topic consist of the development of a diene ester monomer, 2-(10-undecenoyloxy)ethyl methacrylate (MHU), synthesized by enzymatic esterification of UDA

and 2-hydroxyethyl methacrylate (Romera et al. 2019). MHU was used in two different synthesis routes: i) direct thiol-ene polymerization with a dithiol or ii) underwent a Michael addition with a diamine to yield a symmetrical diester diene consequently used for thiol-ene polymerization when reacted with a dithiol. For the thiol-ene bulk polymerization of MHU and dithiol, the presence of methacrylate and an alkene group with different reactivity led to a combination of step- and chain-growth polymerization. These systems present high potential as drug delivery nanoparticles or for transport of antimicrobial and antioxidant compounds.

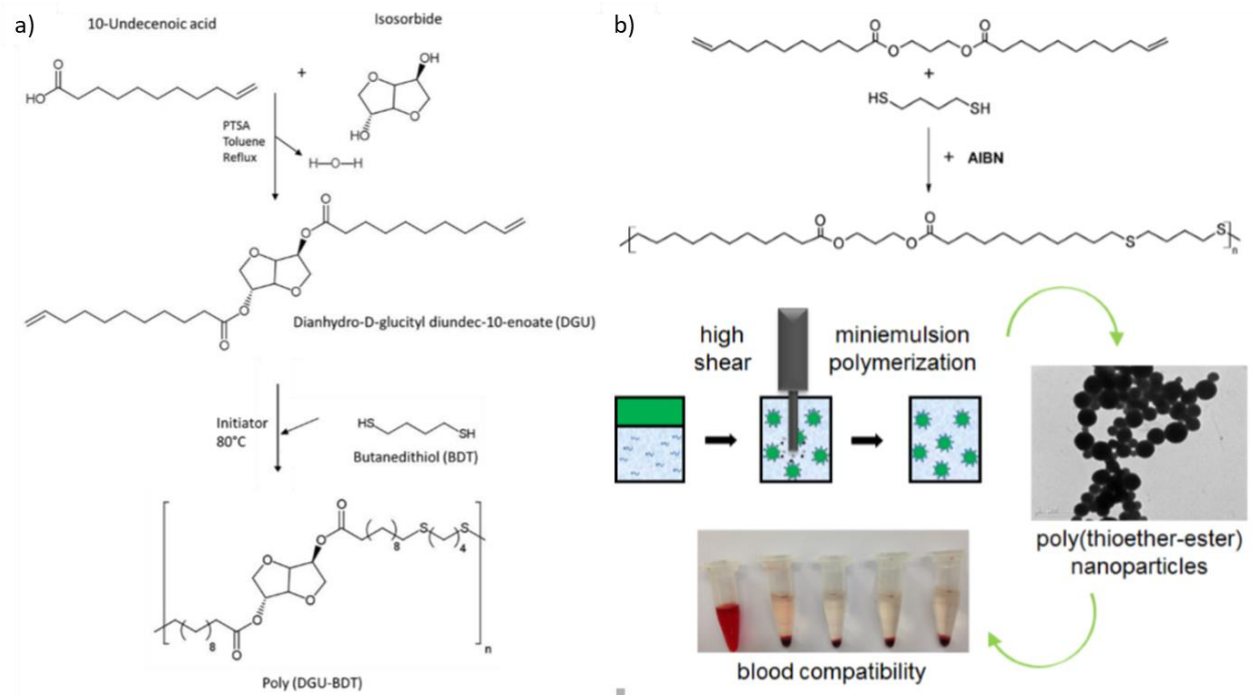

Figure 1.17 – (a) Dianhydro-D-glucityl diundec-10-enoate (DGU) synthesis followed by copolymerization with dithiol via thiol-ene polymerization, adapted from reference (Machado et al. 2017), and (b) synthesis of biocompatible polymeric nanoparticles via thiol-ene polymerization of a biobased monomer in miniemulsion exhibited blood compatibility properties, adapted from reference (Cardoso et al. 2018).

Developing AB monomers containing an alkene moiety at one end and a sulfur moiety at the other end for TEC polymerizations has also been explored. Du Prez and co-workers developed thiolactone (five-membered cyclic thio-ether) derivative of UDA to yield an AB' precursor by two step synthesis (Goethals et al. 2014). First, UDA was rendered more reactive and converted to its corresponding acid chloride and then reacted with DL-homocysteine thiolactone. It is important to note that the synthesis of this AB' monomer requires the use of dangerous chemical products ($SOCl_2$, DCM and isooctane) permitting high yields. The aminolysis of the thiolactone leads the

AB' precursor to generate pendant amide bond and an AB monomer with a free thiol moiety which reacts with terminal double bonds by radical thiol-ene addition to yield PA structures by UV radiation using DMPA at 40 °C. Different AB monomers were synthesized by the nucleophilic aminolysis of the AB' precursor using different primary amines, which led to diverse PA. The sulfide linkages of the polymer backbone could undergo oxidation to lead to sulfoxides and sulfones that consequently impact the final material properties. Thermoset networks were also obtained by the use of diamines. More classically, other authors have developed a panel of AA and AB monomers by the esterification of functional carboxylic acids such as UDA, 11-mercaptoundecanoic acid, and lipoic acid by vinyl ether alcohols such as 1,4-butanediol vinyl ether and 1,6-hexandiol vinyl ether by enzymatic catalysis (Finnveden et al. 2018).

CO is highly utilized for the synthesis of thermosets using TEC to obtain UV-curable coatings. Yang and co-workers functionalized sulfur moieties onto castor oil via the secondary hydroxyl group by esterification of 3-mercaptopropionic acid to yield a highly stable, self-initiated oligomer (CO-SH) for photo-initiator free UV coating (Wang et al. 2017) (Figure 1.18). Thus, CO-SH simultaneously possessed double bonds and thiols moieties. CO-SH exhibited temporal stability with only a slight conversion of double bonds when stored for 7 days at 80 °C or at ambient temperature for 30 days. UV curable films were synthesized by photo-polymerization using CO-SH in conditions respective of green chemistry. By using the same modified castor oil, the authors went on to develop UV-curable coatings with built in flame retardancy (Wang, Li, Wang, et al. 2019). The authors synthesized an organic flame retardant containing terminal double bonds on either side denoted DA. The flame-retardant UV-cured coatings containing phosphorus, silicon, and sulfur were prepared on wood surfaces using varying amounts of CO-SH, DA and 2,4,6-trimethyl-2,4,6-trivinylcyclotrisilazane (TTC). With a molar ratio of 5:3:3 CO-SH: DA: TTC photo-polymerized films (using 0.1 wt. % DMPA) would yield cured films on wood surfaces exhibiting appropriate adhesion and flame retardant properties (Figure 1.18). The authors went to further study this formulation to comprehend the synergistic effectiveness of DA and TTC on flame retardancy (Wang, Li, Wang, et al. 2019). Contrastingly, some authors used CO for the synthesis of hyperbranched urethane acrylate oligomer (CO20-IH). A tetrathiol monomer (PETMP), photoinitiator, a reactive diluent (tripropylene glycol diacrylate) and CO-20IH were used in varying amounts to synthesize by TEC

UV-curable films. The UV-curable films exhibited acid resistance, high hardness, and low water adsorption. Furthermore, soybean oil (Zhang et al. 2015) and rapeseed oil (Fu et al. 2019) have but utilized to obtain polyfunctional molecules to obtain UV-curable coatings via TEC. Terminal double bonds were introduce onto these oils by epoxy-ring opening and were cross-linked by thiols varying in functionality and structure via TEC.

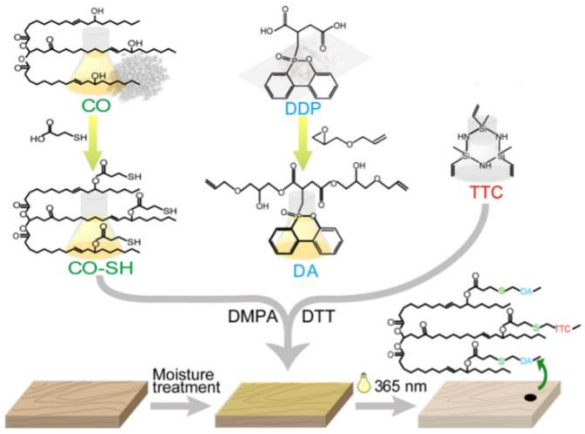

Figure 1.18 – Synthesis of CO-SH followed by the synthesis of UV-cured films via TEC using DTT and TTC on wood surfaces adapted from reference (Wang, Li, Cao, et al. 2019).

5.3.3. Chemical modifications of the polymers

The thiol-ene reaction for the post-polymerization modification of polymer architectures has become an important, conventional and easy tool for polymers functionalization. Heise and co-workers were one of the first to exploit this concept on FA derived polymers (Ates, Thornton, and Heise 2011). The authors synthesized polyesters using enzymatic ring-opening polymerization of globalide, an unsaturated macrolactone synthesized from hydroxyl FAs. The polyester chains were modified by of range of different thiols: butyl-3-mercaptopropionate, mercapto-1-hexanol, and *N*-acetylcisteamine.

Recently, several groups have continued using thiol-ene reaction for post-polymerization modifications. Some authors used the Steglich esterication to synthesize 2-(methacryloyloxy)ethyl oleate (MAEO) (a methylacrylate derivative of OA) and it was polymerized by reversible addition-fragmentation chain transfer (RAFT) to yield poly(2-methacryloyloxy)ethyl oleate (PMAEO) with the aid of a chain transfer agent (Figure 1.19-a) (Maiti, Kumar, and De 2014). The Steglich esterification requires the use of dangerous products such as DCC, DMAP and DCM

and perhaps other means of esterification could be favored to allow for this reaction to adhere to green chemistry principles. The oleate side-chains of PMAEO were further modified via the thiol-ene reaction with AIBN at 60 °C in THF, with quantitative conversions (Figure 1.19-b) for ethanethiol, butanethiol, dodecanethiol, 3-mercaptopropanoic acid, whereas ME gave approximately 90% modified product. Interestingly, the modified of PMAEO by 3-mercaptopropanoic acid would render the polymer water-soluble.

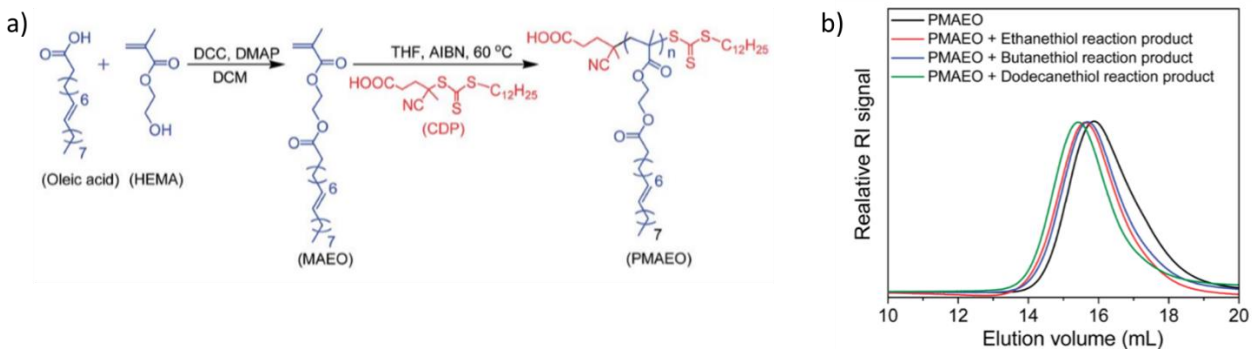

Figure 1.19 – (a) Synthesis of PMAEO by RAFT polymerization, and (b) GPC RI curves of products from thiol-ene reaction of PMAEO with different thiols. Adapted from reference (Maiti, Kumar, and De 2014).

Cramail and co-workers recently published on post-polymerization modifications utilizing TEC. In an initial work (Durand et al. 2018), a polycarbonate polymer is obtained using a synthesized carbonate monomer containing a pendant unsaturation originally derived from MUDO. As shown in Figure 1.20-a, the carbonate monomer is obtained in two steps and further polymerized to yield P(NH-Und-6CC) polycarbonate. The synthesis of the carbonate monomer and subsequent polymer does require the use some dangerous solvents but nevertheless adheres other principles of green chemistry such as energy efficiency. The pendant unsaturation belonging to a fatty chain was functionalized via TEC by a synthesized cinnamate–thiol (Figure 1.20-a) to yield a photoresponsive polycarbonate. TEC onto the polycarbonate took place using a radial initiator in DCM at 40 °C. Functionalization of varying cinnamate-thiol contents onto polycarbonates was achieved by varying the reaction time. Cross-linked polymers were achieved by utilizing the cinnamate moiety. When exposed to UV light, cinnamate groups switch from trans to cis conformation and the cis-cinnamate groups undergo [2+2] cyclo-addition reaction. Consequently, the functionalized polycarbonates exhibited versatile mechanical properties ranging from tough materials (lowest functionalized cinnamate content) to elastomeric networks (highest

functionalized cinnamate content) with the potential of containing self-healing ability (due the reversibility of the cyclobutane ring formed by two cinnamate moieties. The authors went on to further exploit their synthesized polycarbonate P(NH-Und-6CC) by cross-linking this polymer back-bone via TEC by the pendant alkene bond and different dithiols (1,6-hexanedithiol, 1,9-nonanedithiol and 1,4-benzenedimethanethiol) utilizing a radical initiator and UV light for 4 h with minimal use of hazardous solvents in comparison to their previous study. (Figure 1.20-b). The resulting polycarbonates exhibited flexible properties influence by the structure of the dithiols or by the varied thiol/olefin unit ratio used. Moreover, pendant thiol groups were obtained when an excess of dithiols was used which can be utilized for further modifications.

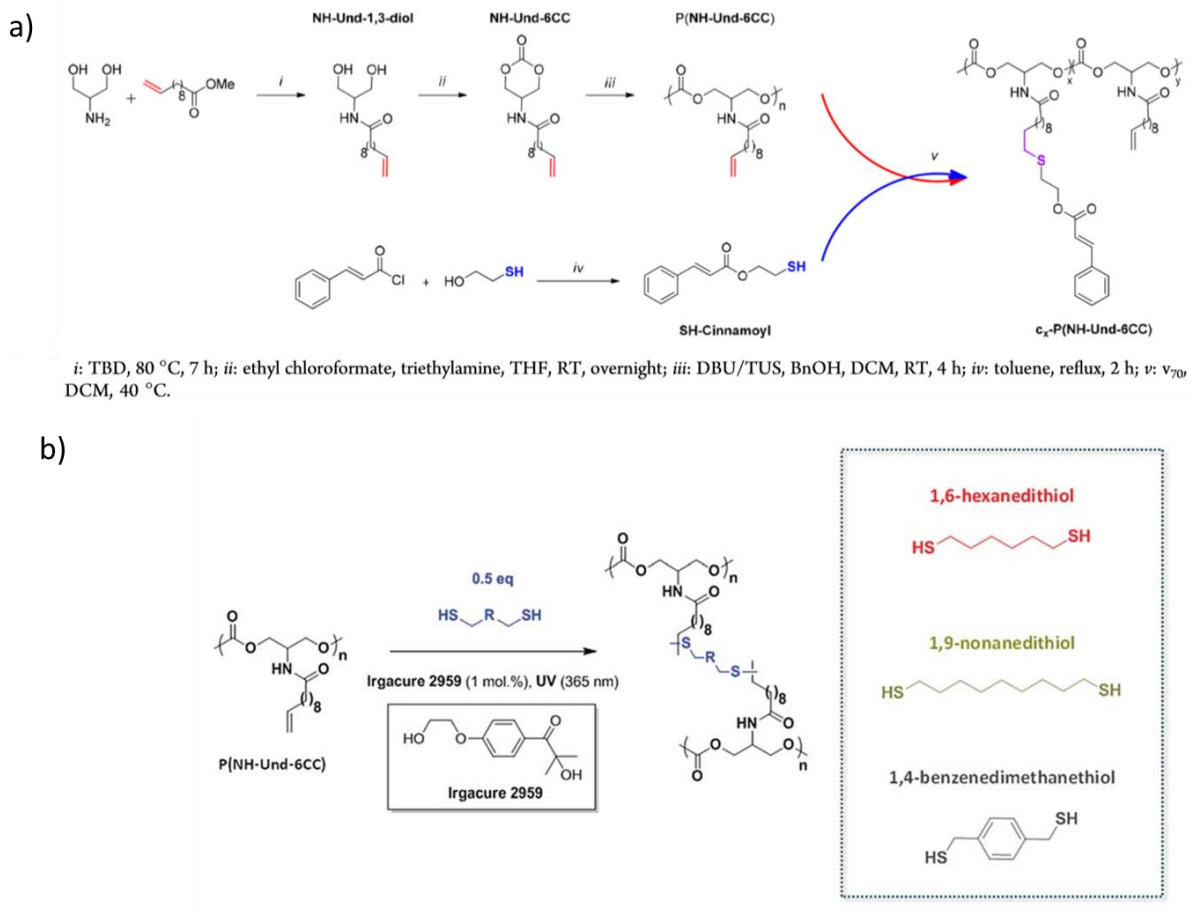

Figure 1.20 – (a) Strategy to access cinnamate-containing aliphatic polycarbonates from FA derivatives, reproduced from reference (Durand et al. 2018), and (b) strategy for the synthesis of cross-linked polyester networks by TEC, reproduced from reference (Durand et al. 2019).

In recent work, TEC is used to modify polyhydroxyalkoanoates (PHAs) using UDA, octanoic acid and/or soybean oil as substrates to yield poly(3-hydroxy undecenoate) (PHU), poly(3-hydrooxy octatanoate-co-undecenoate) (PHOU) and poly(3-hydroxy octanoate-co-soybean oil) (PHOSy) (Hazer 2015). With these different substrates, hydroxyl and carboxyl moieties are functionalized on to these biopolymers via the thiol-ene reaction to improve the mechanical properties and enhance the hydrophilic character of PHAs. Thiol-ene photo click reactions occurred with the use of a radical initiator, the biopolymer and the thiol (3-thio glycerol or merpatopropionic acid) in DCM under UV for 4 h. The functionalization of the PHAs were confirmed by different techniques.

5.4. Thiol – yne reaction

As previously mentioned, there has been limited use of thiol-ene/yne coupling (TEC/TYC) in oleochemistry as acetylenic FAs rarely occur in nature. Several recent scientific works using TEC/TYC have been published for e.g., the synthesis of PU (González-Paz, Lligadas, Ronda, Galià, and Cádiz 2012; González-Paz, Lligadas, Ronda, Galià, Ferreira, et al. 2012; Lligadas 2013) and functional comb-like polymers (Türünç and Meier 2012). The most recent work has continued utilizing TEC/TYC for the synthesis of polyurethanes but well as polyesters.

The majority of work in oleochemistry explored by the TEC/TYC includes the synthesis of polyols for PUs. OA and –α,ω-diacids has been converted into propargylic esters. As is often the case for the functionalization of lipids with alkyne moieties, the esterification of lipids reported herein does not respect several green chemistry principles (use of solvents and dangerous reagents). The propargylic esters were then modified by TEC/TYC using ME for the synthesis of two different polyols using DMPA as the radial initiator and UV radiation (Pham et al. 2014). These polyols were then utilized for the synthesis of PUs using methylene diphenyl diisocyanate (MDI). The reported polyols did not possess dangling chains, consequently the T_g is increased compared to PUs using plant-based polyols with dangling chains. More recently, the use of sunflower oil modified by TEC/TYC to synthesize hyper branched polyols for thermoset PUs, has been reported (Omrani et al. 2016). Generally, alkyne groups were functionalized on to sunflower oil derived triglycerides by the ring opening of epoxides using propargyl alcohol. Although functionalization of triglycerides took place by epoxy ring opening; this still ensued the need for dangerous catalyst

and the use of solvent, however at ambient temperature. TEC/TYC was utilized for the functionalization of primary hydroxyl groups on to the propargyl modified oil by the use of ME, UV radiation at room temperature for 12 h to yield a polyol. The polyol and the subsequent PUs synthesized by the use of isophorone diisocyanate (IPDI) and HDI, with varying NCO/OH ratios. The biobased PU exhibited reasonable thermal stability and gave transparent films useful for the coating industry.

Different research groups have pioneered the use of the TEC/TYC in oleochemistry. Their recent works in the field are applied to the synthesis of polyols for PUs and polyesters. With respect to utilizing TEC/TYC in PUs, the authors have focused their efforts in synthesizing polyols that could further endure post-polymerization modifications. In an initial study (Gonzalez-Paz et al. 2013), the authors synthesized a vinyl-sulphide-containing diol (VSD) from UDA by the pathway described in Figure 1.21-a, utilizing successive bromination, dehydrobromination, esterification, reduction and hydrothiolation. VSD was reacted with MDI to yield PUs. This PU was modified by a successive thiol-ene reaction using 7-mercapto-4-methylcoumarin (Cm-SH), DMPA (dissolved in ACN). In a follow up work (Lluch et al. 2014), the intermediate reaction products to yield VSD, methyl 10-undecynoate (MUDY) and 10-undecynyl alcohol (UDYO), were reacted with 3,6-dioxa-1,8-octandithiol and DMPA at room temperature for 1 h under UV radiation to yield different new polyols (Figure 1.21-b). The polyols were reacted with MDI. The PUs were further modified by the pendant ester moiety by aminolysis using Jeffamine M-600 followed by iodine complexation. These modifications enhanced the hydrophilicity of PUs to impart antimicrobial properties. These PUs could be used in applications such as medical devices, protective clothing, antimicrobial filters and bandages. In their ultimate work pertaining to TEC/TYC and PUs, Cadiz and co-workers synthesized diols from UDC containing allyl and propargyl groups (Comi et al. 2016). These diols were polymerized using IDPI. The alkene and alkyne groups were reacted with thioglycerol via UV radiation using DMPA, to enhanced hydrophilicity. The PUs exhibited highly tunable thermal and mechanical properties. The mechanical properties of these bio-based polymers (modulus from 774 MPa to 6 MPa and elongation at break from 45 to 401 %, respectively) make the suitable materials for a large range of applications.

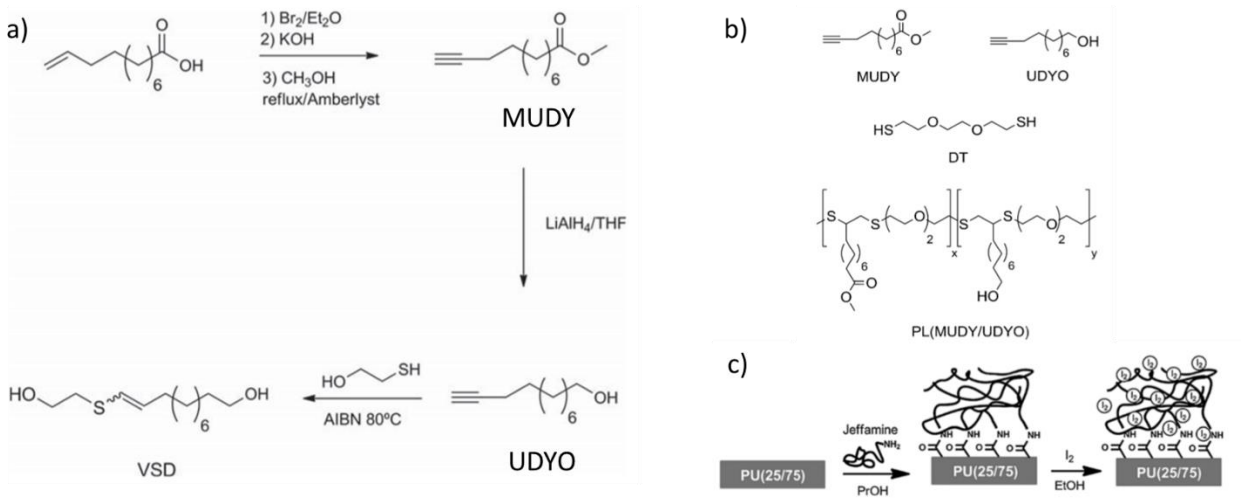

Figure 1.21 – (a) Synthesis of VSD, adapted from reference (Gonzalez-Paz et al. 2013), (b) synthesis of polyols by TEC/TYC using MUDO and UDYO; and (c) functionalization of PU aminolysis and iodine complexation, adapted from reference (Lluch et al. 2014).

Some authors have used TEC/TYC for the synthesis of polyester in recent publications. In an initial work (Beyazkilic et al. 2014), 10-undecynoic acid is used to synthesize vinylsulfide-containing hydroxyacid (VSHA) (Figure 1.22-a) by the use of ME and AIBN at 80 °C (1:1.05 alkyne to thiol ratio) and obtained a moderate mixture of E/Z isomers. The polycondensation of this monomer is accomplished via metal and enzymatic catalyzed means to yield polyesters (PVSHA). Higher MWs were obtained via enzymatic polymerizations. Enzymatic copolymerizations of diblock (VHSA and e-caprolactone (EL)) and triblock of (VHSA, EL and BDO) were also obtained (Figure 1.22-b). More interestingly, VHSA containing polymers could be further reacted via the thiol-ene reaction by: (i) ME to yield pendant hydroxyl groups, (ii) 1,4-butanethiol to yield cross-linked materials and lastly (iii) 7-mercapto-4-methylcoumarin to modify the surface of polyesters. In a follow-up study (Beyazkilic et al. 2015), VHSA and a ketone-containing hydroxy ester (KHE) (Moreno et al. 2014) (derived from methyloleate and synthesized as mentioned in section 5.3) were used to synthesize a series of copolyesters via enzymatic polycondensation. As depicted in Figure 1.22-c, polyesters could be modified after polymerization via the thiol-reaction in VHSA containing segments and via oxyamine for KHE containing segments.

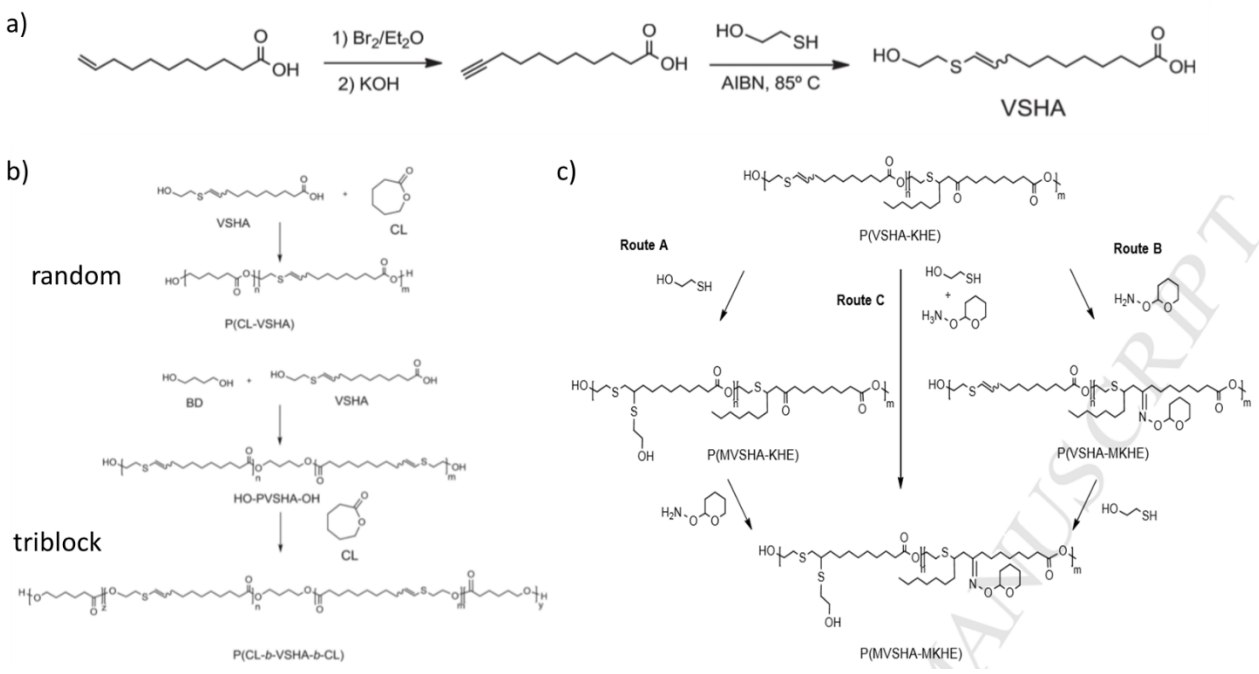

Figure 1.22 – (a) Synthesis of VSHA, (b) copolymerization of VSHA with EL and BDO, adapted from reference (Beyazkilic et al. 2014), and (c) post-polymerization modification of VSHA-KHE copolymers, adapted from reference (Beyazkilic et al. 2015).

5.5. Huisgen 1,3-dipolar cycloaddition

Huisgen 1,3-dipolar cycloaddition represents an efficient method to produce polymers from vegetable oils. The FA chain of epoxidized soybean oil can be functionalized with azide groups by ring-opening nucleophilic addition of sodium azide to the epoxy group (Biswas et al. 2008). Later, this strategy was applied to achieve highly cross-linked biopolymers through the copper-catalyzed and the thermal polyaddition of alkynylated (ASBO) and azidated soybean oil (AzSBO) (Hong, Luo, and Shah 2010). In this work two different approaches were studied. First, alkynylated soybean oil was polymerized by CuAAC reaction with diazide linkers. Then, azidated soybean oil underwent thermal polymerization with diyne moieties and with ethynylated soybean oil at 100 °C. The functionalization of epoxidized soybean oil (ESBO) with azide and alkyl groups is shown in Figure *1*.23-a. For this first approach, ASBO was polymerized with 1,6-diazidohexane and α,α'-diazido-p-xylene at room temperature using copper sulphate and sodium ascorbate as catalysts. The polymerization resulted in highly cross-linked polymers that were insoluble in common organic solvents. AzSBO was in turn polymerized with 1,4-dethynylbenzene and 1,7-octadiyne and with ASBO. The CuAAc results in a 1,4-disubstituted 1,2,3-triazole, whereas the thermal driven reaction

is supposed to be non-stereoselective and results in the formation of both 1,4- and 1,5-disubstituted 1,2,3-triazole rings. The T_g of the polymers obtained by the CuAAC reaction was higher than that of the polymers obtained by the thermal polymerization. We can show that the catalyst-based and solvent free route was better than the pathway based on CuAAC.

New building blocks from castor, canola, corn, soybean and linseed oils were also used on this thermal driven click reaction (Hong et al. 2012). The azidated vegetable oils underwent a step-growth polymerization with ASBO under solvent and catalyst-free conditions (Figure 1.23-b). The azidated oils also showed much higher viscosities than the epoxidized oils, attributed to the presence of stronger intermolecular hydrogen bonds in the azidated ones. The sol fraction and the swelling degree of the materials decreased with the increasing number of azide functionalities in the monomer. A different behavior from azidated castor oil was also observed, showing a higher T_g and elongation at break despite its lower cross-linking density. The higher degree of H-bonding due to additional hydroxyl group per FA chain could explain this behavior. (Hong et al. 2015).

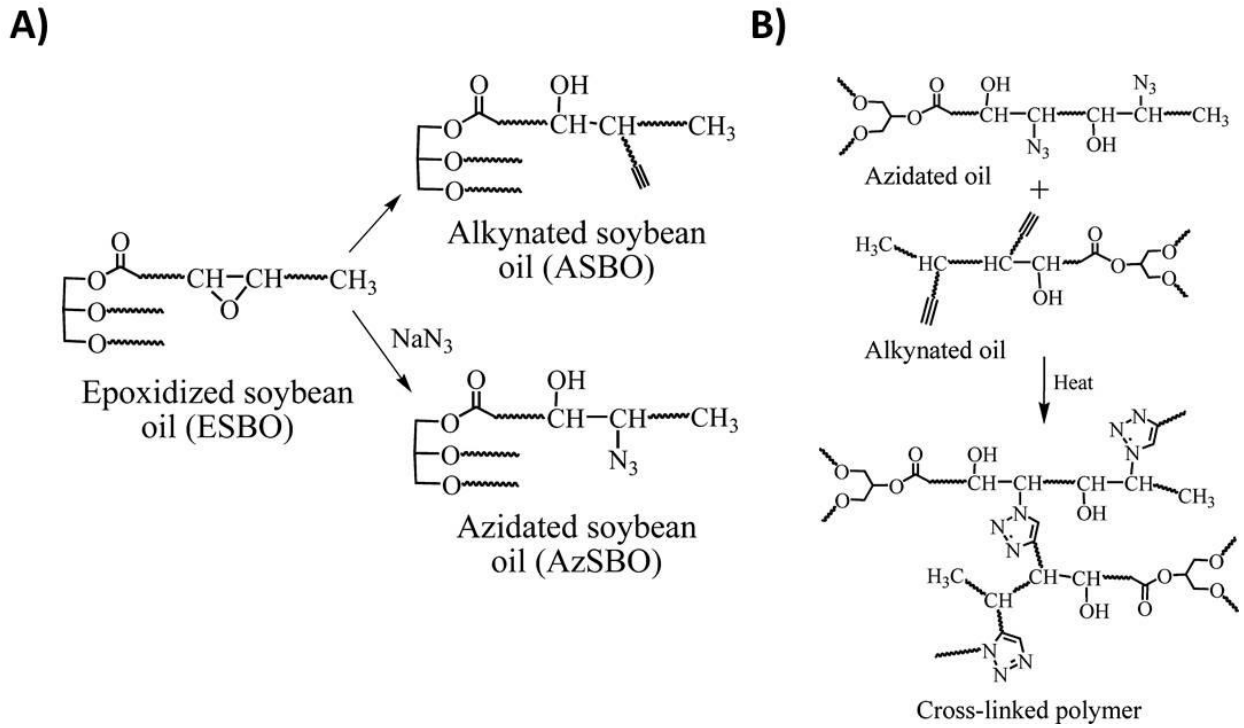

Figure 1.23 – (a) Introduction of terminal alkyde and azide groups on FA chains, and (b) cross-linking of vegetable oil-based polymers via triazole rings. Reprinted with permission from (Hong et al. 2012; Hong, Luo, and Shah 2010)

More recently, the use of photo-induced CuAAC reaction was applied for the polymerization of soybean oils at ambient conditions (Uysal, Acik, and Tasdelen 2017). In this way, the reaction was achieved without solvent with rapid polymerization rates at low temperatures, in good agreement with green chemistry principles. As reported above, azide and alkyne groups were introduced into ESBO by simultaneous ring-opening between epoxides with sodium azide and propargyl alcohol. Then these multifunctional azides and alkynes were polymerized in the presence of a photoinitiator and Cu(II)Br2/N,N,N', N'', N''-pentamethyldiethylenetriamine. The photoinitiator forms reactive free radicals that can reduce Cu(II) into Cu(I), to serve as catalyst for CuAAC.

Polytriazoles with melt-processing properties have also been obtained by the use of the Huisgen cycloaddition without solvent or catalyst. Three thermoplastic polytriazoles were obtained from diester dialkynes and a diazide monomer derived from OA (Floros, Leão, and Narine 2014). The mechanical and thermal properties of the polymer are clearly influenced by the chain length of the ester employed. Polytriazoles have shown excellent coating properties due to their high thermal stability, good mechanical properties and chemical resistance because of the presence of the 1,2,3-triazole five-membered ring, with a high dipole moment and the ability to form hydrogen bonds (Gholami et al. 2015). ASBO has been tested with two different propyfunctional urethane monomers. For the preparation of ASBO, ESBO was reacted with sodium azide in the presence of 1-methylimidazolium tetrafluoroborate as a catalyst. Propyn-terminated urethane monomers were prepared by reaction of propargyl alcohol with isocyanate monomers. All the materials prepared in this study showed only one T_g between 58 and 80 °C, indicating the phase mixing of soft segment from soybean oil-derived structures and hard segment from 1,2,3-triazole rings and urethane linkages.

Huisgen reaction was also used for the preparation of vegetable oil-based PUs for wound dressing applications (Gholami et al. 2018). PUs were prepared from a mixture of castor oil and soybean oil-based polyol containing 1,2,3-triazolium rings (QTSBO). QTSBO was prepared through N-alkylation of 1,2,3-triazole functionalized soybean oil (TSBO) with methyl iodide. TSBO was in turn prepared from an azidated soybean oil and propargyl alcohol through the click reaction. The hydroxyl groups present in the structure of TSBO were employed for the synthesis of PUs. In this

work, castor oil was also employed as co-reactant to impart flexibility and, thus, to tune the physico-mechanical properties of the PU. The resulting materials showed good tensile strength properties for wound dressing applications. Moreover, the presence of 1,2,3-triazolium rings provided antimicrobial activity against different bacterial and fungal stains.

PUs has been also elaborated from 1,2,3-triazole modified soybean oil-based polyols (Bakhshi et al. 2013). Sodium azide was used for the introduction of azides to ESBO and 1-methylimidazolium tetrafluoroborate was selected as catalyst at 65 °C. Then, various alkynes (phenylacetylene, propargyl alcohol and N, N-dimethylpropargyl amine) were used to conduct the cycloaddition in the presence of copper sulphate and sodium ascorbate as the catalyst couple (Figure 1.24). The alkylation of tertiary amine-containing polyol to obtain quaternary ammonium salt-containing polyol to impart biocidal activity to the PU has been performed. The polyols were reacted with IPDI and also mixed with PEG (molar mass of 1000 g/mol) to produce PUs. The results showed that the incorporation of the triazole groups resulted in higher storage modulus at glassy state, T_g, and thermal stability and hardness of the PUs. However, lower adhesion strength and hydrophilicity were also observed.

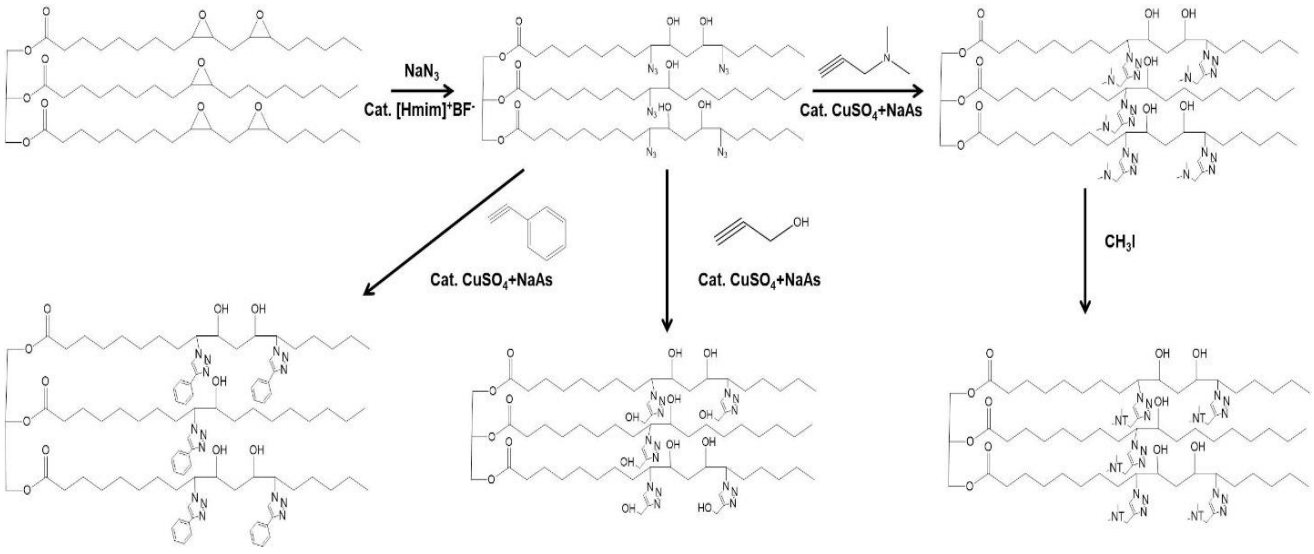

Figure 1.24 – Preparation of polyols from ESBO using Huisgen cycloaddition, reprinted adapted with permission from reference (Bakhshi et al. 2013).

Copper-catalyzed Huisgen cycloaddition has been tested for the cross-linking of waterborne polymer systems to improve their mechanical properties, adhesion strength and water/solvent

resistance when compared with traditional coatings and adhesives (Hu et al. 2016). Clickable alkyne or azide-functionalized monomers were incorporated to WPU, polyester dispersions (PED) or polyacrylate emulsions (PAE). The authors observed that click reactions take place mainly on the particle surface and after polymer diffusion process further cross-linking can take place. Click cross-linked WPU improved the tensile strength and the Young's modulus, whereas the water absorption decreased. The improved mechanical properties were associated to a limitation of the chains mobility. PED cross-linked films showed higher tensile strength and increased T_g. Moreover, clickable groups are still available for further functionalization. The authors claimed that this strategy could replace the use of hardeners, reducing the cost in the coatings preparation.

6. Conclusion

Although plant oils have historically been the most abundantly exploited renewable resources for the use of organic chemistry and polymer science, sustainable polymer production trails behind that of petroleum derived ones. Many different strategies have been exploited to transform plant oils and their derivatives into useful monomers and polymers and lately an emphasis on doing so by green chemistry means has been increasingly important and rightly so. Coordinated with this idea, this review presented the latest results of the utilization of click chemistry for the synthesis of derivates and polymers to yield materials with advanced properties.

This review puts particular emphasis on examining the recent literature pertaining to the subject and whether the chemistry to synthesize these materials abides green chemistry ideals. Click chemistry are efficient and clean reactions from a green chemistry stand point, nevertheless, functionalizing vegetable oils with the required moieties necessary for click chemistry does not always abide by green chemistry ideals.

Thiol-ene addition has classically been the most predominately used of the click chemistry reactions on fats and oils, nevertheless we fully cover the emergence of the Diels-Alder reaction as well as triazolinedione chemistry for the synthesis of advanced sustainable polymers. Click chemistry reaction are powerful reactions that have proven their ability to contribute to the synthesis of sustainable polymers. This review should guide and inspire the uses of these

reactions to develop novel biobased macromolecular architectures derived from vegetable oils, towards several environmental applications for a greener future.

7. References

Alagi, Prakash, Ye Jin Choi, Joonil Seog, and Sung Chul Hong. 2016. 'Efficient and quantitative chemical transformation of vegetable oils to polyols through a thiol-ene reaction for thermoplastic polyurethanes', *Industrial Crops and Products*, 87: 78-88.

Anastas, Paul T., and John Charles Warner. 1998. *Green chemistry : theory and practice* (Oxford University Press: Oxford [England]; New York).

Ates, Zeliha, Paul D Thornton, and Andreas Heise. 2011. 'Side-chain functionalisation of unsaturated polyesters from ring-opening polymerisation of macrolactones by thiol–ene click chemistry', *Polymer Chemistry*, 2: 309-12.

Bakhshi, Hadi, Hamid Yeganeh, Shahram Mehdipour-Ataei, Atefeh Solouk, and Shiva Irani. 2013. 'Polyurethane Coatings Derived from 1,2,3-Triazole-Functionalized Soybean Oil-Based Polyols: Studying their Physical, Mechanical, Thermal, and Biological Properties', *Macromolecules*, 46: 7777-88.

Behr, A., A. Westfechtel, and J. Pérez Gomes. 2008. 'Catalytic Processes for the Technical Use of Natural Fats and Oils', *Chemical Engineering and Technology*, 31: 700-14.

Belgacem, Naceur, and Alessandro Gandini. 2008. *Monomers, Polymers and Composites From Renewable Resources* (Elsevier: Amsterdam).

Bétron, Cyrille, Philippe Cassagnau, and Véronique Bounor-Legaré. 2018. 'EPDM crosslinking from bio-based vegetable oil and Diels–Alder reactions', *Materials Chemistry and Physics*, 211: 361-74.

Beyazkilic, Zeynep, Gerard Lligadas, Juan Carlos Ronda, Marina Galià, and Virginia Cádiz. 2014. 'Vinylsulfide-Containing Polyesters and Copolyesters from Fatty Acids: Thiol-yne Monomer Synthesis and Thiol-ene Functionalization', *Macromol. Chem, Phys.*, 215: 2248-59.

Beyazkilic, Zeynep, Gerard Lligadas, Juan Carlos Ronda, Marina Galià, and Virginia Cádiz. 2015. 'Synthesis and functionalization of vinylsulfide and ketone-containing aliphatic copolyesters from fatty acids', *Polymer*, 79: 290-98.

Biermann, Ursula, Wolfgang Friedt, Siegmund Lang, Wilfried Lühs, Guido Machmüller, Juergen O Metzger, Mark Ruesch gen. Klaas, Hans J Schäfer, and Manfred P Schneider. 2000. 'New syntheses with oils and fats as renewable raw materials for the chemical industry', *Angew. Chem. Int. Ed.*, 39: 2206-24.

Billiet, Stijn, Kevin De Bruycker, Frank Driessen, Hannelore Goossens, Veronique Van Speybroeck, Johan M. Winne, and Filip E. Du Prez. 2014. 'Triazolinediones enable ultrafast and reversible click chemistry for the design of dynamic polymer systems', *Nat Chem*, 6: 815-21.

Biswas, Atanu, H. N. Cheng, Sanghoon Kim, and Zengshe Liu. 2014. 'Modified Triglyceride Oil Through Reactions with Phenyltriazolinedione', *Journal of the American Oil Chemists' Society*, 91: 125-31.

Biswas, Atanu, Brajendra K. Sharma, J. L. Willett, Atanu Advaryu, S. Z. Erhan, and H. N. Cheng. 2008. 'Azide Derivatives of Soybean Oil and Fatty Esters', *Journal of Agricultural and Food Chemistry*, 56: 5611-16.

Bueno-Ferrer, Carmen, Elodie Hablot, María del Carmen Garrigós, Sergio Bocchini, Luc Averous, and Alfonso Jiménez. 2012. 'Relationship between morphology, properties and degradation parameters of novative biobased thermoplastic polyurethanes obtained from dimer fatty acids', *Polymer Degradation and Stability*, 97: 1964-69.

Bueno-Ferrer, Carmen, Elodie Hablot, Florence Perrin-Sarazin, M. Carmen Garrigós, Alfonso Jiménez, and Luc Averous. 2012. 'Structure and Morphology of New Bio-Based Thermoplastic Polyurethanes Obtained From Dimeric Fatty Acids', *Macromolecular Materials and Engineering*, 297: 777-84.

Buono, Pietro, Antoine Duval, Luc Avérous, and Youssef Habibi. 2018. 'Clicking Biobased Polyphenols: A Sustainable Platform for Aromatic Polymeric Materials', *Chemsuschem*, 11: 2472-91.

Calle, Mariola, Gerard Lligadas, Juan Ronda, Marina Galià, and Virginia Cadiz. 2016. 'Non-Isocyanate Route to Biobased Polyurethanes and Polyureas via AB-type Self-Polycondensation', *European Polymer Journal*, 84: 837-48.

Cardoso, Priscilla B., Thiago O. Machado, Paulo E. Feuser, Claudia Sayer, Michael A. R. Meier, and Pedro H. H. Araújo. 2018. 'Biocompatible Polymeric Nanoparticles From Castor Oil Derivatives via Thiol-Ene Miniemulsion Polymerization', *Eur. J. Lipid Sci. Technol.*, 120: 1700212.

Carré, Camille, Yvan Ecochard, Sylvain Caillol, and Luc Averous. 2019. 'From the synthesis of biobased cyclic carbonate to polyhydroxyurethanes: a promising route towards renewable non-isocyanate polyurethanes', *Chemsuschem*, 12: 3410.

Charlon, M., B. Heinrich, Y. Matter, E. Couzigné, B. Donnio, and L. Avérous. 2014. 'Synthesis, structure and properties of fully biobased thermoplastic polyurethanes, obtained from a diisocyanate based on modified dimer fatty acids, and different renewable diols', *European Polymer Journal*, 61: 197-205.

Chattopadhyay, Subrata, and Filip Du Prez. 2016. 'Simple design of chemically crosslinked plant oil nanoparticles by triazolinedione-ene chemistry', *European Polymer Journal*, 81: 77-85.

Claudino, Mauro. 2011. 'Thiol–ene Coupling of Renewable Monomers: at the forefront of bio-based polymeric materials'.

Comi, M., G. Lligadas, J. C. Ronda, M. Galia, and V. Cadiz. 2016. 'Synthesis of castor-oil based polyurethanes bearing alkene/alkyne groups and subsequent thiol-ene/yne post-modification', *Polymer*, 103: 163-70.

Cookson, R. C., S. S. H. Gilani, and I. D. R. Stevens. 1962. '4-Phenyl-1,2,4-triazolin-3,5-dione: a powerful dienophile', *Tetrahedron Letters*, 3: 615-18.

Cookson, R. C., S. S. H. Gilani, and I. D. R. Stevens. 1967. 'Diels–Alder reactions of 4-phenyl-1,2,4-triazoline-3,5-dione', *J. Chem. Soc. C*, 0: 1905-09.

Corma, Avelino, Sara Iborra, and Alexandra Velty. 2007. 'Chemical Routes for the Transformation of Biomass into Chemicals', *Chemical Reviews*, 107: 2411-502.

Cornille, Adrien, Vincent Froidevaux, Claire Negrell, Sylvain Caillol, and Bernard Boutevin. 2014. 'Thiol-ene coupling: An efficient tool for the synthesis of new biobased aliphatic amines for epoxy curing', *Polymer*, 55: 5561-70.

Dannecker, Patrick-Kurt, Ursula Biermann, Alexandra Sink, Fabian R. Bloesser, Jürgen O. Metzger, and Michael A. R. Meier. 2019. 'Fatty Acid–Derived Aliphatic Long Chain Polyethers by a Combination of Catalytic Ester Reduction and ADMET or Thiol-Ene Polymerization', *Macromol. Chem, Phys.*, 220: 1800440.

De Bruycker, Kevin, Stijn Billiet, Hannes A. Houck, Subrata Chattopadhyay, Johan M. Winne, and Filip E. Du Prez. 2016. 'Triazolinediones as Highly Enabling Synthetic Tools', *Chemical Reviews*, 116: 3919-74.

de Espinosa, L. M., and M. A. R. Meier. 2011. 'Plant oils: The perfect renewable resource for polymer science?!', *European Polymer Journal*, 47: 837-52.

Desroches, M., M. Escouvois, R. Auvergne, S. Caillol, and B. Boutevin. 2012. 'From Vegetable Oils to Polyurethanes: Synthetic Routes to Polyols and Main Industrial Products', *Polymer Reviews*, 52: 38-79.

Diels, Otto, and Kurt Alder. 1931. 'Synthesen in der hydroaromatischen Reihe. VIII. Mitteilung: Dien-Synthesen des Anthracens. Anthracen-Formel', *Justus Liebigs Annalen der Chemie*, 486: 191-202.

Diels, Otto, Jacob Hansen Blom, and Werner Koll. 1925. 'Über das aus Cyclopentadien und Azoester entstehende Endomethylen-piperidazin und seine Überführung in 1,3-Diamino-cyclopentan', *Justus Liebigs Annalen der Chemie*, 443: 242-62.

Dumont, Marie-Josée. 2016. 'Polymeric Products Derived From Industrial Oils for Paints, Coatings, and Other Applications', *Industrial Oil Crops, 3*: 43-73.

Durand, Pierre-Luc, Antoine Brège, Guillaume Chollet, Etienne Grau, and Henri Cramail. 2018. 'Simple and Efficient Approach toward Photosensitive Biobased Aliphatic Polycarbonate Materials', *ACS Macro Letters*, 7: 250-54.

Durand, Pierre-Luc, Guillaume Chollet, Etienne Grau, and Henri Cramail. 2019. 'Versatile cross-linked fatty acid-based polycarbonate networks obtained by thiol–ene coupling reaction', *RSC Advances*, 9: 145-50.

Espinosa, Juan P., Vivina Hanazumi, Pablo M. Stefani, and Roxana A. Ruseckaite. 2020. 'Curing behavior and properties of high biosourced epoxy resin blends based on a triepoxy monomer and a tricarboxylic acid hardener from 10-undecenoic acid', *Polymer Testing*, 81: 106208.

Fairbanks, Benjamin D., Timothy F. Scott, Christopher J. Kloxin, Kristi S. Anseth, and Christopher N. Bowman. 2009. 'Thiol-Yne Photopolymerizations: Novel Mechanism, Kinetics, and Step-Growth Formation of Highly Cross-Linked Networks', *Macromolecules*, 42: 211-17.

Feng, Yechang, Haiyan Liang, Ziming Yang, Teng Yuan, Ying Luo, Puwang Li, Zhuohong Yang, and Chaoqun Zhang. 2017. 'A Solvent-Free and Scalable Method To Prepare Soybean-Oil-Based Polyols by Thiol–Ene Photo-Click Reaction and Biobased Polyurethanes Therefrom', *ACS Sustainable Chemistry & Engineering*, 5: 7365-73.

Finnveden, Maja, Sara Brännström, Mats Johansson, Eva Malmström, and Mats Martinelle. 2018. 'Novel sustainable synthesis of vinyl ether ester building blocks, directly from carboxylic acids and the corresponding hydroxyl vinyl ether, and their photopolymerization', *RSC Advances*, 8: 24716-23.

Finnveden, Maja, Peter Hendil-Forssell, Mauro Claudino, Mats Johansson, and Mats Martinelle. 2019. 'Lipase-Catalyzed Synthesis of Renewable Plant Oil-Based Polyamides', *Polymers*, 11: 1730.

Floros, Michael C., Alcides Lopes Leão, and Suresh S. Narine. 2014. 'Vegetable oil derived solvent, and catalyst free "click chemistry" thermoplastic polytriazoles', *BioMed Research International*, 2014: 792901.

Frias, Célia F., Ana C. Fonseca, Jorge F. J. Coelho, and Arménio C. Serra. 2015. 'Straightforward functionalization of acrylated soybean oil by Michael-addition and Diels–Alder reactions', *Industrial Crops and Products*, 64: 33-38.

Fu, Changqing, Jiancheng Liu, Hongying Xia, and Liang Shen. 2015. 'Effect of structure on the properties of polyurethanes based on aromatic cardanol-based polyols prepared by thiol-ene coupling', *Progress in Organic Coatings*, 83: 19-25.

Fu, Changqing, Jiahui Wang, Lie Chen, and Liang Shen. 2019. 'Synthesis of a Fully Biobased Polyfunctional Vinyl Oligomer and Their UV Cured Films Prepared via Thiol-ene Coupling', *Journal of Renewable Materials*, 7: 795-805.

Fu, Changqing, Zhe Yang, Zitong Zheng, and Liang Shen. 2014. 'Properties of alkoxysilane castor oil synthesized via thiol-ene and its polyurethane/siloxane hybrid coating films', *Progress in Organic Coatings*, 77: 1241-48.

Fu, Changqing, Zitong Zheng, Zhe Yang, Yiwang Chen, and Liang Shen. 2014. 'A fully bio-based waterborne polyurethane dispersion from vegetable oils: From synthesis of precursors by thiol-ene reaction to study of final material', *Progress in Organic Coatings*, 77: 53-60.

Gallart-Sirvent, Pau, Anlong Li, Kaichang Li, Gemma Villorbina, and Ramon Canela-Garayoa. 2017. 'Preparation of pressure-sensitive adhesives from tung oil via Diels-Alder reaction', *International Journal of Adhesion and Adhesives*, 78: 67-73.

Gandini, A., D. Coelho, and A. J. D. Silvestre. 2008. 'Reversible click chemistry at the service of macromolecular materials. Part 1: Kinetics of the Diels-Alder reaction applied to furan-maleimide model compounds and linear polymerizations', *European Polymer Journal*, 44: 4029-36.

Gandini, A., A. J. D. Silvestre, and D. Coelho. 2011. 'Reversible click chemistry at the service of macromolecular materials', *Polymer Chemistry*, 2: 1713-19.

Gandini, Alessandro. 2013. 'The furan/maleimide Diels–Alder reaction: A versatile click–unclick tool in macromolecular synthesis', *Progress in Polymer Science*, 38: 1-29.

Gandini, Alessandro, Antonio J. F. Carvalho, Eliane Trovatti, Ricardo K. Kramer, and Talita M. Lacerda. 2018. 'Macromolecular materials based on the application of the Diels–Alder reaction to natural polymers and plant oils', *European Journal of Lipid Science and Technology*, 120: 1700091.

Gandini, Alessandro, and Talita Lacerda. 2018. *Polymers from Plant Oils* (Scrivener Publishing: Beverly, MA, USA).

Gandini, Alessandro, Talita M Lacerda, and Antonio JF Carvalho. 2013. 'A straightforward double coupling of furan moieties onto epoxidized triglycerides: synthesis of monomers based on two renewable resources', *Green Chemistry*, 15: 1514-19.

Gandini, Alessandro, Talita M. Lacerda, Antonio J. F. Carvalho, and Eliane Trovatti. 2016. 'Progress of Polymers from Renewable Resources: Furans, Vegetable Oils, and Polysaccharides', *Chemical Reviews*, 116: 1637-69.

Gandini, Alessandro, Armando J. D. Silvestre, and Dora Coelho. 2010. 'Reversible click chemistry at the service of macromolecular materials. 2. Thermoreversible polymers based on the Diels-Alder reaction of an A-B furan/maleimide monomer', *Journal of Polymer Science Part A: Polymer Chemistry*, 48: 2053-56.

García-Astrain, C., A. Gandini, D. Coelho, I. Mondragon, A. Retegi, A. Eceiza, M. A. Corcuera, and N. Gabilondo. 2013. 'Green chemistry for the synthesis of methacrylate-based hydrogels crosslinked through Diels–Alder reaction', *European Polymer Journal*, 49: 3998-4007.

Gerpen, Jon Van. 2005. 'Biodiesel processing and production', *Fuel Processing Technology*, 86: 1097-107.

Gheneim, R., C. Perez-Berumen, and A. Gandini. 2002. 'Diels-Alder reactions with novel polymeric dienes and dienophiles: Synthesis of reversibly cross-linked elastomers', *Macromolecules*, 35: 7246-53.

Gholami, Hoshyar, Hamid Yeganeh, Saeed Beigi Burujeny, Marziyeh Sorayya, and Elias Shams. 2018. 'Vegetable Oil Based Polyurethane Containing 1,2,3-Triazolium Functional Groups as Antimicrobial Wound Dressing', *Journal of Polymers and the Environment*, 26: 462-73.

Gholami, Hoshyar, Hamid Yeganeh, Reza Gharibi, Mehrdad Jalilian, and Marziyeh Sorayya. 2015. 'Catalyst free-click polymerization: A versatile method for the preparation of soybean oil based poly1,2,3-triazoles as coatings with efficient biocidal activity and excellent cytocompatibility', *Polymer*, 62: 94-108.

Goethals, Fabienne, Steven Martens, Pieter Espeel, Otto van den Berg, and Filip E. Du Prez. 2014. 'Diversely Substituted Polyamide Structures through Thiol–Ene Polymerization of Renewable Thiolactone Building Blocks', *Macromolecules*, 47: 61-69.

Gonzalez-Paz, R. J., G. Lligadas, J. C. Ronda, M. Galia, and V. Cadiz. 2013. 'Thiol-yne Reaction of Alkyne-derivatized Fatty Acids: Thiol-Reactive Linear Polyurethane', *Journal of Renewable Materials*, 1: 187-94.

González-Paz, Rodolfo J., Gerard Lligadas, Juan C. Ronda, Marina Galià, and Virginia Cádiz. 2012. 'Thiol–yne reaction of alkyne-derivatized fatty acids: biobased polyols and cytocompatibility of derived polyurethanes', *Polymer Chemistry*, 3: 2471-78.

González-Paz, Rodolfo J., Gerard Lligadas, Juan C. Ronda, Marina Galià, Ana M. Ferreira, Francesca Boccafoschi, Gianluca Ciardelli, and Virginia Cádiz. 2012. 'Enhancement of Fatty Acid-based Polyurethanes Cytocompatibility by Non-covalent Anchoring of Chondroitin Sulfate', *Macromolecular Bioscience*, 12: 1697-705.

Gousse, C., A. Gandini, and P. Hodge. 1998. 'Application of the Diels-Alder reaction to polymers bearing furan moieties. 2. Diels-Alder and retro-Diels-Alder reactions involving furan rings in some styrene copolymers', *Macromolecules*, 31: 314-21.

Hablot, Elodie, Dan Zheng, Michel Bouquey, and Luc Avérous. 2008. 'Polyurethanes Based on Castor Oil: Kinetics, Chemical, Mechanical and Thermal Properties', *Macromolecular Materials and Engineering*, 293: 922-29.

Hazer, Baki. 2015. 'Simple synthesis of amphiphilic poly(3-hydroxy alkanoate)s with pendant hydroxyl and carboxylic groups via thiol-ene photo click reactions', *Polymer Degradation and Stability*, 119: 159-66.

He, Minghui, Shun Jiang, Ruixin Xu, Jianwen Yang, Zhaohua Zeng, and Guangxue Chen. 2014. 'Facile functionalization of soybean oil by thiol-ene photo-click reaction for the synthesis of polyfunctional acrylate', *Progress in Organic Coatings*, 77: 868-71.

Hong, Jian, Qiang Luo, and Bipin K. Shah. 2010. 'Catalyst- and Solvent-Free “Click” Chemistry: A Facile Approach to Obtain Cross-Linked Biopolymers from Soybean Oil', *Biomacromolecules*, 11: 2960-65.

Hong, Jian, Qiang Luo, Xianmei Wan, Zoran S. Petrović, and Bipin K. Shah. 2012. 'Biopolymers from Vegetable Oils via Catalyst- and Solvent-Free “Click” Chemistry: Effects of Cross-Linking Density', *Biomacromolecules*, 13: 261-66.

Hong, Jian, Dragana Radojčić, Djavan Hairabedian, Xianmei Wan, and Zoran S. Petrović. 2015. 'Alkynated and azidated octadecane as model compounds for kinetic studies of Huisgen 1,3-dipolar cycloaddition in vegetable oils', *European Journal of Lipid Science and Technology*, 117: 266-70.

Hoogenboom, Richard. 2010. 'Thiol–Yne Chemistry: A Powerful Tool for Creating Highly Functional Materials', *Angewandte Chemie International Edition,* 49: 3415-17.

Hoyle, Charles E., and Christopher N. Bowman. 2010. 'Thiol–Ene Click Chemistry', *Angewandte Chemie International Edition*, 49: 1540-73.

Hu, Jianqing, Kaimei Peng, Jinshan Guo, Dingying Shan, Gloria B. Kim, Qiyao Li, Ethan Gerhard, Liang Zhu, Weiping Tu, Weizhong Lv, Michael A. Hickner, and Jian Yang. 2016. 'Click Cross-Linking-Improved Waterborne Polymers for Environment-Friendly Coatings and Adhesives', *ACS Applied Materials & Interfaces*, 8: 17499-510.

Huang, Kun, Zengshe Liu, Jinwen Zhang, Shouhai Li, Mei Li, Jianling Xia, and Yonghong Zhou. 2014. 'Epoxy Monomers Derived from Tung Oil Fatty Acids and Its Regulable Thermosets Cured in Two Synergistic Ways', *Biomacromolecules*, 15: 837-43.

Huang, Kun, Zengshe Liu, Jinwen Zhang, Shouhai Li, Mei Li, Jianling Xia, and Yonghong Zhou. 2015. 'A self-crosslinking thermosetting monomer with both epoxy and anhydride groups derived from tung oil fatty acids: Synthesis and properties', *European Polymer Journal*, 70: 45-54.

Huang, Kun, Pei Zhang, Jinwen Zhang, Shouhai Li, Mei Li, Jianling Xia, and Yonghong Zhou. 2013. 'Preparation of biobased epoxies using tung oil fatty acid-derived C21 diacid and C22 triacid and study of epoxy properties', *Green Chemistry*, 15: 2466-66.

Huang, Yugang, Laixing Pang, Hongliang Wang, Rong Zhong, Zhaohua Zeng, and Jianwen Yang. 2013. 'Synthesis and properties of UV-curable tung oil based resins via modification of Diels–Alder reaction, nonisocyanate polyurethane and acrylates', *Progress in Organic Coatings*, 76: 654-61.

Ionescu, Mihail, Dragana Radojčić, Xianmei Wan, Zoran S. Petrović, and Thomas A. Upshaw. 2015. 'Functionalized vegetable oils as precursors for polymers by thiol-ene reaction', *European Polymer Journal*, 67: 439-48.

Iqbal, Muhammad, Remco Knigge, Hero Heeres, Antonius Broekhuis, and Francesco Picchioni. 2018. 'Diels–Alder-Crosslinked Polymers Derived from Jatropha Oil', *Polymers*, 10: 1177-77.

Jeppesen, Jacob Benjamin, Jean-Francois Devaux, and Jean-Luc Dubois. 2015. "Five Novel Bio Based Diesels Tested in a Light-Duty Road Going Engine." In.: SAE International.

Jia, Puyou, Yufeng Ma, Haoyu Xia, Minrui Zheng, Guodong Feng, Lihong Hu, Meng Zhang, and Yonghong Zhou. 2018. 'Clean Synthesis of Epoxidized Tung Oil Derivatives via Phase Transfer Catalyst and Thiol–ene Reaction: A Detailed Study', *ACS Sustainable Chemistry & Engineering*, 6: 13983-94.

Kade, Matthew J., Daniel J. Burke, and Craig J. Hawker. 2010. 'The power of thiol-ene chemistry', *Journal of Polymer Science Part A: Polymer Chemistry*, 48: 743-50.

Koenig, N. H., and Daniel Swern. 1957. 'Organic Sulfur Derivatives. I. Addition of Mercaptoacetic Acid to Long-chain Monounsaturated Compounds', *Journal of the American Chemical Society*, 79: 362-65.

Kolb, Hartmuth C., M. G. Finn, and K. Barry Sharpless. 2001. 'Click Chemistry: Diverse Chemical Function from a Few Good Reactions', *Angewandte Chemie International Edition*, 40: 2004-21.

Konkolewicz, Dominik, Angus Gray-Weale, and Sébastien Perrier. 2009. 'Hyperbranched Polymers by Thiol−Yne Chemistry: From Small Molecules to Functional Polymers', *Journal of the American Chemical Society*, 131: 18075-77.

Kwart, Harold, and Isabel Burchuk. 1952. 'Isomerism and Adduct Stability in the Diels—Alder Reaction.1a I. The Adducts of Furan and Maleimide', *Journal of the American Chemical Society*, 74: 3094-97.

Lacerda, T. M., A. J. F. Carvalho, and A. Gandini. 2014. 'Two alternative approaches to the Diels-Alder polymerization of tung oil', *RSC Advances*, 4: 26829-37.

Lacerda, T. M., and A. Gandini. 2014. 'Marriage of Furans and Vegetable Oils through Click Chemistry for the Preparation of Macromolecular Materials: A Succinct Review', *Journal of Renewable Materials*, 2: 2-12.

Lamarzelle, Océane, Geoffrey Hibert, Sébastien Lecommandoux, Etienne Grau, and Henri Cramail. 2017. 'A thioglycerol route to bio-based bis-cyclic carbonates: poly(hydroxyurethane) preparation and post-functionalization', *Polymer Chemistry*, 8: 3438-47.

Laurichesse, Stéphanie, and Luc Avérous. 2014. 'Chemical modification of lignins: Towards biobased polymers', *Progress in Polymer Science*, 39: 1266-90.

Ligthelm, S. P., E. von Rudloff, and Donald A. Sutton. 1950. '622. Preparation of unsaturated long-chain alcohols by means of lithium aluminium hydride: some typical members of the series', *Journal of the Chemical Society (Resumed)*: 3187-90.

Liu, Chengguo, Wen Lei, Zhengchun Cai, Jianqiang Chen, Lihong Hu, Yan Dai, and Yonghong Zhou. 2013. 'Use of tung oil as a reactive toughening agent in dicyclopentadiene-terminated unsaturated polyester resins', *Industrial Crops and Products*, 49: 412-18.

Liu, Chengguo, Zengshe Liu, Brent H. Tisserat, Rongpeng Wang, Thomas P. Schuman, Yonghong Zhou, and Lihong Hu. 2015. 'Microwave-assisted maleation of tung oil for bio-based products with versatile applications', *Industrial Crops and Products*, 71: 185-96.

Lligadas, Gerard. 2013. 'Renewable Polyols for Polyurethane Synthesis via Thiol-ene/yne Couplings of Plant Oils', *Macromol. Chem, Phys.*, 214: 415-22.

Lligadas, Gerard, Joan C. Ronda, Marina Galià, and Virginia Cádiz. 2007. 'Polyurethane Networks from Fatty-Acid-Based Aromatic Triols: Synthesis and Characterization', *Biomacromolecules*, 8: 1858-64.

Lligadas, Gerard, Juan C. Ronda, Marina Galià, and Virginia Cádiz. 2013. 'Monomers and polymers from plant oils via click chemistry reactions', *Journal of Polymer Science Part A: Polymer Chemistry*, 51: 2111-24.

Lluch, Cristina, Braulio Esteve-Zarzoso, Albert Bordons, Gerard Lligadas, Juan C. Ronda, Marina Galià, and Virginia Cádiz. 2014. 'Antimicrobial Polyurethane Thermosets Based on Undecylenic Acid: Synthesis and Evaluation', *Macromolecular Bioscience*, 14: 1170-80.

Lu, Yongshang, and Richard C. Larock. 2009. 'Novel Polymeric Materials from Vegetable Oils and Vinyl Monomers: Preparation, Properties, and Applications', *Chemsuschem*, 2: 136-47.

Ma, Guozhang, Tong Zhang, Jianbing Wu, Caiying Hou, Lixia Ling, and Baojun Wang. 2013. 'Preparation and properties of glycerin ester of tung oil modified rosin', *Journal of Applied Polymer Science*, 130: 1700-06.

Machado, Thiago O., Priscilla B. Cardoso, Paulo Emilio Feuser, Claudia Sayer, and Pedro H. H. Araújo. 2017. 'Thiol-ene miniemulsion polymerization of a biobased monomer for biomedical applications', *Colloids and Surfaces B: Biointerfaces*, 159: 509-17.

Maisonneuve, Lise, Anne-Laure Wirotius, Carine Alfos, Etienne Grau, and Henri Cramail. 2014. 'Fatty acid-based (bis) 6-membered cyclic carbonates as efficient isocyanate free poly(hydroxyurethane) precursors', *Polymer Chemistry*, 5: 6142-47.

Maiti, Binoy, Sonu Kumar, and Priyadarsi De. 2014. 'Controlled RAFT synthesis of side-chain oleic acid containing polymers and their post-polymerization functionalization', *RSC Advances*, 4: 56415-23.

Mangeon, Carine, France Thevenieau, Estelle Renard, and Valérie Langlois. 2017. 'Straightforward Route To Design Biorenewable Networks Based on Terpenes and Sunflower Oil', *ACS Sustainable Chemistry & Engineering*, 5: 6707-15.

Meier, Michael A. R., Jurgen O. Metzger, and Ulrich S. Schubert. 2007. 'Plant oil renewable resources as green alternatives in polymer science', *Chemical Society Reviews*, 36: 1788-802.

Miao, Shida, Ping Wang, Zhiguo Su, and Songping Zhang. 2014. 'Vegetable-oil-based polymers as future polymeric biomaterials', *Acta Biomaterialia*, 10: 1692-704.

Montero de Espinosa, L., J. C. Ronda, M. Galià, and V. Cádiz. 2008. 'A new enone-containing triglyceride derivative as precursor of thermosets from renewable resources', *Journal of Polymer Science Part A: Polymer Chemistry*, 46: 6843-50.

Montero de Espinosa, Lucas, Andreas Gevers, Benjamin Woldt, Michael Graß, and Michael A. R. Meier. 2014. 'Sulfur-containing fatty acid-based plasticizers via thiol–ene addition and oxidation: synthesis and evaluation in PVC formulations', *Green Chemistry*, 16: 1883-96.

Moreno, Maryluz, Gerard Lligadas, Juan C. Ronda, Marina Galià, and Virginia Cádiz. 2014. 'Polyketoesters from oleic acid. Synthesis and functionalization', *Green Chemistry*, 16: 1847-53.

Moser, Bryan R., Kenneth M. Doll, and Steven C. Peterson. 2019. 'Renewable Poly(Thioether-Ester)s from Fatty Acid Derivatives via Thiol-Ene Photopolymerization', *Journal of the American Oil Chemists' Society*, 96: 825-37.

Moses, John E., and Adam D. Moorhouse. 2007. 'The growing applications of click chemistry', *Chemical Society Reviews*, 36: 1249-62.

Mubofu, Egid B. 2016. 'Castor oil as a potential renewable resource for the production of functional materials', *Sustainable Chemical Processes*, 4: 11.

Nalawade, Priyanka P., Brinda Mehta, Coleen Pugh, and Mark D. Soucek. 2014. 'Modified soybean oil as a reactive diluent: Synthesis and characterization', *Journal of Polymer Science Part A: Polymer Chemistry*, 52: 3045-59.

Nguyen, Phan Huy, Steven Spoljaric, and Jukka Seppälä. 2018. 'Renewable polyamides via thiol-ene 'click' chemistry and long-chain aliphatic segments', *Polymer*, 153: 183-92.

Omrani, Ismail, Abdolreza Farhadian, Niloofar Babanejad, Hasan Kashef Shendi, Abbas Ahmadi, and Mohammad Reza Nabid. 2016. 'Synthesis of novel high primary hydroxyl functionality polyol from sunflower oil using thiol-yne reaction and their application in polyurethane coating', *European Polymer Journal*, 82: 220-31.

Pang, Chengcai, Jie Zhang, Guolin Wu, Yinong Wang, Hui Gao, and Jianbiao Ma. 2014. 'Renewable polyesters derived from 10-undecenoic acid and vanillic acid with versatile properties', *Polymer Chemistry*, 5: 2843-53.

Petrovic, Z. S. 2008. 'Polyurethanes from vegetable oils', *Polymer Reviews*, 48: 109-55.

Petrović, Zoran S, Alisa Zlatanić, Charlene C Lava, and Snežana Sinadinović-Fišer. 2002. 'Epoxidation of soybean oil in toluene with peroxoacetic and peroxoformic acids—kinetics and side reactions', *European Journal of Lipid Science and Technology*, 104: 293-99.

Petrović, Zoran S., Wei Zhang, and Ivan Javni. 2005. 'Structure and Properties of Polyurethanes Prepared from Triglyceride Polyols by Ozonolysis', *Biomacromolecules*, 6: 713-19.

Peyrton, Julien, Clémence Chambaretaud, and Luc Avérous. 2019. 'New Insight on the Study of the Kinetic of Biobased Polyurethanes Synthesis Based on Oleo-Chemistry', *Molecules*, 24: 4332.

Pham, Phuoc Dien, Vincent Lapinte, Yann Raoul, and Jean-Jacques Robin. 2014. 'Lipidic polyols using thiol-ene/yne strategy for crosslinked polyurethanes', *Journal of Polymer Science Part A: Polymer Chemistry*, 52: 1597-606.

Qin, Anjun, Jacky W. Y. Lam, and Ben Zhong Tang. 2010. 'Click polymerization', *Chemical Society Reviews*, 39: 2522-44.

Reulier, M., R. Matadi Boumbimba, Z. Walsh Korb, R. Vaudemont, and L. Avérous. 2017. 'Thermomechanical and cyclic behavior of biocomposites based on renewable thermoplastics from dimer fatty acids', *Journal of Applied Polymer Science*, 134: 44610.

Reulier, M., R. Perrin, and L. Avérous. 2016. 'Biocomposites based on chemically modified cellulose fibers with renewable fatty-acid-based thermoplastic systems: Effect of different fiber treatments', 133: 43878.

Reulier, Marie, and Luc Avérous. 2015. 'Elaboration, morphology and properties of renewable thermoplastics blends, based on polyamide and polyurethane synthesized from dimer fatty acids', *European Polymer Journal*, 67: 418-27.

Reulier, Marie, Rodrigue Matadi Boumbimba, Damien Rasselet, and Luc Avérous. 2016. 'Renewable thermoplastic multiphase systems from dimer fatty acids, with mineral microfillers', *Journal of Applied Polymer Science*, 133: 43055

Romera, Cristian de Oliveira, Débora de Oliveira, Pedro Henrique Hermes de Araújo, and Claudia Sayer. 2019. 'Biobased Ester 2-(10-Undecenoyloxy)ethyl Methacrylate as an Asymmetrical Diene Monomer in Thiol–Ene Polymerization', *Industrial & Engineering Chemistry Research*, 58: 21044-55.

Ronda, J. C., G. Lligadas, M. Galia, and V. Cadiz. 2011. 'Vegetable oils as platform chemicals for polymer synthesis', *European Journal of Lipid Science and Technology*, 113: 46-58.

Rostovtsev, Vsevolod V., Luke G. Green, Valery V. Fokin, and K. Barry Sharpless. 2002. 'A Stepwise Huisgen Cycloaddition Process: Copper(I)-Catalyzed Regioselective "Ligation" of Azides and Terminal Alkynes', *Angew. Chem. Int. Ed.*, 41: 2596-99.

Ruiz, L., G. Lligadas, J. C. Ronda, M. Galià, and V. Cádiz. 2019. 'Synthesis of acid degradable oxidation responsive poly(β-thioether ester)s from castor oil', *European Polymer Journal*, 110: 183-91.

Rybak, Anastasiya, Patrice A. Fokou, and Michael A. R. Meier. 2008. 'Metathesis as a versatile tool in oleochemistry', *Eur. J. Lipid Sci. Technol.*, 110: 797-804.

Salehpour, Somaieh, and Marc A. Dubé. 2008. 'Biodiesel: a green polymerization solvent', *Green Chemistry*, 10: 321-26.

Shrestha, Maha L., Mihail Ionescu, Xianmei Wan, Bili, Nikola, Petrovi, Zoran S., and Tom Upshaw. 2018. 'Biobased Aromatic-Aliphatic Polyols from Cardanol by Thermal Thiol-Ene Reaction', *Journal of Renewable Materials*, 6: 87-101.

Silbert, Leonard S. 1984. 'Facile dehydrobromination of vic-dibromo fatty acids: A one-vessel bromination-dehydrobromination of oleic acid to stearolic acid', *Journal of the American Chemical Society*, 61: 1090-92.

Song, Lingzhi, Tianyu Zhu, Liang Yuan, Jiangjun Zhou, Yaqiong Zhang, Zhongkai Wang, and Chuanbing Tang. 2019. 'Ultra-strong long-chain polyamide elastomers with programmable supramolecular interactions and oriented crystalline microstructures', *Nature Communications*, 10: 1315.

Stemmelen, Mylène, Vincent Lapinte, Jean-Pierre Habas, and Jean-Jacques Robin. 2015. 'Plant oil-based epoxy resins from fatty diamines and epoxidized vegetable oil', *European Polymer Journal*, 68: 536-45.

Tornøe, Christian W., Caspar Christensen, and Morten Meldal. 2002. 'Peptidotriazoles on Solid Phase: [1,2,3]-Triazoles by Regiospecific Copper(I)-Catalyzed 1,3-Dipolar Cycloadditions of Terminal Alkynes to Azides', *The Journal of Organic Chemistry*, 67: 3057-64.

Türünç, Oğuz, Stijn Billiet, Kevin De Bruycker, Samira Ouardad, Johan Winne, and Filip E. Du Prez. 2015. 'From plant oils to plant foils: Straightforward functionalization and crosslinking of natural plant oils with triazolinediones', *European Polymer Journal*, 65: 286-97.

Türünç, Oğuz, and Michael A. R. Meier. 2012. 'A novel polymerization approach via thiol-yne addition', *Journal of Polymer Science Part A: Polymer Chemistry*, 50: 1689-95.

Türünç, Oğuz, and Michael A. R. Meier. 2013. 'The thiol-ene (click) reaction for the synthesis of plant oil derived polymers', *Eur. J. Lipid Sci. Technol.*, 115: 41-54.

Unverferth, Maike, and Michael A. R. Meier. 2016. 'Selective formation of C36-dimer fatty acids via thiol-ene addition for copolyamide synthesis', *European Journal of Lipid Science and Technology*, 118: 1470-74.

Ursula, Biermann, Bornscheuer Uwe, Meier Michael A. R., Metzger Jürgen O., and Schäfer Hans J. 2011. 'Oils and Fats as Renewable Raw Materials in Chemistry', *Angewandte Chemie International Edition*, 50: 3854-71.

Uysal, Naci, Gokhan Acik, and Mehmet Atilla Tasdelen. 2017. 'Soybean oil based thermoset networks via photoinduced CuAAC click chemistry', *Polymer International*, 66: 999-1004.

Vilela, Carla, Letizia Cruciani, Armando J. D. Silvestre, and Alessandro Gandini. 2011. 'A Double Click Strategy Applied to the Reversible Polymerization of Furan/Vegetable Oil Monomers', *Macromolecular Rapid Communications*, 32: 1319-23.

Vilela, Carla, Letizia Cruciani, Armando J. D. Silvestre, and Alessandro Gandini. 2012. 'Reversible polymerization of novel monomers bearing furan and plant oil moieties: a double click exploitation of renewable resources', *RSC Advances*, 2: 2966-74.

Vilela, Carla, Armando J. D. Silvestre, and Alessandro Gandini. 2013. 'Thermoreversible nonlinear diels-alder polymerization of furan/plant oil monomers', *Journal of Polymer Science Part A: Polymer Chemistry*, 51: 2260-70.

Wang, Haoran, and Qixin Zhou. 2018. 'Synthesis of Cardanol-Based Polyols via Thiol-ene/Thiol-epoxy Dual Click-Reactions and Thermosetting Polyurethanes Therefrom', *ACS Sustainable Chemistry & Engineering*, 6: 12088-95.

Wang, Qing, Guangxue Chen, Yanyan Cui, Junfei Tian, Minghui He, and Jian-Wen Yang. 2017. 'Castor Oil Based Biothiol as a Highly Stable and Self-Initiated Oligomer for Photoinitiator-Free UV Coatings', *ACS Sustainable Chemistry & Engineering*, 5: 376-81.

Wang, Tiansheng, Liping Li, Yongjian Cao, Qingwen Wang, and Chuigen Guo. 2019. 'Preparation and flame retardancy of castor oil based UV-cured flame retardant coating containing P/Si/S on wood surface', *Industrial Crops and Products*, 130: 562-70.

Wang, Tiansheng, Liping Li, Qingwen Wang, Guijun Xie, and Chuigen Guo. 2019. 'Castor oil based UV-cured coatings using thiol-ene click reaction for thermal degradation with flame retardance', *Industrial Crops and Products*, 141: 111798.

Wang, Z. K., Y. Q. Zhang, L. Yuan, J. Hayat, N. M. Trenor, M. E. Lamm, L. Vlaminck, S. Billiet, F. E. Du Prez, Z. G. Wang, and C. B. Tang. 2016. 'Biomass Approach toward Robust, Sustainable, Multiple-Shape-Memory Materials', *ACS Macro Letters*, 5: 602-06.

Wu, Wan-Xia, Jun Li, Xian-Ling Yang, Na Wang, and Xiao-Qi Yu. 2019. 'Lipase-catalyzed synthesis of renewable acid-degradable poly(β-thioether ester) and poly(β-thioether ester-co-ricinoleic acid) copolymers derived from castor oil', *European Polymer Journal,* 121: 109315.

Xia, Ying, and Richard C. Larock. 2010. 'Vegetable oil-based polymeric materials: synthesis, properties, and applications', *Green Chemistry*, 12: 1893-909.

Xu, Dongdong, Zhiyuan Cao, Tong Wang, Jiang Zhong, Jinze Zhao, Fei Gao, Xuyang Luo, Zhaoli Fang, Jinsong Cao, Suzhen Xu, and Liang Shen. 2019. 'An ambient-cured coating film obtained via a Knoevenagel and Michael addition reactions based on modified acetoacetylated castor oil prepared by a thiol-ene coupling reaction', *Progress in Organic Coatings*, 135: 510-16.

Yang, Xuejuan, Shouhai Li, Jianling Xia, Jian Song, Kun Huang, and Mei Li. 2015. 'Novel renewable resource-based UV-curable copolymers derived from myrcene and tung oil: Preparation, characterization and properties', *Industrial Crops and Products*, 63: 17-25.

Yang, Xuejuan, Chunpeng Wang, Shouhai Li, Kun Huang, Mei Li, Wei Mao, Shan Cao, and Jianling Xia. 2017. 'Study on the synthesis of bio-based epoxy curing agent derived from myrcene and castor oil and the properties of the cured products', *RSC Advances*, 7: 238-47.

Zhang, Dandan, Hongbo Liang, Jiang Bu, Lei Xiong, Shengmei Huang, D. D. Zhang, H. B. Liang, J. Bu, L. Xiong, and S. M. Huang. 2015. 'UV curable soybean-oil hybrid systems based on thiol-acrylate and thiol-ene-acrylate chemistry', *Journal of Applied Polymer Science*, 132: 42095.

Zheng, Kaiwen, Yazhou Tian, Mengjin Fan, Junying Zhang, and Jue Cheng. 2018. 'Recyclable, shape-memory, and self-healing soy oil-based polyurethane crosslinked by a thermoreversible Diels-Alder reaction', *Journal of Applied Polymer Science*, 135: 46049-49.

Zlatanic, Alisa, Charlene Lava, Wei Zhang, and Zoran Petrović. 2004. 'Effect of Structure on Properties of Polyols and Polyurethanes Based on Different Vegetable Oils', *Journal of Polymer Science Part B: Polymer Physics*, 42: 809-19.

Zuo, Hanqi, Zhiyuan Cao, Jinbing Shu, Dongdong Xu, Jiang Zhong, Jinze Zhao, Tong Wang, Yongming Chen, Fei Gao, and Liang Shen. 2019. 'Effect of structure on the properties of ambient-cured coating films prepared via a Michael addition reaction based on an acetoacetate-modified castor oil prepared by thiol-ene coupling', *Progress in Organic Coatings*, 135: 27-33.

Conclusion

The literature review of this chapter puts forth the notion that click chemistry is a known and useful tool in organic chemistry and polymer synthesis for the elaboration of high-performance macromolecular architectures. Consequently, the use of click chemistry to synthesize monomers or polymers derived from vegetable oils further renders the use of vegetable oils and their derivatives prevalent for a wide range of applications. Click chemistry reactions are efficient reactions that quite commonly abide the principles of green chemistry. We further examined the recently literature on the synthesis of materials using click chemistry from a green chemistry stand point, as functionalizing vegetable oils with the required moieties necessary for click chemistry does not always abide by green chemistry ideals.

In terms of the use of click chemistry reactions, thiol-ene additions has been the most common exploited reaction on vegetable oils. Nevertheless we fully cover the emergence of the Diels-Alder reaction as well as triazolinedione chemistry for the synthesis of advanced sustainable polymers. This analysis of the literature made it possible to understand and foresee the intricacies of using click chemistry as a means of synthesis, most notably the use of the DA reaction by the furan maleimide coupling. The use of the furan-maleimide DA reaction for the synthesis vegetable oil-based networks is in its infancy. As the furan-maleimide DA reaction is a thermally reversible click chemistry reaction that instills itself well in the ideals of green chemistry, it is also an established reaction for the synthesis of dissociative covalent adaptable networks (CANs). CANs have been known to display advanced properties such as recyclability and controlled end-of-life of materials. They contain dynamic cross-links which allows them to be reprocessed like thermoplastics, as well as maintain the benefits of thermosets. In dissociative CANs, cross-links are cleaved back into their individual reactive moieties before reforming again by exposure to a stimuli.

The thorough examination of the furan-maleimide DA reaction of this review was instrumental for the development of the following experimental chapters.

Chapter 2. Renewable responsive systems based on original on click and polyurethane cross-linked architectures with advanced properties

Chapter 1: State of the art – Click chemistry and vegetable oils

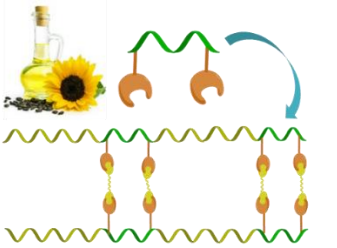

Chapter 2: Synthesis of Furan Oligomer and biobased PU CANs

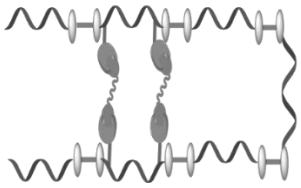

Chapter 3: Further elaboration of biobased PU CANs containing FO

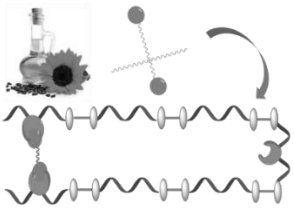

Chapter 4: Synthesis of Methyl oleate bismaleimide and biobased PU CANs

Introduction of Chapter 2

The literature review showed (i) the richness of click chemistry on vegetable oils, thus making it possible to obtain materials with varied and original properties and (ii) the latest progress made (academic and industrial) for the sustainable production of these architectures.

The objective of the work described in this chapter is to synthesize biosourced polyurethane architectures with crosslinking points. These cross-linking points consist of a reversible click covalent bonds, formed by the Diels-Alder reaction between a furan and maleimide functions that can undergo a reversion reaction by the retro-Diels-Alder reaction. To achieve this, a diol structure containing pedant furan rings is synthesized from oleic acid derived from sunflower oil denoted the Furan Oligomer (FO). The purpose of synthesizing a molecule with such an architecture is to utilize the hydroxyl groups to incorporate the molecule into the polyurethane chain and use the pendant furan groups for cross-linking site with the use of widely available bismaleimide molecules. The FO was synthesized in three reactional steps and fully characterized. The furan group was first functionalized on the fatty acid via an esterification reaction with furfuryl alcohol at the end of the carboxylic acid chain. The double bond located between the ninth and tenth carbon of the fatty chain was then epoxidized. The FO was obtained by the ring opening polymerization (ROP) by acid catalysis. Different polyurethane materials were synthesized with varied crosslinking densities. They were prepared by varying the ratio between the polyester polyol derived from fatty acids of rapeseed oil and FO reacted with hexamethylene diisocyanate. These materials were crosslinked with a short bismaleimide based on polypropylene oxide. The physical, mechanical and self-repair properties of these different materials were studied.

Renewable responsive systems based on original click and polyurethane cross-linked architectures with advanced properties

Khantutta-Kim Tremblay-Parrado[1], Luc Avérous*[,1]

(1) BioTeam/ICPEES-ECPM, UMR CNRS 7515, Université de Strasbourg, 25 rue Becquerel, 67087 Strasbourg Cedex 2, France

(*) Corresponding author: luc.averous@unistra.fr

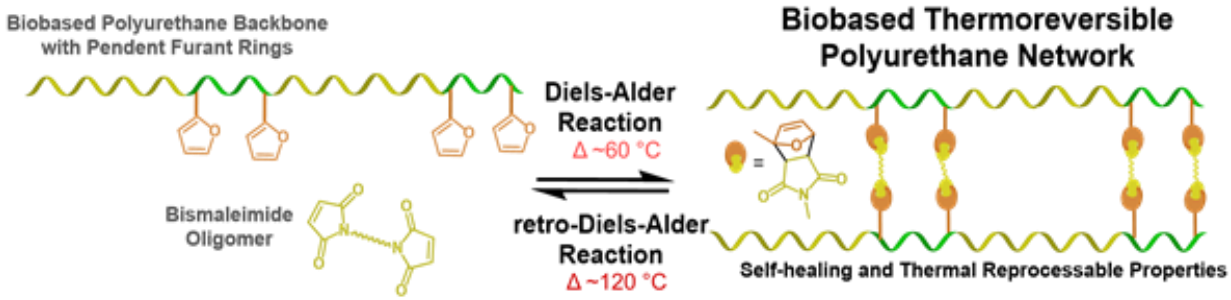

1. Abstract

A new chemical architecture from oleic acid, consisting of a diol structure containing pendant furan rings denoted the Furan Oligomer (FO) was synthesized and fully characterized. The FO was integrated into a linear rapeseed-based polyurethane (PU) backbone and cross-linked via Diels-Alder (DA) reaction by using the pendant furan rings and a short polypropylene oxide based bismaleimide. This is the first time a thermo-reversible PU network based on vegetable oil is reported. The effects of varying proportions of FO in linear and cross-linked systems, by DA, were studied. These materials were analyzed by classic characterization techniques. The stability and recyclability of the cross-linked materials were shown by successive reprocessing cycles and reanalyzing the mechanical properties. Self-healing properties were macroscopically exhibited and investigated by tensile tests of healed materials. The resulting cross-linked materials present a large range of properties such as tunable mechanical and thermoresponsive behavior, good thermal recyclability and self-healing abilities.

Keywords: Renewable Resources, Oleic acid, Biobased polymers, Polyurethane, Diels-Alder Cycloaddition

2. Introduction

Nowadays, developing biobased and environmentally friendly materials is not enough. Science has to face developing advanced materials with extended lifetimes and with a controlled end-of-life. Polymer materials with innovative architectures allowing for cutting-edge properties such as self-healing and reprocessability, do not only extend the life of end-user materials, but also allow for the reduction of energy use, resources and waste. Polyurethanes (PUs) are of particular interest to integrate these novel properties due to their global versatility. PUs are used for a wide range of applications such as adhesives, coatings, and in the automotive and construction industry (Haponiuk and Formela 2017). Their production is ranked 6th among all polymers (Carré et al. 2019), with a planned production of approximately 23 million tons in 2019 (Akindoyo et al. 2016). Although the biobased PU market is expanding, limited work has been conducted to explore the development biobased PUs with particular architectures to allow for dynamic and adaptable materials. Developing biobased materials and PUs is a starting point to a circular economy, but, by designing biobased PUs with dynamic architectures, this truly takes in to account the cradle-to-grave reasoning of materials to facilitate recyclability and the extension of material lifetimes.

To develop renewable materials, vegetable oils have a particular importance because they are abundantly available at rather low costs, with attractive chemical structures for rich chemistry (Lligadas et al. 2013). Soybean oil is the most abundantly produced vegetable oil and has been particularly explored by academics and industrials for PU thermoset applications (Meier, Metzger, and Schubert 2007; Desroches, Escouvois, et al. 2012; Lligadas et al. 2013). Studies reporting the use of vegetable oils to synthesize diols for linear thermoplastic PUs (TPUs) include (i) the use of methyl oleate and ricinoleic acid through transesterification, epoxidation, ring-opening of epoxides and thiol-ene addition (Palaskar et al. 2012), (ii) methyl ester of rapeseed oil through transesterification and thiol-ene coupling (Desroches, Caillol, et al. 2012), (iii) polyricinoleate diol by polycondensation (Petrović et al. 2008; Xu et al. 2008) and (iv) the dimerization of rapeseed oil fatty acids at high temperature by a Diels-Alder (DA) mechanism (Ionescu 2005). Consequently, the use of vegetable oils for the development of biobased PUs is a favorable starting point. Nevertheless, there is an apparent lack, particularly at the industrial level, in the development of

advanced biobased PUs materials with dynamic architectures for a well-thought-out reflection of the extension of polymer material lifetimes.

To extend the lifetime of polymers, many efforts have been made to develop dynamic and reversible polymers. Such a behavior is based on the development of dynamic covalent bonds that can be formed and cleaved by exposure to an external stimulus or autonomously. Cross-linked polymers containing reversible covalent bonds are defined as Covalent Adaptive Networks (CANs) (Kloxin et al. 2010) and can be further subdivide in two categories, dissociative and associative systems (Denissen, Winne, and Du Prez 2016). Associative CANs consists of bond exchange between polymer chains, where the overall cross-linking density is preserved because a new covalent bond can only be formed if another has been broken, such as vitrimers (Montarnal et al. 2011), which can also be biobased (Dhers, Vantomme, and Avérous 2019). Dissociative CANs consist of chemical bond exchanges in which bonds are first broken and then formed again in another place. Reversible covalent bonds such as the DA (Sanyal 2010) reaction or alkoxyamine (Otsuka et al. 2007) chemistry can be used. As highlighted by the work of Gandini and co-workers, the thermoreversible furan-maleimide [4+2] cycloaddition DA reaction is the most extensively studied reversible covalent bond of dissociative CANs used in the synthesis of macromolecular architectures (Gandini et al. 2018; Gandini et al. 2016; Lacerda and Gandini 2014; Gandini 2013). The DA reaction between a furan and maleimide moiety is considered to be a click cycloaddition reaction, which generally occurs at moderate temperature (below 90 °C) and the reverse reaction, which is denoted as the retro-DA (r-DA) reaction, occurs between 110 and 130 °C (Chen et al. 2002). The reactivity and reversibility of the DA and r-DA reactions can be tuned significantly depending on the substituents located on a furan and maleimide moiety (Boutelle and Northrop 2011). Several biobased CANs have been synthesized using the thermoreversible DA reaction derived from lignins (Duval et al. 2015; Buono et al. 2017), tannins (Duval et al. 2017), alginate (García-Astrain and Avérous 2018), chitosan (García Astrain et al. 2016; Guaresti, García–Astrain, et al. 2018; Guaresti, García Astrain, et al. 2018), starch (González et al. 2018) or vegetable oils (Gandini et al. 2018).

Use of the DA reaction in PUs is of particular interest because it is believed that the shape memory behavior of PUs facilitates the self-healing by DA reaction (Heo and Sodano 2014). Consequently,

reversibly cross-linked PUs have been studied through a multitude of different strategies (Truong et al. 2018; Truong et al. 2019; Willocq et al. 2017; Irusta, Fernandez-Berridi, and Aizpurua 2017; Dolci et al. 2015; Dolci et al. 2017; Lakatos et al. 2016; Du et al. 2016; Rivero et al. 2014). Nevertheless, very few studies have explored the use of biobased PUs as a canvas to investigate reversibly cross-linked polymers. Gu *et al*. synthesized a biobased TPU backbone using a renewable polylactide copolymer diol and 2,5-furandimethanol as a soft segment and chain extender respectively. The reversible covalent bonds were located in the hard segments where, at which the DA reaction took place between the furan ring of the chain extender and bismaleimide (BMI) (Gu and Wu 2018). Wilson *et al.* synthesized an original C_{11} difuranic diol from furfural and 5-hydroxymethylfurufral, which they used to synthesize polyesters and reversibly cross-linked polyurethanes networks with a BMI (Wilson and Chen 2019).

Herein, we produced reversibly cross-linked PUs based on vegetable oils using thermally reversible furan-maleimide DA reaction. We synthesized a new chemical architecture from oleic acid, consisting of a diol structure, containing pendant furan rings, which was thoroughly characterized and denoted as the Furan Oligomer (FO). As depicted in Scheme 2.1, FO was incorporated into the linear polymer backbone and further cross-linked with the use of a BMI based on polypropylene oxide (PPO BMI). The corresponding materials with varying cross-linker contents were tested as remendable and self-healing PUs.

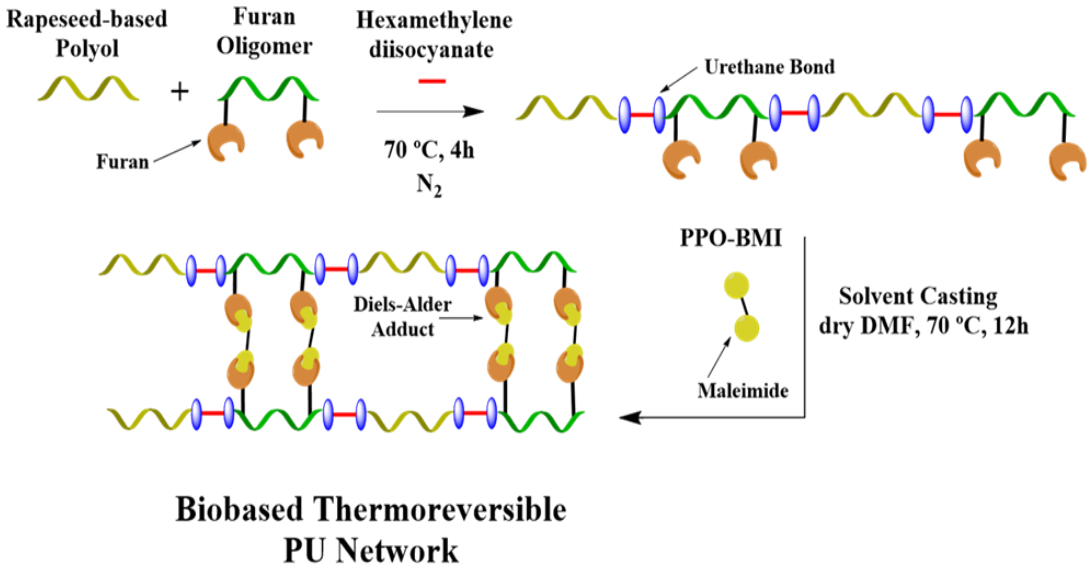

Scheme 2.1 – Illustration of the general synthesis of biobased thermoreversible PU-based systems from FO.

3. Experimental Section

3.1. Reagents and materials

Octadec-9-enoic acid (OA) from sunflower oil was kindly supplied by ITERG. It is a technical grade fatty acid with an acid value of 185 mg KOH per g. Furfuryl alcohol (FA, 98%), 4-dimethylaminopyridine (DMAP, 99%), hydrogen peroxide (H_2O_2, 30% *w/v* aqueous solution), 2-chloro-4,4,5,5-tetramethyl-1,3,2-dioxaphospholane (CL-TDP, 95%), chromium(III) acetylacetonate (99.99%), cholesterol (>99%), [D_6]dimethyl sulfoxide (DMSO, 100%, 99.96% atom D) were purchased from Sigma Aldrich; N,N'-dicyclohexylcarboiimide (DCC, 99%), $HSbF_6$ (65% *w/w* aqueous solution) were purchased from Alfa Aesar; hexamethylene diisocyanate (HDI, 99%), chloroform-d ($CDCl_3$, 100%, 99.96% atom D) were purchased from Acros Organics; dichloromethane (dried over molecular sieve, DCM, >99%, stabilized with amylene), diethyl ether (stabilized with BHT) were purchased from Carlo Erba; toluene (100%,) was purchased from VWR Chemicals; glacial acetic acid (GAA, >99%), N,N-dimethylformamide (DMF, 99.8%) was purchased from Fisher Scientific; and amberlite IR-120 H from Fluka Chemicals. Biobased polyester polyol (purchased from Oleon) was derived from dimeric fatty acids from rapeseed oil with purity greater than 98% and MW around 3 000 g mol^{-1}. Hydroxyl and acid values were 33 and 0.253 mg per gram of KOH, respectively. The poly(propylene oxide) based bismaleimide (degree of polymerization (DP) = 3) cross-linker was purchased from Specific Polymers (Castries, France). 2,3,4,5,6-pentafluorobenzaldehyde (PFB,98%) was purchased from fluorochem.

3.2. Syntheses and material processing

3.2.1. Esterification of Furan-2-ylmethanol and Octadec-9-enoic Acid from sunflower oil

The esterification of Octadec-9-enoic acid (OA) was adapted from Vilela *et al*. and Rauf *et al*. (Vilela et al. 2011; Rauf and Parveen 2004), for an esterification conducted under mild conditions. A solution included one molar equivalent of OA, *N,N'*-dicyclohexylcarboiimide (DCC, 1.1 mol equiv.), 4-dimethylaminopyridine (DMAP, 0.1 mol equiv.) in 25% *w/v* of dried dichloromethane (DCM) was stirred magnetically for 1 h in a two-necked round bottom flask at room temperature. Furfuryl Alcohol (FA, 1.1 mol equiv.) was then added dropwise through a dropping funnel. The

reaction mixture was left stirring overnight at room temperature and under nitrogen. *N,N'* – dicyclohexylurea (DCU) formed during the reaction, precipitated, and was filtered off. The filtrate was washed twice with water, twice with 5% acetic acid solution, and finally again with water until a neutral pH was attained. The organic phase was dried over anhydrous sodium sulphate. The solvent was evaporated under reduced pressure. The ester formed, Furan-2-ylmethyl-octadec-9-enoate (FMO) was then further purified over a silica gel plug using petroleum ether/diethyl ether (95:5, *v/v*) as eluents to remove remnants of DCU. FMO was dried under vacuum overnight vacuum, at 50 °C.

Furan-2-ylmethyl-octadec-9-enoate (FMO) - ^{1}H NMR (400 MHz, $CDCl_3$): δ = 7.41 (dd, 1H; 5-H of 2-furan)), 6.39 (d, 1H; 3-H of 2-furan), 6.36 (dd, 1H; 4-H of 2-furan), 5.34 (m, 2H; C*H*=C*H*), 5.06 (s, 2H; OCH_2) 2.32 (t, 2H; CH_2C(=O)), 1.99 (m, 2H; CH=CHCH_2) 1.62 (m, 2H; CH_2CH_2C(=O)), 1.37-1.18 (m, 20H; aliphatic CH_2), 0.88 (t, 3H; CH_3). ^{13}C NMR (500 MHz, $CDCl_3$,): δ = 173 (*C*=O), 150 (C-2 of 2-furan), 143 (C-5 of 2-furan), 130 (*C*H=CH), 130 (CH=*C*H), 111 (C-3 of 2-furan), 111 (C-4 of 2-furan), 57.9 (O*C*H_2–2-furan), 34.2 (*C*H_2–C(=O)), 31.9-22.7 (aliphatic *C*H_2), 14.1 (*C*H_3)

3.2.2. Epoxidation of Furan-2-lymethyl-octadec-9-enoate (FMO)

The epoxidation of FMO was conducted by the in situ formation of peracetic acid from glacial acetic acid (GAA) and H_2O_2, and was adapted from Arbenz et al (Arbenz, Perrin, and Avérous 2017). In a two-necked, round bottom flask, equipped with a magnetic stirrer and a dropping funnel, FMO (1 mol equiv. of unsaturations), amberlite IR-120 H (25 wt% of FMO), GAA (0.2 mol equiv.) was inserted into the flask and dissolved in toluene (12.5 wt% w/v). The solution was stirred to 70 °C and then H_2O_2 (1.2 mol equiv.) was added dropwise. The mixture was stirred at 70 °C for 7 h. In comparison to current literature (Petrović et al. 2002; Arbenz, Perrin, and Avérous 2017), a lower amounts acetic acid and H_2O_2 but increased toluene content, are required to yield a high conversion of the alkene bond into an epoxy moiety, while minimizing the hydrolysis of the newly formed ester bond. Optimization trials of the stoichiometry of reactional components can be found in SI Table S2.5. Amberlite IR-120 H was filtered off and the solution was washed with distilled water until a neutral pH was attained. The organic phase was dried with anhydrous sodium sulphate and then filtered. The solvent was evaporated under reduced pressure.

Epoxidized FMO (EFMO) was dried under vacuum overnight, at 50 °C. The reaction product, Furan-2-ylmethlyl 8-(3-octyloxiran-2-yl)octonoate (FMOO), was clear yellow oil.

Furan-2-ylmethlyl 8-(3-octyloxiran-2-yl)octonoate (FMOO) - ^{1}H NMR (400 MHz, $CDCl_3$): δ=7.41 (dd, 1H; 5-H of 2-furan)), 6.39 (d, 1H; 3-H of 2-furan), 6.36 (dd, 1H; 4-H of 2-furan), 5.06 (s, 2H; OC*H*$_2$), 2.90 (m, 2H; C*H*OC*H*), 2.32 (t, 2H; C*H*$_2$C(=O)), 1.62 (m, 2H; C*H*$_2$CH$_2$C(=O)), 1.37-1.18 (m, 24H; aliphatic C*H*$_2$), 0.88 (t, 3H; C*H*$_3$). ^{13}C NMR (500 MHz, $CDCl_3$): δ = 174 (*C*=O), 150 (C-2 of 2-furan), 143 (C-5 of 2-furan), 111 (C-3 of 2-furan), 111 (C-4 of 2-furan), 57.9 (O*C*H$_2$–2-furan), 57.2 (H*C*-*O*-*C*H), 34.2 (*C*H$_2$–C(=O)), 31.9-22.7 (aliphatic *C*H$_2$), 14.1 (*C*H$_3$)

3.2.3. Oligomerization of epoxidized Furan-2-lymethyl-octadec-9enoate (FMOO)

H_2O (0.7 mol equiv.) was added to FMOO (1 mol equiv.) in a two-necked round bottom flask and stirred mechanically. A cationic initiator, $HSbF_6$ (1.5 wt% of FMOO) was added dropwise. The mixture was stirred at room temperature for 1 h. The reaction was quenched by the addition of water and dissolved in diethyl ether. The organic solution was washed with a 5% sodium bicarbonate solution and distilled water until a neutral pH was attained. The solution was dried over anhydrous sodium sulfate and filtered. The solvent was evaporated under reduced pressure and the oligomer was dried under vacuum overnight, at 50 °C. The oligomerization resulted in FO as an orange, clear, viscous oil.

Furan Oligomer: ^{1}H NMR (400 MHz, $CDCl_3$): δ = 7.41 (dd, 1H; 5-H of 2-furan)), 6.39 (d, 1H; 3-H of 2-furan), 6.36 (dd, 1H; 4-H of 2-furan), 5.06 (s, 2H; OC*H*$_2$), 3.80 - 2.82 (m; polyether backbone), 2.32 (t, 2H; C*H*$_2$C(=O)), 1.62 (m, 2H; C*H*$_2$CH$_2$C(=O)), 1.37-1.18 (m, 24H; aliphatic C*H*$_2$), 0.88 (t, 3H; C*H*$_3$. ^{13}C NMR (500 MHz, $CDCl_3$): δ = 174 (*C*=O), 150 (C-2 of 2-furan), 143 (C-5 of 2-furan), 111 (C-3 of 2-furan), 111 (C-4 of 2-furan), 85.0-70.0 (polyether backbone *C*-O-*C*), 57.9 (O*C*H$_2$–2-furan), 34.2 (*C*H$_2$–C(=O)), 31.9-22.7 (aliphatic *C*H$_2$), 14.1 (*C*H$_3$)

3.2.4. Model reaction between FO and N-methylmaleimide

FO (200 mg, 0.378 mmol of furan) was dissolved in [D_6]DMSO (2 mL) in a 10 mL round bottom flask. *N*-methylmaleimide (0.378 mmol of maleimide) was added to obtain a furan/maleimide ratio of 1:1 (mol/mol). The solution was placed in an oil bath regulated to 65 °C and samples (200

µL) were taken at regular intervals over 5 days. The samples were further diluted to 650 µL and analyzed by ^{1}H NMR spectroscopy to determine the reaction conversion and *endo*/*exo* ratio of the DA adducts.

3.2.5. Diels-Alder and retro-Diels-Alder Reaction between FO and a bismaleimide

FO and a PPO-based BMI were mixed together in a small flask at a 1:1 furan/maleimide ratio (mol/mol) and dissolved in DMSO at 40 wt% concentration. The sample was heated in an oven at 60 °C without stirring. Once gelation occurred (typically after 24 h), sample were heated to 120 °C for 1 h in an oven to perform the r-DA reaction, and the mixture returned to a liquid state. The sample underwent the same cycle one more time. After cross-linking in solution, the gel was washed with water and dried in an oven at 40 °C under vacuum. The gel was analyzed by FTIR spectroscopy comparison with the initial mixture of FO and BMI.

3.2.6. Synthesis of PUs containing FO

All glassware and reactants were previously dried. Four different kinds of polyurethanes films were prepared with varying amounts of FO (0%, 10%, 20% and 30% of total the hydroxyl value required was derived from the FO, for example, for FO-20%, 2.96 mmol OH from FO). Under nitrogen, in a three-necked, round bottom flask, biobased rapeseed polyester polyol (11.8 mmol OH) and FO (2.96 mmol OH) was added to hexamethylene di-isocyanate (HDI, 15.5 mmol NCO) and the mixture was mechanically stirred at 70 °C for 3-4 h. The ratio –NCO/-OH functional groups were fixed to 1.05 in all cases.

3.2.7. Cross-linking of PUs containing FO

The PU was dissolved in dry DMF. To this, BMI was added in a 1:1 furan/maleimide ratio (mol/mol). The reaction mixture was stirred at 70 °C for 12 h to allow for the DA adducts to form. The solution was poured into a polyetrafluoroethylene (PTFE) mold and put into the oven to evaporate the solvent (70 °C, 48 h). Solvent traces were removed by placing material under vacuum at 70 °C for 24h.

3.2.8. Material reprocessing of cross-linked PUs

PU films are reprocessed by compression molding in a tile mold (10 cm x 10 cm x 1 mm) at 150 °C in LabTech Scientific press hot press. First, the films were cut in several small pieces and placed in the center of the tile and left to undergo a 10 min preheating cycle to soften the material. This was followed by several venting steps and the material was pressed with a constant applied force of 16 MPa between the two plates. The square materials were then cured at 60 °C in the oven for 48 h and post cured for 24 h at room temperature.

3.2.9. Study of the self-healing behavior

The macroscopic self-healing ability of material PU-FO-30XL was determined by observing how a dumbbell-shaped sample cut in half healed. To accomplish this, a dumbbell-shaped sample was cut in half in the middle and subsequently healed by placing the halves in contact for 1 h at 120 °C, followed by 60 °C overnight and 24 h at room temperature.

3.3. Methods

3.3.1. Acid value

Acid value (AV) was determined according to ISO 660. OA (≈0.1 g) of was dissolved in a 50:50 solution (50 mL) of ethanol and diethyl ether. One drop of phenolphthalein solution, used an indicator, was added to the solution. Then titration is performed with 0.1M potassium hydroxide (KOH) aqueous solution. AV is express in mg of KOH per gram OA, according to Equation (1):

$$AV = \frac{(V_{eq} * C) * 56.1}{Ws} \quad (1)$$

in which V_{eq} (mL) is the titration equivalent volume, C ($molL^{-1}$) is the concentration of KOH solution and W_s (g) is the weight of OA.

3.3.2. Iodine value

Iodine value (IV), known as the measure of the double bond content, was determined using the Wijs method. This result is expressed in grams I_2 per 100 g of sample. A sample (0.5 g) was dissolved in a 50:50 mixture (20 mL) of cyclohexane and GAA. Then, the Wijs solution (25 mL,

0.1M) composed of iodine chloride in GAA was added; the corresponding solution was stirred for 1 h in the dark. Then, a 10 wt% potassium iodide aqueous solution (20 mL) and water (150 mL) was added to quench the reaction. The solution was then titrated with a 0.1 M solution of $Na_2S_2O_3$ with starch solution as indicator. IV (in I_2 g/100 g) was determined according to Equation (2):

$$IV = \frac{(V_{blank} - V_s) * C * 126.9}{Ws} * 100 \quad (2)$$

in which V_{blank} (mL) and V_S (mL) are the volumes of solution of $Na_2S_2O_3$ required for blank and sample titrations, respectively; C ($molL^{-1}$) is the concentration of $Na_2S_2O_3$ solution; and W_S (g) is the sample weight. It is important to note that Wijs method does not involve a reaction with the conjugated double bonds of the furan ring.

3.3.3. NMR spectroscopy

All NMR spectra were recorded on a Bruker Ascend 400 or 500 MHz spectrometer. Sample were dissolved in deuterated chloroform ($CDCl_3$) or deuterated dimethyl sulfoxide ([D_6]DMSO) with concentrations varying between 8-10 and 20-30 mg mL^{-1} for ^{1}H-NMR and ^{13}C-NMR spectroscopy, respectively. The number of scans was set to 128 for ^{1}H-NMR spectroscopy and 2048 for ^{13}C-NMR spectroscopy. The calibration of ^{1}H-NMR and ^{13}C-NMR spectra was performed using the chloroform peak at δ = 7.26 and 77.16 ppm, respectively and DMSO peak at δ=2.50 ppm.

^{31}P NMR analysis was performed on FO and polyester polyol samples phosphytilated with 2-chloro-4,4,5,5-tetramethyl-1,3,2-dioxaphospholane. Cholesterol was used as an internal standard, as described in standard protocols (Spyros 2002). Scans (128) were recorded with a 15 s delay and a spectral width of 80 ppm (180-100 ppm).

For quantitative ^{1}H NMR spectroscopic analysis, FO (≈ 20 mg) was dissolved in [D_6]DMSO (0.5 mL) before the addition standard solution (100 µL) of pentafluorobenzaldehyde in [D_6]DMSO; 32 scans were collected 10 s delay.

3.3.4. Fourier transform infrared (FTIR) spectroscopy

FTIR spectroscopy was performed using a Nicolet 380 FTIR spectrometer in reflection mode equipped with an ATR diamond module (FTIR-ATR). A background spectrum was collected before each sample was analyzed (32 scans, resolution 4 cm^{-1}).

3.3.5. Mass spectroscopy – MALDI-TOF

Mass spectra were acquired on a time-of-flight mass spectrometer (MALDI-TOF-TOF Autoflex Speed LRF, Bruker Daltonics, Bremen, Germany) equipped with a nitrogen laser (λ = 337 nm). An external multi-point calibration was carried out before each measurement. Scan accumulation and data processing were performed with FlexAnalysis 3.0 software. 2,5-dihydroxybenzoic acid (DHB) was obtained from Sigma-Aldrich. Matrix solutions was freshly prepared: DHB was dissolved to saturation in a H_2O/CH_3CN/HCOOH (50:50, 1%) solution. Typically, a mixture (0.5 µL) containing the sample solution and the matrix (1:1) was deposited on the stainless-steel plate.

3.3.6. Rheological measurements

Time required to form a gel between FO and BMI at 60 °C (gelation time, t_{gel}) was determined by dynamic oscillatory rheology measurements performed on a TA Instruments Discovery HR-3 using ETC parallel geometry; 25 mm upper plate and 60 mm lower plate. The viscometer was equipped with a Peltier system for temperature control. The evolution of storage (G´) and loss (G´´) modulus was measured at 60 °C at a constant shear strain (1%) and at 1 Hz. The gel point was considered as the time where the curves of storage and loss moduli crossover at a fixed temperature and frequency.

3.3.7. Thermal gravimetric analysis (TGA)

TGA was performed using a TA Instrument Hi-Res TGA Q5000 at a heating rate of 10 °Cmin^{-1} from room temperature to 700 °C under nitrogen atmosphere (flow rate 25 mL min^{-1}). Sample weighed between 1-3 mg.

3.3.8. Differential scanning calorimetry (DSC)

DSC was performed using a TA Instrument Q200 under nitrogen flow (50 mL min^{-1}). Samples of 1-3 mg were sealed in standard aluminum pans. Depending on the information to be acquired,

different heating runs were performed. For the qualitative studies on the DA adduct and r-DA, the FO and PPO-based BMI mixtures were heated up from -30 °C to 175 °C with a heating ramp of 2.5 °C min^{-1}. The glass transition temperature (T_g) of cross-linked materials were recorded using a single heating ramp, from -80 °C to 175 °C at 10 °C min^{-1}. The T_g of the non-cross-linked materials were recorded using cyclic procedure involving a heating ramp from -80 °C to 175 °C at 10 °C min^{-1}, followed by a cooling ramp down to -80 °C at 5 °C min^{-1} and finally a second heating to 175 °C at 10 °C min^{-1}. The temperature was kept constant for 2 min at the end of each temperature ramp.

3.3.9. Uniaxial tensile tests

Tensile properties of materials were determined with an Instron tensile testing machine (model 5567 H, USA), at a rate of 20 mm min^{-1}, using dumbbell specimens (dimensions: 30 X 5 X 1 mm^3). For each formulation at least five dumbbell samples were tested.

3.3.10. Swelling Index and gel content determination

Swelling measurements of the polymer networks were carried out in DMF. The swelling percentage was determined using the weight difference between dried and swollen samples. The sample (written m_i and ranging from 10 to 20 mg) was immersed in solvent (15 mL). After 24h, the sample was removed from the solution, the surfaces were dried superficially with filter paper, and the weight was recorded (m_s). Three repetitions were conducted for each material. For each sample, a swelling ratio (SR) was calculated according to the Equation (3):

$$SR = \frac{m_s - m_i}{m_i} * 100 \ (3)$$

The sample was then dried in a vacuum oven at 40 °C for 24 h. The resulting weight was recorded (m_f) and the insoluble fraction (IF) was calculated according to the Equation (4):

$$IF = \frac{m_f}{m_i} * 100 \ (4)$$

4. Results and Discussion

4.1. Analysis of the synthesis of FO

The acid moiety and alkene site of octadec-9-enoic acid (OA) were used as reaction sites to yield an oligomer with a diol structure containing pendant furan rings (Scheme 3.1). OA was esterified using furan-2-ylmethanol (FM) at ambient temperature to yield furan-2-ylmethyl-oleate (FMO). The advantage of this type of esterification reaction (Steglich esterification) is that no energy source is required; thus minimizing the global energy requirement, in agreement with one of the main principles for a green chemistry (Vilela et al. 2012). Nevertheless, this esterification reaction can also be accomplished using *Candida Antarctic* lipase B, an enzymatic catalyst, with greener conditions as explored by Sengupta *et al* (Sengupta et al. 2012). More recently, Muthusamy *et al.* used the same enzymatic catalyst to obtain furan based oligoesters (Muthusamy et al. 2018). The use of enzymes as green catalysts for macromolecular synthesis has become prevalent in the recent years, as highlighted by Kobayashi and co-workers (Shoda et al. 2016). The FTIR spectrum of FMO exhibits a predominant band at $\tilde{\nu}$ = 1738 cm^{-1}, which confirms the presence of an ester carbonyl group, and the furan heterocycle bands at $\tilde{\nu}$ = 1503, 1375, 1347, 1228, 1080, 920, 885, 739 and 599 cm^{-1} (Figure 2.1-b). The appearance of the resonances of the methylene protons of the ester moiety at δ = 5.1 ppm and the furan ring protons at δ = 6.36, 6.39, and 7.41 ppm in the ^{1}H NMR spectrum of FMO confirms the expected structure (Figure 2.2-b). The technical grade oleic acid received contained small amounts of ethyl ester impurities because the saponification of the triglycerides took place in ethanol. This is evidenced by the quartet signal associated with the CH_2 of the ethyl ester at δ = 4.21 ppm. The results of ^{13}C NMR spectroscopic analysis of FMO agreed with the assigned structure (Figure S2.11) in the supplementary information (SI) in section 7.

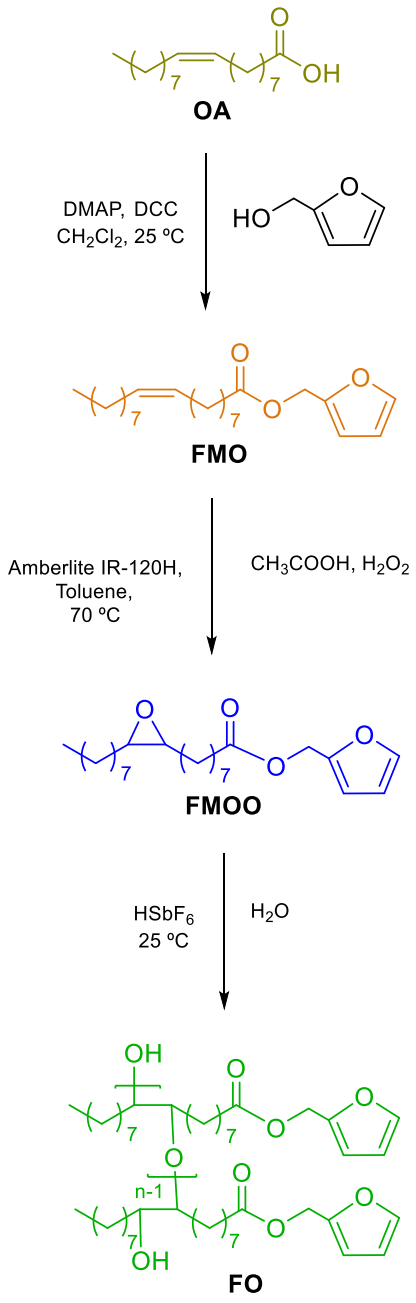

Scheme 2.2 – Global reaction pathway of FO. DMAP=4-dimethylaminopyridine, DCC=N,N'-dicyclohexylcarboiimide, FMO=furan-2-ylmethyl oleate, FMOO=furan-2-ylmethlyl 8-(3-octyloxiran-2-yl)octonoate.

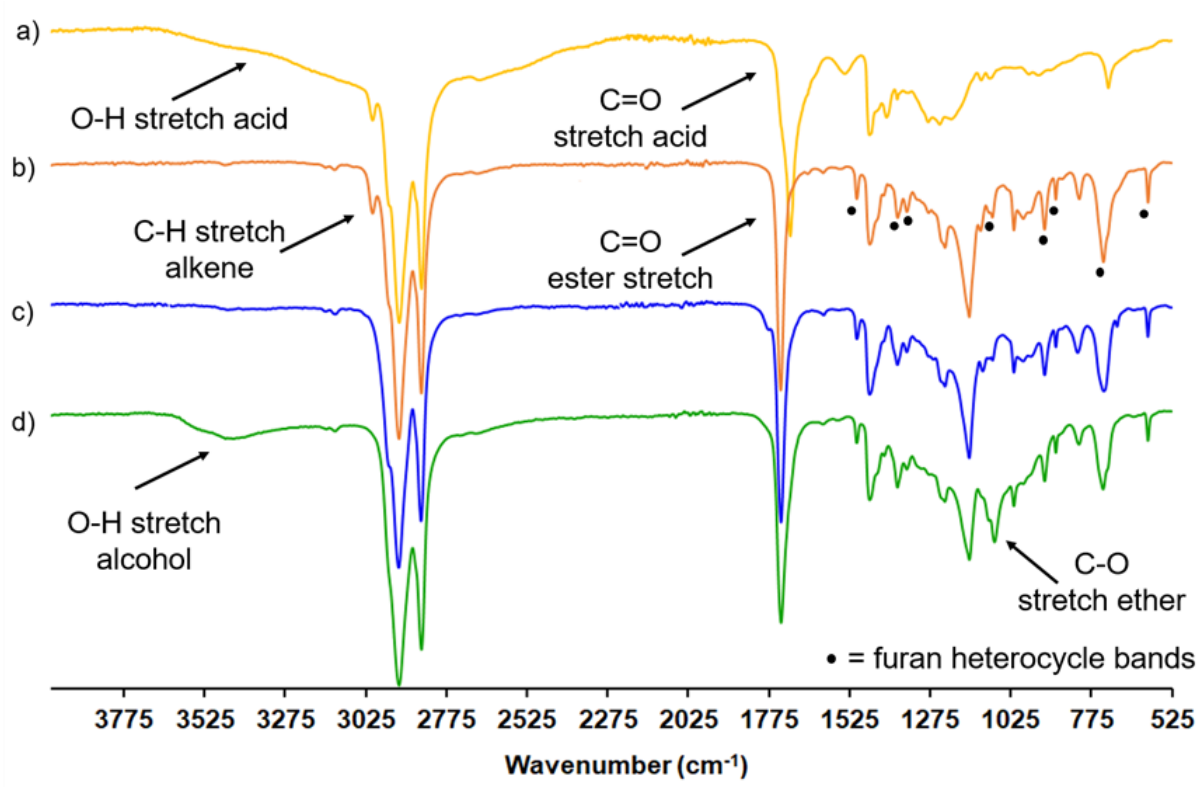

Figure 2.1 – FTIR spectra of (a) OA, (b) FMO, (c) FMOO, and (d) FO.

Thereafter, FMO underwent an in situ epoxidation with the use of GAA, H_2O_2, and acid catalyst in toluene to yield furan-2-ylmethlyl 8-(3-octyloxiran-2-yl)octonoate (FMOO). GAA is converted to the oxidizing agent peroxyacetic acid and is regenerated. This type of epoxidation is nowadays routinely used on vegetable oils (Petrović et al. 2002). Compared to conventional academic epoxidation based on *meta*-chloroperoxybenzoic acid (mCPBA) as an oxidizing agent in solvent (Kim, Traylor, and Perrin 1998), in situ epoxidation uses milder oxidizing agents and globally adheres better to green chemistry principles. The FTIR spectrum of FMOO (Figure 2.1-c) shows the disappearance of the double bonds at $\tilde{\nu}$ = 3009 cm^{-1}. By ^{1}H NMR spectroscopic analysis (Figure 2.2-c), the structure is confirmed by the disappearance of the vinyl and allyl protons at δ = 5.35 and 1.99 ppm respectively, and by the appearance of the epoxide and protons alpha to the epoxides at δ = 2.90 and 1.45 ppm respectively. The results of ^{13}C NMR spectroscopic analysis of FMOO agreed with the assigned structure (Figure S2.12 in SI).

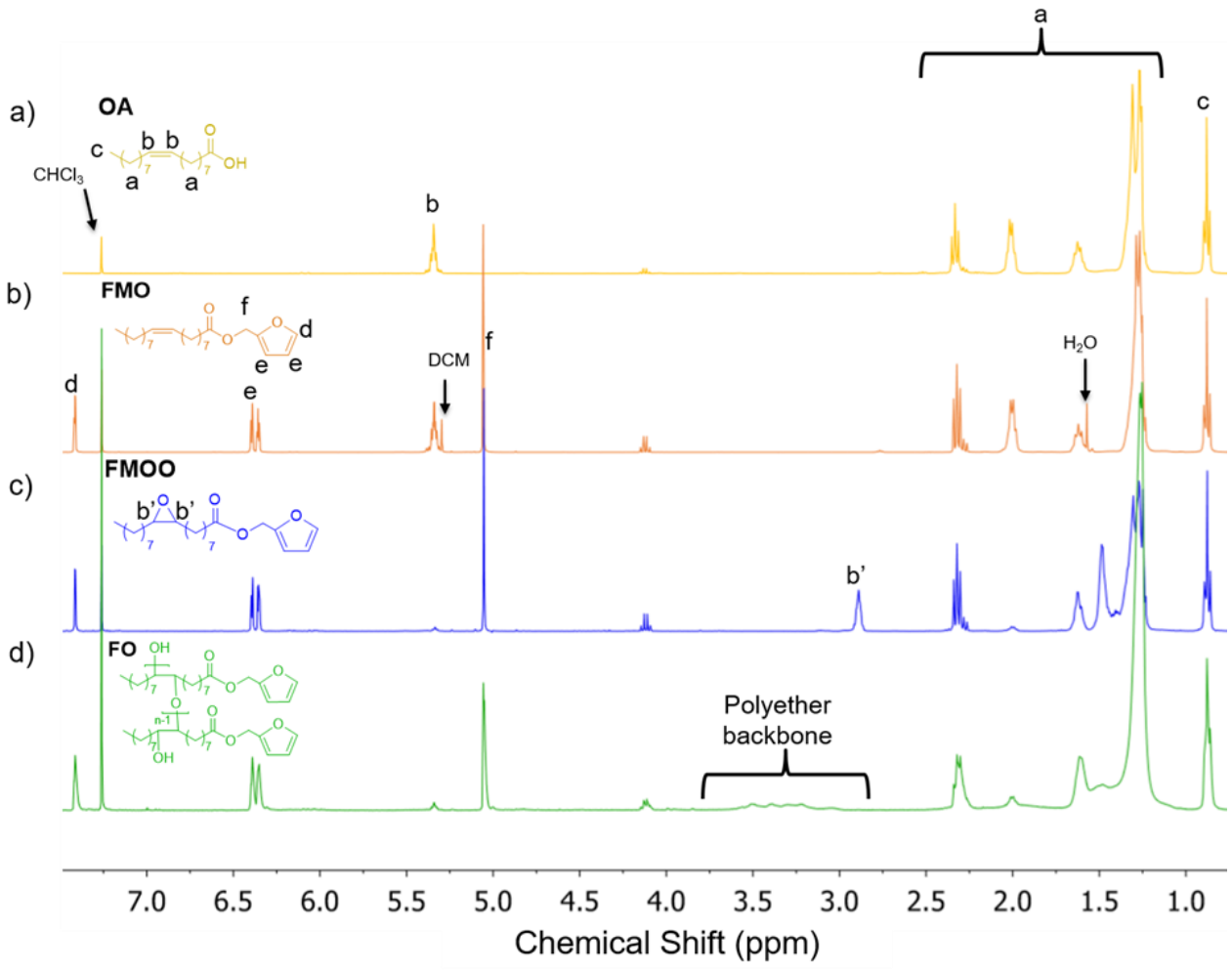

Figure 2.2 – ^{1}H NMR spectra of (a) OA, (b) FMO, (c) FMOO, and (d) FO.

An oligomer polyether diol was finally obtained by the acid-catalyzed ring-opening polymerization (ROP) of FMOO and denoted as Furan Oligomer (FO). This cationic polymerization was accomplished using fluoroantimonic acid, $HSbF_6$, because it predominantly achieved oligoether species (Lligadas et al. 2006). It was observed that 1.5 wt % of initiator was required to achieve complete oligomerization. The reaction was performed in bulk and followed by ^{1}H NMR spectroscopic analysis. The FTIR spectrum (Figure 2.1-d) exhibits the broad stretch of the hydroxyl groups at $\tilde{\nu}$ = 3440 cm^{-1}. The FO structure was further confirmed by ^{1}H NMR spectroscopic analysis (Figure 2.2-d) by the disappearance of the epoxide protons and protons in alpha to the epoxides at δ = 2.90 and 1.45 ppm, respectively, and the appearance of the formed polyether backbone between δ = 3.00-3.60 ppm (for detailed integration see Figure S2.13). By ^{13}C NMR and ^{13}C NMR DEPT 135 spectroscopy (Figure S2.14 and Figure S2.15 in the SI respectively), carbons associated

to the polyether backbone corresponding to ether and carbon containing secondary hydroxyl groups clearly appear. Concurring with Lligadas *et al. (Lligadas et al. 2006)*, water was introduced in the oligomerization synthesis to suppress the occurrence of macrocyclization. This allowed for the nucleophilic attack of water to compete with intramolecular attacks, consequently favoring the proportion of linear species. Three different oligomers architectures were synthesized. As highlighted in Table 2.1, introducing higher water equivalents limits the oligomerization and yields overall higher hydroxyl values (HVs) of the synthesized oligomers. The oligomer hydroxyl functionality was determined by using the M_n and HV and remains very close to two for all oligomers synthesized. This was further confirmed by the MALDI-TOF MS analysis of Oligomer Sample B (Figure S2.16 and Figure S2.17 in SI), in which the repeating units, *n*, varied from two to nine. The most intense signals belonged to the series of oligomers with *n* values of three to five. The HV was determined using ^{31}P-NMR spectroscopic analysis and quantification results can be found in Figure S2.18 and Table S2.6 in SI (Spyros 2002; Korntner et al. 2015). Quantitative ^{1}H NMR spectroscopy was used to determine the furan content ($mmol_{furan}g^{-1}$) of FO and quantification results are available in Figure S2.19 and Table S2.7 in SI. Oligomer B was then used for the PU synthesis.

Table 2.1 – Synthesis and properties of different FO obtained by cationic ROP of FMO.

Oligomer sample	$HSbF_6$ [wt %]	H_2O [mol %]	HV[a] [$mg_{KOH}\,g^{-1}$]	EW[b] [g $equiv^{-1}$]	M_n[c] [g mol^{-1}]	Đ[d]	Functionality[e]	Furan content[f] [mmol g^{-1}]
A	1.5	80	60	935	1179	1.75	1.90	1.89
B	1.5	70	55	1020	1983	1.69	1.94	1.89
C	1.5	60	49	1145	2222	1.94	1.94	1.74

[a] Determined from ^{31}P NMR spectroscopic analysis. [b] EW = equivalent weight, which was calculated from HV. [c] Determined from size-exclusion chromatography analysis. [d] Dispersity = Mw/Mn. [e] Obtained from Mn/EW. [f] Determined from 1H NMR spectroscopic analysis

4.2. Analysis of DA cycloaddition of FO and *N*-Methylmaleimide

FO was reacted with monofunctional *N*-methylmaleimide in DMSO at 65 °C to study the DA adduct formation by ^{1}H NMR spectroscopy in absence of gelation. ^{1}H NMR spectroscopy results

attest to the formation of the DA adduct (Figure 2.3 – (a) ^{1}H NMR spectra of mixture of FO and N-methylmaleimide after 0 and 24 h. (b) Conversion and percentage of endo structure with respect to time at 65 °C.Figure 2.3-a). Proton assignment was achieved using the ^{1}H NMR spectra of initial compounds and comparison to the literature (Froidevaux et al. 2015; Buono et al. 2017). To quantify the conversion, proton signals, f_1 and f_4 (in the furan) and m_2 (in the maleimide) and f_1', $f_4'$and m_2' (in the adduct) were used because they are free from overlap with other signals (Figure 2.3-a). The conversion (X) was calculated in accordance with Equation (5) for proton set f_1 and f_1' as follows; where Int_{f1} *and* $Int_{f1'}$ represent the integral values of their respective protons:

$$X\,(\%) = \frac{Int_{f_1'}}{Int_{f_1} + Int_{f_1'}} * 100 \quad (5)$$

Similar results could be obtained with proton sets f_4, f_4' and m_2, m_2'. The evolution of the conversion with respect to time at 65 °C is depicted on Figure 3b. An equilibrium conversion of 65% was attained after 121 h of reaction, as similarly reported in literature (Adzima et al. 2008; Scheltjens et al. 2013). Furthermore, proton signals, f_1' and m_2', were used to quantify the evolution of two diastereomers of the DA adduct (*endo* and *exo)* with respect to time (Figure 2.3-b), because the chemical shift differed slightly for each diastereomer. The *endo* adduct, which is kinetically favored (Froidevaux et al. 2015), is first formed at 62%. As the reaction progresses, the thermodynamically stable *exo* diastereomer becomes the predominant entity (91 wt %) after 121 h.

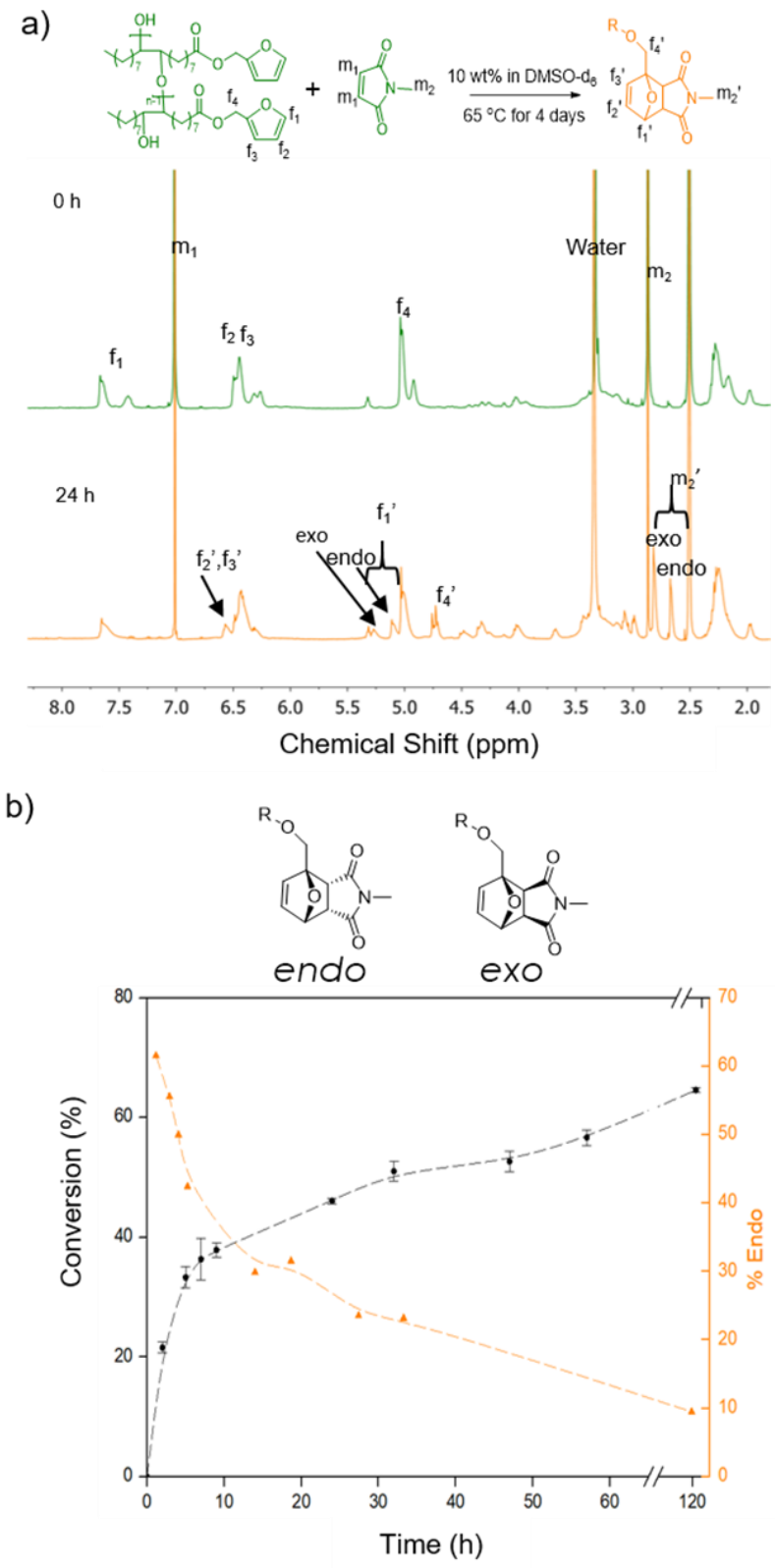

Figure 2.3 – (a) ^{1}H NMR spectra of mixture of FO and N-methylmaleimide after 0 and 24 h. (b) Conversion and percentage of endo structure with respect to time at 65 °C.

4.3. Analysis of DA and r-DA reactions between FO and a BMI

To test and simulate the formation of DA adducts between PU chains, the FO was reacted with PPOBMI. DSC was used to monitor the formation of the DA adducts and the r-DA reaction. A stoichiometric mixture of FO and PPOBMI was heated from -30 to 175 °C. As controls, FO and PPOBMI were separately investigated under the same conditions. As observed in the thermograms reported in Figure 2.4-a, no thermodynamic phenomena take place for each separate entity. However, in the thermogram of the mixture (orange), an exothermic peak begins to appear between 50 and 60 °C, which indicates the DA reaction. Two endothermic peaks, corresponding to the r-DA, follow the exothermic peak. The first one, between 90 and 120 °C, corresponds to the r-DA of the *endo* diastereomer, whereas the second one refers to the r-DA of the *exo* diastereomer, between 120 and 150 °C (Froidevaux et al. 2015).

The thermoreversibility of the network formed between the FO and the PPOBMI was further qualitatively studied by dissolving the mixture in DMSO and exposing it to different heating cycles. As depicted in Figure 2.4-b-i, the mixture is first completely soluble in DMSO. Once exposed to 60 °C for 24 h, a gel is formed by cross-linking (Figure 2.4-b-ii). The mixture was then exposed to 120 °C for 1 h, causing the disassembly of the network due to the r-DA reaction (Figure 2.4-b-iii). When repeating the heating cycle, the same phenomenon took place (Figure 2.4-b-iv). To further evidence the DA reaction, the mixture was studied prior and after gel formation by FTIR spectroscopy. Before cross-linking, the FTIR spectrum of the mixture contains signals of free furan ($\tilde{\nu}$ = 739 and 1503 cm^{-1}) and maleimide rings ($\tilde{\nu}$ = 695 and 826 cm^{-1}) (Figure 2.4-c). After gel formation, the FTIR spectrum revealed a complete disappearance of the respective free furan and maleimide ring signals. To quantitatively study the DA reaction and r-DA between FO and PPOBMI, the rheological behavior of gel formation between the two entities was evaluated by a dynamic experiment. As observed in Figure S2.20 the gelation reaction was analyzed by a time sweep test at 60 °C at 1% strain and 1 Hz, while recording the variation of the two dynamic moduli. Gelation occurs when the moduli cross over at 1740 s (29 min, G’ ≈ G’’ ≈ 650 Pa). Thereafter, heating steps were imposed to evaluate the thermoreversibility of the gel; 60 °C for the DA reaction and 120 °C for the r-DA. During the r-DA heating steps, the gel would disassemble and the two moduli shoot back to zero. The gel was reassembled two more times; each time leading

to quicker gelation times. This proves the thermoreversibility of the cross-linking points of the PU materials made using these two building blocks.

a)

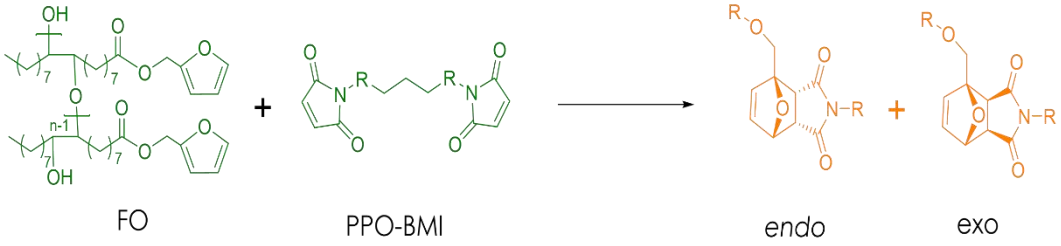

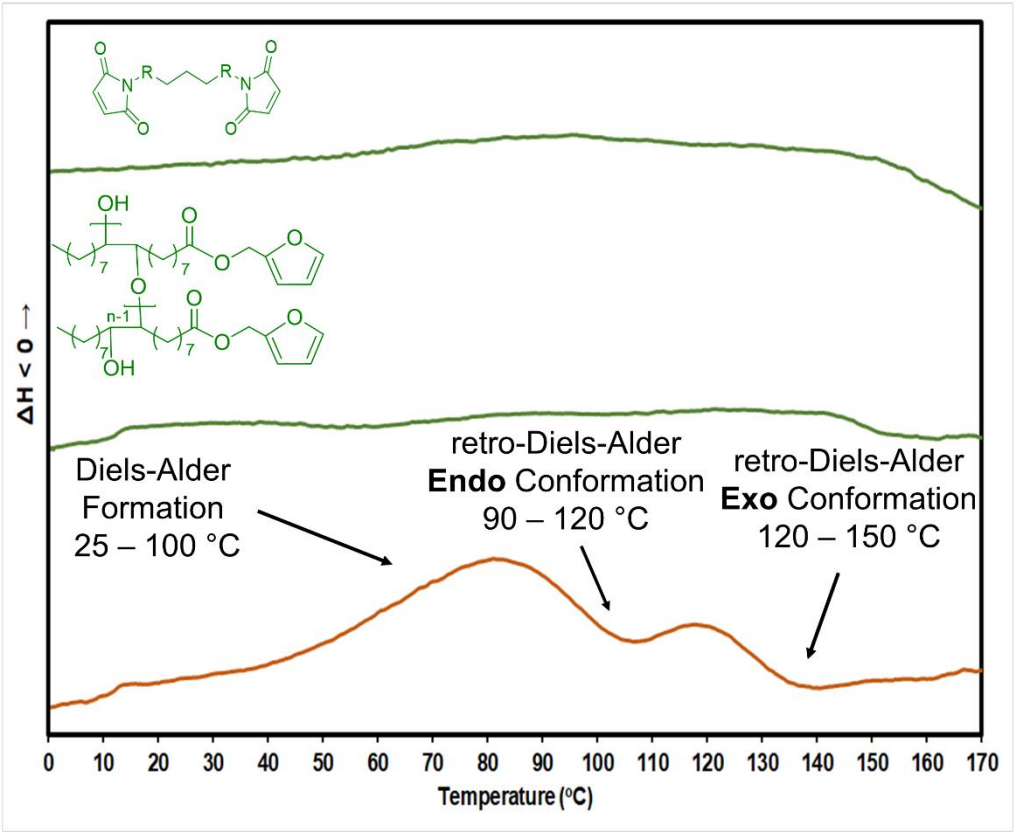

b)

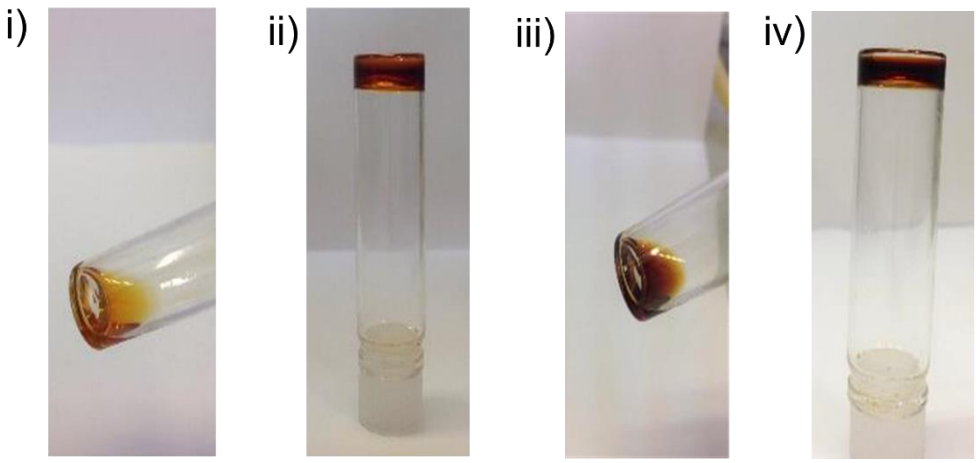

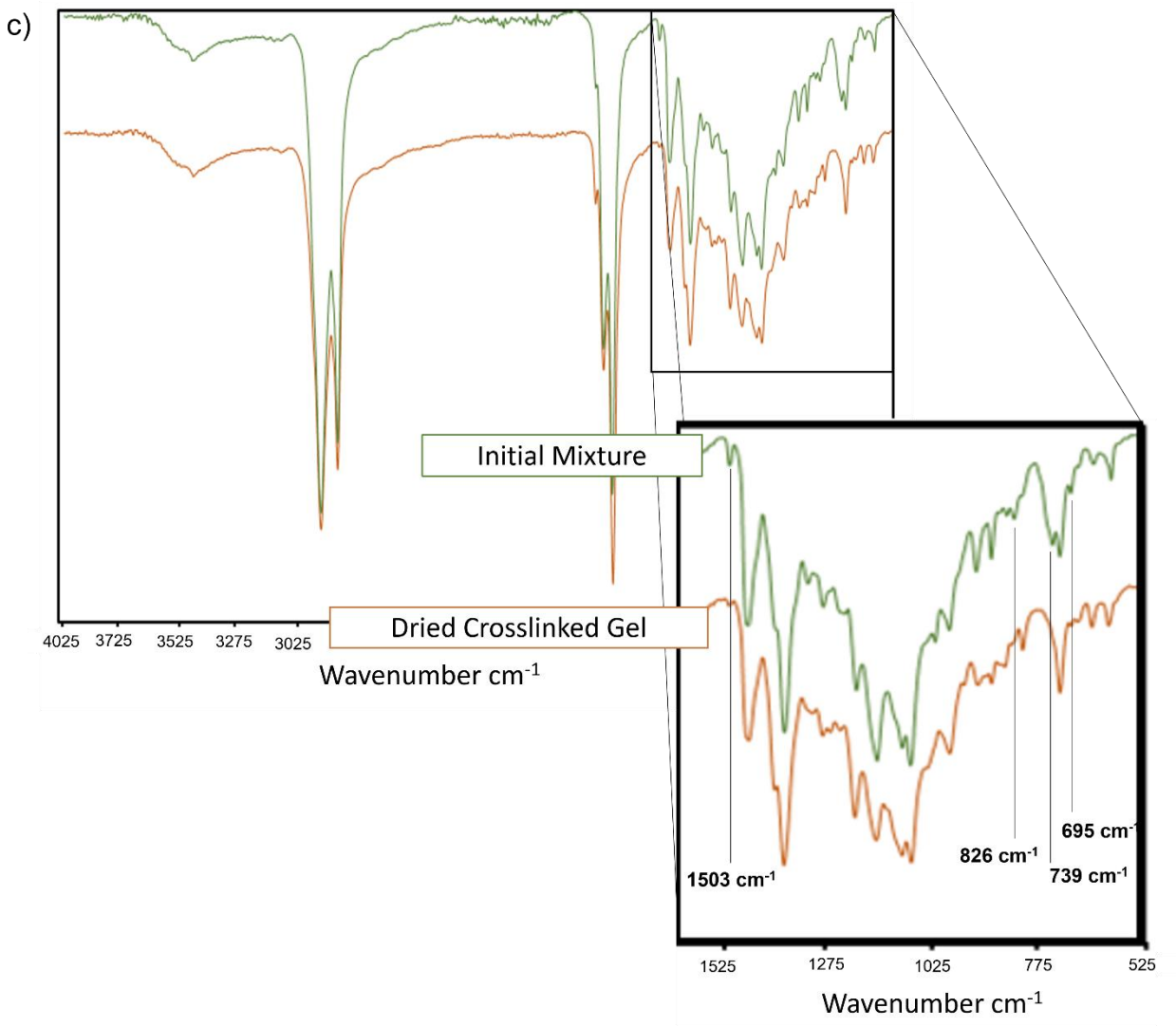

Figure 2.4 – (a) DSC thermograms of PPOBMI, FO, and a mixture of both, from 0 to 170 °C. (b) Photographs of i) the initial mixture of FO and PPOBMI; ii) the mixture after 24 h at 60 °C; iii) the mixture after additional 1 h at 120 °C; and iv) the mixture after additional 24 h at 60 °C. (c) FTIR spectra of the initial mixture (green) and final dried cross-linked gel (orange).

4.4. Analysis of the synthesis of biobased cross-linked PU containing FO and BMI

The synthesis of cross-linked biobased PUs containing thermoreversible DA adducts was achieved by using FO and PPO BMI. Scheme 2.1 illustrates the route for the preparation of the control (linear PUs, reaction 1) systems and cross-linked PUs (reactions 1 and 2). Different types of PUs were prepared by varying the proportion of FO in a PU system by the polyaddition between the biobased polyester polyol (structure given in Figure 2.5) and HDI. The FO content in the PU

systems was varied from 0 to 30% of the total number of moles of hydroxyl required to synthesize PUs with a final NCO/OH ratio of 1.05. PUs were obtained without hard segments (segments synthesized with short diols and diisocyanates) to study the effect of the FO on a model of a simple system. The nomenclature of all PU systems synthesized is summarized in Table 2.2. Different control PU systems, with varying amounts of FO content were denoted as PU-FO-0, PU-FO-10, PU-FO-20, and PU-FO-30. Thermoreversible cross-linked PU systems were obtained by dissolving the corresponding linear PU in dry DMF, adding the required amount of PPOBMI and letting the solution stir overnight at 70 °C, to allow the DA reaction to take place. These solutions then underwent solvent casting in a PTFE square mold for 48 h at 70 °C followed by 24 h under vacuum at 70 °C to yield a cross-linked PU. Cross-linked PUs containing the required PPOBMI mass to yield a 1:1 furan to maleimide ratio were denoted as PU-FO-10XL, PU-FO-20XL and PU-FO-30XL. Two additional cross-linked PUs were synthesized using the linear PU-FO-20 but with furan/maleimide ratios of 1: 0.7 and 1: 0.5, and denoted as PU-FO-20XL-0.7BMI and PU-FO-20XL-0.5BMI, respectively.

Table 2.2 – Linear PU (control) and cross-linked systems: nomenclature and corresponding formulations.

PU system	Type of system	FO content [a] [%]	Rapeseed polyol content [a] [%]	PPO BMI [equiv.] [b]
PU-FO-0	linear	0	100	0
PU-FO-10	linear	10	90	0
PU-FO-10XL	cross-link	10	90	1
PU-FO-20	linear	20	80	0
PU-FO-20XL	cross-link	20	80	1
PU-FO-20-0.7BMI	cross-link	20	80	0.7
PU-FO-20-0.5BMI	cross-link	20	80	0.5
PU-FO-30	linear	30	70	0
PU-FO-30XL	cross-link	30	70	1

[a] The FO content in the PU systems was varied from 0 to 30% of the total hydroxyl moles required to synthesize PUs with a final NCO/OH equivalent of 1.05. [b] Equivalents of maleimide moiety from PPOBMI with respect to furan moiety of FO.

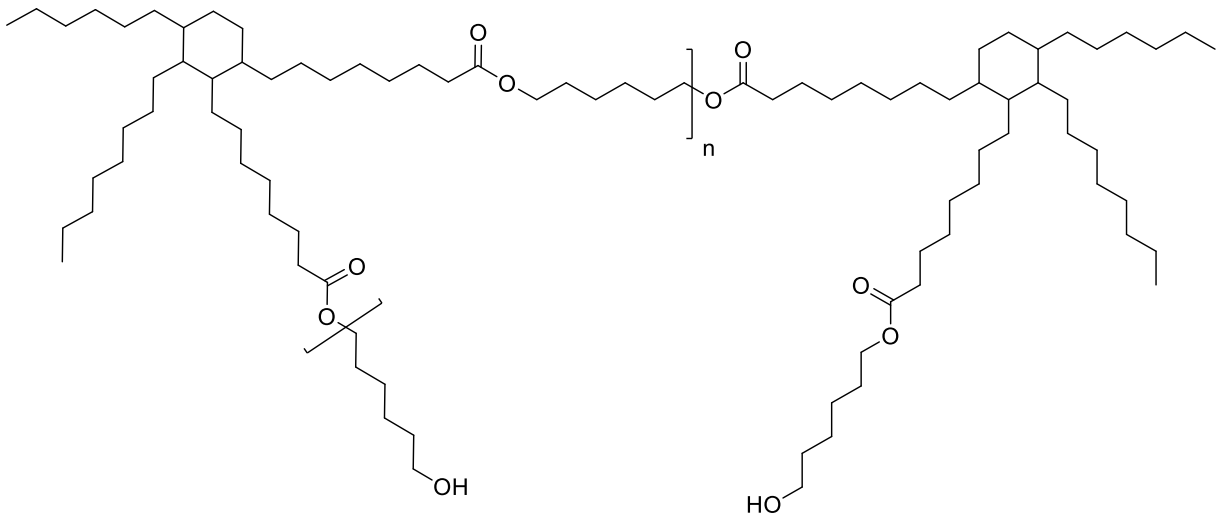

Figure 2.5 – Structure of the biobased polyester polyol supplied by the provider. This polyol is based on dimeric fatty acids found in rapeseed oil.

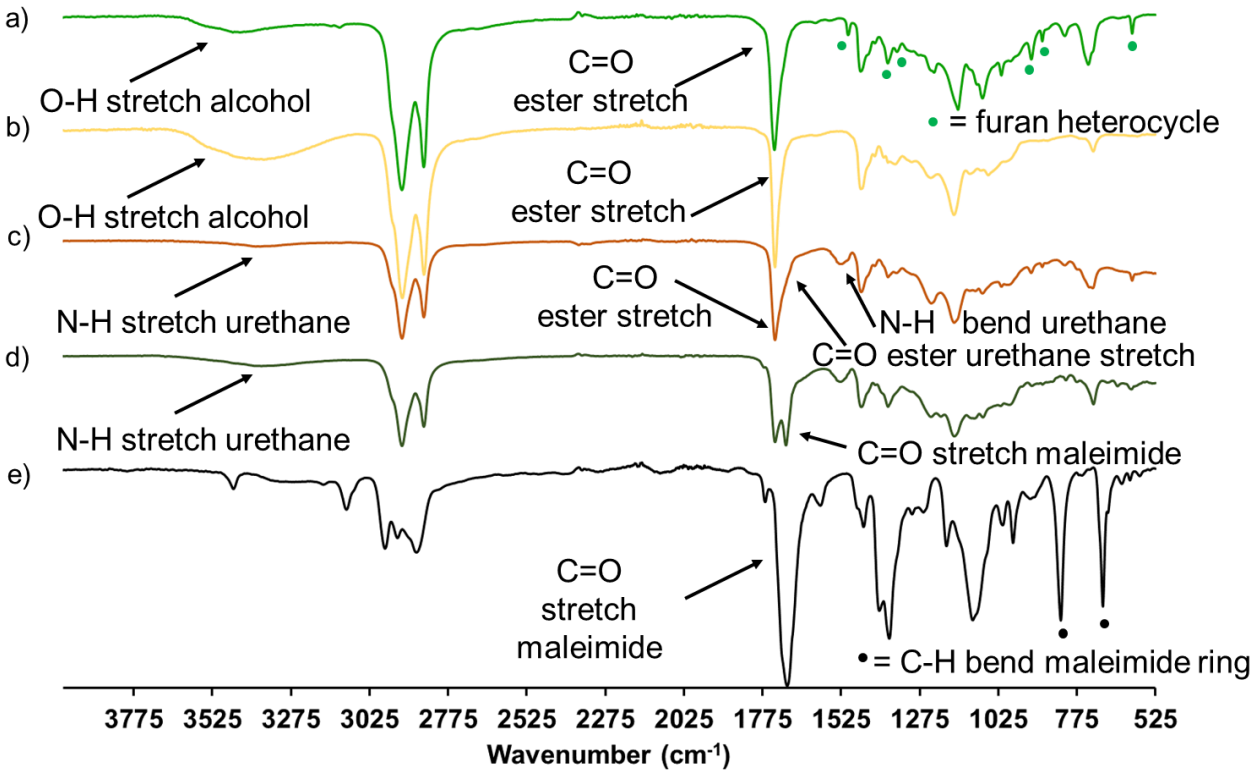

Figure 2.6 – FTIR spectra of (a) FO, (b) rapeseed polyol, (c) PU-FO-30, (d) PU-FO-30XL, and (e) PPO BMI.

All PU systems post curing (linear and cross-linked) were insoluble in conventional solvents ($CHCl_3$, DMSO, THF, DMF) and thus, were examined by FTIR. Symmetrical diisocyanates, such as HDI, increase the crystallinity and hard segment packing of PUs which may account for the lack of solubility that occurs in the presented networks (Das et al. 2007). A comparison of the FTIR spectra of FO, biobased polyester rapeseed polyol, PU-FO-30, PU-FO-30-XL and PPOBMI is displayed in Figure 2.6. In FTIR spectrum PU-FO-30 (Figure 2.6-c), the disappearance the hydroxyl stretches (at $\tilde{\nu} \approx 3440$ cm^{-1}) associated with the hydroxyls of FO and rapeseed polyol is observed. Consequently, the appearance of vibrations at $\tilde{\nu} = 3380$ and 1550 cm^{-1} corresponding to -N-H stretching and bending, respectively, of urethane group, whereas the ester urethane stretch is presented as a shoulder at $\tilde{\nu} = 1700$ cm^{-1}. The FTIR spectrum of PU-FO-30XL (Figure 2.6-d) displays a similar spectrum than that of PU-FO-30. However, the addition of PPOBMI to yield a cross-linked system results in the appearance of the carbonyl groups of the maleimides at $\tilde{\nu} = 1705$ cm-^{1}. Moreover, as the PU-FO-30XL is cross-linked via DA reaction, the disappearance of furan heterocycle and C-H bending of maleimide ring ($\tilde{\nu} = 826$ and 692 cm^{-1}) is observed.

4.5. Characterization of biobased cross-linked PUs

The thermal stability of all PU materials was evaluated by means of TGA. Detailed TGA results are found in Figure S2.21 in SI. As exhibited in Table 2.3, the initial thermal degradation ($T_{5\%}$) for all materials begins at temperatures above that of the r-DA reaction. This is indicative that reprocessing and disassembly of cross-linked points is thus possible without thermal degradation, although the introduction of the FO seems to decrease the $T_{5\%}$ (from 337 to 250 °C for PU-FO-0 to PU-FO-30, respectively). Furthermore, the respective cross-linked materials have lower $T_{5\%}$, with except of PU-FO-10XL. The glass transition temperatures (T_g) were measured by DSC (Table 2.3). The T_g of cross-linked materials were recorded using a single heating ramp, from -80 °C to 175 °C in order to avoid any significant degradation, as indicated by TGA results. Upon comparing control PU-FO-30 with its respective cross-linked PU counterpart (PU-FO-30XL), T_g increases due to a high level of cross-linking. Furthermore, as observed in Figure 2.7, the thermograms of cross-linked PUs exhibit the presence of an endothermic peak between 90 and 150 °C corresponding to the r-DA reaction, whereas, their control PU counterparts are flat-lined as no BMI is present. Materials containing increased amounts of FO, (and consequently increased cross-linking density)

logically exhibit a more prominent endothermic r-DA peak between 90 and 150 °C. A slight endothermic peak seems to appear in all cross-linked materials of Figure 6 between 30 to 60 °C. As previously mentioned, cross-linked materials are evaluated by a single heating ramp from -80 to 175 °C. These endothermic peaks were present in linear material upon first heating, but disappeared upon second heating as the thermal history of the material was erased. Thus, these slight endothermic peaks appear to be associated the thermal history of the material. Detailed DSC results are found in Figure S2.22.

Table 2.3 – Characterizations of synthesized biobased polyurethanes.

PU system	TGA $T_{5\%}$ [°C]	DSC T_g [°C]	Young's modulus [MPa]	σ[a] [MPa]	ε[b] [%]	SR[c] in DMF [%]	IF[d] [%]
PU-FO-0	337	-50	0.39 ± 0.03	0.58 ± 0.02	563 ± 36	36.9 ± 1.8	96.4 ± 0.3
PU-FO-10	327	-51	0.14 ± 0.01	0.36 ± 0.02	368 ± 27	51.6 ± 2.3	94.4 ± 0.6
PU-FO-10XL	333	-51	0.32 ± 0.01	0.51 ± 0.03	409 ± 54	44.3 ± 0.6	95.0 ± 0.9
PU-FO-20	298	-51	0.11 ± 0.01	0.38 ± 0.03	288 ± 4	58.5 ± 3.4	92.9 ± 0.6
PU-FO-20XL	267	-50	0.32 ± 0.01	0.50 ± 0.01	232 ± 2	46.9 ± 0.1	95.2 ± 2.9
PU-FO-20-0.7BMI	287	-51	0.30 ± 0.01	0.40 ± 0.02	208 ± 2	48.2 ± 6.3	92.0 ± 2.9
PU-FO-20-0.5BMI	293	-50	0.26 ± 0.01	0.32 ± 0.01	232 ± 11	55.7 ± 3.0	90.6 ± 1.2
PU-FO-30	250	-55	NA[e]	NA[e]	NA[e]	146.1 ± 7.4	77.5 ± 0.8
PU-FO-30XL	234	-51	0.57 ± 0.09	0.49 ± 0.04	107 ± 9	70.4 ± 2.7	92.5 ± 0.6

[a] Tensile strength. [b] Elongation. [c] SR=swelling ratio. [d] IF=insoluble fraction. [e] NA=not available

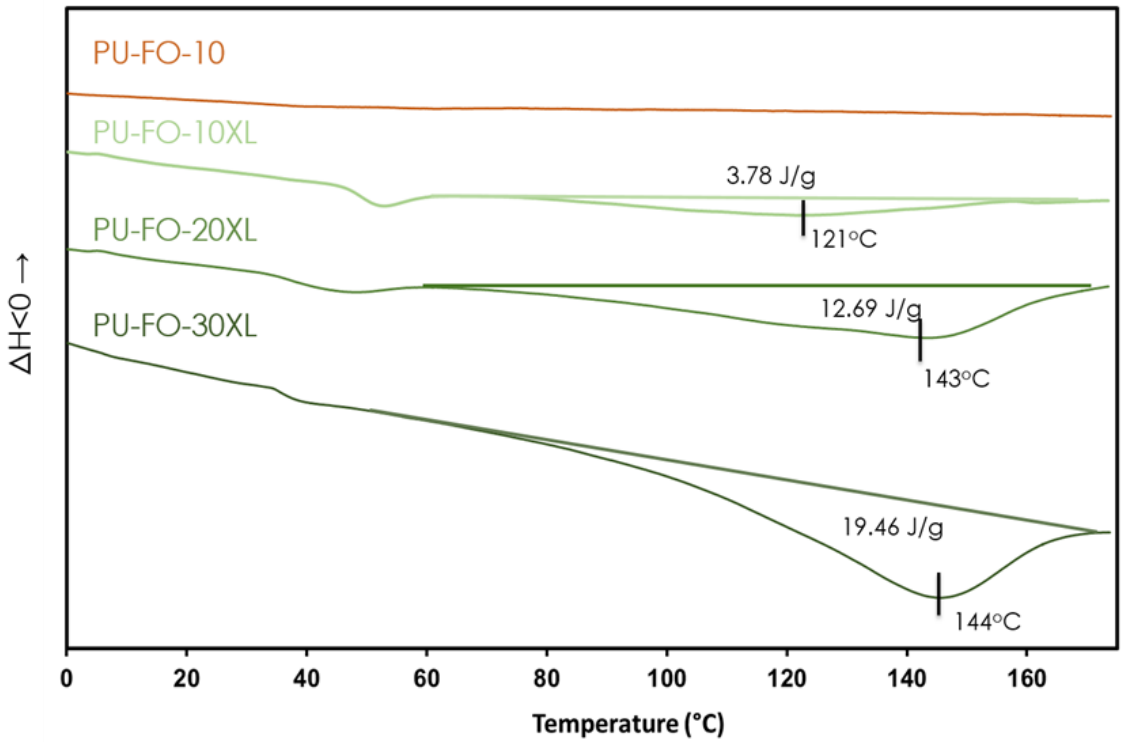

Figure 2.7 – Thermograms of PUs: PU-FO-10, PU-FO-10XL, PU-FO-20XL, and PU-FO-30XL from 0 to 175 °C.

The mechanical properties of the PUs were evaluated by uniaxial tensile tests at room temperature. The "sticky" and weak behavior of control PU, PU-FO-30, rendered the material untestable because it was nonprocessable for dumbbell shaping because molding these samples was impossible. Upon examining the results in Table 2.3 and more specifically control PUs results, the incorporation of FO into the PU structure weakens the material as there is an apparent decrease in tensile strength and Young's modulus of PU-FO10, PU-FO-20 in comparison to PU-FO-0. Furthermore, the addition of FO also reduces the elasticity of the material because the elongation of PU-FO-10, PU-FO-20 is decreased with respect to PU-FO-0. Nevertheless, upon examining the mechanical properties of cross-linked PU-FO-10XL, PU-FO-20XL and PU-FO-30XL, cross-linking as a result of the DA reaction improves the tensile strength of the materials, but most notably the Young's modulus.

From the stress-strain curves of PU-FO-0, PU-FO-10XL, PU-FO-20XL and PU-FO-30XL, in Figure 2.8, it can be deduced that, by increasing the portion of FO in the PU structure and cross-linking by PPOBMI, the material properties vary from a thermoplastic elastomer (PU-FO-0) to a thermoset

material (PU-FO-30XL). Furthermore, the mechanical properties can be further tuned by varying the number of equivalents of PPOBMI introduced into the material. This is evidenced by the mechanical properties of PU-FO-20XL-0.7BMI and PU-FO-20XL-0.5BMI, whereby varying the number of equivalents of PPOBMI between 0.7 and 0.5, relative to the number of furan, resulted in tensile strengths and Young's moduli in an intermediate range between those of PU-FO-20 and PU-FO-20XL (Table 2.3).

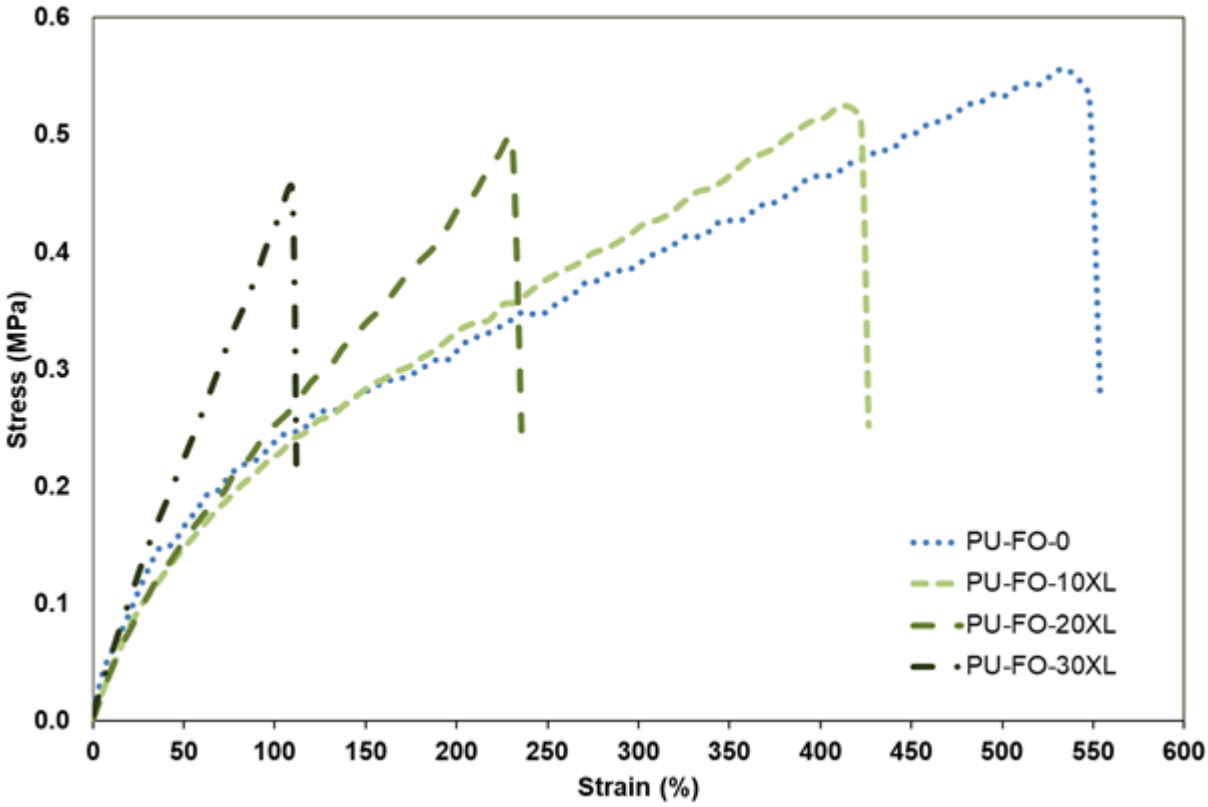

Figure 2.8 – Stress-strain curves of PU-FO-0, PU-FO-10XL, PU-FO-20XL, and PU-FO-30XL.

All PU materials were finally characterized by swelling test in DMF. As observed from the results in Table 2.3, upon first examining linear materials PU-FO-0, PU-FO10, PU-FO-20, and PU-FO-30, it can be observed that the polymer networks experience higher swelling with an increasing amount of FO in the polymer architecture. In contrast, due the cross-linking by the DA reaction, the results of cross-linked PUs yield considerably lower swelling ratios in comparison with that of their respective control PUs. The most considerable effect of DA cross-linking is observed for the highest cross-linked content, between PU-FO-30 to PU-FO-30XL, for which the swelling ratio

decreased from 146 to 70%, respectively, and the insoluble fraction increased from 78 to 93%, respectively. Except PU-FO-30, all PU material were relatively insoluble. Furthermore, the swelling ratio of PU material PU-FO-20XL-0.7BMI and PU-FO-20XL-0.5BMI yields intermediate results between that of the cross-linked material, PU-FO-20XL and the linear control PU, PU-FO-20. This is a testament to the tunablity of properties upon varying not only the FO content, but also PPOBMI concentration.

4.6. Thermoreversibility of biobased cross-linked PU leading to remendable and self-healing behaviors

Initial studies conducted to prove the thermoreversible between FO and the monofunctional *N*-methylmaleimide or PPOBMI permitted to testing and simulating of the thermoreversibility of cross-linked PU by the DA and r-DA reactions. To first evaluate the thermoreversibility of cross-linked materials, PU-FO-20XL was examined by FTIR spectroscopy after exposing the material to different heating cycles. As depicted in Figure 2.9, upon heating the material for 2 h at 120 °C, free maleimide ring bands appear to be prevalent at $\tilde{\nu}$ = 692 and 825 cm^{-1} due the occurrence the r-DA reaction. These free maleimide ring bands disappear once the DA reaction takes place, if the material is reexposed to 70 °C for 20 h. This heating cycle was repeated and yielded the same results (Figure 2.9), which indicates that the materials cross-linked by DA had the potential to be reprocessable and could be self-healing.

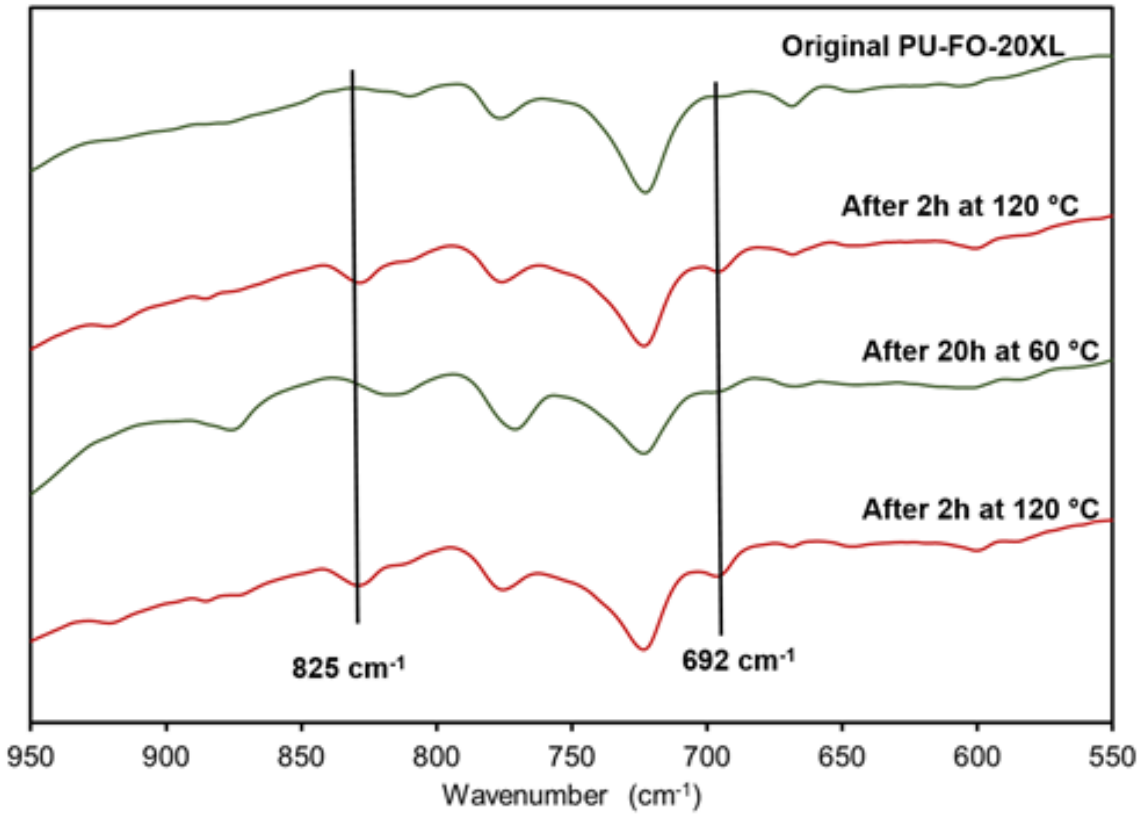

Figure 2.9 – FTIR spectra of PU-FO-20XL, PU-FO-20XL heated for 2 h at 120 °C, PU-FO-20XL heated for 20 h at 60 °C, and PU-FO-20XL heated for 2 h at 120 °C.

Reprocessability was also studied on PU-FO-30XL, which was first processed by solvent casting and then characterized (Table 2.4). This material was then reprocessed by compression molding at 150 °C for 25 min. The material was cured at 60 °C in the oven for 48 h and post cured for 24 h at room temperature. The uniaxial tensile test and T_g were studied for this material labeled PU-FO-30XL-RP1. The material was then reprocessed, reevaluated, and labeled PU-FO-30XL-RP2. The results are summarized in Table 4 and are conclusive that the material can indeed be reprocessed without significant material degradation. The T_g of the reprocessed material is stable, as is the Young's modulus. Nevertheless, reprocessing does induce only some light decrease in the material performances because the tensile strength and elongation at break slightly decrease.

Table 2.4 – Characterization of biobased PU-FO-30XL reprocessed several times.

PU System	DSC T_g [°C]	Young's Modulus [MPa]	σ [MPa]	ε [%]
PU-FO-30XL	-51	0.57 ± 0.09	0.49 ± 0.04	107 ± 9
PU-FO-30XL-RP1	-50	0.62 ± 0.03	0.47 ± 0.04	83 ± 5
PU-FO-30XL-RP2	-50	0.58 ± 0.02	0.40 ± 0.03	74 ± 6

As depicted in Figure 2.10-a, self-healing was studied by cutting a dumbbell sample of PU-FO-30XL in half and exposing it to 1 h at 120 °C and 2 days at 60 °C; this is denoted PU-FO-30XL-HL1. By utilizing the thermo-reversibility of the DA bonds, the breaking and reforming of the cross-links allows a severed dumbbell sample to be healed upon exposed to such heating cycles. The initial heating at 120 °C for 1 h allows to break the cross-links, thus enhancing network mobility. Consequently, the polymer chains can locally flow, giving rise to adhesion to the two severed pieces. The final heating step at 60 °C for 2 days allows the network to be reformed by the DA reaction. As observed Figure 2.10-b, the healed materials show a novel integrity and recovery in terms of Young's modulus with around 0.5 MP; a value equivalent to the initial material. Only at high elongation, a decrease of the performances is visible. This behavior is largely indicative that the thermoreversible DA cross-linking of PUs allows the material to have self-healing properties.

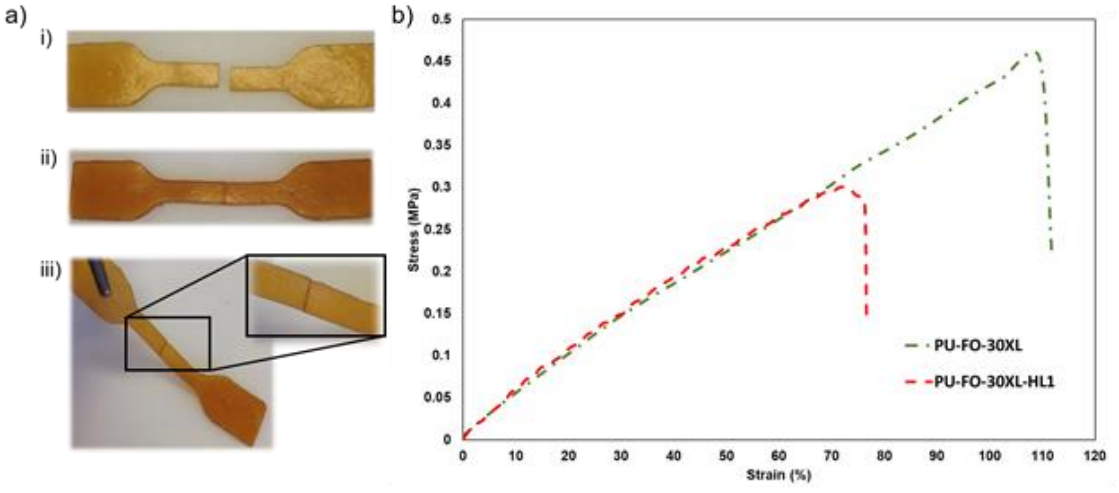

Figure 2.10 – Self-healing evaluation. (a) Photographs of (i) PU-FO-30XL dumbbell sample cut in half; (ii) healed dumbbell sample of PU-FO-30XL after heating 1 h at 120 °C and 2 days at 60 °C; (iii) lifted healed dumbbell with close-up on healed section, and (b) stress-strain curves of PU-FO-30XL and PU-FO-30XL-HL1.

5. Conclusion

Thermoreversible and self-healing cross-linked biobased systems based on urethane groups and clickable functions were successfully synthesized using vegetable oil derivatives and utilizing Diels-Alder reaction to control the design of their macromolecular architectures. A new biobased building block has been designed. The furan oligomer (FO) was developed from oleic acid in a sustainable way, largely in agreement with different green chemistry principles. As a general trend, cross-linked systems had characteristically higher T_g, and insoluble ratio and enhanced stiffness and strength, and lower swelling ratio when compared with those of their control polyurethane (PU) counterparts. The cross-linked materials exhibit modular mechanical properties with respect to FO content. These biobased materials present a wide range of behavior, from a typical thermoplastic elastomer-like material (least cross-linked material) to a thermoset (most cross-linked material). Reprocessing cycles were successfully performed and exhibited stable material properties. The systems also present self-healing properties. Dumbbell samples were cut in half, healed by joining the pieces together and exposing them to 120 °C, and cured at 60 °C. Both parts were able to recombine and considerably mend the material. To this end, this work is a stepping-stone in developing vegetable oil-based architectures with integrated dynamicity for evolution of high-performance and advanced biobased materials.

Future efforts will be dedicated to develop a greener chemistry with e.g. the reduction of the solvent consumption and the use of more sustainable solvents. In the near future, similar cross-linked vegetable oil based polyurethane formulation varying hard segment content can be studied for material application such as adhesives and coatings; thus providing exciting perspectives for a greener future with advanced behavior to decrease the global impact of these materials, with a controlled end-of-life.

Ackowledgements

We would like to thank BPI-France for the funding through the Trans'Alg Project and the corresponding consortium. Iterg for kindly providing technical grade oleic acid. The authors would like to thank Dr. Antoine Duval for his input, the R&D Team of Soprema (France) and Sophie Wendels for help with rheological measurements.

6. References

Adzima, Brian J., H. Alan Aguirre, Christopher J. Kloxin, Timothy F. Scott, and Christopher N. Bowman. 2008. 'Rheological and Chemical Analysis of Reverse Gelation in a Covalently Cross-Linked Diels−Alder Polymer Network', *Macromolecules*, 41: 9112-17.

Akindoyo, John, Mohammad Beg, Suriati Ghazali, Muhammad Islam, Nitthiyah Jeyaratnam, and Yuvaraj Ar. 2016. 'Polyurethane types, synthesis and applications-a review', *RSC Advances*, 6: 114453-82.

Arbenz, Alice, Rémi Perrin, and Luc Avérous. 2017. 'Elaboration and Properties of Innovative Biobased PUIR Foams from Microalgae', *Journal of Polymers and the Environment*, 26: 254-62.

Boutelle, Robert C., and Brian H. Northrop. 2011. 'Substituent Effects on the Reversibility of Furan–Maleimide Cycloadditions', *The Journal of Organic Chemistry*, 76: 7994-8002.

Buono, Pietro, Antoine Duval, Luc Averous, and Youssef Habibi. 2017. 'Thermally healable and remendable lignin-based materials through Diels – Alder click polymerization', *Polymer*, 133: 78-88.

Carré, Camille, Yvan Ecochard, Sylvain Caillol, and Luc Averous. 2019. 'From the synthesis of biobased cyclic carbonate to polyhydroxyurethanes: a promising route towards renewable non-isocyanate polyurethanes', *Chemsuschem*, 12: 3410.

Chen, Xiangxu, Matheus A. Dam, Kanji Ono, Ajit Mal, Hongbin Shen, Steven R. Nutt, Kevin Sheran, and Fred Wudl. 2002. 'A Thermally Re-mendable Cross-Linked Polymeric Material', *Science*, 295: 1698-702.

Das, Sudipto, David F. Cox, Garth L. Wilkes, Derek B. Klinedinst, Iskender Yilgor, Emel Yilgor, and Frederick L. Beyer. 2007. 'Effect of Symmetry and H-bond Strength of Hard Segments on the Structure-Property Relationships of Segmented, Nonchain Extended Polyurethanes and Polyureas', *Journal of Macromolecular Science, Part B*, 46: 853-75.

Denissen, Wim, Johan M. Winne, and Filip E. Du Prez. 2016. 'Vitrimers: permanent organic networks with glass-like fluidity', *Chemical Science*, 7: 30-38.

Desroches, M., S. Caillol, R. Auvergne, and B. Boutevin. 2012. 'Synthesis of pseudo-telechelic diols by transesterification and thiol-ene coupling', *European Journal of Lipid Science and Technology*, 114: 84-91.

Desroches, M., M. Escouvois, R. Auvergne, S. Caillol, and B. Boutevin. 2012. 'From Vegetable Oils to Polyurethanes: Synthetic Routes to Polyols and Main Industrial Products', *Polymer Reviews*, 52: 38-79.

Dhers, Sébastien, Ghislaine Vantomme, and Luc Avérous. 2019. 'A fully bio-based polyimine vitrimer derived from fructose', *Green Chemistry*, 21: 1596-601.

Dolci, E., V. Froidevaux, G. Michaud, F. Simon, R. Auvergne, S. Fouquay, and S. Caillol. 2017. 'Thermoresponsive crosslinked isocyanate-free polyurethanes by Diels-Alder polymerization', *Journal of Applied Polymer Science*, 134: 44408.

Dolci, Elena, Guillaume Michaud, Frédéric Simon, Bernard Boutevin, Stéphane Fouquay, and Sylvain Caillol. 2015. 'Remendable thermosetting polymers for isocyanate-free adhesives: a preliminary study', *Polymer Chemistry*, 6: 7851-61.

Du, P. F., H. Y. Jia, Q. H. Chen, Z. Zheng, X. L. Wang, and D. L. Chen. 2016. 'Slightly crosslinked polyurethane with Diels-Alder adducts from trimethylolpropane', *Journal of Applied Polymer Science*, 133: 43971.

Duval, A., G. Couture, S. Caillol, and L. Averous. 2017. 'Biobased and Aromatic Reversible Thermoset Networks from Condensed Tannins via the Diels-Alder Reaction', *ACS Sustainable Chemistry & Engineering*, 5: 1199-207.

Duval, Antoine, Heiko Lange, Martin Lawoko, and Claudia Crestini. 2015. 'Reversible crosslinking of lignin via the furan-maleimide Diels-Alder reaction', *Green Chemistry*, 17: 4991-5000.

Froidevaux, V, M Borne, E Laborbe, R Auvergne, A Gandini, and B Boutevin. 2015. 'Study of the Diels–Alder and retro-Diels–Alder reaction between furan derivatives and maleimide for the creation of new materials', *RSC Advances*, 5: 37742-54.

Gandini, Alessandro. 2013. 'The furan/maleimide Diels–Alder reaction: A versatile click–unclick tool in macromolecular synthesis', *Progress in Polymer Science*, 38: 1-29.

Gandini, Alessandro, Antonio J. F. Carvalho, Eliane Trovatti, Ricardo K. Kramer, and Talita M. Lacerda. 2018. 'Macromolecular materials based on the application of the Diels–Alder reaction to natural polymers and plant oils', *European Journal of Lipid Science and Technology*, 120: 1700091.

Gandini, Alessandro, Talita M. Lacerda, Antonio J. F. Carvalho, and Eliane Trovatti. 2016. 'Progress of Polymers from Renewable Resources: Furans, Vegetable Oils, and Polysaccharides', *Chemical Reviews*, 116: 1637-69.

García-Astrain, Clara, and Luc Avérous. 2018. 'Synthesis and evaluation of functional alginate hydrogels based on click chemistry for drug delivery applications', *Carbohydrate Polymers*, 190: 271-80.

García Astrain, Clara, Rebeca Hernandez, Olatz Guaresti, Ljiljana Fruk, Carmen Mijangos, Arantxa Eceiza, and Nagore Gabilondo. 2016. *Click Crosslinked Chitosan/Gold Nanocomposite Hydrogels*. *Macromol. Mater. Eng.*, 301: 1295-1300.

González, Kizkitza, Clara García-Astrain, Arantzazu Santamaria-Echart, Lorena Ugarte, Luc Avérous, Arantxa Eceiza, and Nagore Gabilondo. 2018. 'Starch/graphene hydrogels via click chemistry with relevant electrical and antibacterial properties', *Carbohydrate Polymers*, 202: 372-81.

Gu, Lin, and Qing-Yun Wu. 2018. 'Recyclable bio-based crosslinked polyurethanes with self-healing ability', *Journal of Applied Polymer Science*, 135: 46272.

Guaresti, O., C. García–Astrain, R. H. Aguirresarobe, A. Eceiza, and N. Gabilondo. 2018. 'Synthesis of stimuli–responsive chitosan–based hydrogels by Diels–Alder cross–linking `click´ reaction as potential carriers for drug administration', *Carbohydrate Polymers*, 183: 278-86.

Guaresti, Olatz, Clara García Astrain, Leire Urbina, Arantxa Eceiza, and Nagore Gabilondo. 2018. 'Reversible swelling behaviour of Diels-Alder clicked chitosan hydrogels in response to pH changes', *Express Polymer Letters*, 13: 27-36.

Haponiuk, Józef T., and Krzysztof Formela. 2017. 'Chapter 1 - PU Polymers, Their Composites, and Nanocomposites: State of the Art and New Challenges.' in Sabu Thomas, Janusz Datta, Józef T. Haponiuk and Arunima Reghunadhan (eds.), *Polyurethane Polymers* (Elsevier: Amsterdam).

Heo, Yunseon, and Henry A. Sodano. 2014. 'Self-Healing Polyurethanes with Shape Recovery', *Advanced Functional Materials*, 24: 5261-68.

Ionescu, M. 2005. *Chemistry and Technology of Polyols for Polyurethanes.* Milhail Ionescu. Rapra Technology, Shrewsbury, UK. Polym. Int.

Irusta, L., M. J. Fernandez-Berridi, and J. Aizpurua. 2017. 'Polyurethanes based on isophorone diisocyanate trimer and polypropylene glycol crosslinked by thermal reversible diels alder reactions', *Journal of Applied Polymer Science*, 134: 9.

Kim, Cheal, Teddy G. Traylor, and Charles L. Perrin. 1998. 'MCPBA Epoxidation of Alkenes: Reinvestigation of Correlation between Rate and Ionization Potential', *Journal of the American Chemical Society*, 120: 9513-16.

Kloxin, Christopher J., Timothy F. Scott, Brian J. Adzima, and Christopher N. Bowman. 2010. 'Covalent Adaptable Networks (CANs): A Unique Paradigm in Cross-Linked Polymers', *Macromolecules*, 43: 2643-53.

Korntner, Philipp, Ivan Sumerskii, Markus Bacher, Thomas Rosenau, and Antje Potthast. 2015. 'Characterization of technical lignins by NMR spectroscopy: optimization of functional group analysis by 31P NMR spectroscopy', *Holzforschung*, 69: 807-14.

Lacerda, T. M., and A. Gandini. 2014. 'Marriage of Furans and Vegetable Oils through Click Chemistry for the Preparation of Macromolecular Materials: A Succinct Review', *Journal of Renewable Materials*, 2: 2-12.

Lakatos, C., K. Czifrak, J. Karger-Kocsis, L. Daroczi, M. Zsuga, and S. Keki. 2016. 'Shape memory crosslinked polyurethanes containing thermoreversible Diels-Alder couplings', *Journal of Applied Polymer Science*, 133: 44145.

Lligadas, G., J. C. Ronda, M. Galià, U. Biermann, and J. O. Metzger. 2006. 'Synthesis and characterization of polyurethanes from epoxidized methyl oleate based polyether polyols as renewable resources', *Journal of Polymer Science Part A: Polymer Chemistry*, 44: 634-45.

Lligadas, G., J. C. Ronda, M. Galia, and V. Cadiz. 2013. 'Renewable polymeric materials from vegetable oils: a perspective', *Materials Today*, 16: 337-43.

Meier, Michael A. R., Jurgen O. Metzger, and Ulrich S. Schubert. 2007. 'Plant oil renewable resources as green alternatives in polymer science', *Chemical Society Reviews*, 36: 1788-802.

Montarnal, D., M. Capelot, F. Tournilhac, and L. Leibler. 2011. 'Silica-Like Malleable Materials from Permanent Organic Networks', *Science*, 334: 965-68.

Muthusamy, Kumarasamy, Krishnamoorthy Lalitha, Yadavali Siva Prasad, Ayyapillai Thamizhanban, Vellaisamy Sridharan, C. Uma Maheswari, and Subbiah Nagarajan. 2018. 'Lipase-Catalyzed Synthesis of Furan-Based Oligoesters and their Self-Assembly-Assisted Polymerization', *Chemsuschem,* 11: 2453-63.

Otsuka, Hideyuki, Koichiro Aotani, Yuji Higaki, Yoshifumi Amamoto, and Atsushi Takahara. 2007. 'Thermal Reorganization and Molecular Weight Control of Dynamic Covalent Polymers Containing Alkoxyamines in Their Main Chains', *Macromolecules*, 40: 1429-34.

Palaskar, Dnyaneshwar V., Aurélie Boyer, Eric Cloutet, Jean-François Le Meins, Benoit Gadenne, Carine Alfos, Céline Farcet, and Henri Cramail. 2012. 'Original diols from sunflower and ricin oils: Synthesis, characterization, and use as polyurethane building blocks', *Journal of Polymer Science Part A: Polymer Chemistry*, 50: 1766-82.

Petrović, Zoran S, Alisa Zlatanić, Charlene C Lava, and Snežana Sinadinović-Fišer. 2002. 'Epoxidation of soybean oil in toluene with peroxoacetic and peroxoformic acids—kinetics and side reactions', *European Journal of Lipid Science and Technology*, 104: 293-99.

Petrović, Zoran S., Ivana Cvetković, DooPyo Hong, Xianmei Wan, Wei Zhang, Tim Abraham, and Jeff Malsam. 2008. 'Polyester polyols and polyurethanes from ricinoleic acid', *Journal of Applied Polymer Science*, 108: 1184-90.

Rauf, Abdul, and Humaira Parveen. 2004. 'Direct esterification of fatty acids with phenylalkanols by using dicyclohexylcarbodiimide', *European Journal of Lipid Science and Technology*, 106: 97-100.

Rivero, Guadalupe, Le-Thu T. Nguyen, Xander K. D. Hillewaere, and Filip E. Du Prez. 2014. 'One-Pot Thermo-Remendable Shape Memory Polyurethanes', *Macromolecules*, 47: 2010-18.

Sanyal, Amitav. 2010. 'Diels–Alder Cycloaddition-Cycloreversion: A Powerful Combo in Materials Design', *Macromolecular Chemistry and Physics*, 211: 1417-25.

Scheltjens, G., M. M. Diaz, Joost Brancart, Guy Van Assche, and Bruno Mele. 2013. 'A self-healing polymer network based on reversible covalent bonding', *Reactive and Functional Polymers,* 73: 413-20.

Sengupta, Avery, Tanmoy Dey, Mahua Ghosh, Jaydip Ghosh, and Santinath Ghosh. 2012. 'Enzymatic Synthesis of Furfuryl Alcohol Ester with Oleic Acid by Candida antarctica Lipase B and Its Kinetic Study', *Journal of The Insitution of Engineers (India)*, 93: 31-36.

Shoda, Shin-ichiro, Hiroshi Uyama, Jun-ichi Kadokawa, Shunsaku Kimura, and Shiro Kobayashi. 2016. 'Enzymes as Green Catalysts for Precision Macromolecular Synthesis', *Chemical Reviews*, 116: 2307-413.

Spyros, A. 2002. 'Quantitative determination of the distribution of free hydroxylic and carboxylic groups in unsaturated polyester and alkyd resins by 31P-NMR spectroscopy', *Journal of Applied Polymer Science*, 83: 1635-42.

Truong, Thuy Thu, Ha Tran Nguyen, Man Ngoc Phan, and Le-Thu T. Nguyen. 2018. 'Study of Diels–Alder reactions between furan and maleimide model compounds and the preparation of a healable thermo-reversible polyurethane', *Journal of Polymer Science Part A: Polymer Chemistry*, 56: 1806-14.

Truong, Thuy Thu, Son Hong Thai, Ha Tran Nguyen, Dung Thuy Thi Phung, Loc Tan Nguyen, Hung Quang Pham, and Le-Thu T. Nguyen. 2019. 'Tailoring the Hard–Soft Interface with Dynamic Diels–Alder Linkages in Polyurethanes: Toward Superior Mechanical Properties and Healability at Mild Temperature', *Chemistry of Materials*, 31: 2347-57.

Vilela, Carla, Letizia Cruciani, Armando J. D. Silvestre, and Alessandro Gandini. 2011. 'A Double Click Strategy Applied to the Reversible Polymerization of Furan/Vegetable Oil Monomers', *Macromolecular Rapid Communications*, 32: 1319-23.

Vilela, Carla, Letizia Cruciani, Armando JD Silvestre, and Alessandro Gandini. 2012. 'Reversible polymerization of novel monomers bearing furan and plant oil moieties: a double click exploitation of renewable resources', *RSC Advances*, 2: 2966-74.

Willocq, B., F. Khelifa, J. Brancart, G. Van Assche, Ph Dubois, and J. M. Raquez. 2017. 'One-component Diels-Alder based polyurethanes: a unique way to self-heal', *RSC Advances*, 7: 48047-53.

Wilson, Jedediah F., and Eugene Y. X. Chen. 2019. 'Difuranic Diols for Renewable Polymers with Pendent Furan Rings', *ACS Sustainable Chemistry & Engineering*, 7: 7035-46.

Xu, Y. J., Z. Petrovic, S. Das, and G. L. Wilkes. 2008. 'Morphology and properties of thermoplastic polyurethanes with dangling chains in ricinoleate-based soft segments', *Polymer*, 49: 4248-58.

7. Supporting Information

7.1. Synthesis of FO

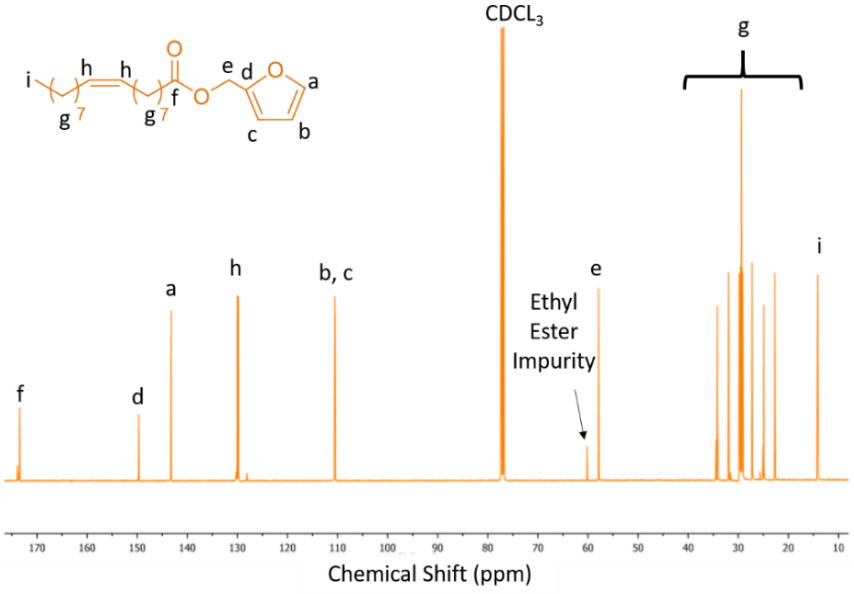

Figure S2.11 –^{13}C NMR spectrum of FMO.

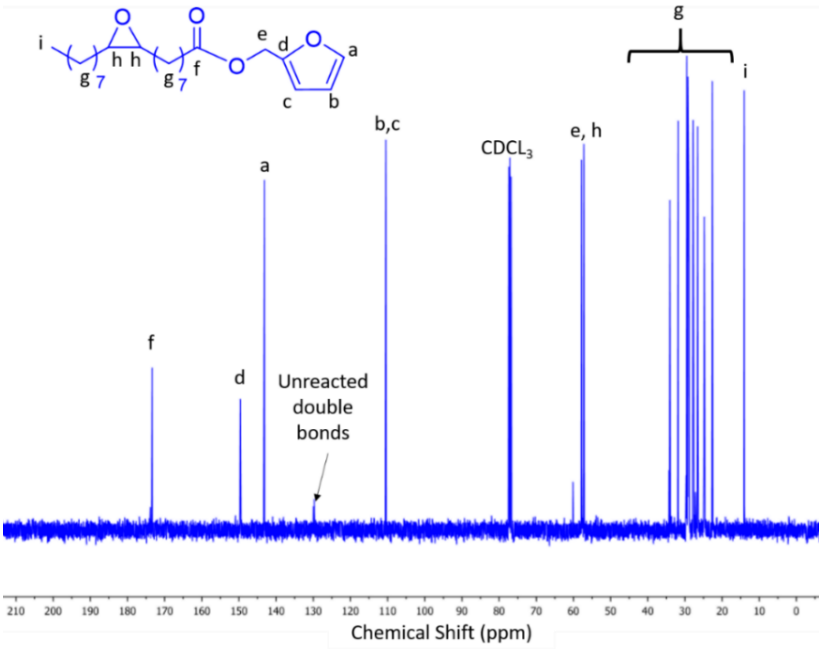

Figure S2.12 – ^{13}C NMR spectrum of FMOO.

Table S2.5 – Epoxidation reaction conditions. Optimization of FMO content for the synthesis of FMOO.

Trial	Eq. H_2O_2	Eq. Glacial Acetic Acid	Toluene Amount	Double Bond Relative Conversion [a]	Epoxy Formation Relative Conversion [a]	(%) Intact Ester [a]
1	1.5	0.5	0.5 ml /g oil	100	0	25
2	1.2	0.5	0.5 ml /g oil	100	63	63
3	1.2	0.5	12.5 w.t. % reactants	100	95	80
4	1.2	0.5	8.0 w.t. % reactants	100	82	66
5	1.2	0.2	12.5 w.t. % reactants	97	92	92

[a] Determined by ^{1}H NMR relative conversion

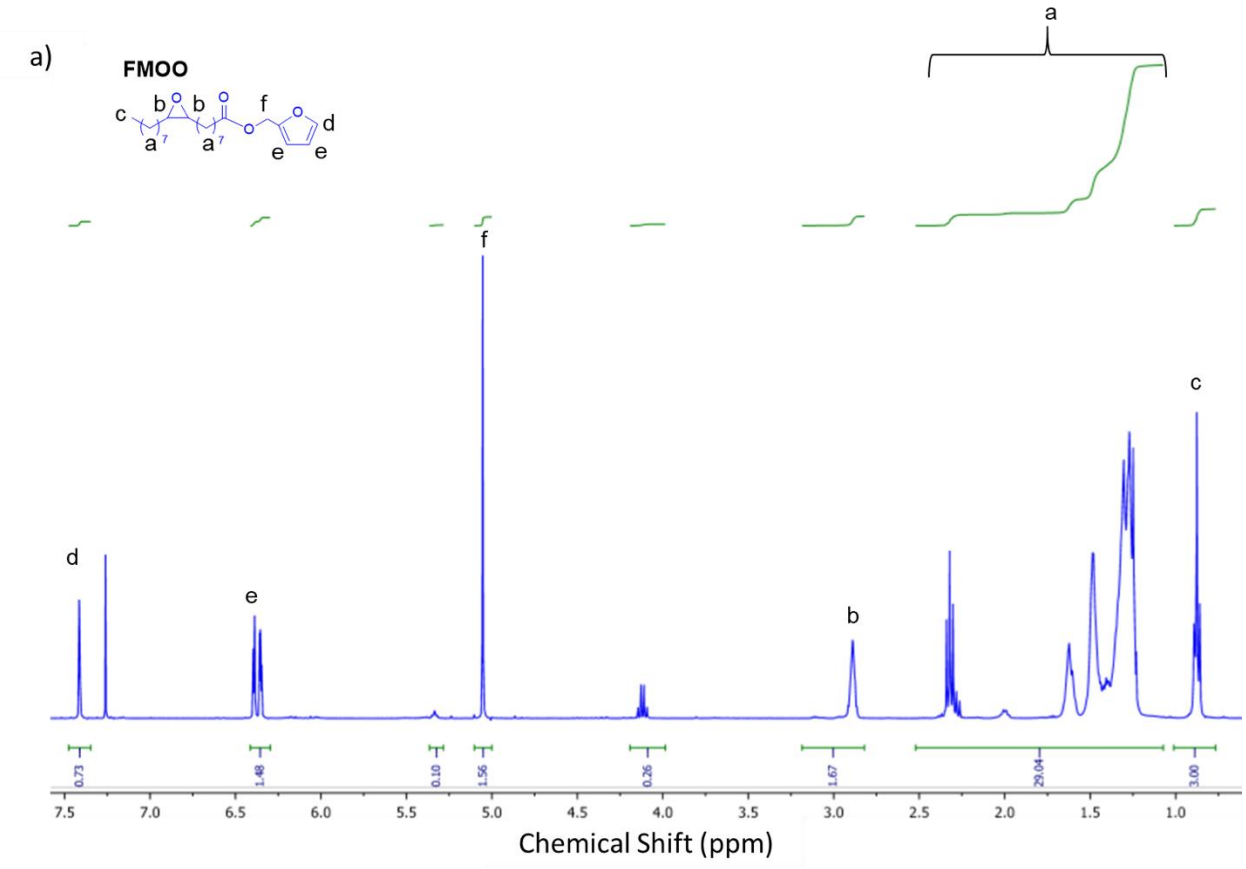

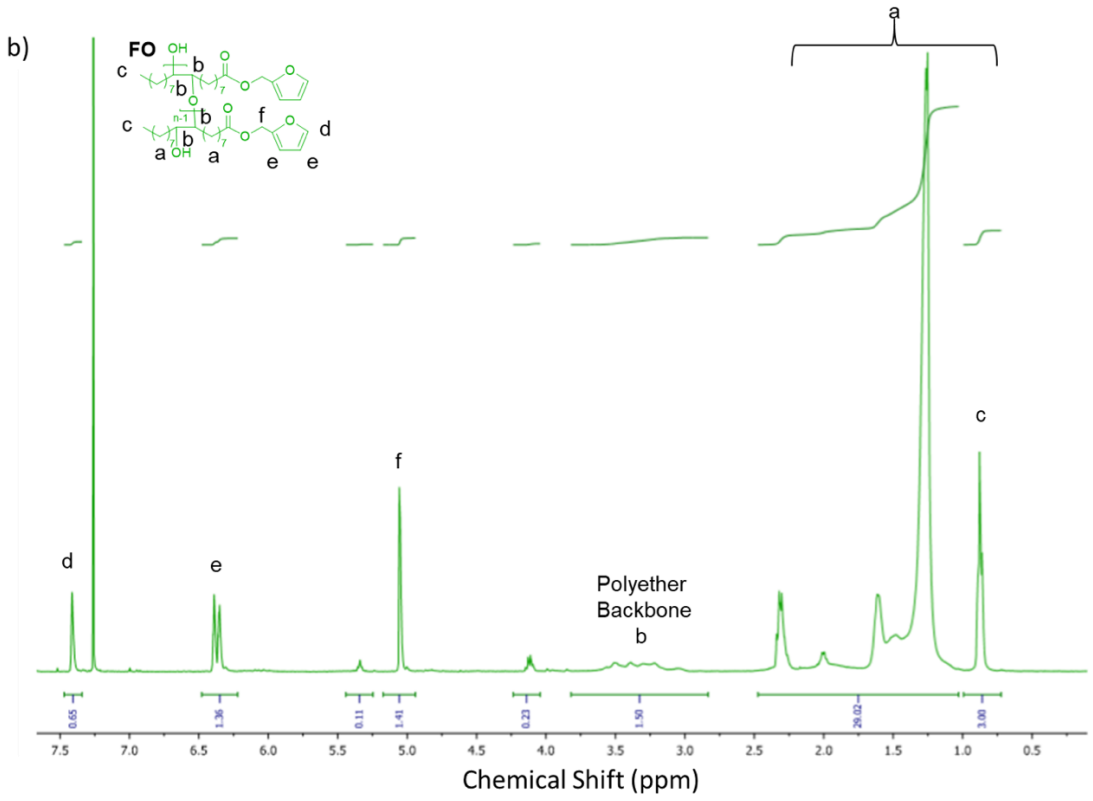

Figure S2.13 – ^{1}H NMR spectra of (a) FMOO and (b) FO with integrations.

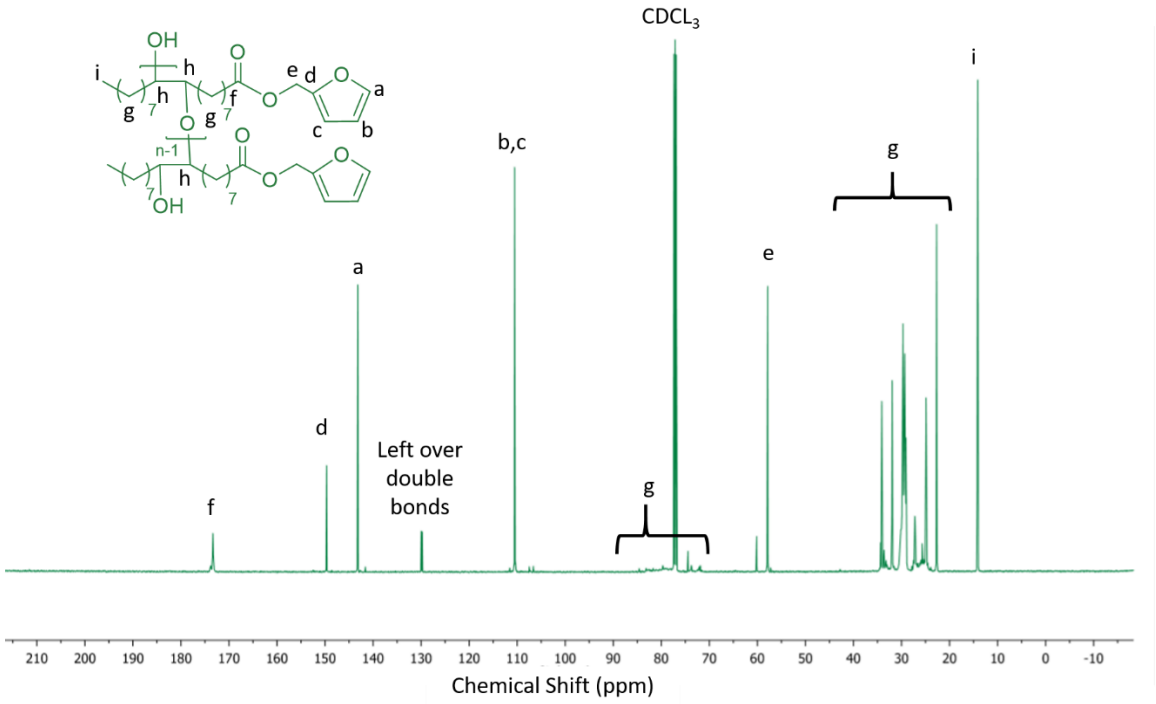

Figure S2.14 – ^{13}C NMR spectrum of FO.

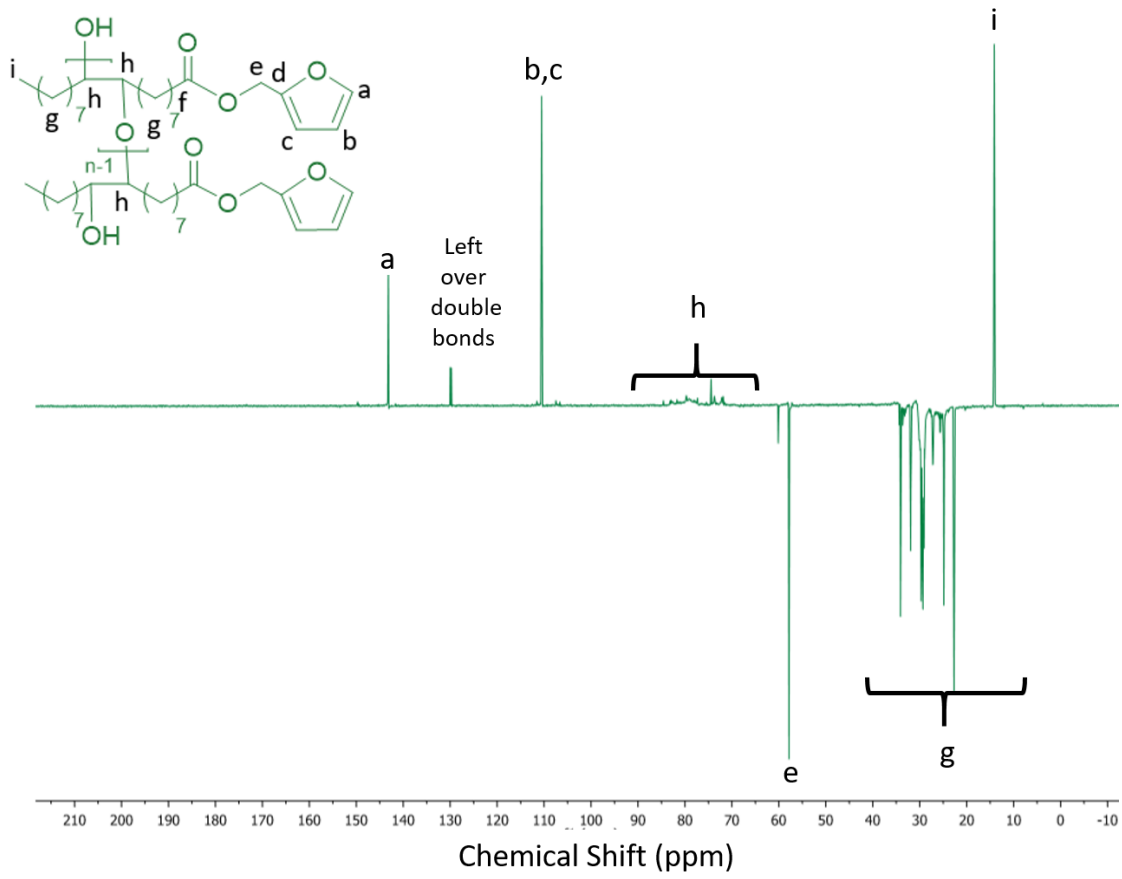

Figure S2.15 – ^{13}C NMR DEPT spectrum of FO.

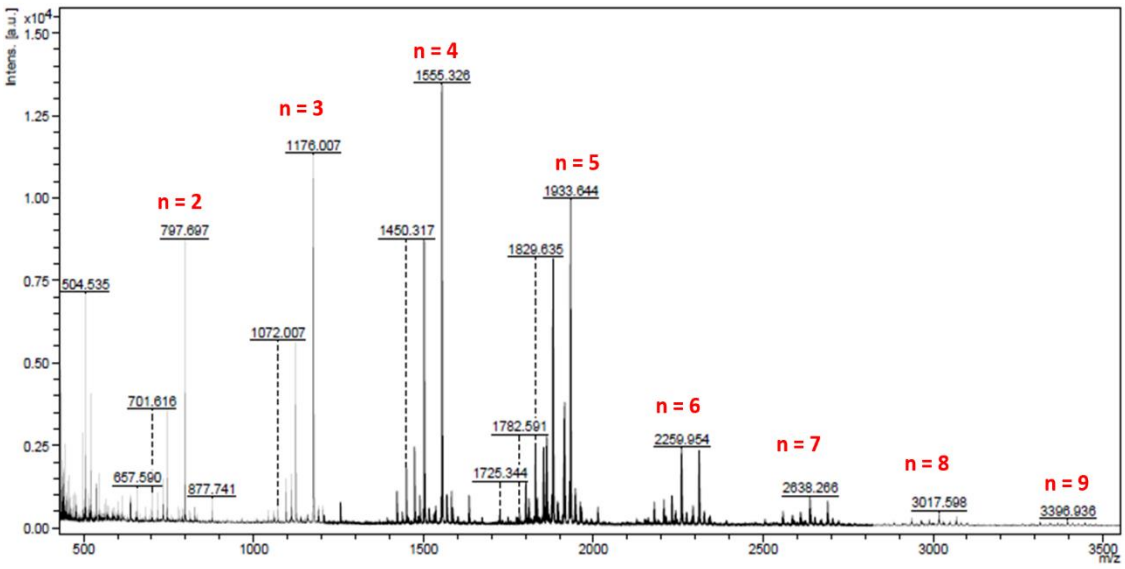

Figure S2.16 – MALDI-TOF MS spectrum of oligomer B on the ion series H-[O-$C_{23}H_{38}O_4$]$_n$-OH-Na^+ (mass = 379n + 18 + $Na^{+)}$ in majority. Matrix solution was freshly prepared: DHB was dissolved to saturation in a H_2O/CH_3CN/HCOOH (50/50,1%) solution.

Figure S2.16 shows the MALDI-TOF MS spectrum of oligomer B, which is dominated by a series of peaks ranging from 750 to 3400 Da, corresponding to linear hydroxyl-terminated oligomers doped with Na^+ ions of type H-$[O\text{-}C_{23}H_{38}O_4]_n$-OH-$Na^+$ (mass = 379n + 18 + Na^+); *n* values from 2-9. The three most intense peaks belonging to series of oligomers with *n* values of 3-5. The oleic acid received is isolated through the saponification of the triglyceride using ethanol as solvent and thus traces of ethyl ester impurities can be observed. As traces of ethyl ester are observed in ^1H NMR and ^{13}C NMR spectra and so can some peaks of these ethyl ester be detected by MALDI-TOF MS. This is further addressed in the analysis of zoom on series *n* = 4 peaks in Figure S2.17.

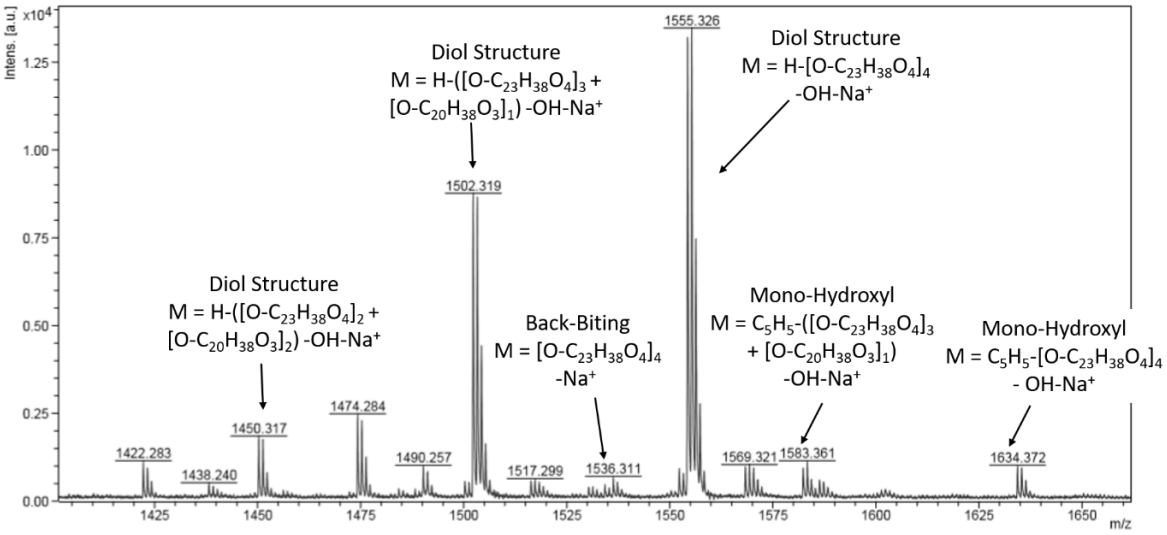

Figure S2.17 – MALDI-TOF MS spectrum of oligomer B zoom on series n = 4 on the ion. Matrix solutions was freshly prepared: DHB was dissolved to saturation in a H_2O/CH_3CN/HCOOH (50/50,1%) solution.

Figure S2.17 shows the MALDI-TOF MS spectrum oligomer B zoomed in series *n* = 4. The most intense peak at 1555 DA corresponds to the linear hydroxyl-terminated oligomer doped with Na^+ ions of type H-$[O\text{-}C_{23}H_{38}O_4]_4$-OH-$Na^+$ (mass = 379(4) + 18 + Na^+). The two following most intense peaks corresponding to 1502 Da and 1450 Da correspond to linear hydroxyl-terminated oligomer doped with Na^+ ions of type H-($[O\text{-}C_{23}H_{38}O_4]_3$ + $[O\text{-}C_{20}H_{38}O_3]_1$) -OH-$Na^+$ and H-($[O\text{-}C_{23}H_{38}O_4]_2$ + $[O\text{-}C_{20}H_{38}O_3]_2$) -OH-$Na^+$, respectively. As previously mentioned, the presence of ethyl ester impurities is detected by MALDI-TOF MS and accounts for these lower intensity peaks with such masses. When further analyzing series *n* = 4 of MALDI-TOF MS of oligomer B, it can be concluded that mainly diol structures are achieved with very little occurrence of monohydroxyl or cyclic architectures.

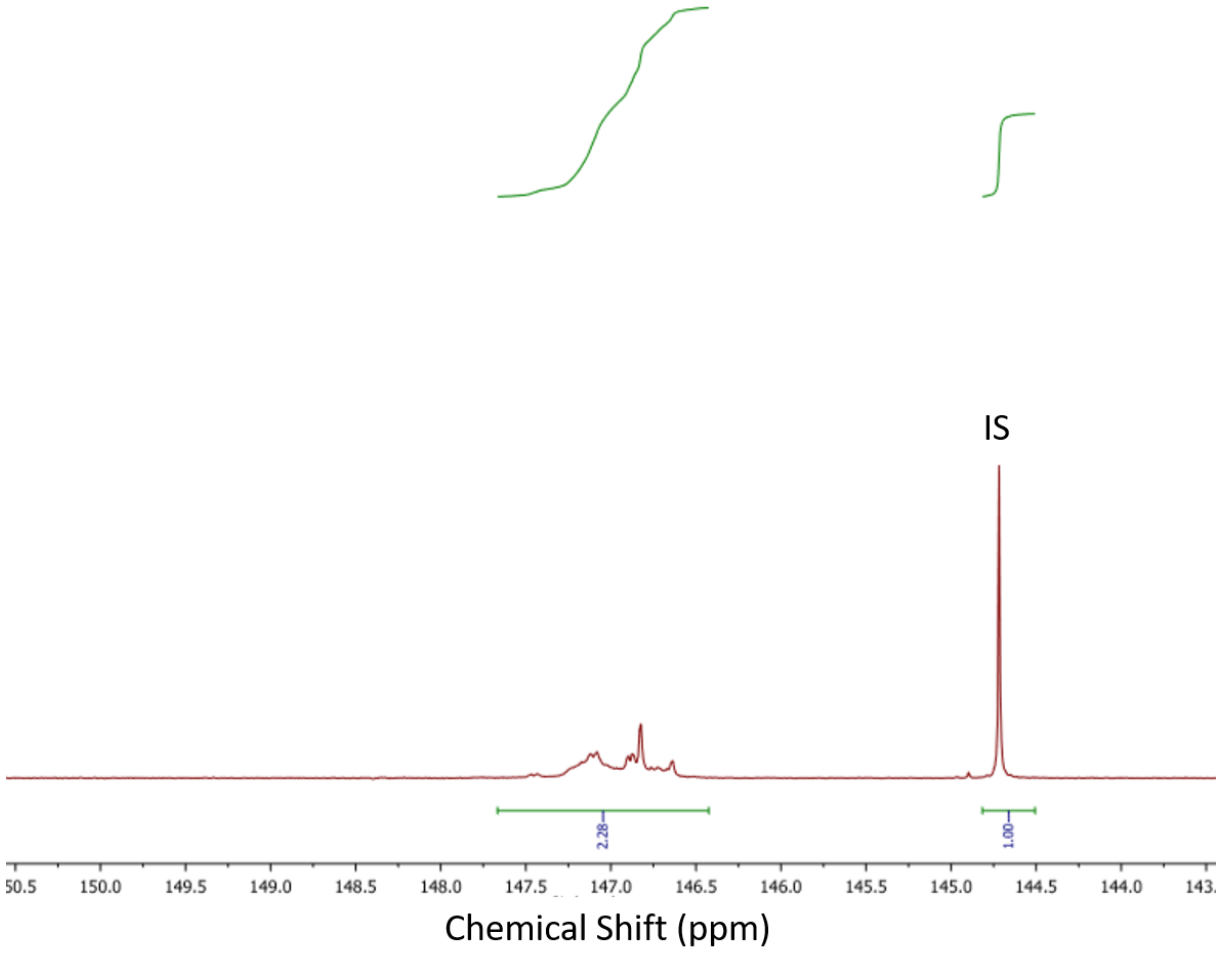

Figure S2.18 – ^{31}P NMR of FO Oligomer B with integrations. IS = internal standard (cholesterol). ^{31}P-NMR was performed with Cl-TDP as phospholane reagent. Phospilated product clearly indicated signals linked to the OH area (146.5-147.8ppm) of secondary hydroxyl.

Table S2.6 – HV of Oligomer B determined by ^{31}P NMR (mg KOH/g) from Figure S2.18.

Sample	Mass [mg]	Secondary Hydroxyl δ [ppm]	Area	mmol/g	HV [mg KOH/g]
Oligomer B	23.3	146.5 -147.8	2.28	0.91	55

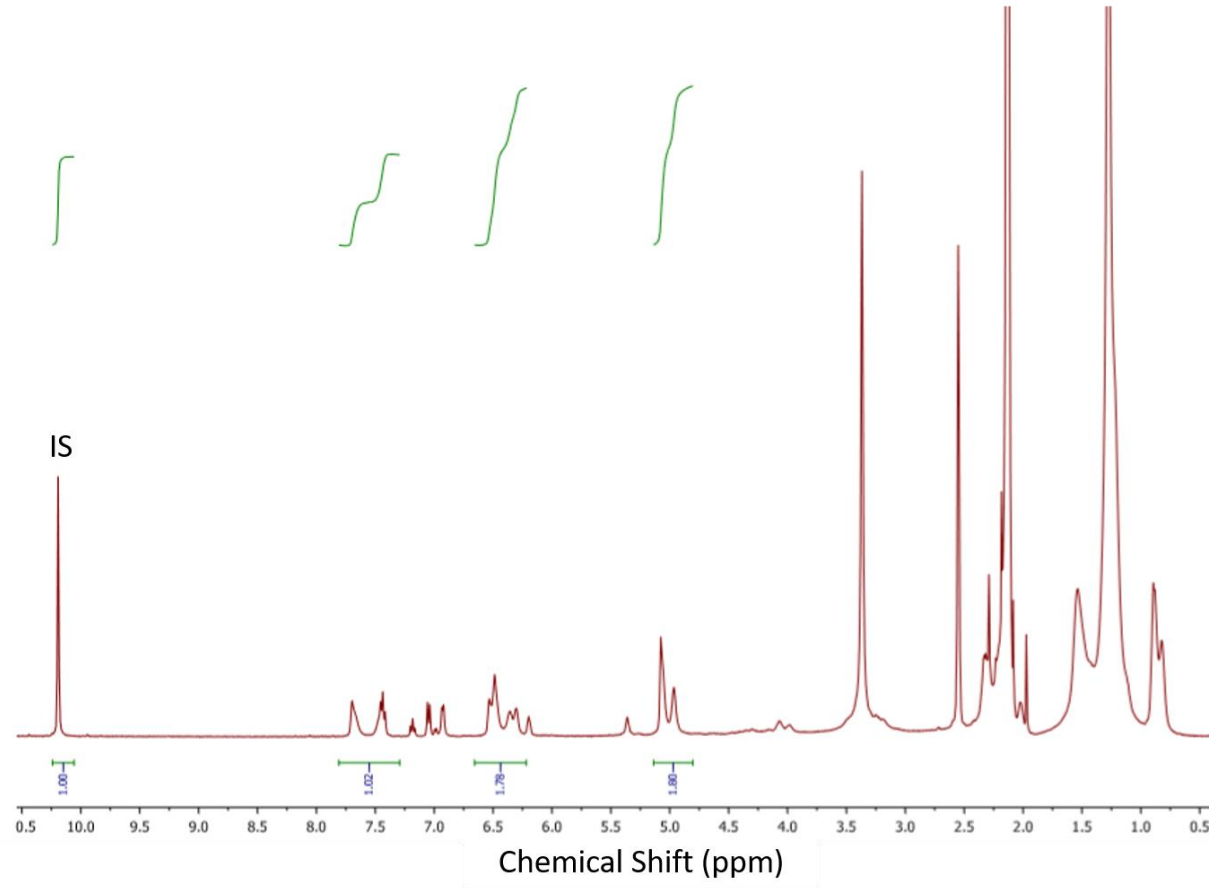

Figure S2.19 – Quantitative ^{1}H NMR of FO with integrations, internal standard PFB in DMSO.

Table S2.7 – Furan content in mmol/g of Oligomer B determined by Quantitative ^{1}H NMR from Figure 2.19.

Sample	Mass [mg]	Signal	Δ (ppm)	Area	mmol/g
Oligomer B	24.8	5-H of 2-furan	7.3 - 7.8	1.02	2.06
		3-H & 4-H of 2-furan	6.3 – 6.7	1.78	1.79
		2-H of OCH_2	4.7 – 5.3	1.80	1.81
Average	--	--	--	--	1.89

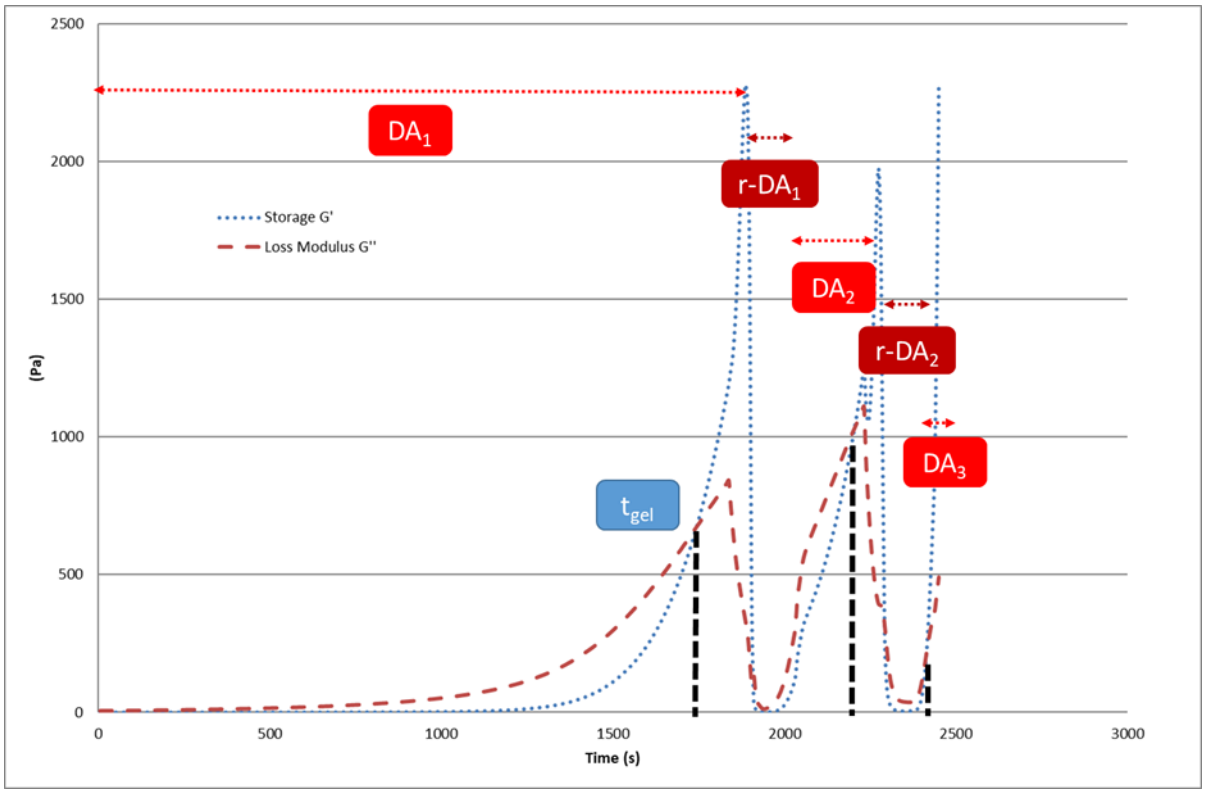

Figure S2.20 – Storage modulus (G', blue round dotted line) and loss modulus (G'', red dashed dotted line) versus time for FO and BMI furan:maleimide ratio 1:1 with different heating steps, DA at 60 °C and r-DA at 120 °C.

7.2. Characterization of biobased PUs

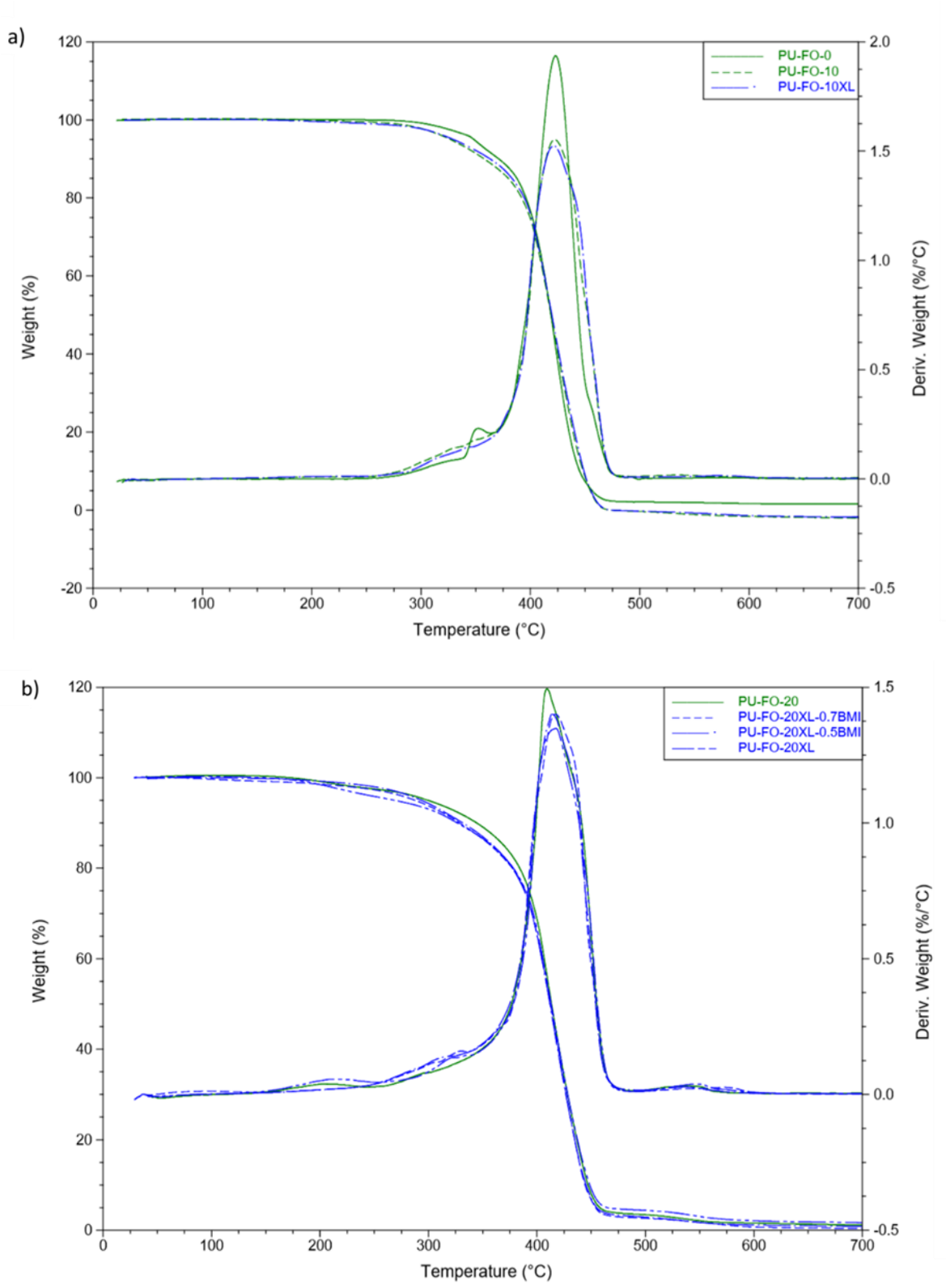

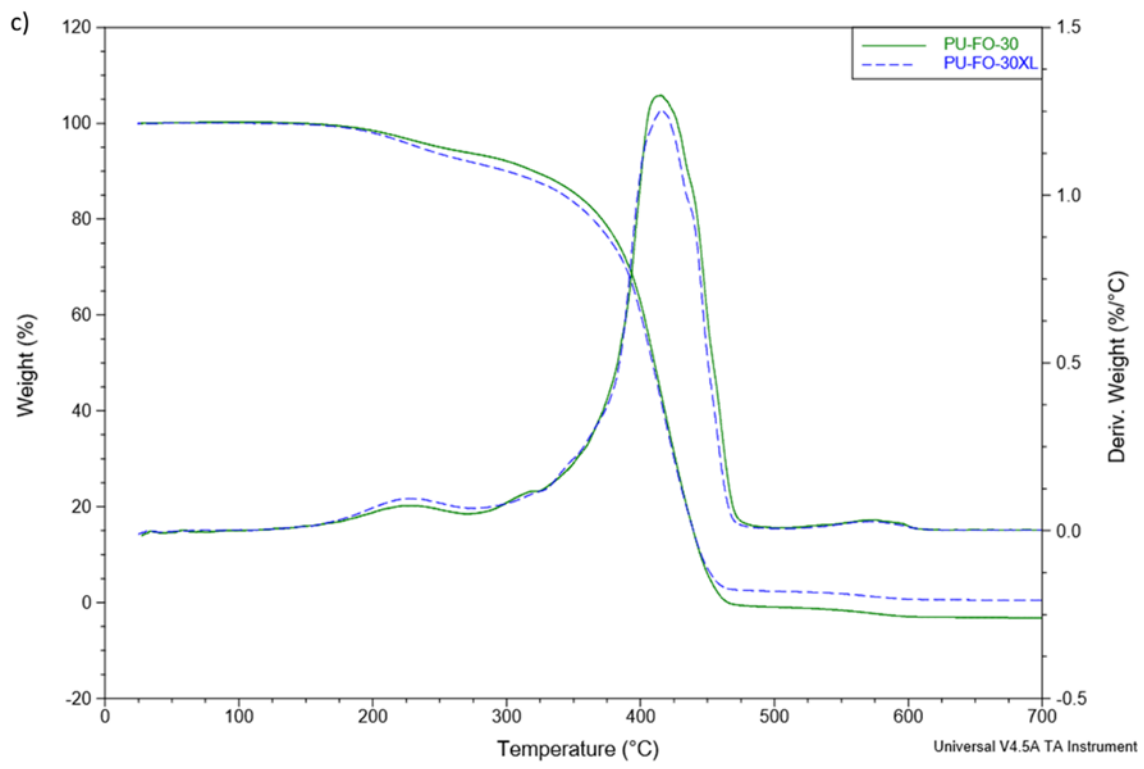

Figure S2.21 – Thermogravimetric analysis curves (TGA) and derivative thermogravimetric analysis curve (DTG) of materials a) PU-FO-0 (green, sold), PU-FO-10 (green, dashed), PU-FO-10XL (blue, dash-dot), b) PU-FO-20 (green, sold), PU-FO-20XL-0.7BMI (blue, dashed), PU-FO-20XL-0.5BMI (blue, dash-dot), PU-FO-20XL (blue, line-double dash), c) PU-FO-30 (green, sold) and PU-FO-30XL (blue, dashed).

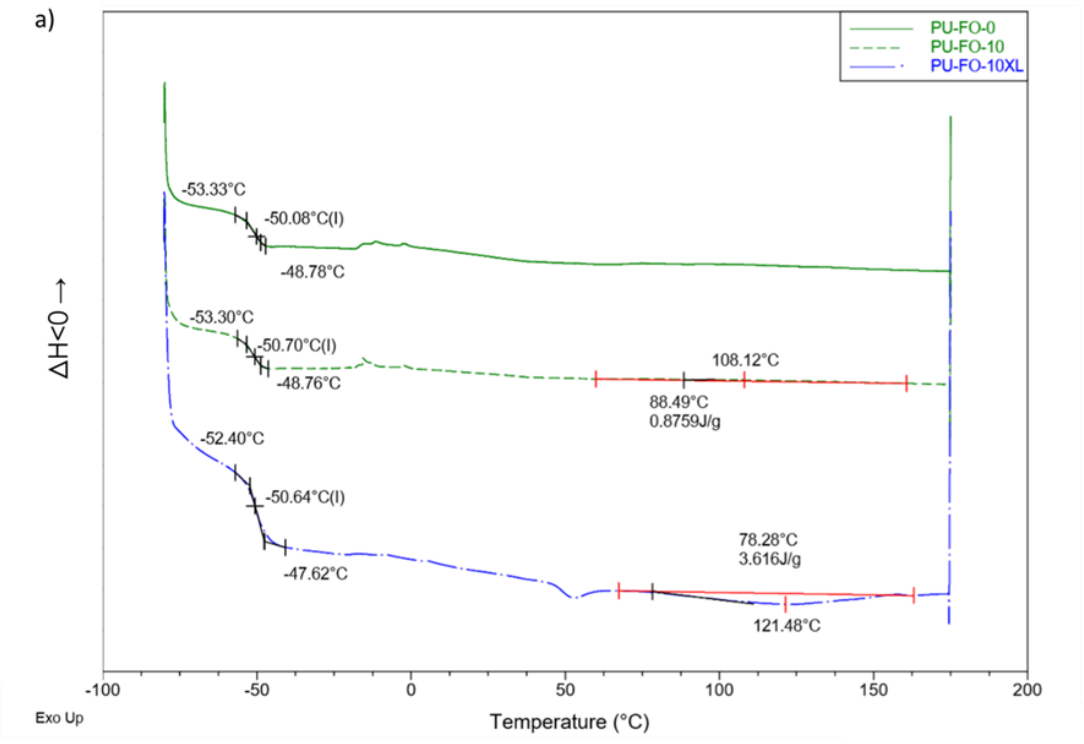

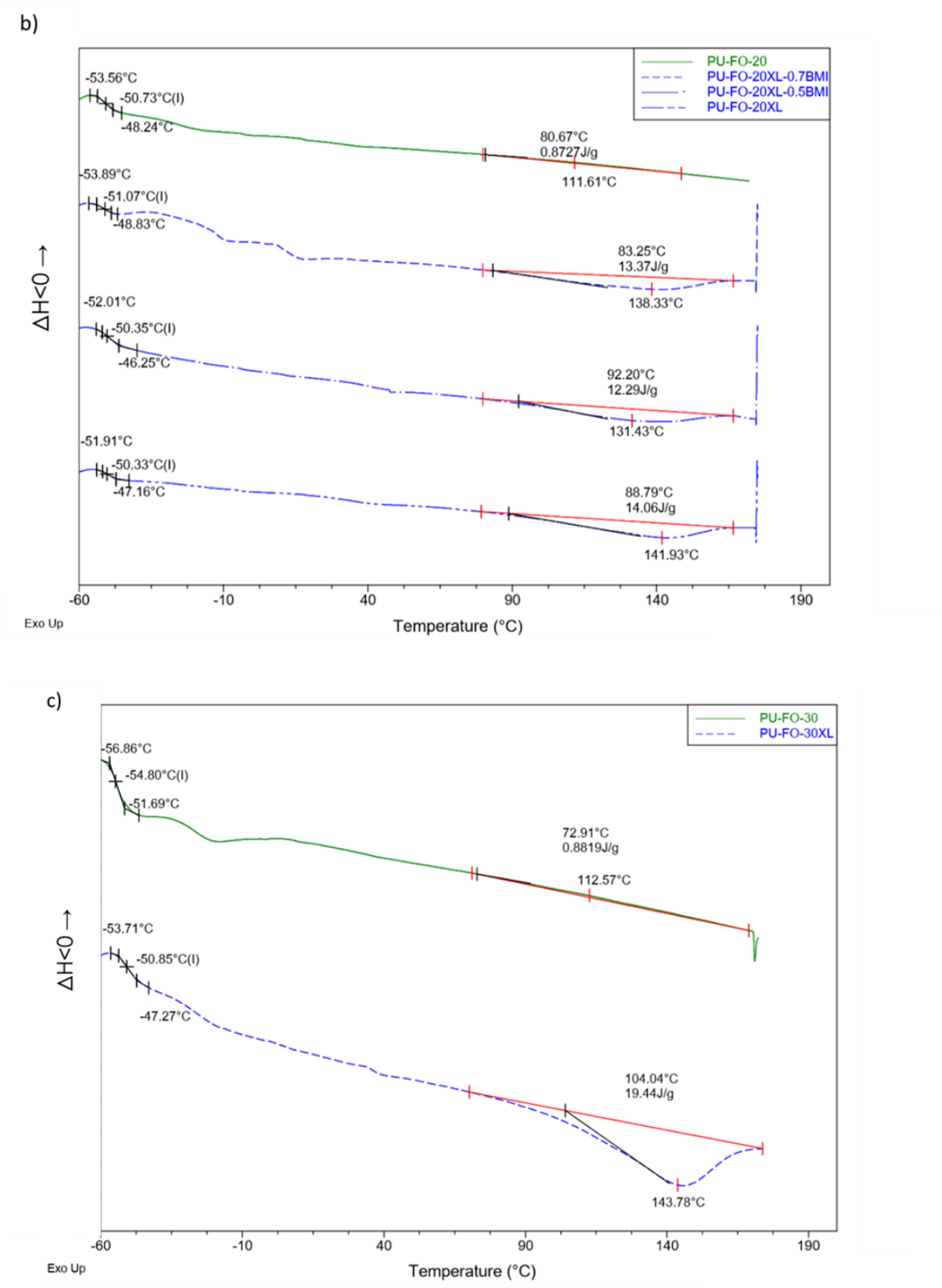

Figure S2.22 – Differential scanning calorimetry (DSC) thermograms of materials a) PU-FO-0 (green, sold), PU-FO-10 (green, dashed), PU-FO-10XL (blue, dash-dot), b) PU-FO-20 (green, sold), PU-FO-20XL-0.7BMI (blue, dashed), PU-FO-20XL-0.5BMI (blue, dash-dot), PU-FO-20XL (blue, line-double dash), c) PU-FO-30 (green, sold) and PU-FO-30XL (blue, dashed).

Conclusion of Chapter 2

The aim of this chapter was to synthesize cross-linked and reversible biosourced polyurethane architectures as a proof of concept. To achieve this, a fatty acid-based diol derived from oleic acid of sunflower oil, functionalized with pendant furan groups (called "Furan Oligomer" or FO) was synthesized. The FO was incorporated into backbone of polyurethane chains and the pendant furan groups were used as cross-linking sites with a short polypropylene oxide-based bismaleimide. FO and synthesis intermediates were fully characterized. In order to model the reversible linking of cross-linking sites and the thermo-reversibility of the polyurethane networks, the Diels-Alder and retro-Diels-Alder reaction between the FO and the commercial bismaleimide was studied by differential scanning calorimetry, gel formation and FTIR.

The cross-linked systems developed within the framework of this chapter have an increased glass transition temperature, an insolubility ratio, improved rigidity and mechanical resistance as well as a lower swelling ratios when compared to reference PUs. Cross-linked materials have modular mechanical properties depending on the amount of FO added. These bio-based materials exhibit a wide range of behaviors; from that of thermoplastics (low crosslinking) to that of the behavior of thermosets (most crosslinked). Material recycling cycles have been successfully carried out and has shown stable properties after the different cycles. The materials have self-healing properties. For this, tensile test dumbbells were cut in half, repaired by joining the pieces together, treating them at 120 ° C, followed by a heat treatment at 60 ° C. The two parts recombined by the means of heat induced self-repair.

Consequently, cross-linked thermoreversible and self-repairing biosourced systems based on urethane groups and clickable functions have been successfully synthesized starting from vegetable oil derivatives by the Diels-Alder reaction by controlling the syntheses and macromolecular architectures.

Chapter 3. Synthesis and behavior of responsive biobased polyurethane networks cross-linked by click chemistry: Effect of the cross-linkers and backbone structures.

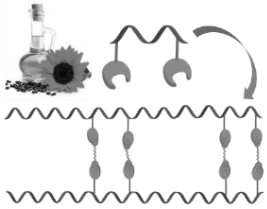

Chapter 2: Synthesis of Furan Oligomer and biobased PU CANs

Chapter 1: State of the art – Click chemistry and vegetable oils

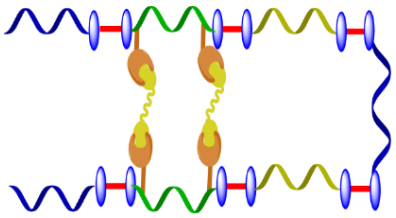

Chapter 3: Further elaboration of biobased PU CANs containing FO

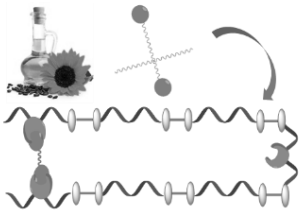

Chapter 4: Synthesis of Methyl oleate bismaleimide and biobased PU CANs

Introduction of Chapter 3

The preceding chapter established the proof of concept of designing biobased polyurethane (PU) responsive systems with dynamic cross-linking points to yield advance polymer properties. Developing such systems was deemed possible by the synthesis of new biobased synthon denoted as the Furan Oligomer (FO) and its interaction with a bismaleimide (BMI) in PU networks. As previously explored in the preceding chapter, the FO consists of diol structure containing pendant furan rings derived from oleic acid. Its diol structure allows for FO to react with diisocyanates and be incorporated into PU backbone, whereas the pendant furan moiety end can then react with a BMI to form dynamic cross-linking points via the Diels-Alder and retro-Diels-Alder reaction.

This chapter aims to further examine biobased PU responsive cross-linked systems using the FO while studying, (i) the effect of varying the BMI length and structure and (ii) the incorporation of phase segregation by the of addition of 1,4 – butanediol (BDO) to produce hard segments (HS) in the PU network. Four different types of bismaleimides were used: 1'-(Methylenedi-4,1-phenylene) bismaleimide (MPBMI), poly(propylene oxide) (PPO) based BMI with a degree of polymerization (DP) = 6 (PPOBMI-DP6), PPO-poly(ethylene-oxide)(PEO)-based BMI with an overall DP = 13 (PPOPEOBMI-DP13) and PPO-based BMI with a DP = 33 (PPOBMI-DP33). Two series of materials were synthesized using simple PU structures (no HS). The first consisted of varying in the amount of FO in PU structures and cross-linking by MPBMI. A second PU series involved keeping the FO amount content constant and cross-linking the structures by the different aforementioned BMIs. Lastly, a control and cross-linked system were synthesized using 20 % by weight of HS by the incorporation of BDO. All PUs were characterized by different and complementary techniques to better understand their structures and behaviors. For instance, the effect of varying parameters on the thermal recyclability and heat induced healing of all cross-linked architectures was also studied and shown.

Synthesis and behavior of responsive biobased polyurethane networks cross-linked by click chemistry: Effect of the cross-linkers and backbone structures.

Khantutta-Kim Tremblay-Parrado[1], Luc Avérous*[,1]

(1) BioTeam/ICPEES-ECPM, UMR CNRS 7515, Université de Strasbourg, 25 rue Becquerel, 67087 Strasbourg Cedex 2, France

(*) Corresponding author: luc.averous@unistra.fr

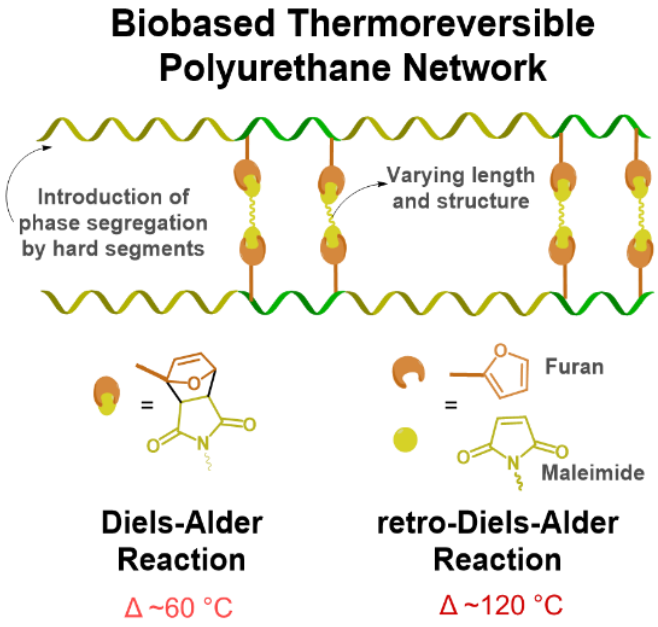

1. Abstract

Distinct bismaleimides (BMIs) of differing molar masses and chemical architectures were studied as cross-linkers of different polyurethane (PUs) backbones containing pendant furan rings via Diels-Alder (DA) reaction to form responsive biobased networks. Pendant furan rings were introduced during PU synthesis by addition of diol structures containing pendant furan rings denoted as the Furan Oligomer (FO), which is derived from oleic acid. The effects of varying the proportions of FO in cross-linked systems as well as the type of BMIs were particularly studied. The corresponding materials were fully analyzed through several complementary approaches to evaluate their performances. PUs cross-linked by an aromatic BMI yield superior mechanical properties, whereas the chain length and structure clearly influenced the swelling, reprocessability and heat induced healing of the networks. The introduction of hard segments (HS) into the PU backbone was also examined in terms of micro-segregation. It was found that the effect of hydrogen bonding of HS in combination with the cross-links by DA would yield superior mechanical properties with good thermal recyclability and self-healing behaviors.

Keywords: Renewable Resources, Oleic acid, Biobased polymers, Polyurethane, Diels-Alder-Cycloaddition, Reversible network

2. Introduction

The modern era was revolutionized by the invention of plastics and as such have gained prevalence in most aspects of our daily lives, with its existence found amongst consumer and industrial goods as well as medical devices. Consequently, its ubiquitous presence has hailed emerging concerns for its increasing appearance in landfills and oceans (Thompson et al. 2009). Furthermore, most plastics used are synthetic and originate from non-renewable petroleum resources, and thus if their end-of-life is managed poorly, remain and effect natural environments for decades. It is for this reason that polymer and material design should not only take in account the origin of materials (by developing biobased and environmentally friendly materials) but as well as factor in of advanced properties to manage the end-of-life as well as extending lifetimes of materials. Cross-linked polymers (or thermosets) are the most present type of materials (up to 20% of the produced polymers (American Chemistry Council 2017)), mainly due to their high strength and chemical stability, but, have been historically mismanaged in their end-of-life given their inability to be recycled by traditional techniques. In contrast, the incorporation of dynamic interactions in linear and polymer networks can give rise to advanced properties such as healing and reprocessability which can extend the life of end user materials, but as well reduce the use of energy, resources and creation of waste (Fortman et al. 2018).

Polymer networks with dynamic cross-links have recently skewed the frontier between the conventional division of polymeric materials, thermoplastics and thermosets. The recent work of Sumerlin et al. outlines the fundamental theory of these networks and provides a critical assessment of their status (Scheutz et al. 2019). Generally, these networks are based on dynamic covalent bonds which are assembled and disassembled by “associative” or “dissociative” processes by the exposure to external stimuli (thermal) or autonomously (Denissen, Winne, and Du Prez 2016). Cross-linked polymers containing dynamic covalent bonds were coined by Kloxin et al. as Covalent Adaptive Networks (CANs) (Kloxin et al. 2010). Associative CANs consists of bond exchange between polymer chains, with a preserved cross-linking density as a new covalent bond can only be formed if another has been broken. As discovered by Liebler and co-workers, vitrimers are an example of this (Montarnal et al. 2011) and can also be exclusively biobased (Dhers,

Vantomme, and Avérous 2019). Alternatively, dissociative CANs exhibit chemical bond exchanges where bonds are first broken and reformed again. Many networks containing thermoreversible cross-linking covalent chemistries have been explored such as the Diels-Alder (DA) cycloaddition (Chen et al. 2002), hindered urea exchange (Ying, Zhang, and Cheng 2014), and 1,2,3-trazolium salts (Obadia et al. 2017). The thermoreversible furan-maleimide [4+2] cycloaddition DA reaction is the most prominently studied reversible chemistry used to synthesize dissociative CANs (Canary and Stevens 1992; Chujo, Sada, and Saegusa 1990; Gandini 2013). Regardless of the corresponding chemistry, the association between the design of these thermosets and the notion of recyclability at the end-of-life using dynamic cross-links allows to develop sustainable materials.

Polyurethanes (PUs) are a versatile and major polymer family that can be tuned for a wide range of applications e.g.; the construction, automotive and medical industry. Consequently, PUs are ranked 6th in term of worldwide production (Carré et al. 2016). In addition, their chemical structures can be utilized for the incorporation of thermoreversible chemistry such as that of the DA reaction to further enhance the sustainability of cross-linked PUs (Heo and Sodano 2014; Rivero et al. 2014; Dolci et al. 2015; Lakatos et al. 2016; Du et al. 2016; Dolci et al. 2017; Willocq et al. 2017; Irusta, Fernandez-Berridi, and Aizpurua 2017; Truong et al. 2018; Truong et al. 2019; Oh et al. 2019) Nevertheless, to design truly sustainable materials, they must be derived from renewable resources. Nowadays, the biobased PU market is expanding with a particular emphasis on use of vegetable oils consisting of adequate architectures for the developments of polyols for thermosets (Meier, Metzger, and Schubert 2007; Desroches, Escouvois, et al. 2012; Lligadas et al. 2013) or for thermoplastic PU applications (Ionescu 2005; Palaskar et al. 2012; Desroches et al. 2012; Petrović et al. 2008; Xu et al. 2008), by controlling the corresponding functionality.

There seems to be an increasing research in developing biobased CANs from diverse biobased resources such as lignins (Duval et al. 2015; Buono et al. 2017), tannins (Duval et al. 2017), alginate (García-Astrain and Avérous 2018; García-Astrain and Avérous 2019), chitosan (García Astrain et al. 2016; Guaresti, García–Astrain, et al. 2018; Guaresti, García Astrain, et al. 2018), starch (González et al. 2018), 5-hydroxymethyfurfural (Yoshie, Yoshida, and Matsuoka 2019), natural rubber (Feng et al. 2019) or vegetable oils (Lacerda and Gandini 2014; Lacerda, Carvalho, and

Gandini 2014; Gandini, Lacerda, and Carvalho 2013; Vilela, Silvestre, and Gandini 2013; Vilela et al. 2012; Vilela et al. 2011). Nevertheless, according to the literature, the development of dynamic biobased PU architectures is until now largely limited (Gu and Wu 2018; Wilson and Chen 2019; Zhang, Michel Jr, and Co 2019; Hu, Chen, and Torkelson 2019). Besides, in a recent work (Tremblay-Parrado and Avérous 2019), we have addressed this challenge by synthesizing reversibly cross-linked PUs based on vegetable oils using the thermally reversible furan-maleimide DA reaction. The DA reaction between furan and maleimide functions is defined as a click cycloaddition reaction and occurs at modest temperatures (below 90 °C), whereas the retro-DA (r-DA) reaction, occurs between 110 and 130 °C (Chen et al. 2002). A PU cross-linked system was proved to be thermally recyclable and self-healing by the incorporation of diol containing pendant furan rings called the Furan Oligomer (FO), which was derived from oleic acid. The pendant furan rings of the PU backbone were reacted with a short poly(propylene oxide) (PPO) based bismaleimide (BMI) to form cross-linking points.

The aim of this study is to examine more particularly the effect the BMI structure and length (Scheme 3.1 – Route 1) onto the polymer properties such as the thermal recyclability and heat induce healing of the corresponding biobased PU networks. Besides, new macromolecular architectures with increased hydrogen bonding concentration was developed (Scheme 3.1– Route 2), by incorporation of hard segments into the PU backbone via the addition of 1,4 – butanediol and studied.

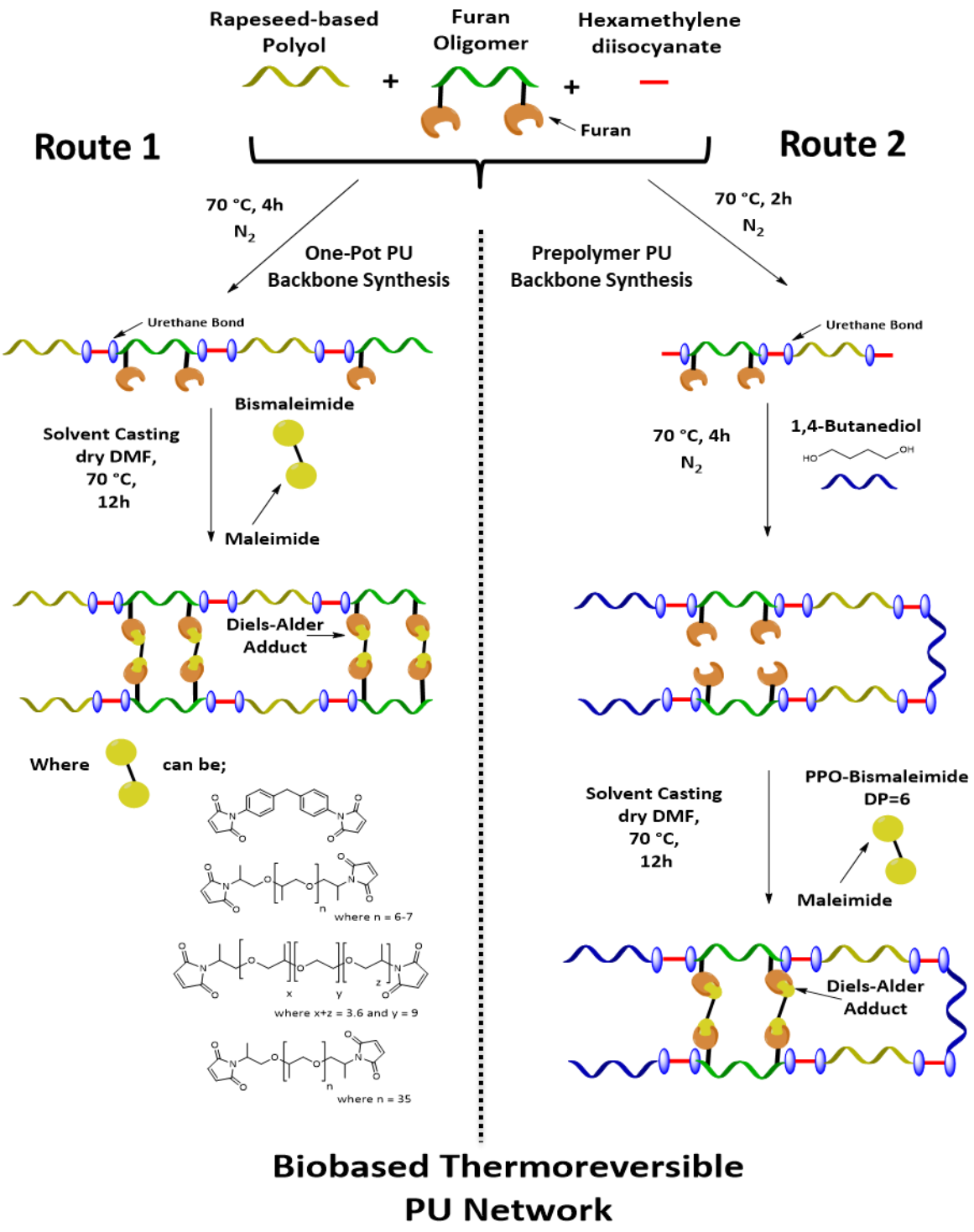

Scheme 3.1 – Illustration of the general synthesis of biobased thermoreversible PU-based systems using FO.

3. Experimental Section

3.1. Reagents and materials

Octadec-9-enoic acid (OA) from sunflower oil was supplied by ITERG. Acid value is 185 mg KOH per g. Biobased polyester polyol (purchased from Oleon) was derived from dimeric fatty acids from rapeseed oil with purity greater than 98% and weight average molar mass (M_w) around 3 000 g/mol. Hydroxyl and acid values were 33.7 and 0.253 mg/g KOH, respectively.The different cross-linkers such as poly(propylene oxide) bismaleimide (degree of polymerization or DP = 6 and 35) and poly(propylene oxide)-b-poly(ethylene oxide)-b-poly(propylene oxide) bismaleimide were obtained from Specific Polymers (Castries, France). 4-dimethylaminopyridine (DMAP, 99%), 2-chloro-4,4,5,5-tetramethyl-1,3,2-dioxaphospholane (CL-TDP, 95%), Furfuryl alcohol (FA, 98%), hydrogen peroxide (H_2O_2, 30% *w/v* aqueous solution), chromium (III) acetylacetonate (99.99%), [D_6]dimethyl sulfoxide (DMSO, 100%, 99.96% atom D) and cholesterol (>99%) were purchased from Sigma Aldrich. N,N'-dicyclohexylcarboiimide (DCC, 99%), chloroform-d ($CDCl_3$, 100%, 99.96% atom D), 1,1'-(Methylenedi-4,1-phenylene)bismaleimide (95%, MPBMI) and $HSbF_6$ (65% *w/w* aqueous solution), were purchased from Alfa Aesar. Dichloromethane dried over molecular sieve (DCM, >99%, stabilized with amylene) and diethyl ether (stabilized with BHT) were purchased from Carlo Erba. N,N-dimethylformamide (DMF, 99.8%) Glacial acetic acid (GAA, >99%) and 1,4-Butanediol (BDO, 98%) were purchased from Fisher Scientific.Amberlite IR-120 H, Toluene (100%), 2,3,4,5,6-pentafluorobenzaldehyde (PFB,98%) and hexamethylene diisocyanate (HDI, 99%) was purchased from Fluka Chemicals, VWR Chemicals, Fluorochem, and Acros Organics, respectively. Most of these reagents and solvents were used without additional purification.

3.2. Syntheses and material processing

3.2.1. Synthesis of Furan Oligomer from Oleic Acid

The Furan Oligomer was synthesized by a previously reported 3-step synthesis procedure (Tremblay-Parrado and Avérous 2019). The detailed procedure can be found in the Supporting Information (SI) section. First, the esterification of Octadec-9-enoic acid (OA) by furfuryl alcohol in mild conditions by a Steglich Esterification was achieved. *N,N'*-dicyclohexylcarboiimide (DCC)

was used as an activating agent, whereas 4-dimethylaminopyridine (DMAP) was used as a catalyst. This was followed by the Prilezhaez reaction to accomplish the in-situ epoxidation of the sole alkene bond on the fatty aliphatic chain by the use of H_2O_2 and glacial acetic acid. Lastly, FO diol structure was attained by the acid-catalyzed ring-opening polymerization (ROP) using fluoroantimonic acid, $HSbF_6$, and water to limit the polymerization.

3.2.2. Diels-Alder and retro-Diels-Alder reaction between FO and different BMIs

To explore the dynamicity of the DA reaction between the furan moieties of the FO and maleimide moieties of BMIs, FO and each BMI were mixed together with a furan / maleimide molar ratio of 1, in a small flask and then dissolved in DMSO and exposed to different heating cycles. After 24 h exposure to 60 °C without stirring gelation occurs due to the DA reaction. To prove the r-DA reaction, the flask was exposed to 120 °C for 1 h. The mixture returns to a disassembled state. Each heating step was repeated another time. Final gels were washed with water, dried and examined by FTIR to compare with spectra of the initial system.

3.2.3. Synthesis of PUs containing FO

Rapeseed polyester polyol, FO as well as glassware were previously dried. PUs films were synthesized using different amounts of FO under nitrogen flow. For the synthesis of PU containing 20% FO the formulation included 11.8 mmol of OH from rapeseed polyester polyol, 3.01 mmol OH from FO and 15.5 mmol NCO from HDI, stirred mechanically for 3-4 h. The –NCO/-OH ratio was established to 1.05 for all syntheses.

3.2.4. Synthesis of PUs containing FO and BDO

All glassware and reactants were previously dried. A single type of PU containing FO and BDO was prepared with a -NCO/-OH ratio equal to 1.05: 1, with a hard segment (HS) content of 20 %. This type of PU was synthesized by a two-step prepolymer process. In a first step, the polyol (15.8 g, 9.52 mmol OH,) FO (1.75 g, 2.38 mmol OH) and HDI (3.27 g, 38.9 mmol NCO) was reacted for 2 h in a three-necked, round-bottom flask, under a nitrogen flow, mechanical stirring at 70 °C. During the synthesis a sample was extracted to determine the NCO content to control the NCO consumption during the reaction.

A specific method has been performed to determine the amount of isocyanate that reacts with on equivalent of *N*-dibutylamine, and gives NCO content by weight percent. A sample of the prepolymer (≈ 1.2 g) of was diluted in a standard solution (20 mL) of dibutylamine 0.2M in THF for a reaction between the residual diisocyanate. The excess amine was back-titrated with a 0.5 aqueous solution of HCl. NCO content by weight percent was determined using Equation (1):

$$\%NCO = \frac{(V_{blank} - V_s) * 42 * 0.1}{m_s} \quad (1)$$

in which V_{blank} (mL) is the HCl solution volume required for a blank titration of the dibutylamine solution, while V_s is the volume required for the prepolymer titration and m_s is the prepolymer weight. It was calculated from this experiment that the NCO content for the prepolymer should approximately 5.4%. This result was used for the addition for the precise amount of BDO (≈ 1.13 g of BDO). The BDO was added and left reacting for 3 h and followed by FTIR.

3.2.5. Cross-linking of PUs containing of FO and PUs containing FO and BDO

After the initial synthesis of linear PU, they were dissolved in dry DMF. The respective BMI was added in the required amount (to yield an overall furan to maleimide moiety ratio 1:1 between the FO and BMI). In order for the DA reaction and cross-linking to occur the contents were stirred overnight at 70 °C. Then, the solution was transferred into a polytetrafluoroethylene mold for solvent casting by slow evaporation of DMF for 48 h at 70 °C followed by 24 h at 70 °C under vacuum to remove traces of solvent.

3.2.6. Material reprocessing of cross-linked PUs

Reprocessing of synthesized PUs was preformed using a LabTech Scientific hot press. PU we cut into small pieces and placed in the middle of tile mold (10 cm x 10 cm x 1 mm) at 150 °C. The material was softened by a 10 min preheating cycle, followed by venting cycles, a pressing cycle of 15 min with applied force of 16 MPa. Prior to punching the film into dumbbell traction samples, the film was cured at 60 °C for 48 h, followed by 24 h at room temperature.

3.2.7. Study of the self-healing Behavior

Dumbbell-shaped samples where cut in two and put back in contact and exposed to 120 °C for 1 h, followed by a 24 h exposure to 60 °C. Prior to tensile test, the sample was left 24 h at ambient temperature.

3.3. Methods and characterization techniques

3.3.1. Iodine Value

Iodine value (IV) was determined using the Wijs method to quantify the double bond content according to ISO 3961:2018(E)

3.3.2. NMR Spectroscopies

All NMR spectra were recorded on a Bruker Ascend 400 or 500 MHz spectrometer. Sample were dissolved in deuterated chloroform ($CDCl_3$) or deuterated dimethyl sulfoxide ([D_6]DMSO) with contents between 8-10 and 20-30 mg/mL for ^{1}H-NMR and ^{13}C-NMR spectroscopy, respectively. The calibration of ^{1}H- and ^{13}C-NMR spectra was performed using the chloroform peaks at δ = 7.26 and 77.16 ppm, respectively and DMSO peak at δ = 2.50 ppm as references.

^{31}P NMR analysis was performed by 2-chloro-4,4,5,5-tetramethyl-1,3,2-dioxaphospholane as phosphytilating agent. Scans (128) were recorded with a 15 s delay and a spectral width of 80 ppm (180-100 ppm). Cholesterol was used as an internal standard, as described in standard protocols (Spyros 2002).

In the case of quantitative ^{1}H NMR spectroscopic analysis, 20 mg was dissolved in [D_6]DMSO (0.5 mL) for each sample before the addition of a standard solution (100 µL) of pentafluorobenzaldehyde in [D_6]DMSO. 32 scans were collected 10 s delay.

3.3.3. Fourier transform infrared (FTIR) spectroscopy

For FTIR spectroscopy of experimental samples, a blank background was performed prior to examining samples (32 scans, resolution 4 cm^{-1}) on a Nicolet 380 spectrometer equipped with an ATR diamond module (FTIR-ATR) in reflection mode.

3.3.4. Rheological measurements

Dynamic rheological measurements were performed with a TA Instruments Discovery HR-3, using plate-plate parallel geometry equipped with a Peltier temperature control system. The lower plate had a 60 mm diameter whereas the upper plate had a 25 mm diameter. Gel formation between FO and BMI studied by examining the progression of the (G´) and loss (G´´) modulus at 60 °C at a constant shear strain (1%), at 1 Hz. The gel point is defined at the gel time (t_{gel}) when the curves of G' and G'' crossover. The dynamicity of the gel formed on the viscometer was evaluated by exposing it heating cycles of 120 °C to disassemble the gel (r-DA reaction) followed by 60 °C to re-assemble it (DA reaction). This heating cycles were repeated.

3.3.5. Thermal Gravimetric Analysis (TGA)

Sample weighing between 1-3 mg were evaluated by TGA (TA Instrument Hi-Res TGA Q5000) at a heating rate of 10 °C min^{-1} from 25 to 700 °C, without oxidative atmosphere, under nitrogen flow rate atmosphere at 25 mL min^{-1}.

3.3.6. Differential Scanning Calorimetry (DSC)

In standard aluminum pans, samples between 1 to 3 mg by weight were examined by DSC (TA Instrument Q200) under nitrogen flow at 50 mL min^{-1}. To study the dynamicity between furan and maleimide moieties by DSC, FO and PPOBMI-DP6 were mixed together in equimolar equivalents of the moieties and placed in an aluminum pan and exposed to a heating ramp of 2.5 °C min^{-1} from -80 to 165 °C. For cross-linked PUs, a single heating ramp of 10 °C min^{-1} over the same aforementioned temperature range. Non crosslinked materials were evaluated using a cyclical heating ramp.

3.3.7. Uniaxial Tensile Test

Uniaxial tensile testing was performed on an Instron model 5567 H, USA at strain rate of 20 mm min^{-1} on dumbbell specimens of approximately 30 X 5 X 1 mm^3. For each synthesized or reprocessed PU, five dumbbell samples were tested.

3.3.8. Swelling Index and Gel Determination

The swelling ratio (SR) for each PU was determined between dried (m_i) and swollen samples (m_s) in DMF according to Equation 2:

$$SR = \frac{m_s - m_i}{m_i} * 100 \ (2)$$

PU samples of approximately 10-20 mg were swollen in 15 mL of solvent over an entire day. Three repetitions were examined for each PU formulation. The insoluble fraction (IF) was determined by drying the swollen sample (m_f) according to Equation 3:

$$IF = \frac{m_f}{m_i} * 100 \ (3)$$

4. Results and Discussion

4.1. Analysis of synthesis of FO

The FO was synthesized from the acid moiety and alkene site of OA as per the previous procedure (Tremblay-Parrado and Avérous 2019). OA underwent a Steglich esterification using DCC as an activating agent, DMAP as the catalyst and FA as the reagent to yield FMO. FMO was subjected to an in-situ epoxidation with the use of H_2O_2, GAA and acid catalyst to yield the oxidizing agent, peroxyacetic acid in toluene to yield FMOO. Finally, the oligomer diol, FO (Scheme 3.2), was obtained by the acid-catalyzed ring-opening polymerization of FMOO using $HSbF_6$ (1.5 wt %) and H_2O (0.7 mol equiv.). FO was fully characterized by FTIR, ^{31}P NMR and ^{1}H NMR spectroscopy. The corresponding data, which clearly confirms the successful synthesis is available in Supporting Information (SI) (Figure S3.8). The furan content of the FO was calculated as 1.88 mmol furan/g as an average of the quantitative ^{1}H NMR spectroscopic analysis of distinctive signals, whereas the hydroxyl value was calculated to 54.1 mg KOH/g by quantitative ^{31}P NMR spectroscopic analysis, and was in accordance with our previous study (Tremblay-Parrado and Avérous 2019) and the results are summarized in SI Table S3.4

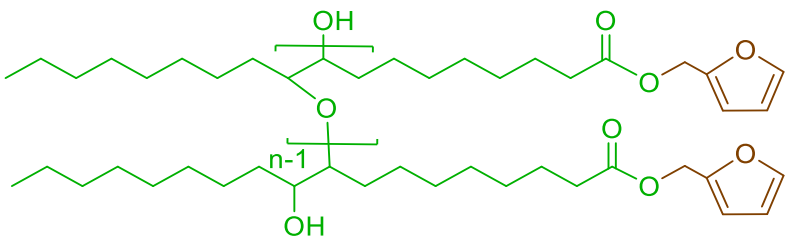

Scheme 3.2 – Chemical model structure of FO.

4.2. Analysis of DA and r-DA reactions between FO and different BMIs

In order to verify the occurrence of the DA reaction between PU chains and consequently the r-DA, the FO was reacted with each BMI according to a previously described procedure (Tremblay-Parrado and Avérous 2019). Four different bismaleimides were used: 1,1'-(Methylenedi-4,1-phenylene) bismaleimide (MPBMI), PPO-based BMI with a DP = 6 (PPOBMI-DP6), PPO-poly(ethylene-oxide)-based BMI with a DP = 13 (PPOPEOBMI-DP13) and PPO-based BMI with a DP = 33 (PPOBMI-DP33). The dynamicity (DA and r-DA) of the corresponding structures (FO with each BMI) was evaluated by dissolving FO and the respective BMI into DMSO under different heating processes at controlled temperature and time. Figure 3.1-a shows the results of a system between FO and PPOBMI-DP6 dissolved in DMSO and exposed to heating cycles. As observed in Figure 3.1-a-i, the system is initially soluble is DMSO. Since the functionality in furan groups of FO is greater than two, a gel is then formed by DA reaction after an exposure to 60 °C for 24 h (Figure 3.1-a-ii). This step was followed by exposing the gel to 120 °C for 1 h. The gel is disassembled by r-DA reaction (Figure 3.1-a-iii). The heating cycle at 60 °C was repeated, and a gel network was reformed by DA reaction (Figure 3.1-a-iv). All other systems and results between FO and other BMIs can be found in SI Figure S3.9. Similar observations can be made. To confirm the DA reaction took place, the system was evaluated before and after gel assembly by FTIR spectroscopy. The initial mix contained signals of free furan ($\tilde{\nu}$ = 739 and 1503 cm^{-1}) and maleimide rings ($\tilde{\nu}$ = 695 and 826 cm^{-1}) (Figure 3.1-b). Upon network assembly, the FTIR spectrum shows the loss of free furan and maleimide ring signals.

In order to follow the occurrence of thermal reaction between FO and PPOBMI-DP6, DSC was used. A stoichiometric system of FO and PPOBMI-DP6 was heated from -80 to 165 °C. Under the same conditions, FO and PPOBMI-DP6 were separately investigated. No thermodynamic

phenomena occurred in the case of separated reagents (Figure 3.1-c). In the thermogram of the mixed system (Figure 3.1-c, orange), an exothermic peak spans between 40 to 90°C, marking the DA reaction. This is followed by two endothermic peaks, corresponding to the r-DA. The peak of r-DA of the *endo* diastereomer occurred between 90 and 120 °C, meanwhile the r-DA of the *exo* diastereomer peak occurred by 120 and 145 °C (Froidevaux et al. 2015). This is highly indicative of the thermo-dynamicity of the cross-linking linkages with in PUs from FO and each of the four different BMIs.

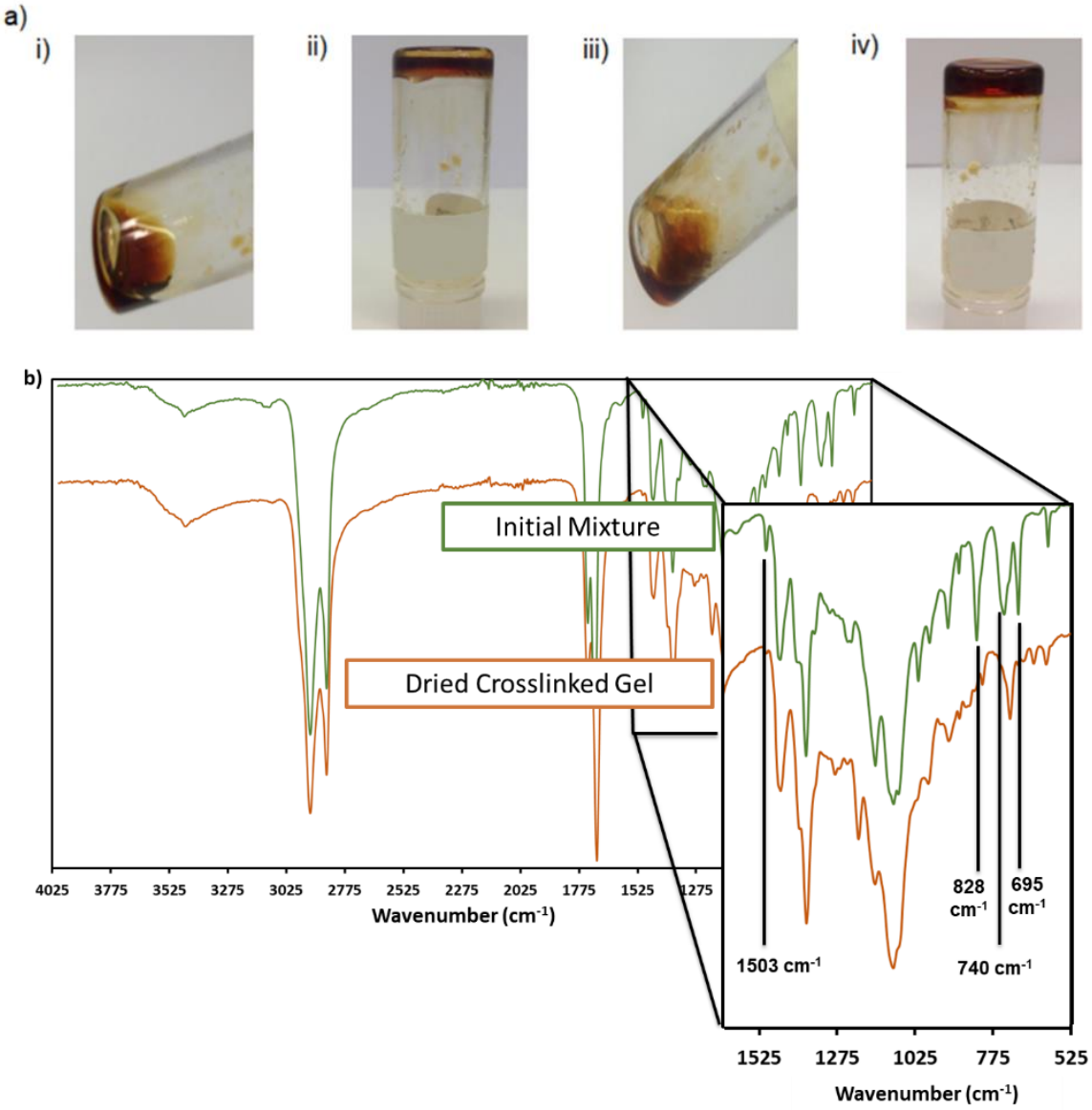

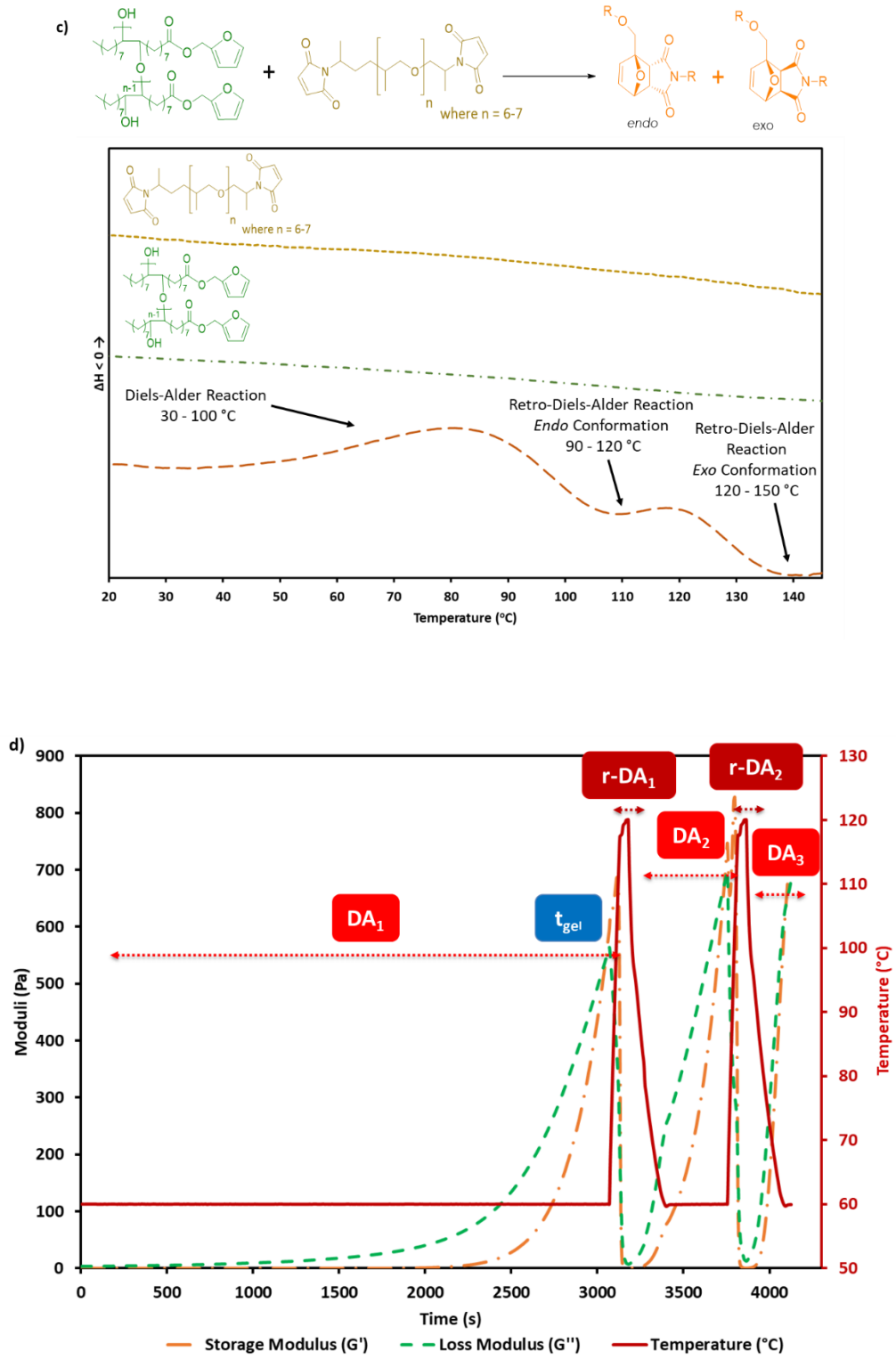

Figure 3.1 – (a) Photographs of (i) initial mixture of FO and PPOBMI-DP6; (ii) mixture after 24 h at 60 °C, (iii) mixture after additional 1 h at 120 °C; (iv) mixture after additional 24 h at 60 °C; (b) FTIR spectra of initial mixture (green) and final dried cross-linked gel (orange), (c) DSC thermograms of PPOBMI-DP6, FO and the mixture of both, from 20 to 170 °C, and (d) rheological behavior of gel formation between FO and PPOBMI-DP6.

To evaluate the rheological behavior of the gel formation between FO and liquid state BMIs, and to further study the DA reaction and r-DA between these reagents, dynamic experiments were performed. Gelation between FO and PPOBMI-DP6 occurred as the moduli overlap at 3046 s (51 min, G' ≈ G'' ≈ 538 Pa) (Figure 3.1-d). To study the reversibility of the gel, heating steps were induced; 60 °C for the DA and 120 °C for r-DA. Upon the 120 °C heating steps (r-DA), the gel disassembled and the moduli descended back to zero. The network was assembled two additional times with shorter gelation times. The same experiments were conducted between FO and different viscous state BMIs and can be found in SI (Figure S3.10), with the exception of MPBMI as it a powder that only melts at temperatures above 150 °C. Table 3.1 summarizes these experiments. It was observed that as the length of the BMI increased, the longer the time interval required to achieve initial gelation times (3046 and 7401 s for PPOBMI-DP6 and PPOBMI-DP35, respectively) and the weaker these gels appeared (538 and 185 Pa for PPOBMI-DP6 and PPOBMI-DP35, respectively).

Table 3.1 – Summary of rheological behavior of gel formation between FO and BMIs.

Gel type	Time to gel point [s]	Moduli at gel point [Pa]
FO-PPOBMI-DP6	3046	538
FO-PPOPEOBMI-DP13	3209	294
FO-PPOBMI-DP35	7401	185

4.3. Analysis of biobased cross-linked PUs from FO and different BMIs

FO and different BMIs were used to obtain biobased PUs consisting of thermally dynamic DA adducts as cross-linking points. Via route 1 (Scheme 3.1), the portion of FO in the PU network was varied to prepare distinctive types of PUs. The FO content was varied from 10 to 30% of the total number of moles of hydroxyl required to prepare PUs with a final NCO/OH ratio of 1.05. Cross-linking took place by dissolving the PU backbone in dry DMF immediately after its synthesis, and adding the appropriate amount of BMI and the solution stirred overnight at 70 °C. These solutions then underwent solvent casting in a PTFE square mold for 48 h at 70 °C followed by 24 h under

vacuum at 70 °C. Three different PUs cross-linked by MPBMI were synthesized and denoted PU-FO10-MPBMI, PU-FO20-MPBMI or PU-FO30-MPBMI according to FO composition, 10, 20 or 30% of the total hydroxyl moles required, respectively. To evaluate the influence of the BMI structure and length on biobased PUs cross-linked mechanical, reprocessing and healing properties, PUs with 20 % FO content were cross-linked via three different BMIs, PPOBMI-DP6, PPOPEOBMI-DP13 or PPOBMI-DP35 and denoted as PU-FO20-PPOBMI-DP6, PU-FO20-PPOPEOBMI-DP13 or PU-FO20-PPOBMI-DP35, respectively. Two additional PUs were synthesized via route 2 (Scheme 3.1), based on HS content. First a prepolymer was achieved using the rapeseed-based polyol, FO and HDI. FO was substituted in order to represent 20% of the number of moles of hydroxyl required for the synthesis of the prepolymer. Once the prepolymer synthesis was achieved (confirmed by NCO content titration), BDO was added to yield a final PU with 20% of HS. The reference PU for this route was denoted as PU-HS20-FO20. In order to cross-link this system via the pendant furan rings of the FO in the soft segments of the PU, the reference PU was immediately dissolved in dry DMF. Then PPOBMI-DP6 was added in stoichiometric equivalents and the solution was stirred overnight at 70 °C, in order for the DA reaction to take place. This final PU system was denoted PU-HS20-FO20-PPOBMI-DP6. Similarly, these solutions underwent solvent casting in PTFE square molds. Table 3.2 summarizes the different nomenclatures and the detailed formulations of all PU prepared systems.

Table 3.2 – Linear PU (reference) and cross-linked systems: nomenclature and corresponding formulations.

PU system	Type of system	FO content[a] [%]	Rapeseed polyol content [%]	Targeted HS content [%]	BMI [b] [equiv.]
PU-FO10-MPBMI	cross-link	10	90	0	1
PU-FO20-MPBMI	cross-link	20	80	0	1
PU-FO30-MPBMI	cross-link	30	70	0	1
PU-FO20-PPOBMI-DP6	cross-link	20	80	0	1
PU-FO20-PPOPEOBMI-DP13	cross-link	20	80	0	1
PU-FO20-PPOBMI-DP33	cross-link	20	80	0	1
PU-HS20-FO20	linear (reference)	20	80	20	1
PU-HS20-FO20-PPOBMI-DP6	cross-link	20	80	20	1

[a] The FO content in the PU systems was varied from 0 to 30% of the total hydroxyl moles required to synthesize PUs with a final NCO/OH equivalent of 1.05. For samples PU-HS20-FO20 and PU-HS20-FO20-PPOBMI-DP6. [b] Equivalents of maleimide moiety from BMI with respect to furan moiety of FO.

In order to characterize the successful synthesis of all PU systems, they were evaluated by FTIR spectroscopy. Even, PU-HS20-FO20-DP6, a reference linear PU was found to be insoluble in common solvents ($CHCl_3$, DMSO, THF, DMF). Figure 3.2 compares the FTIR spectra of FO, biobased polyol, BDO, PU-HS20-FO20, PU-HS20-FO20-PPOBMI-DP6 and PPOBMI-DP6. In Figure 3.2-d of the FTIR spectrum PU-HS20-FO20, the signals at $\tilde{\nu}$ = 3375 and 1555 cm^{-1} correlating with the -N-H stretching and bending appropriately of urethane group appear; the ester urethane stretch presents itself at $\tilde{\nu}$ = 1690 cm^{-1}. The hydroxyl signals (at $\tilde{\nu} \approx$ 3440 cm^{-1}) corresponding to the FO, rapeseed polyol and BDO disappeared due to the polyaddition reaction between –NCO/-OH. Figure 3.2-e displays the FTIR spectrum of PU-HS20-FO20-PPOBMI-DP6 which is quite similar to spectrum of PU-HS20-FO20. Nevertheless, the presence of the carbonyls of the maleimides at $\tilde{\nu}$ = 1710 cm^{-1} from the addition of PPOBMI-DP6 to achieve a cross-linked system becomes slightly apparent. Furthermore, because the PU-HS20-FO20-PPOBMI-DP6 is cross-linked by the DA reaction and a loss of free furan maleimide ring is observed. The FTIR spectrum of cross-linked PUs without HS can be found in SI (Figure S3.11, Figure S3.12, Figure S3.13 and Figure S3.14).

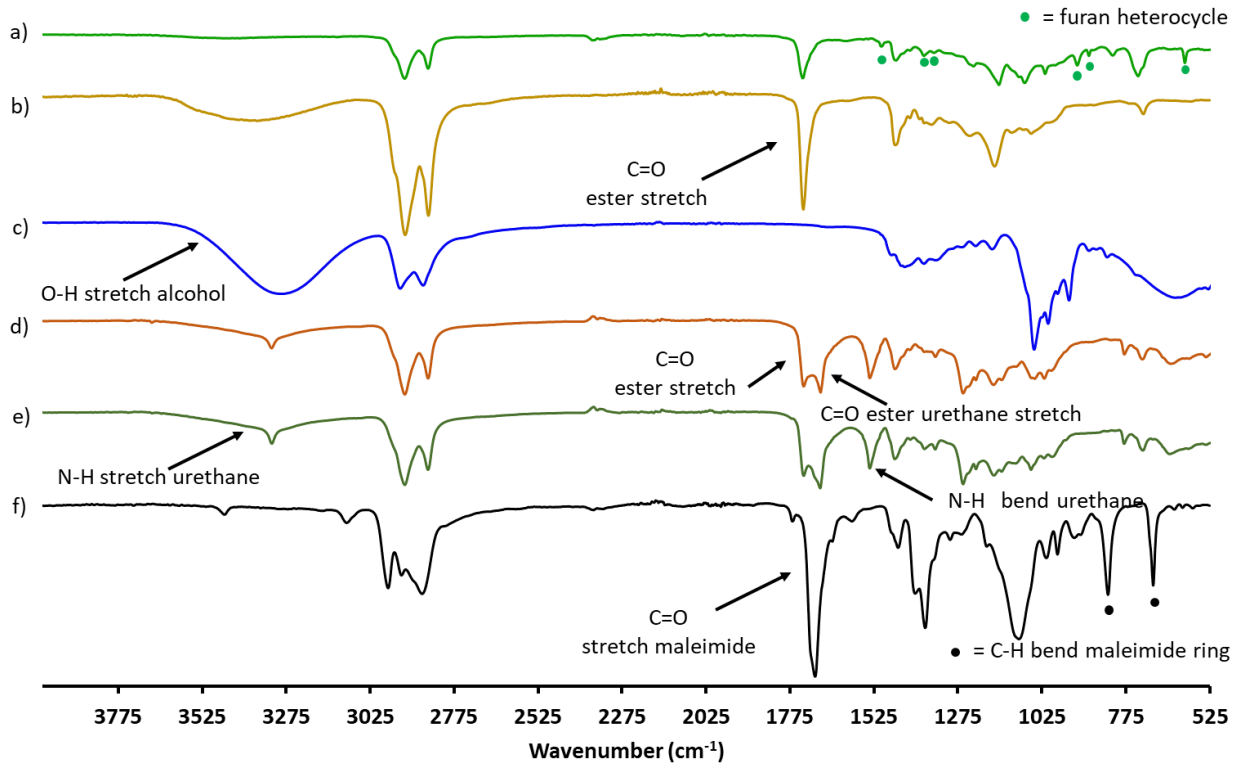

Figure 3.2 – FTIR spectra of (a) FO, (b) rapeseed polyol, (c) BDO, (d) PU-HS20-FO20, (e) PU-HS20-FO20-PPOBMI-DP6, and (f) PPOBMI-DP6.

4.4. Mechanical and thermal evaluations of the biobased cross-linked PUs

TGA was use to evaluate the thermal stability of the cross-linked PU materials. Table 3.3, displays the material properties and it can be observed that the initial thermal degradations ($T_{5\%}$) for the prepared PUs commenced at temperatures greater than 120 °C. This suggests that a reprocessing at temperature of 120 °C based on r-DA can occur without thermal degradation. Similarly to previously reported results (Tremblay-Parrado and Avérous 2019), an increase in FO content, decreases the $T_{5\%}$ in the PU networks. This is notable by the $T_{5\%}$ of PU-FO10-MPBMI compared to PU-FO30-MPBMI. Furthermore, all PU materials synthesized with a consistent amount of FO (20 %) and cross-linked by the different maleimides, remained with a $T_{5\%}$ steadily around 330 °C. It is known that degradation of PUs is a complex multistep process, nevertheless, it generally accepted that an increase in HS also renders those materials more susceptible to degradation, suggesting that initial degradation takes place predominantly in HS (Bueno-Ferrer et al. 2012). This is consistent with the results of PU-HS20-FO20 and PU-HS20-FO20-PPOBMI-DP6 which observed

decreased and similar $T_{5\%}$ in comparison to all other PU networks. The thorough TGA results are found in SI (Figure S3.15).

Table 3.3 – Main results of the characterizations of cross-linked biobased PUs.

PU system	TGA $T_{5\%}$ [°C]	DSC T_g [°C]	Young's modulus [MPa]	σ[a] [MPa]	ε[b] [%]	SR[c] in DMF [%]	IF[d] [%]
PU-FO10-MPBMI	344	-51	1.86 ± 0.12	0.95 ± 0.08	265 ± 27	36.8 ± 1.0	97.5 ± 0.2
PU-FO20-MPBMI	332	-51	2.40 ± 0.22	1.10 ± 0.04	120 ± 5	45.6 ± 2.8	97.3 ± 0.4
PU-FO30-MPBMI	314	-51	2.22 ± 0.19	1.58 ± 0.16	118 ± 10	49.9 ± 1.5	96.4 ± 0.2
PU-FO20-PPOBMI-DP6	333	-50	1.65 ± 0.15	1.10 ± 0.03	129 ± 8	49.5 ± 2.6	96.7 ± 0.2
PU-FO20-PPOPEOBMI-DP13	324	-52	1.57 ± 0.21	0.86 ± 0.01	131 ± 5	54.5 ± 1.0	96.7 ± 0.3
PU-FO20-PPOBMI-DP33	326	-52	1.22 ± 0.10	0.80 ± 0.07	120 ± 7	71.5 ± 1.6	96.0 ± 0.2
PU-HS20-FO20	298	-50	11.84 ± 1.16	1.15 ± 0.11	30 ± 9	50.1 ± 1.7	95.6 ± 0.3
PU-HS20-FO20-PPOBMI-DP6	299	-49	14.47 ± 3.50	1.74 ± 0.20	24 ± 10	52.1 ± 2.5	96.1 ± 0.8

[a] Ultimate tensile strength. [b] Elongation at rupture. [c] SR=swelling ratio. [d] IF=insoluble fraction.

TGA results show that no degradation occurs in the studied DSC temperature range. Main DSC results are summarized in Table 3.3. Detailed DSC thermograms are found in SI (Figure S3.16). The T_g for all materials remains close to -51 °C. In a previous study (Tremblay-Parrado and Avérous 2019), it was observed that networks containing increasing amounts of FO, (and increased cross-linking density) displayed more pronounced endothermic r-DA peak between 90 and 150 °C. This was also observed in series of PUs cross-linked by MPBMI (PU-FO10-MPBBMI, PU-FO20-MPBMI and PU-FO30-MPBMI) as shown in SI (Figure S3.16-a). Furthermore, for the series of PUs cross-linked with varied BMIs and consistent amount of FO (20 %), as the length of the BMI increased, a decrease is observed in the prominence of the endothermic related to the r-DA reaction (Figure 3.3-a). The increase in the length of the BMIs decreased the cross-linking density by weight of the materials. A slight decrease in the T_g of PU-HS20-FO20-PPOBMI-DP6 was observed, when compared to its linear counterpart. Furthermore, as observed in Figure 3.3-b, the thermograms of cross-linked PU-HS20-FO20-PPOBMI-DP6 displayed the appearance of an endothermic signal

between 90 and 150 °C correlating to the r-DA reaction. Contrastingly, without BMI, the reference PU counterpart remained unchanged.

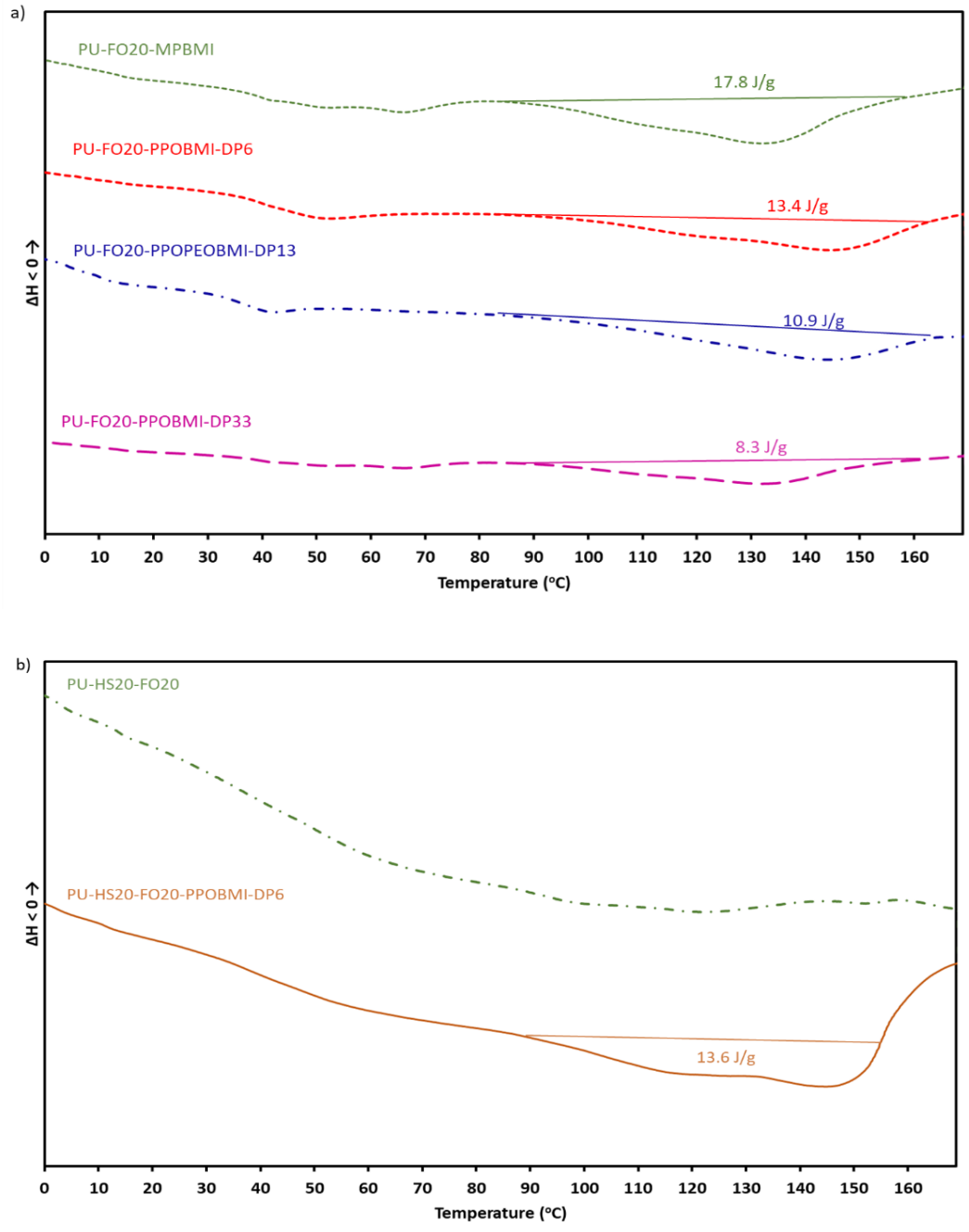

Figure 3.3 – Thermograms of (a) PU-FO20-MPBMI, PU-FO20-PPOBMI-DP6, PU-FO20-PPOPEOBMI-DP13, PU-FO20-PPOBMI-DP33 and (b) PU-HS20-FO20, PU-HS20-FO20-PPOBMI-DP6 from 0 to 170 °C.

All PUs synthesized were evaluated for their mechanical properties by uniaxial tensile testing at room temperature to analyze the influence of the structure and length of the BMIs. Main results

were summarized in Table 3.3. The PUs series cross-linked by MPBMI with increasing amount of FO displayed a similar trend as cross-linked PUs in a previous study (Tremblay-Parrado and Avérous 2019) by a PPO-based BMI with a DP = 3. That is, with increasing amount of FO (and consequently increasing cross-linking density), PUs materials displayed behaviors from thermoplastic elastomer (PU-FO10-MPBMI) to thermoset (PU-FO30-MPBMI) with an increase of tensile strength and a decrease of maximum elongation (Figure 3.4-a). Furthermore, in comparison to previously published results (Tremblay-Parrado and Avérous 2019), the Young's modulus and tensile strength of this PU series considerably increased and this can be in part due to the aromatic structure of MPBMI.

The material properties of PU series with FO (20 %) and then cross-linked by different BMIs (PU-FO20-MPBMI, PU-FO20-PPOBMI-DP6, PU-FO20-PPOPEOBMI-DP13 and PU-FO20-PPOBMI-DP33) yield interesting results. As seen in Figure 3.4-b, PU-FO20-MPBMI presents the highest Young's modulus and tensile strength, which can be due to the phenyl structure of the MPBMI. PUs materials cross-linked with linear aliphatic BMIs yield very similar Young's modulus, tensile strength and elongation regardless of their varying lengths. Although PU-FO20-PPOBMI-DP6 claims the highest average Young's modulus and tensile strength, and PU-FO20-PPOBMI-DP35 the lowest, the standard deviations of these results are overlapping and then can be considered as similar. Although the cross-linking density by weight for this series of materials is varied, the overall moles of cross-linking points remained the same. Furthermore, entanglements have a higher prevalence of occurring for BMIs with the longest lengths and can be a contributing factor to explain the similar results achieved between PU systems. Lastly, PUs containing HS, PU-HS20-FO20 and its cross-linked counterparts PU-HS20-FO20-PPOBMI-DP6, exhibit superior mechanical properties, as evidenced by the mechanical properties of the reference PU. As seen in Figure 3.4-c, the cross-linked counterpart, PU-HS20-FO20-PPOBMI-DP6, exhibited an increased Young's modulus, tensile strength and decrease elongation due to the presence of cross-linking points.

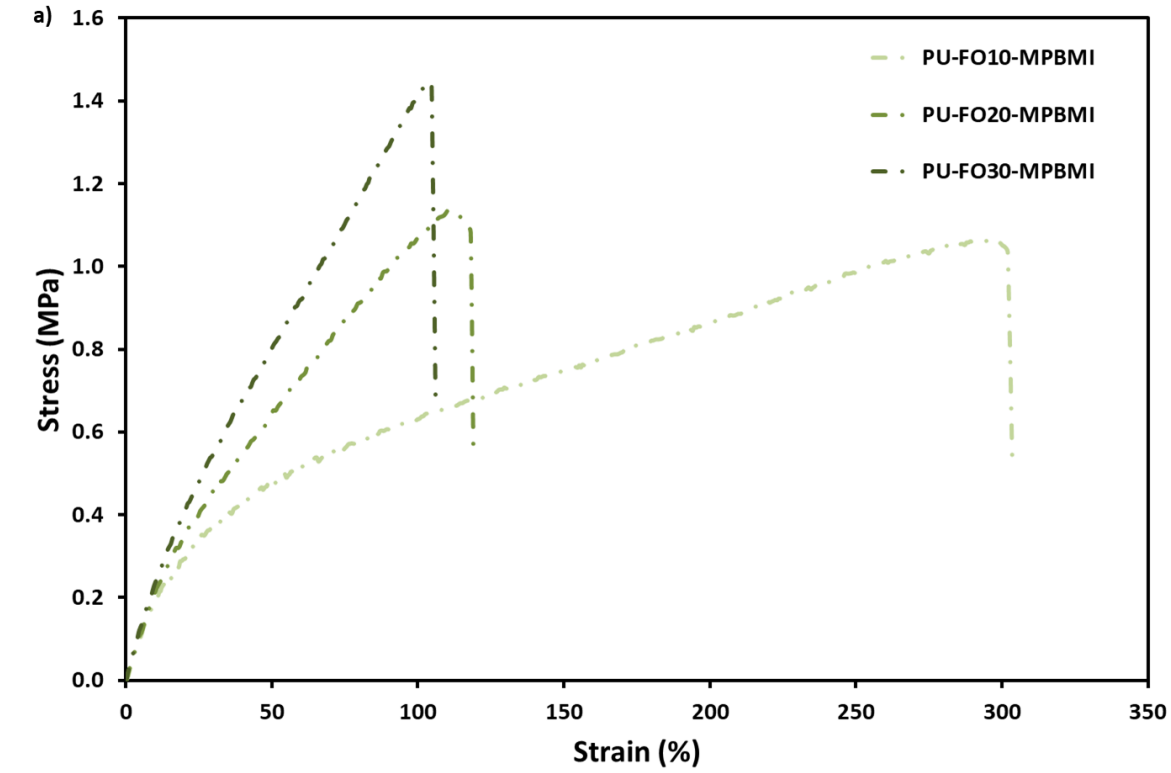
a)
PU-FO10-MPBMI
PU-FO20-MPBMI
PU-FO30-MPBMI
Stress (MPa)
Strain (%)
0.0
0.2
0.4
0.6
0.8
1.0
1.2
1.4
1.6
0
50
100
150
200
250
300
350

.

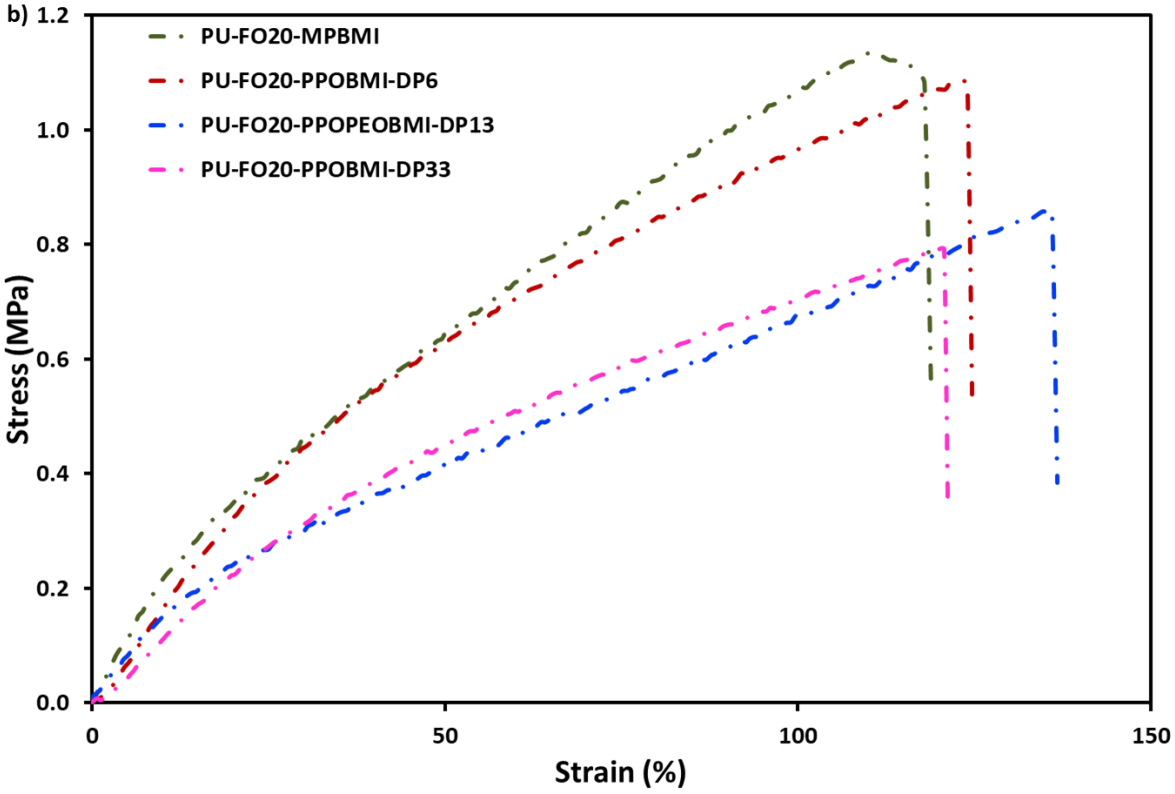
b)
PU-FO20-MPBMI
PU-FO20-PPOBMI-DP6
PU-FO20-PPOPEOBMI-DP13
PU-FO20-PPOBMI-DP33
Stress (MPa)
Strain (%)
0.0
0.2
0.4
0.6
0.8
1.0
1.2
0
50
100
150

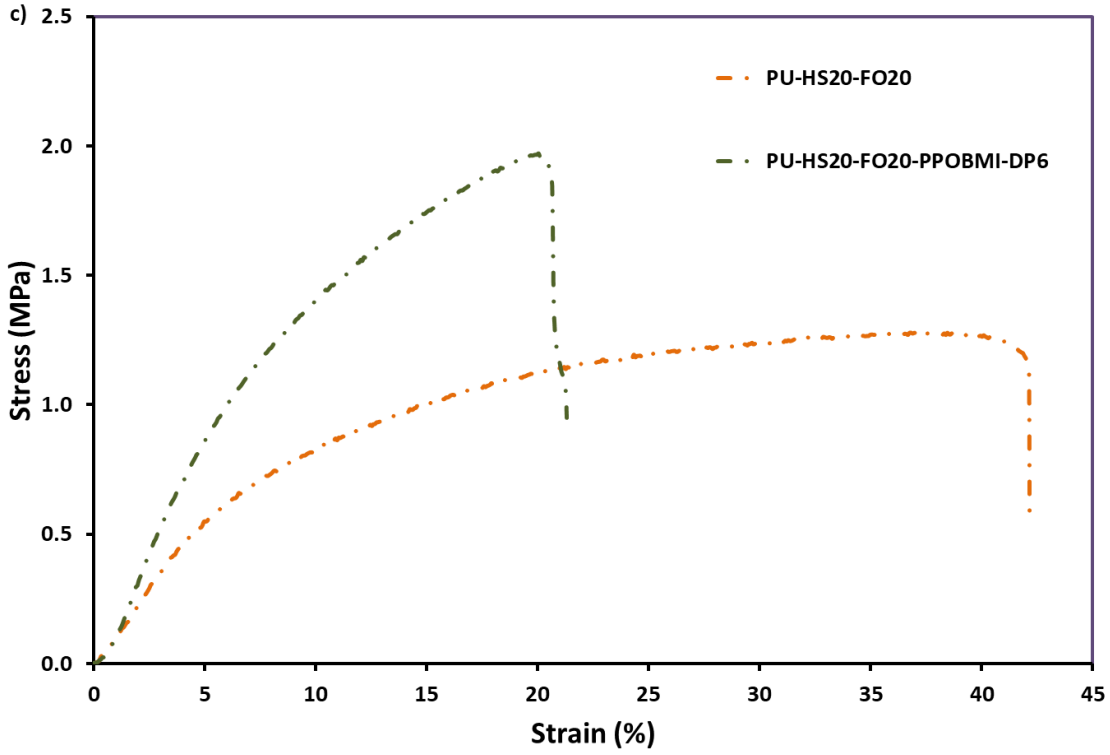

Figure 3.4 – Stress-strain curves of (a) PU-FO10-MPBMI, PU-FO20-MPBMI, PU-FO30-MPBMI (b) PU-FO20-PPOBMI-DP6, PU-FO20-PPOPEOBMI-DP13, PU-FO20-PPOBMI-DP33 and (c) PU-HS20-FO20, PU-HS20-FO20-PPOBMI-DP6.

The structures of the PU materials were evaluated by swelling tests in DMF and the results are displayed in Table 3.3. As similarly observed in a previous study, although PU-FO10-MPBMI, PU-FO20-MPBMI, and PU-FO30-MPBMI, consist of increasing cross-linking densities, it was observed that the PU networks experienced higher swelling ratios (SRs), due to the affinity of the FO to swell in the given solvent. Furthermore, PU networks cross-linked with the aromatic bismaleimides reveal to have the lowest SRs for PUs with respect to FO content, in part because MPBMI has the shortest length between maleimide functions. In the series of PUs prepared with equivalent amounts of FO (20%), cross-linked with increasing lengths of the aliphatic bismaleimides; it was observed that SRs increased with the BMI length. Nevertheless, this did not affect the initial mechanical properties of these PU systems. Finally, PUs containing HS, reference or cross-linked samples seemed to display statistically indifferentiable SRs despite the differences they yield in mechanical properties. All prepared materials were relatively insoluble with lowest insoluble fraction (IF) reported at 95.6 % for e.g., the linear reference PU-HS20-FO20.

4.5. Evaluation of the remendable and self-healing behaviors

Previously published results (Tremblay-Parrado and Avérous 2019) suggest PU materials could exhibit reprocessable and heat-induced self-healing behavior. Characterizing the reprocessability of all PUs synthesized was evaluated by comparing the initial T_g and mechanical properties of materials first processed by solvent casting, to that of PUs reprocessed by compression molding over two compression molding reprocessing cycles. As mentioned in a previous study, reprocessing by compression molding was conducted as follows: material was cut into several small pieces and placed in a square mold and left to preheat at 150 °C for 15 mins (to soften the material and allow for the r-DA reaction to take place), material was then compressed for 10 mins at 150 °C, followed by 48 h at 60 °C (to allow for the DA reaction to take place). To add further comparisons to the study, a dumbbell of each initial PU synthesized was exposed to 120 °C for a 2 h thermal treatment and cooled over 12 h at room temperature prior to uniaxial tensile testing. The results of mechanical properties of PUs of initial and reprocessed materials exposed to 120 °C treatment are shown Figure 3.5 (PUs without HS) and Figure 3.6 (PUs with HS) and all detailed results are summarized in SI (Table S3.5).

The reprocessability of PU series containing varying FO contents and cross-linked by MPBMI were generally reprocessable over one reprocessing cycle for all materials (PU-FO10-MPBMI, PU-FO20-MPBMI and PU-FO30-MPBMI). However, PU-FO10-MPBMI and PU-FO20-MPBMI experienced a notable loss in the Young's modulus after a second reprocessing cycles, whereas PU-FO30-MPBMI evidenced diminished mechanical properties after a second reprocessing cycle on all fronts. In a previous study (Tremblay-Parrado and Avérous 2019), a PU material was synthesized with 30 % substitution of FO and cross-linked with a PPO BMI DP = 3 would yield a confirmed reprocessable material after two compression molding reprocessing cycles. Thus, it can be concluded that although the aromatic nature for the MPBMI can yield superior mechanical properties, it can affect the reprocessing ability of the material by this specified procedure of reprocessing by compression molding. A contributing factor effecting the reprocessing ability can be the high melting temperature of MPBMI (approximately 150 °C), this can effect the curing step (DA reaction) of the reprocessing procedure as this limits the local mobility of MPBMI in the material.

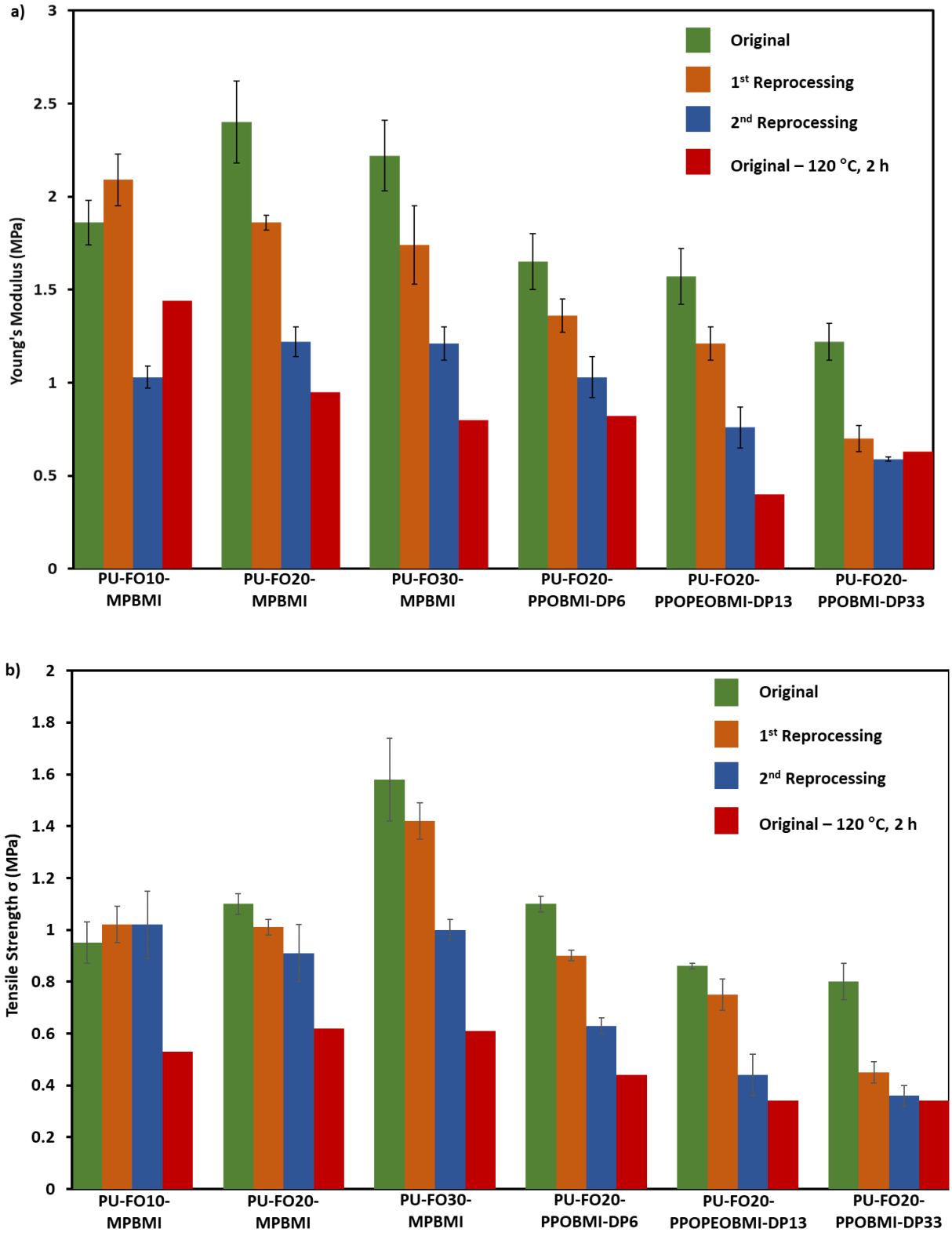
a)
Young's Modulus (MPa)
3
2.5
2
1.5
1
0.5
0
Original
1st Reprocessing
2nd Reprocessing
Original – 120 °C, 2 h
PU-FO10-MPBMI
PU-FO20-MPBMI
PU-FO30-MPBMI
PU-FO20-PPOBMI-DP6
PU-FO20-PPOPEOBMI-DP13
PU-FO20-PPOBMI-DP33
b)
Tensile Strength σ (MPa)
2
1.8
1.6
1.4
1.2
1
0.8
0.6
0.4
0.2
0
Original
1st Reprocessing
2nd Reprocessing
Original – 120 °C, 2 h
PU-FO10-MPBMI
PU-FO20-MPBMI
PU-FO30-MPBMI
PU-FO20-PPOBMI-DP6
PU-FO20-PPOPEOBMI-DP13
PU-FO20-PPOBMI-DP33

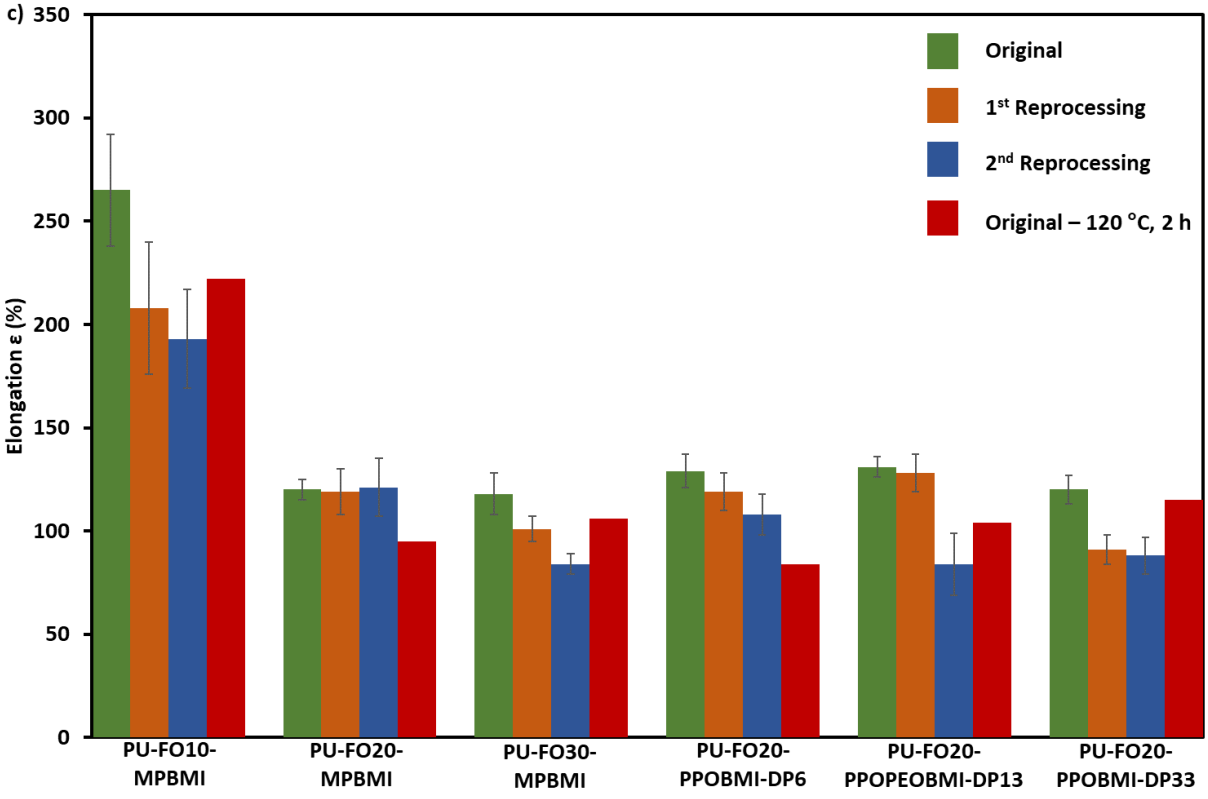

Figure 3.5 – Comparison of mechanical properties of biobased PUs: original, reprocessed and original heated to 120 °C, (a) Young's modulus, (b) tensile strength (σ), and (c) elongation (ε).

The effect of varying the BMI length and structure while keeping the FO content constant (20 %) was seen most prevalent in the ability PU materials to be reprocessable by the specified reprocessing procedure. PU materials PU-FO20-MPBMI, PU-FO20-PPOBMI-DP6 and PU-FO20-PPOPEO-DP6 were generally reprocessable after one reprocessing cycles, with slight but noticeable loss in Young's modulus. In contrast, PU-FO20-PPOBMI-DP33 experienced considerably diminished mechanical properties after a single reprocessing single. Upon a second reprocessing, PU materials PU-FO20-MPBMI, PU-FO20-PPOBMI-DP6 and PU-FO20-PPOPEO-DP6 experienced significant loss in mechanical properties and slightly superior results when compared to an original sample exposed to a 120 °C thermal treatment. This is indicative that upon a second reprocessing some cross-linking points are apparent. Nevertheless, these results contrast with initially reported findings for similar PU systems cross-linked by a shorter PPO BMI DP = 3 and which were deemed reprocessable. Thus, increasing significantly the length of the BMIs can affect the reprocessing ability, by this specific reprocessing procedure. Dissociative CANs often exhibit

different cross-link densities after reprocessing and thus effect mechanical properties for a multitude of reasons, such as: chain rearrangement, vitrification or cross-link degradation (Kloxin et al. 2010). Furthermore, it is not to say that the PUs system cross-linked with longer chain BMIs could not exhibit enhanced reprocessing ability by a reprocessing procedure specifically adapted to the network. As explained by Sumerlin and coworkers, two attributes profoundly impact the temperature-dependent viscoelastic behaviour of dissociative CANs: the dynamic equilibrium of dissociative bond exchange and the gel point in association with the gel-point temperature of the system (Scheutz et al. 2019). Thus, the gel point temperature of these PU systems may have varied with respect to the BMI introduced and can also be a contributing factor effecting the repro cessing ability.

PU material containing HS, PU-HS20-FO20-PPOBMI-DP6, was deemed reprocessable as it exhibited consistent mechanical properties over reprocessing cycles, as well superior results when compared to an original sample exposed to a thermal treatment and control results. It would be of interest to determine how the gel point temperature varied with by varying the HS concentration and consequently for a fixed HS, determining if indeed the length and structure of the BMI effects the gel point temperature of these systems.

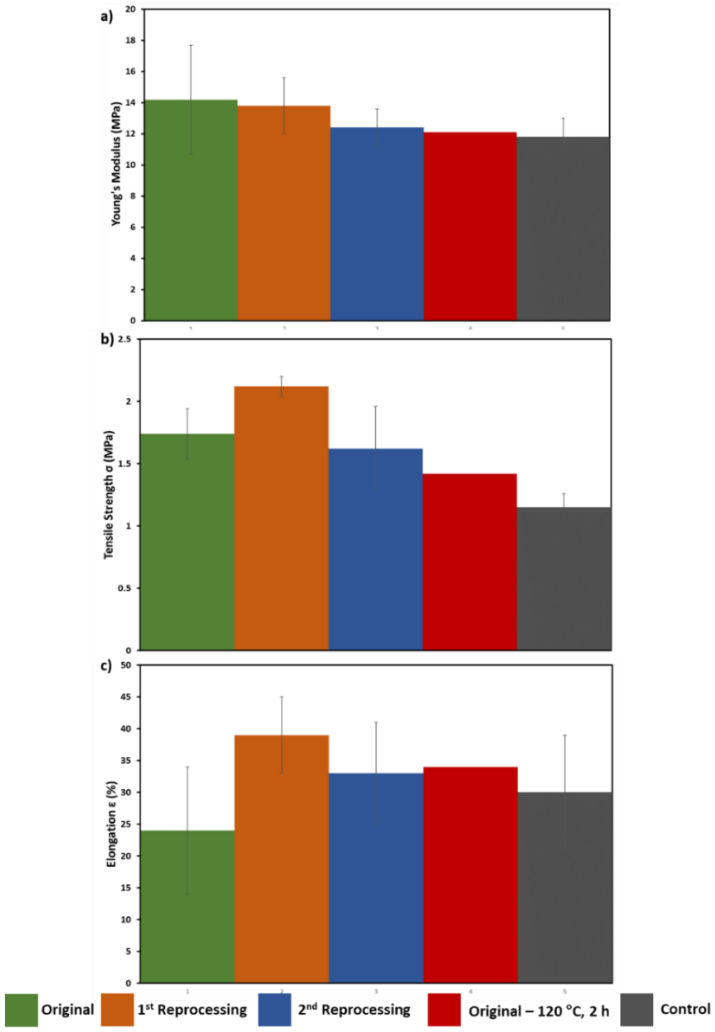

Figure 3.6 – Comparison of mechanical properties of biobased PU-HS20-FO20-PPOBMI-DP6: original, reprocessed, original heated to 120 °C, and control, (a) Young's modulus, (b) tensile strength (σ), and (c) elongation (ε).

Heat induced self-healing experiments were conducted on dumbbells of initial synthesized PU materials by (i) cutting a dumbbell in half, (ii) joining the cut ends of the dumbbell, exposing it to 1 h at 120 °C treatment to allow for the r-DA reaction to take place and for adhesion of two both ends and lastly (iii) a final heating at 60 °C for 48 h allowing the network to be reformed by the DA reaction. The integrity of these dumbbells was then evaluated by uniaxial tensile testing. In contrast to previously reported results (Tremblay-Parrado and Avérous 2019), the heat induced self-healing ability of PU materials synthesized in this study seem to be considerably affected by the BMI length and structure. Detailed results of the self-healing ability of simple PU networks (without HS) is summarized in Table S3.6.

For the series of PUs containing increasing amount of FO cross-linked by MPBMI, sample PU-FO10-MPBMI would yield the most prevalent recovery of original material properties. As depicted in Figure 3.7-a, the sample PU-FO10-MPBMI appears to heal relatively well to the naked eye. Nevertheless, uniaxial tensile test reveal healing of the sample with recovery of 64% of the average original Young's modulus, 41 and 47% of tensile strength and elongation, respectively (Figure 3.7-b). For the series of PUs with 20% substitution of FO and cross-linked with different BMIs, materials seem to heal relatively similarly with an approximate recovery of mechanical properties as follows: 39% of Young's modulus, 31% of tensile strength and 50 percent elongation. Similarly to sample PU-FO10-MPBMI, sample PU-FO20-MPBMI seems to heal relatively well to the naked eye (Figure 3.7-c), but as illustrated in Figure 3.7-d, PU-FO20-MPBMI heals poorly with a recovery of original material properties as follows of 33% Young's modulus; 36% of tensile strength and 58% of elongation. Although, PU-FO20-MPBMI exhibits the highest recovery in tensile strength with comparison to the other PU of this series, it is still a result considerably diminished when compared to that of reported healing results of a previous study (Tremblay-Parrado and Avérous 2019). Thus, although PU-FO10-MPBMI and PU-FO20-MPBMI demonstrate the most prevalent healing results due to the shorter chain length of the BMI, the aromatic structure and consequently high melting temperature further impedes its healing ability.

For sample PU-HS20-FO20-PPOBMI-DP6, the stiffness of the dumbbell did not allow for adhesion of the cut ends without an applied constant pressure. Given that the surface area of the dumbbells, an adhesion test between an overlap of two pieces consisting of 1.5 cm^2 surface area (Figure 3.7-e) was deemed appropriate. The two pieces of overlapped sample PU-HS20-FO20-PPOBMI-DP6 were exposed to 120 °C for 1h with a 100 g weight to apply slight pressure to the overlap. The overlap sample was then exposed to 60 °C for 48 h. As seen Figure 3.7-e, the adhesion test displayed an overlap good adhesion and the overlap could be submitted to 250 g which represented a shear stress of approximately 1.67×10^4 Pa (250 g x 10 N / 1000 g)/(1.5 cm^2)). The thermal treatment endured by the overlap allows for a network to be formed by chemical association of the interfacial Diels-Alder moieties. This is a highly favorable result for adhesive applications of such PU systems.

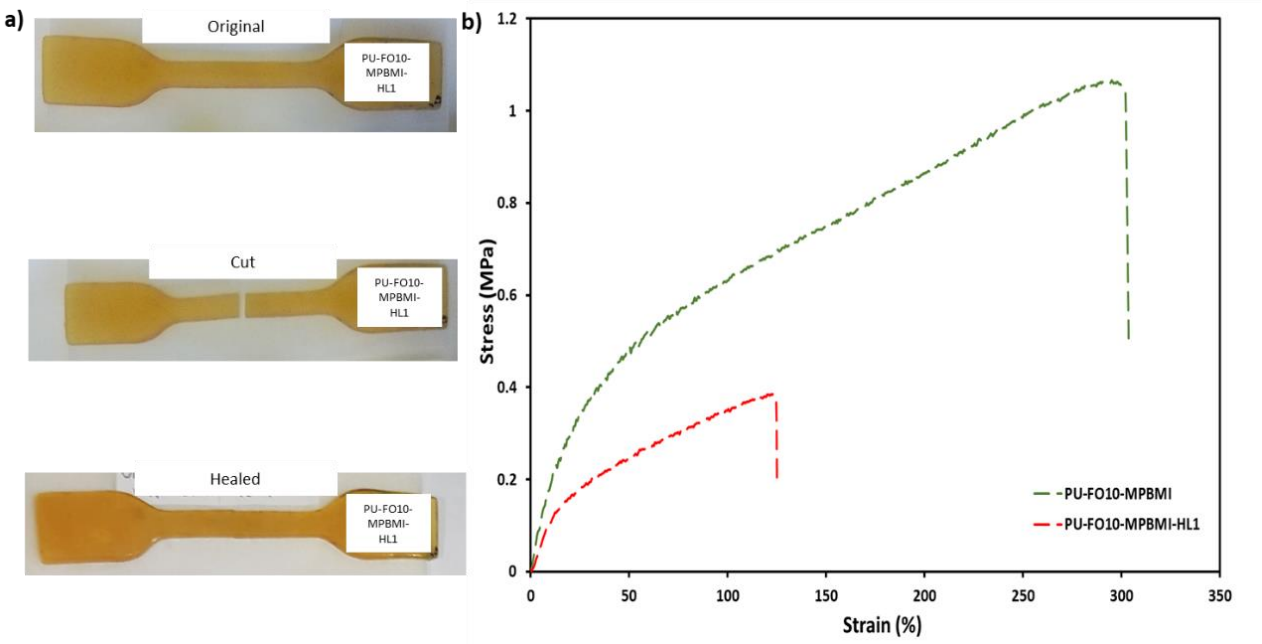
a)
Original
PU-FO10-MPBMI-HL1
Cut
PU-FO10-MPBMI-HL1
Healed
PU-FO10-MPBMI-HL1
b)
Stress (MPa)
Strain (%)
PU-FO10-MPBMI
PU-FO10-MPBMI-HL1

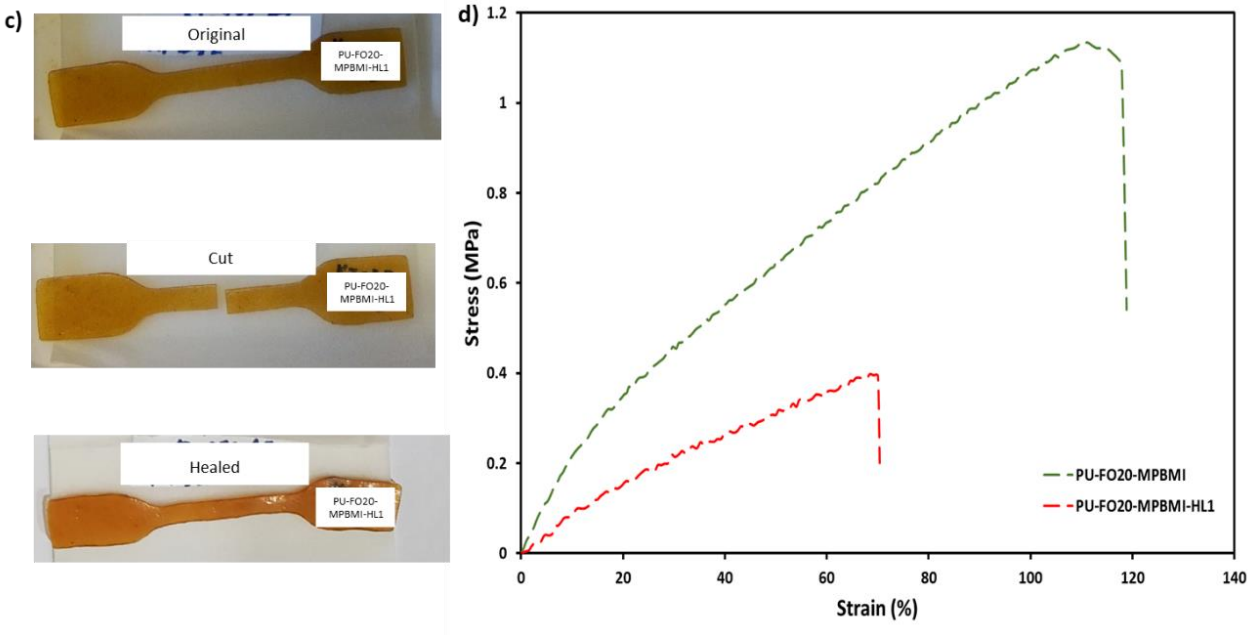
c)
Original
PU-FO20-MPBMI-HL1
Cut
PU-FO20-MPBMI-HL1
Healed
PU-FO20-MPBMI-HL1
d)
Stress (MPa)
Strain (%)
PU-FO20-MPBMI
PU-FO20-MPBMI-HL1

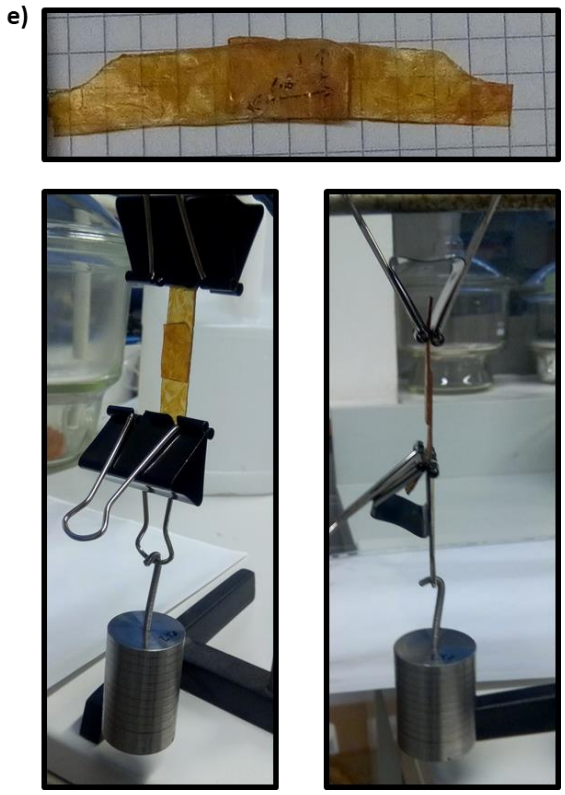

Figure 3.7 – Observation of healing of materials (a) photographs of original, cut and healed dumbbell sample PU-FO10-MPBMI, (b) stress-strain curves of PU-FO10-MPBMI original and healed sample, (c) photographs of original, cut and healed dumbbell sample PU-FO20-MPBMI, (d) stress-strain curves of PU-FO20-MPBMI original and healed sample, and (e) photographs of adhesion of PU-HS20-FO20-PPOBMI-DP6 films submitted to 250 g load.

5. Conclusion

This study examined the effect of various BMIs which varied in length and structure (four different bismaleimides where used) on the materials properties, thermal recyclability and heated induced healing of different biobased cross-linked PU networks. A PU material series containing varying amount of FO substitution (10, 20 or 30%) cross-linked by MPBMI exhibited modular mechanical properties and were as well superior to previous published works (Tremblay-Parrado and Avérous 2019). Nevertheless, the high melting temperature of MPBMI diminished the thermal recyclability and heat induce healing ability of these PU materials. The PU material series with 20% substitution of FO and cross-linked by the different BMIs showed that cross-linking by MPBMI would yield superior mechanical properties compared to aliphatic counterparts. The distinguishment of PU networks cross-linked by different BMIs was evidenced. The corresponding cross-linked materials presented superior mechanical properties (when compared to linear reference counterpart) with

good thermal recyclability and self-healing behavior. Lastly, the introduction phase segregation in PU materials was examined. A control and cross-linked architecture was examined. Both architecture would yield superior mechanical properties than all previously synthesized systems. The cross-linked material presented good thermal recyclability and adhesion properties. The corresponding preliminary results on these latter systems containing specific HS provides interesting results to be applied to industrial applications such as adhesives and coatings.

Developing these PUs provides a thrilling prospect to the notion of reconceiving sustainable material design by elaborating polymer architectures with advanced performances allowing for intrinsic recyclability and a controlled end-of-life. Finally, this work constitutes a springboard in the development of innovative, biobased and dynamic macromolecular architectures for a large range of advanced domains.

Acknowledgements

The authors would like to thank BPI-France for the funding of Trans'Alg Project and the corresponding consortium. Iterg (France) for kindly providing technical grade oleic acid. The authors would like to thank the R&D Team of Soprema (France).

6. References

Bueno-Ferrer, Carmen, Elodie Hablot, María del Carmen Garrigós, Sergio Bocchini, Luc Averous, and Alfonso Jiménez. 2012. 'Relationship between morphology, properties and degradation parameters of novative biobased thermoplastic polyurethanes obtained from dimer fatty acids', *Polymer Degradation and Stability*, 97: 1964-69.

Buono, Pietro, Antoine Duval, Luc Averous, and Youssef Habibi. 2017. 'Thermally healable and remendable lignin-based materials through Diels – Alder click polymerization', *Polymer*, 133: 78-88.

Canary, Stephen A., and Malcolm P. Stevens. 1992. 'Thermally reversible crosslinking of polystyrene via the furan–maleimide Diels–Alder reaction', *Journal of Polymer Science Part A: Polymer Chemistry*, 30: 1755-60.

Carré, Camille, Yvan Ecochard, Sylvain Caillol, and Luc Averous. 2019. 'From the synthesis of biobased cyclic carbonate to polyhydroxyurethanes: a promising route towards renewable NonIsocyanate Polyurethanes', *Chemsuschem*, 12, 3410.

Chen, Xiangxu, Matheus A. Dam, Kanji Ono, Ajit Mal, Hongbin Shen, Steven R. Nutt, Kevin Sheran, and Fred Wudl. 2002. 'A Thermally Re-mendable Cross-Linked Polymeric Material', *Science*, 295: 1698-02.

Chujo, Yoshiki, Kazuki Sada, and Takeo Saegusa. 1990. 'Reversible gelation of polyoxazoline by means of Diels-Alder reaction', *Macromolecules*, 23: 2636-41.

American Chemistry Council. 2017. 'U.S. Resin Production and Sales', Accessed 19/11/2019. https://plastics.americanchemistry.com/PlasticsStatistics/ACC-PIPS-Year-End-2017-Resin-Stats-vs-2016.pdf.

Denissen, Wim, Johan M. Winne, and Filip E. Du Prez. 2016. 'Vitrimers: permanent organic networks with glass-like fluidity', *Chemical Science,* 7: 30-38.

Desroches, M., M. Escouvois, R. Auvergne, S. Caillol, and B. Boutevin. 2012. 'From Vegetable Oils to Polyurethanes: Synthetic Routes to Polyols and Main Industrial Products', *Polymer Reviews*, 52: 38-79.

Dhers, Sébastien, Ghislaine Vantomme, and Luc Avérous. 2019. 'A fully bio-based polyimine vitrimer derived from fructose', *Green Chemistry*, 21: 1596-601.

Dolci, E., V. Froidevaux, G. Michaud, F. Simon, R. Auvergne, S. Fouquay, and S. Caillol. 2017. 'Thermoresponsive crosslinked isocyanate-free polyurethanes by Diels-Alder polymerization', *Journal of Applied Polymer Science*, 134: 11.

Dolci, Elena, Guillaume Michaud, Frédéric Simon, Bernard Boutevin, Stéphane Fouquay, and Sylvain Caillol. 2015. 'Remendable thermosetting polymers for isocyanate-free adhesives: a preliminary study', *Polymer Chemistry*, 6: 7851-61.

Du, P. F., H. Y. Jia, Q. H. Chen, Z. Zheng, X. L. Wang, and D. L. Chen. 2016. 'Slightly crosslinked polyurethane with Diels-Alder adducts from trimethylolpropane', *Journal of Applied Polymer Science,* 133: 43791.

Duval, A., G. Couture, S. Caillol, and L. Averous. 2017. 'Biobased and Aromatic Reversible Thermoset Networks from Condensed Tannins via the Diels-Alder Reaction', *ACS Sustainable Chemistry & Engineering,* 5: 1199-207.

Duval, Antoine, Heiko Lange, Martin Lawoko, and Claudia Crestini. 2015. 'Reversible crosslinking of lignin via the furan-maleimide Diels-Alder reaction', *Green Chemistry*, 17: 4991-5000.

Feng, Zhanbin, Jing Hu, Bing Yu, Hongchi Tian, Hongli Zuo, Nanying Ning, Ming Tian, and Liqun Zhang. 2019. 'Environmentally Friendly Method To Prepare Thermo-Reversible, Self-Healable Biobased Elastomers by One-Step Melt Processing', *ACS Applied Polymer Materials,* 1: 169-77.

Fortman, D. J., J. P. Brutman, G. X. De Hoe, R. L. Snyder, W. R. Dichtel, and M. A. Hillmyer. 2018. 'Approaches to Sustainable and Continually Recyclable Cross-Linked Polymers', *ACS Sustainable Chemistry & Engineering,* 6: 11145-59.

Froidevaux, V, M Borne, E Laborbe, R Auvergne, A Gandini, and B Boutevin. 2015. 'Study of the Diels–Alder and retro-Diels–Alder reaction between furan derivatives and maleimide for the creation of new materials', *RSC Advances*, 5: 37742-54.

Gandini, Alessandro. 2013. 'The furan/maleimide Diels–Alder reaction: A versatile click–unclick tool in macromolecular synthesis', *Progress in Polymer Science,* 38: 1-29.

Gandini, Alessandro, Talita M Lacerda, and Antonio JF Carvalho. 2013. 'A straightforward double coupling of furan moieties onto epoxidized triglycerides: synthesis of monomers based on two renewable resources', *Green Chemistry,* 15: 1514-19.

García-Astrain, Clara, and Luc Avérous. 2018. 'Synthesis and evaluation of functional alginate hydrogels based on click chemistry for drug delivery applications', *Carbohydrate Polymers*, 190: 271-80.

García-Astrain, Clara, and Luc Avérous. 2019. 'Synthesis and behavior of click cross-linked alginate hydrogels: Effect of cross-linker length and functionality', International Journal of Biological Macromolecules, 137: 612-19.

García Astrain, Clara, Rebeca Hernandez, Olatz Guaresti, Ljiljana Fruk, Carmen Mijangos, Arantxa Eceiza, and Nagore Gabilondo. 2016. 'Click Crosslinked Chitosan/Gold Nanocomposite Hydrogels', Macromolecular Materials and Engineering, 301:1295-1300.

González, Kizkitza, Clara García-Astrain, Arantzazu Santamaria-Echart, Lorena Ugarte, Luc Avérous, Arantxa Eceiza, and Nagore Gabilondo. 2018. 'Starch/graphene hydrogels via click chemistry with relevant electrical and antibacterial properties', Carbohydrate Polymers, 202: 372-81.

Gu, Lin, and Qing-Yun Wu. 2018. 'Recyclable bio-based crosslinked polyurethanes with self-healing ability', *Journal of Applied Polymer Science*, 135: 46272.

Guaresti, O., C. García–Astrain, R. H. Aguirresarobe, A. Eceiza, and N. Gabilondo. 2018. 'Synthesis of stimuli–responsive chitosan–based hydrogels by Diels–Alder cross–linking `click´ reaction as potential carriers for drug administration', *Carbohydrate Polymers*, 183: 278-86.

Guaresti, Olatz, Clara García Astrain, Leire Urbina, Arantxa Eceiza, and Nagore Gabilondo. 2018. 'Reversible swelling behaviour of Diels-Alder clicked chitosan hydrogels in response to pH changes', *Express Polymer Letters*, 13: 27-36.

Heo, Yunseon, and Henry A. Sodano. 2014. 'Self-Healing Polyurethanes with Shape Recovery', *Advanced Functional Materials*, 24: 5261-68.

Hu, Sumeng, Xi Chen, and John M. Torkelson. 2019. 'Biobased Reprocessable Polyhydroxyurethane Networks: Full Recovery of Crosslink Density with Three Concurrent Dynamic Chemistries', *ACS Sustainable Chemistry & Engineering*, 7: 10025-34.

Ionescu, M. 2005. Chemistry and Technology of Polyols for Polyurethanes. Milhail Ionescu. Rapra Technology, Shrewsbury, UK. Polym. Int.

Irusta, L., M. J. Fernandez-Berridi, and J. Aizpurua. 2017. 'Polyurethanes based on isophorone diisocyanate trimer and polypropylene glycol crosslinked by thermal reversible diels alder reactions', *Journal of Applied Polymer Science,* 134: 9.

Kloxin, Christopher J., Timothy F. Scott, Brian J. Adzima, and Christopher N. Bowman. 2010. 'Covalent Adaptable Networks (CANs): A Unique Paradigm in Cross-Linked Polymers', *Macromolecules*, 43: 2643-53.

Lacerda, T. M., A. J. F. Carvalho, and A. Gandini. 2014. 'Two alternative approaches to the Diels-Alder polymerization of tung oil', *RSC Advances,* 4: 26829-37.

Lacerda, T. M., and A. Gandini. 2014. 'Marriage of Furans and Vegetable Oils through Click Chemistry for the Preparation of Macromolecular Materials: A Succinct Review', *Journal of Renewable Materials,* 2: 2-12.

Lakatos, C., K. Czifrak, J. Karger-Kocsis, L. Daroczi, M. Zsuga, and S. Keki. 2016. 'Shape memory crosslinked polyurethanes containing thermoreversible Diels-Alder couplings', *Journal of Applied Polymer Science*, 133: 44145.

Lligadas, G., J. C. Ronda, M. Galia, and V. Cadiz. 2013. 'Renewable polymeric materials from vegetable oils: a perspective'*, Materials Today*, 16: 337-43.

Meier, Michael A. R., Jurgen O. Metzger, and Ulrich S. Schubert. 2007. 'Plant oil renewable resources as green alternatives in polymer science', *Chemical Society Reviews*, 36: 1788-802.

Montarnal, D., M. Capelot, F. Tournilhac, and L. Leibler. 2011. 'Silica-Like Malleable Materials from Permanent Organic Networks', *Science,* 334: 965-68.

Obadia, Mona M., Antoine Jourdain, Philippe Cassagnau, Damien Montarnal, and Eric Drockenmuller. 2017. 'Tuning the Viscosity Profile of Ionic Vitrimers Incorporating 1,2,3-Triazolium Cross-Links', *Advanced Functional Materials*, 27: 1703258.

Oh, Cho-Rong, Sang-Hyub Lee, Jun-Hong Park, and Dai-Soo Lee. 2019. 'Thermally Self-Healing Graphene-Nanoplate/Polyurethane Nanocomposites via Diels–Alder Reaction through a One-Shot Process', *Nanomaterials*, 9: 434.

Palaskar, Dnyaneshwar V., Aurélie Boyer, Eric Cloutet, Jean-François Le Meins, Benoit Gadenne, Carine Alfos, Céline Farcet, and Henri Cramail. 2012. 'Original diols from sunflower and ricin oils: Synthesis, characterization, and use as polyurethane building blocks', *Journal of Polymer Science Part A: Polymer Chemistry,* 50: 1766-82.

Petrović, Zoran S., Ivana Cvetković, DooPyo Hong, Xianmei Wan, Wei Zhang, Tim Abraham, and Jeff Malsam. 2008. 'Polyester polyols and polyurethanes from ricinoleic acid', *Journal of Applied Polymer Science,* 108: 1184-1190.

Rivero, Guadalupe, Le-Thu T. Nguyen, Xander K. D. Hillewaere, and Filip E. Du Prez. 2014. 'One-Pot Thermo-Remendable Shape Memory Polyurethanes'*, Macromolecules*, 47: 2010-18.

Scheutz, Georg M., Jacob J. Lessard, Michael B. Sims, and Brent S. Sumerlin. 2019. 'Adaptable Crosslinks in Polymeric Materials: Resolving the Intersection of Thermoplastics and Thermosets', *Journal of the American Chemical Society,* 141: 16181-96.

Thompson, Richard C., Charles J. Moore, Frederick S. vom Saal, and Shanna H. Swan. 2009. 'Plastics, the environment and human health: current consensus and future trends', *Philosophical transactions of the Royal Society of London. Series B, Biological Sciences,* 364: 2153-66.

Tremblay-Parrado, Khantutta-Kim, and Luc Avérous. 2019. 'Renewable Responsive Systems Based on Original Click and Polyurethane Cross-Linked Architectures with Advanced Properties', *Chemsuschem*, 13: 238.

Truong, Thuy Thu, Ha Tran Nguyen, Man Ngoc Phan, and Le-Thu T. Nguyen. 2018. 'Study of Diels–Alder reactions between furan and maleimide model compounds and the preparation of a healable thermo-reversible polyurethane'*, Journal of Polymer Science Part A: Polymer Chemistry,* 56: 1806-14.

Truong, Thuy Thu, Son Hong Thai, Ha Tran Nguyen, Dung Thuy Thi Phung, Loc Tan Nguyen, Hung Quang Pham, and Le-Thu T. Nguyen. 2019. 'Tailoring the Hard–Soft Interface with Dynamic Diels–Alder Linkages in Polyurethanes: Toward Superior Mechanical Properties and Healability at Mild Temperature', *Chemistry of Materials,* 31: 2347-57.

Vilela, Carla, Letizia Cruciani, Armando J. D. Silvestre, and Alessandro Gandini. 2011. 'A Double Click Strategy Applied to the Reversible Polymerization of Furan/Vegetable Oil Monomers', *Macromolecular Rapid Communications*, 32: 1319-23.

Vilela, Carla, Letizia Cruciani, Armando JD Silvestre, and Alessandro Gandini. 2012. 'Reversible polymerization of novel monomers bearing furan and plant oil moieties: a double click exploitation of renewable resources', *RSC Advances,* 2: 2966-74.

Vilela, Carla, Armando J. D. Silvestre, and Alessandro Gandini. 2013. 'Thermoreversible nonlinear diels-alder polymerization of furan/plant oil monomers', *Journal of Polymer Science Part A: Polymer Chemistry*, 51: 2260-70.

Willocq, B., F. Khelifa, J. Brancart, G. Van Assche, Ph Dubois, and J. M. Raquez. 2017. 'One-component Diels-Alder based polyurethanes: a unique way to self-heal', *RSC Advances, 7*: 48047-53.

Wilson, Jedediah F., and Eugene Y. X. Chen. 2019. 'Difuranic Diols for Renewable Polymers with Pendent Furan Rings', *ACS Sustainable Chemistry & Engineering,* 7: 7035-46.

Xu, Y. J., Z. Petrovic, S. Das, and G. L. Wilkes. 2008. 'Morphology and properties of thermoplastic polyurethanes with dangling chains in ricinoleate-based soft segments', *Polymer*, 49: 4248-58.

Ying, Hanze, Yanfeng Zhang, and Jianjun Cheng. 2014. 'Dynamic urea bond for the design of reversible and self-healing polymers', *Nature Communications*, 5: 3218.

Yoshie, Naoko, Shoma Yoshida, and Koji Matsuoka. 2019. 'Self-healing of biobased furan polymers: Recovery of high mechanical strength by mild heating', *Polymer Degradation and Stability*, 161: 13-18.

Zhang, Lu, Frederick C. Michel Jr, and Anne C. Co. 2019. 'Nonisocyanate route to 2,5-bis(hydroxymethyl)furan-based polyurethanes crosslinked by reversible diels–alder reactions', *Journal of Polymer Science Part A: Polymer Chemistry*, 57: 1495-99.

7. Supporting Information

7.1. Synthesis of FO

Esterification of OA by Furfuryl Alcohol to yield Furan-2-ylmethyl-octadec-9-enoate (FMO)

A solution including OA (1 mol equiv.), *N,N'*-dicyclohexylcarboiimide (DCC, 1.1 mol equiv.), 4-dimethylaminopyridine (DMAP, 0.1 mol equiv.) in 25% *w/v* % dried dichloromethane (DCM) was stirred magnetically for 1 h in a two-necked round bottom flask at room temperature. Then, furfuryl alcohol (FA, 1.1 mol equiv.) was added dropwise through a dropping funnel. The reaction mixture was left stirring overnight at room temperature and under nitrogen. *N,N'* – dicyclohexylurea (DCU) formed during the reaction, precipitated, and was filtered off. The filtrate was washed twice with water, twice with 5% acetic acid solution and finally again with water until a neutral pH was attained. The organic phase was dried over anhydrous sodium sulfate. The solvent was evaporated under reduced pressure. The ester formed, Furan-2-ylmethyl-octadec-9-enoate (FMO) was then further purified over a silica gel plug using petroleum ether/diethyl ether (95:5, *v/v*) as eluents to remove remnants of DCU. FMO was dried under vacuum overnight vacuum, at 50 °C.

Epoxidation of FMO

The epoxidation of FMO was conducted by the in-situ formation of peracetic acid from glacial acetic acid (GAA) and H_2O_2. In a two-necked round bottom flask, equipped with a magnetic stirrer and a dropping funnel, FMO (1 mol equiv. of unsaturations), amberlite IR-120 H (25 wt % of FMO), GAA (0.2 mol equiv.) was inserted into the flask and dissolved in toluene (12.5 wt % *w/v*). The solution was stirred to 70 °C and then H_2O_2 (1.2 mol equiv.) was added dropwise. The mixture was stirred at 70 °C for 7 h. The organic phase was dried with anhydrous sodium sulphate and then filtered. The solvent was evaporated under reduced pressure. Epoxidized FMO (EFMO) was

dried under vacuum overnight, at 50 °C. The reaction product, Furan-2-ylmethlyl 8-(3-octyloxiran-2-yl)octonoate (FMOO), was clear yellow oil.

Oligomerization of FMOO

For a molar equivalent of FMOO, H_2O (0.7 mol equiv.) was added in a two-necked round bottom flask and stirred mechanically. A cationic initiator, $HSbF_6$ (1.5 wt % of FMOO) was added dropwise. The mixture was stirred at room temperature for 1 h. The reaction was quenched by the addition of water and dissolved in diethyl ether. The organic solution was washed with a 5% sodium bicarbonate solution and distilled water until a neutral pH was attained. The solution was dried over anhydrous sodium sulfate, and filtered. The solvent was evaporated under reduced pressure and the oligomer was dried under vacuum overnight, at 50 °C. The oligomerization resulted in an orange clear viscous oil. A master batch of about 35 g was prepared.

Furan Oligomer: ^{1}H NMR (400 MHz, $CDCl_3$): δ = 7.41 (dd, 1H; 5-H of 2-furan)), 6.39 (d, 1H; 3-H of 2-furan), 6.36 (dd, 1H; 4-H of 2-furan), 5.06 (s, 2H; OC*H*$_2$), 3.80 - 2.82 (m; polyether backbone), 2.32 (t, 2H; C*H*$_2$C(=O)), 1.62 (m, 2H; C*H*$_2$CH$_2$C(=O)), 1.37-1.18 (m, 24H; aliphatic C*H*$_2$), 0.88 (t, 3H; C*H*$_3$. ^{13}C NMR (500 MHz, $CDCl_3$): δ = 174 (*C*=O), 150 (C-2 of 2-furan), 143 (C-5 of 2-furan), 111 (C-3 of 2-furan), 111 (C-4 of 2-furan), 85.0-70.0 (polyether backbone *C*-O-*C*), 57.9 (O*C*H$_2$–2-furan), 34.2 (*C*H$_2$–C(=O)), 31.9-22.7 (aliphatic *C*H$_2$), 14.1 (*C*H$_3$)

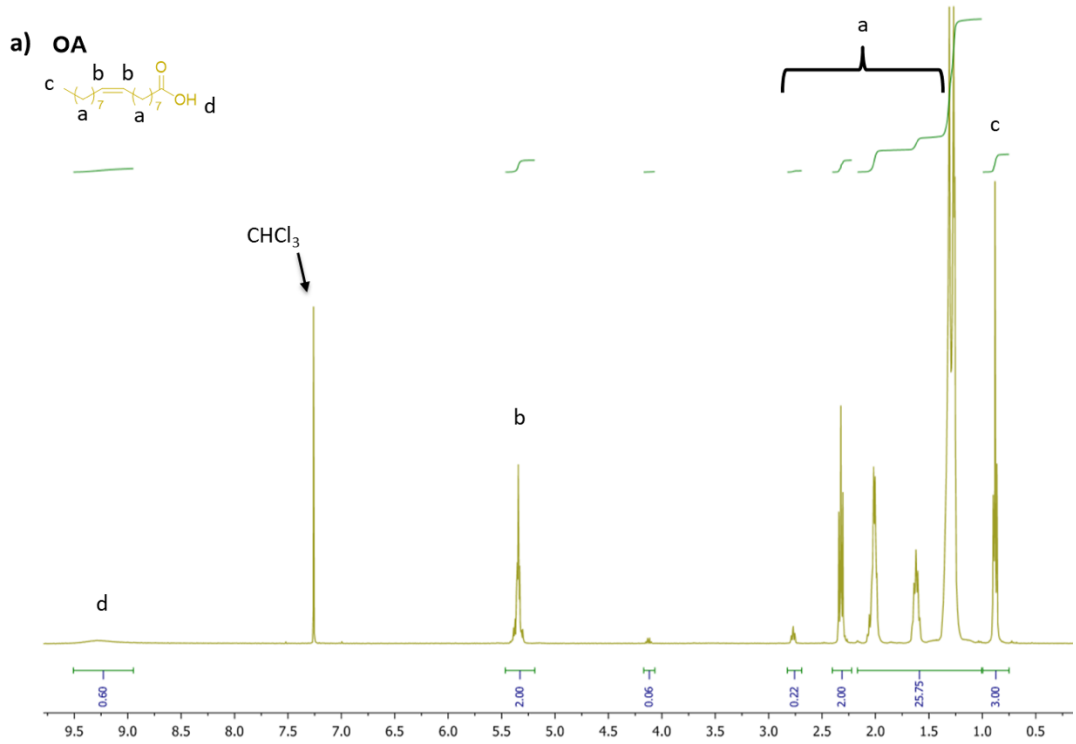
a) OA
c
b b
a a
d
OH
a
c
CHCl3
b
d
0.60
2.00
0.06
0.22
2.00
25.75
3.00
9.5 9.0 8.5 8.0 7.5 7.0 6.5 6.0 5.5 5.0 4.5 4.0 3.5 3.0 2.5 2.0 1.5 1.0 0.5

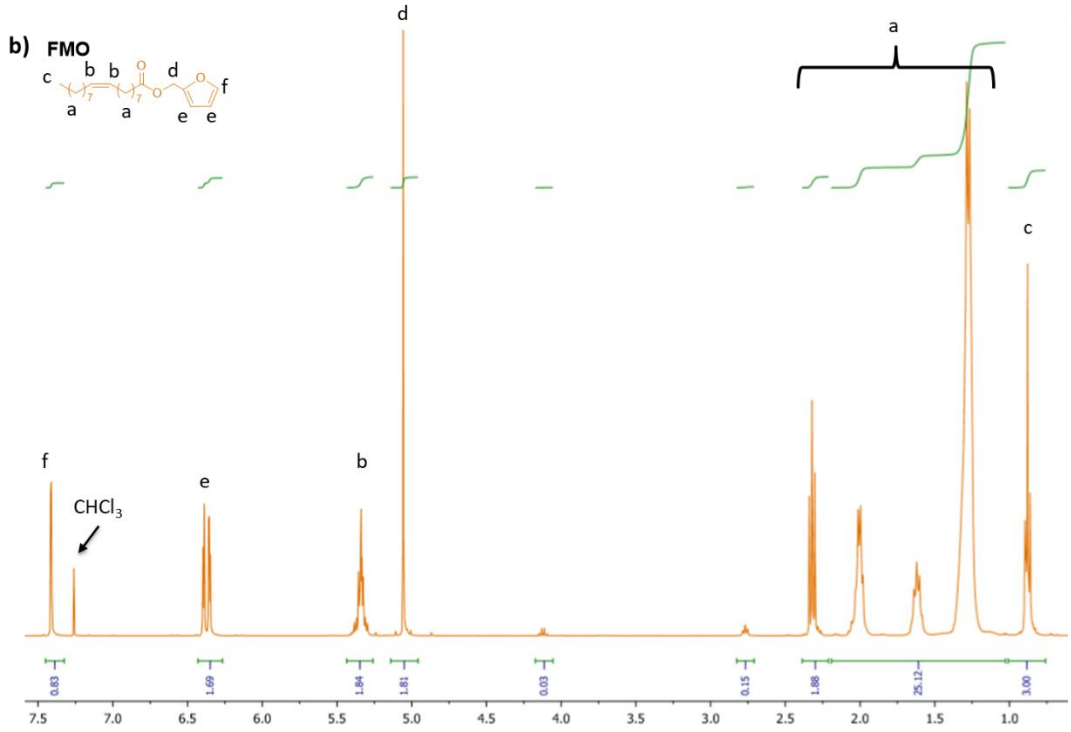
b) FMO
c
b b
d
f
a a
e e
d
a
c
f
CHCl3
e
b
0.83
1.69
1.84
1.81
0.03
0.15
1.88
25.12
3.00
7.5 7.0 6.5 6.0 5.5 5.0 4.5 4.0 3.5 3.0 2.5 2.0 1.5 1.0

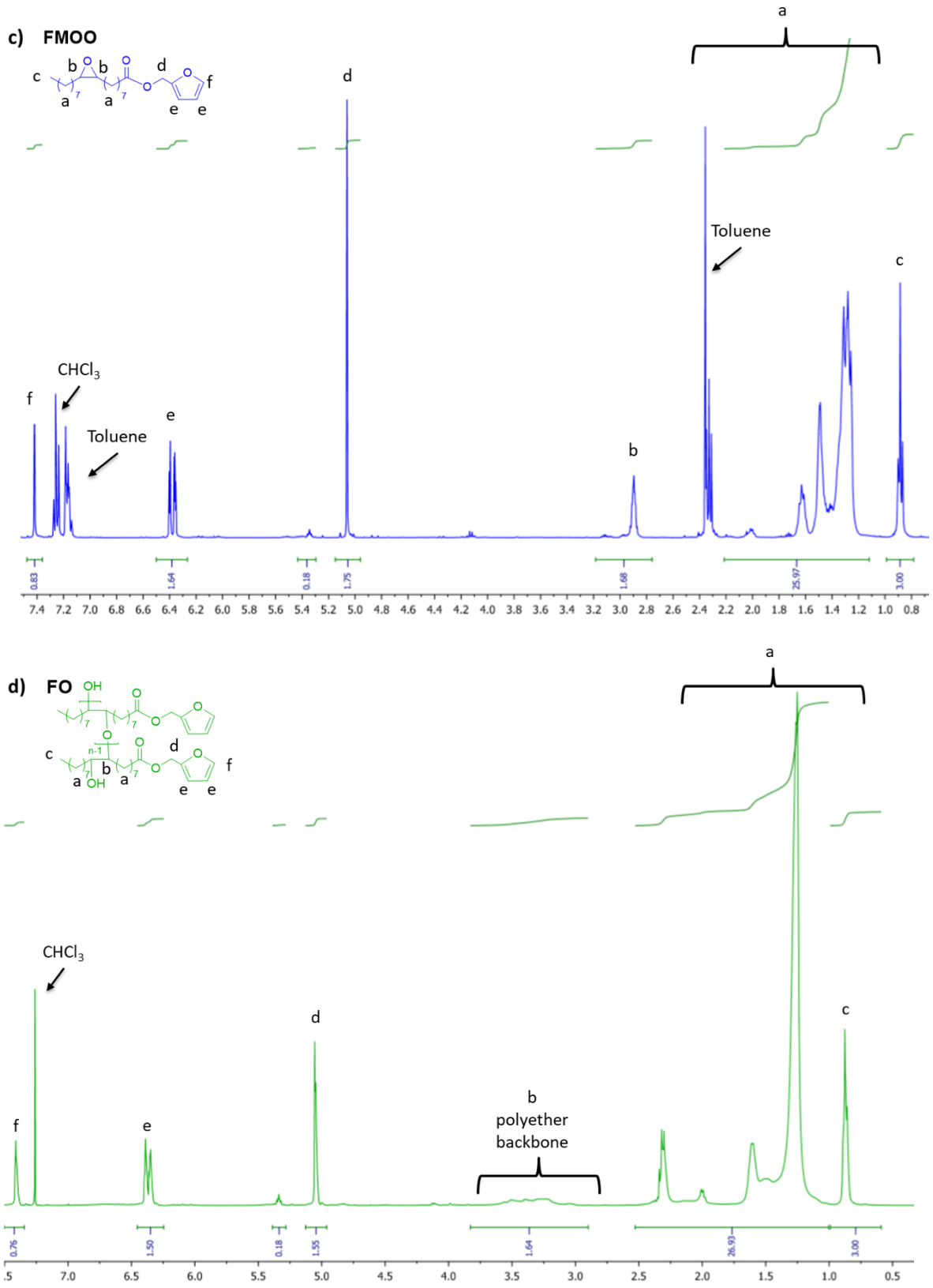

Figure S3.8 – ^{1}H NMR spectra of (a) OA (b) FMO (c) FMOO and (d) FO, with integrations.

Table S3.4 – Properties of FO used for the synthesis of PU materials.

Oligomer Sample	$HSbF_6$ [w.t. %]	H_2O [mol %]	HV[a] [mg_{KOH}/g]	Furan Content[b] [mmol/g]
Batch 1	1.5	70	54	1.89

[a] Determined from ^{31}P NMR spectroscopic analysis. [b] Determined from ^{1}H NMR spectroscopic analysis

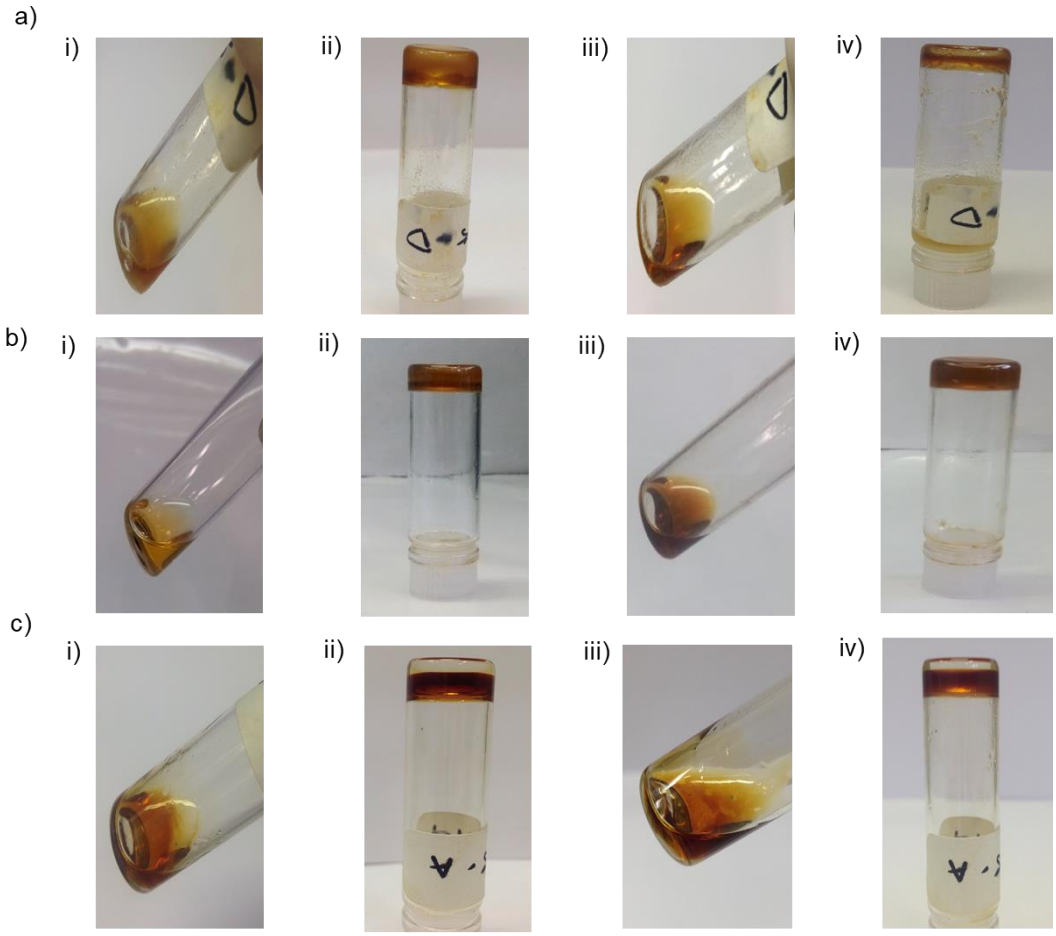

Figure S3.9 – (a) Photographs of i) the initial mixture of FO and MP BMI; ii) the mixture after 24 h at 60 °C; iii) the mixture after additional 1 h at 120 °C; and iv) the mixture after additional 24 h at 60 °C. (b) Photographs of i) the initial mixture of FO and PPOPEOBMI-DP13; ii) the mixture after 24 h at 60 °C; iii) the mixture after additional 1 h at 120 °C; and iv) the mixture after additional 24 h at 60 °C. (c) Photographs of i) the initial mixture of FO and PPOBMI-DP33; ii) the mixture after 24 h at 60 °C; iii) the mixture after additional 1 h at 120 °C; and iv) the mixture after additional 24 h at 60 °C.

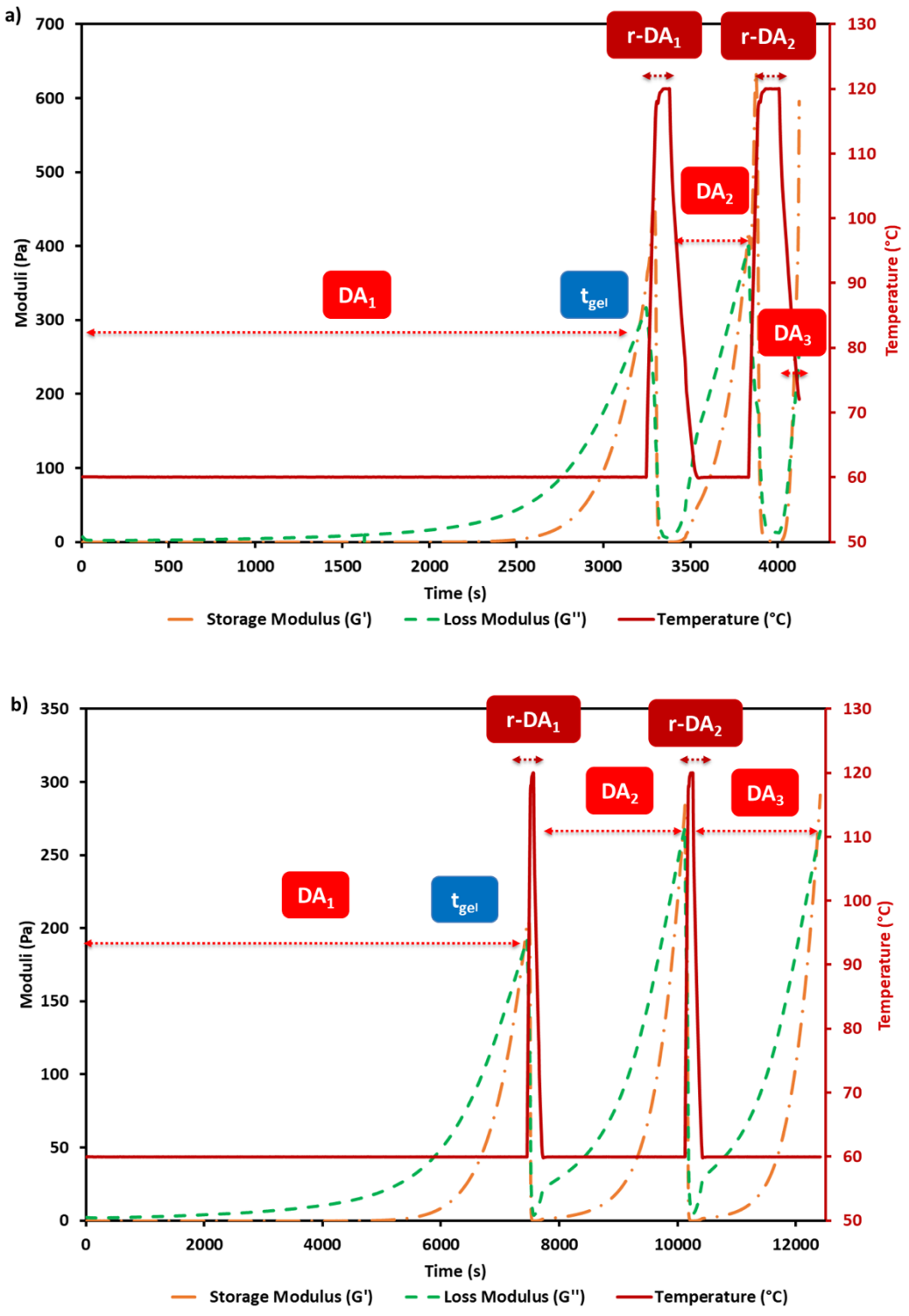

Figure S3.10 – Rheological experiments (a) storage modulus (G', blue round dotted line) and loss modulus (G'', red dashed dotted line) versus time for FO and PPOPEOBMI-DP6 furan:maleimide ratio 1:1 with different heating steps, DA at 60 °C and r-DA at 120 °C, (b) storage modulus (G', blue round dotted line) and loss modulus (G'', red dashed dotted line) versus time for FO and PPOBMI-DP33 furan:maleimide ratio 1:1 with different heating steps, DA at 60 °C and r-DA at 120 °C.

7.2. Characterization of biobased PUs

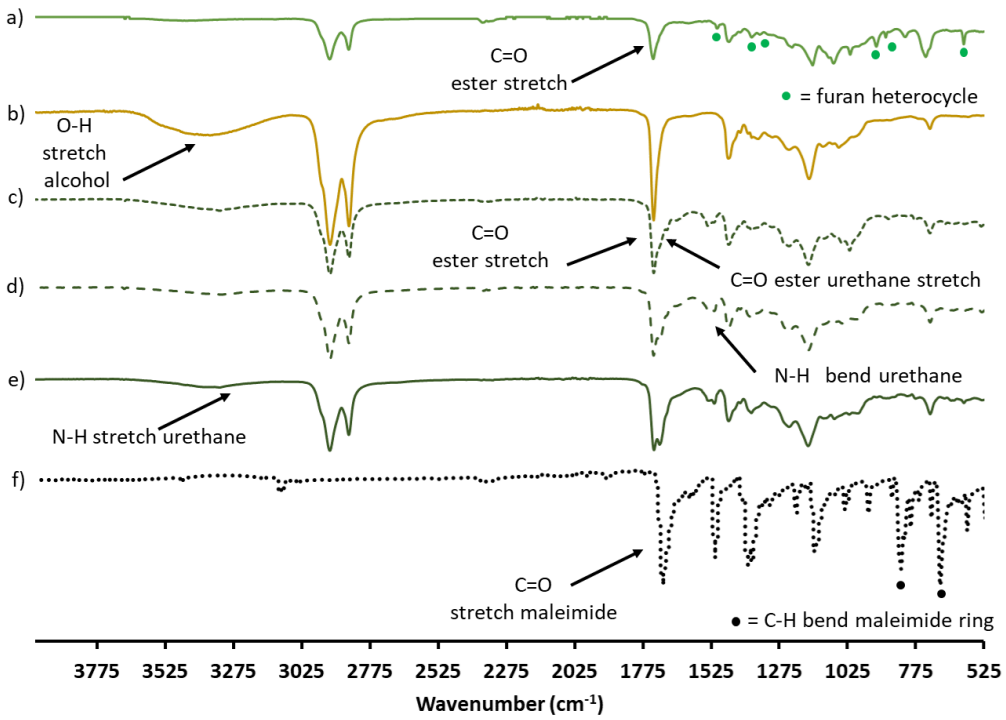

Figure S3.11 – FTIR spectra of (a) FO, (b) biobased polyol, (c) PU-FO10-MPBMI, (d) PU-FO20-MPBMI, (e) PU-FO30-MPBMI, and (f) MPBMI.

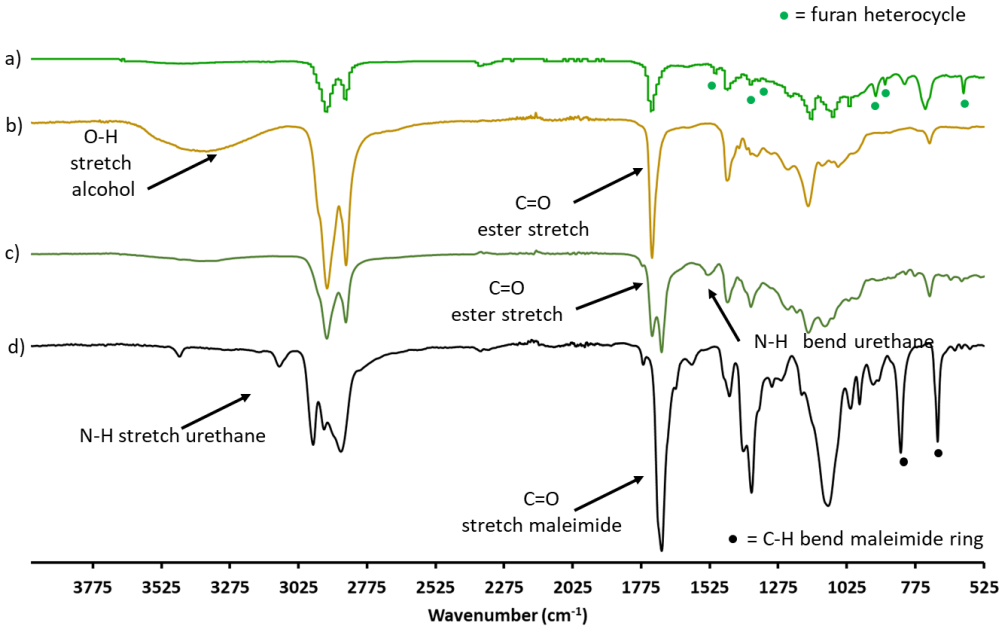

Figure S3.12 – FTIR spectra of (a) FO, (b) biobased polyol, (c) PU-FO20-PPOBMI-DP6, and (d) PPOBMI-DP6.

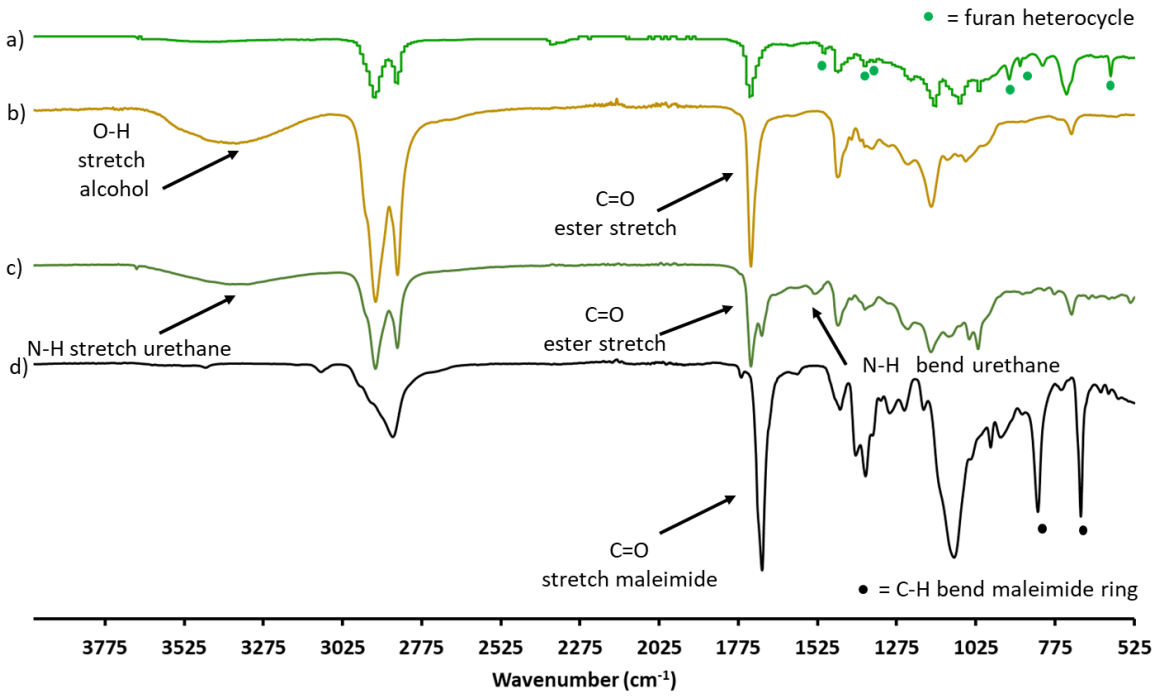

Figure S3.13 – FTIR spectra of (a) FO, (b) biobased polyol, (c) PU-FO20-PPOPEOBMI-DP13, and (d) PPOPEOBMI-DP13.

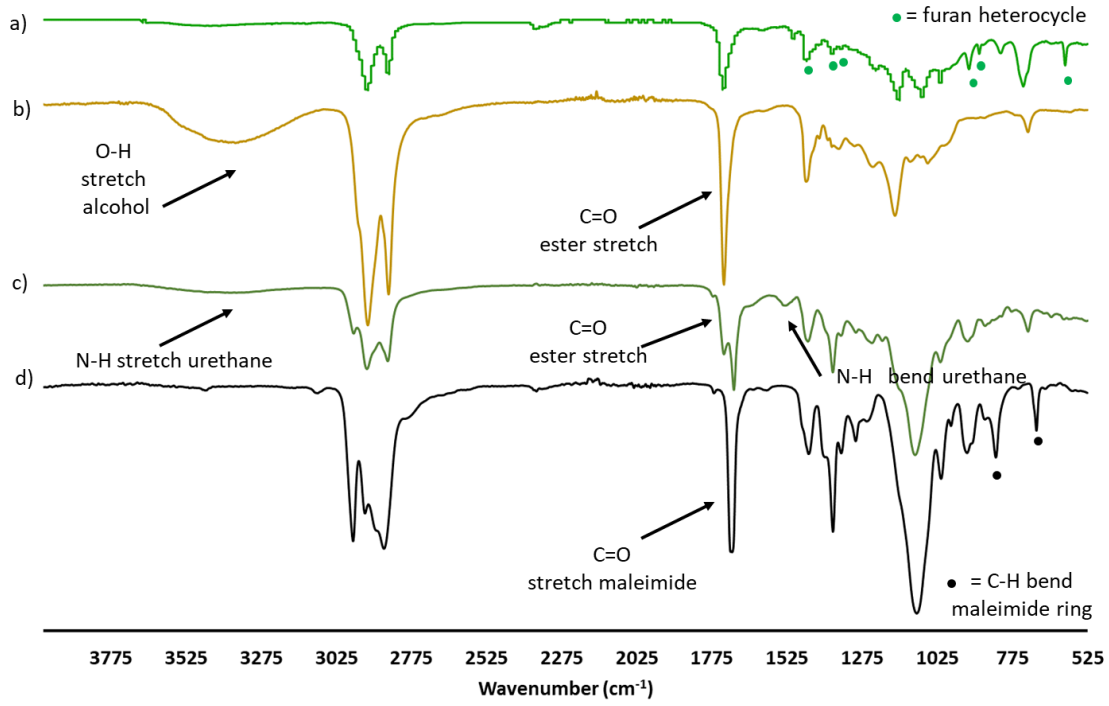

Figure S3.14 – FTIR spectra of (a) FO, (b) biobased polyol, (c) PU-FO20-PPOBMI-DP33, and (d) PPOBMI-DP33.

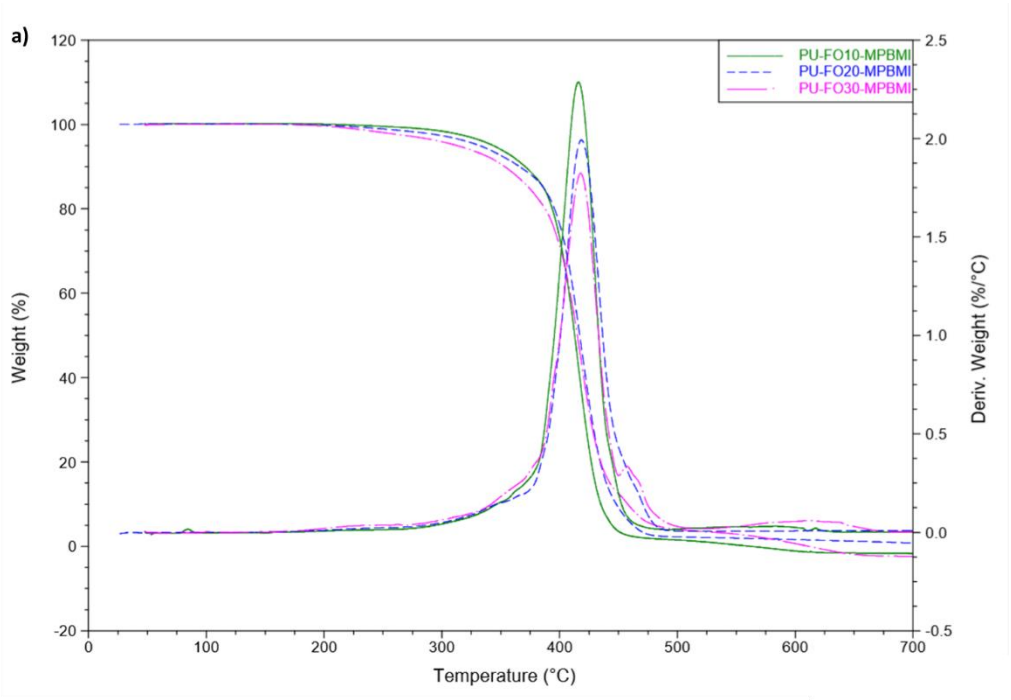
a)
PU-FO10-MPBMI
PU-FO20-MPBMI
PU-FO30-MPBMI
Weight (%)
Deriv. Weight (%/°C)
Temperature (°C)

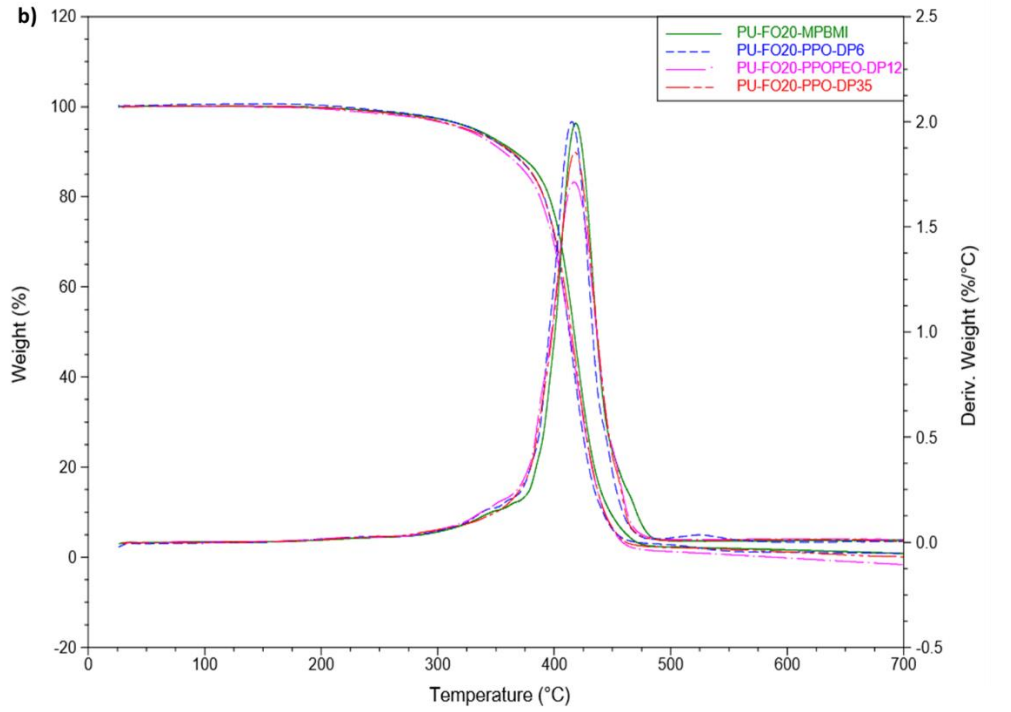
b)
PU-FO20-MPBMI
PU-FO20-PPO-DP6
PU-FO20-PPOPEO-DP12
PU-FO20-PPO-DP35
Weight (%)
Deriv. Weight (%/°C)
Temperature (°C)

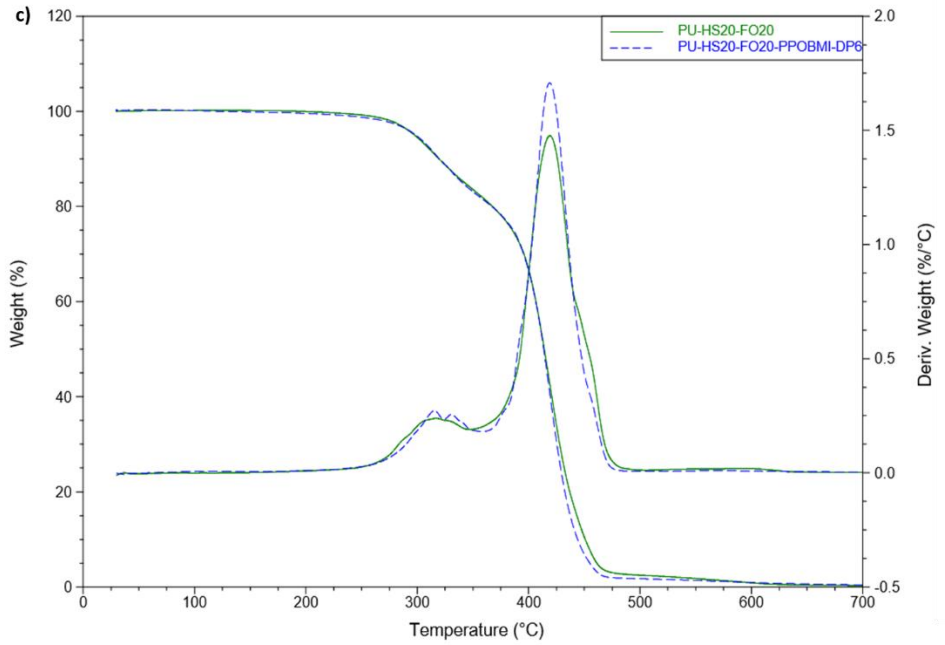

Figure S3.15 – Thermogravimetric analysis curves (TGA) and derivative thermogravimetric analysis curve (DTG) of materials (a) PU-FO10-MPBMI (green, sold), PU-FO20-MPBMI (blue, dashed), PU-FO30-MPBMI (pink, dash-dot), (b) PU-FO20-MPBMI (green, sold), PU-FO20-PPOBMI-DP6 (blue, dashed), PU-FO20-PPOPEO-DP13 (blue, dash-dot), PU-FO20-PPOBMI-DP6 (pink, dash-dot), PU-FO20-PPOBMI-DP33 (red, line-dash), (c) PU-HS20-FO20 (green, sold), PU-HS20-FO20-PPOBMI-DP6 (blue, dashed).

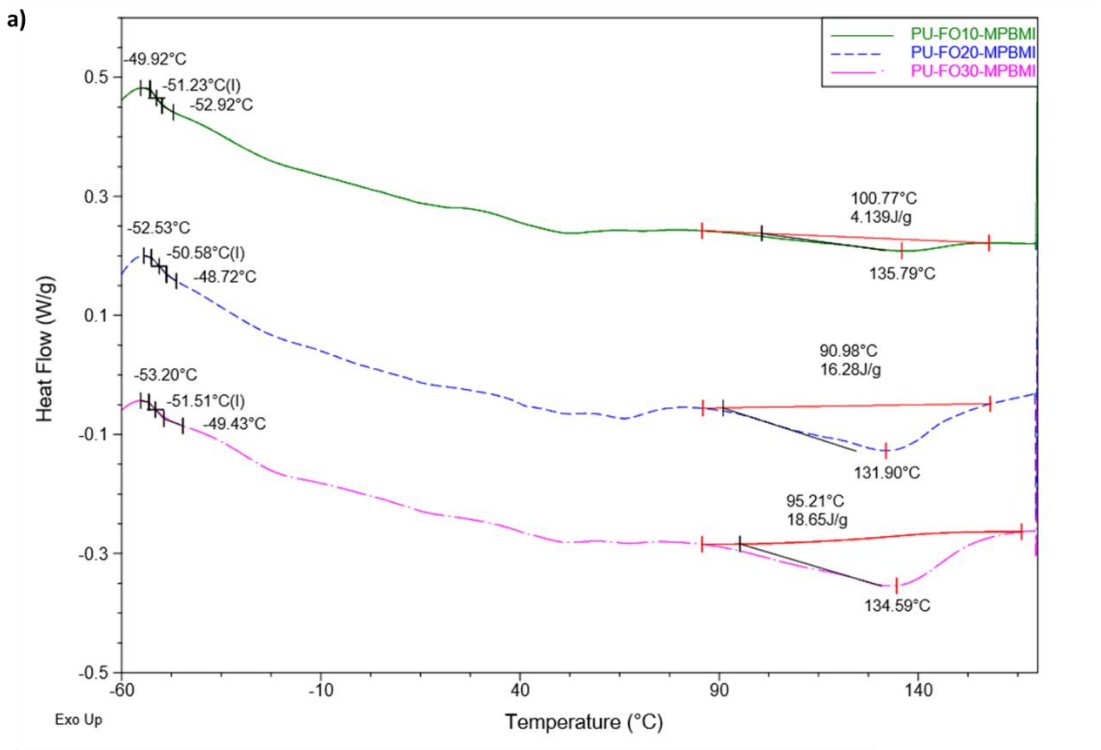

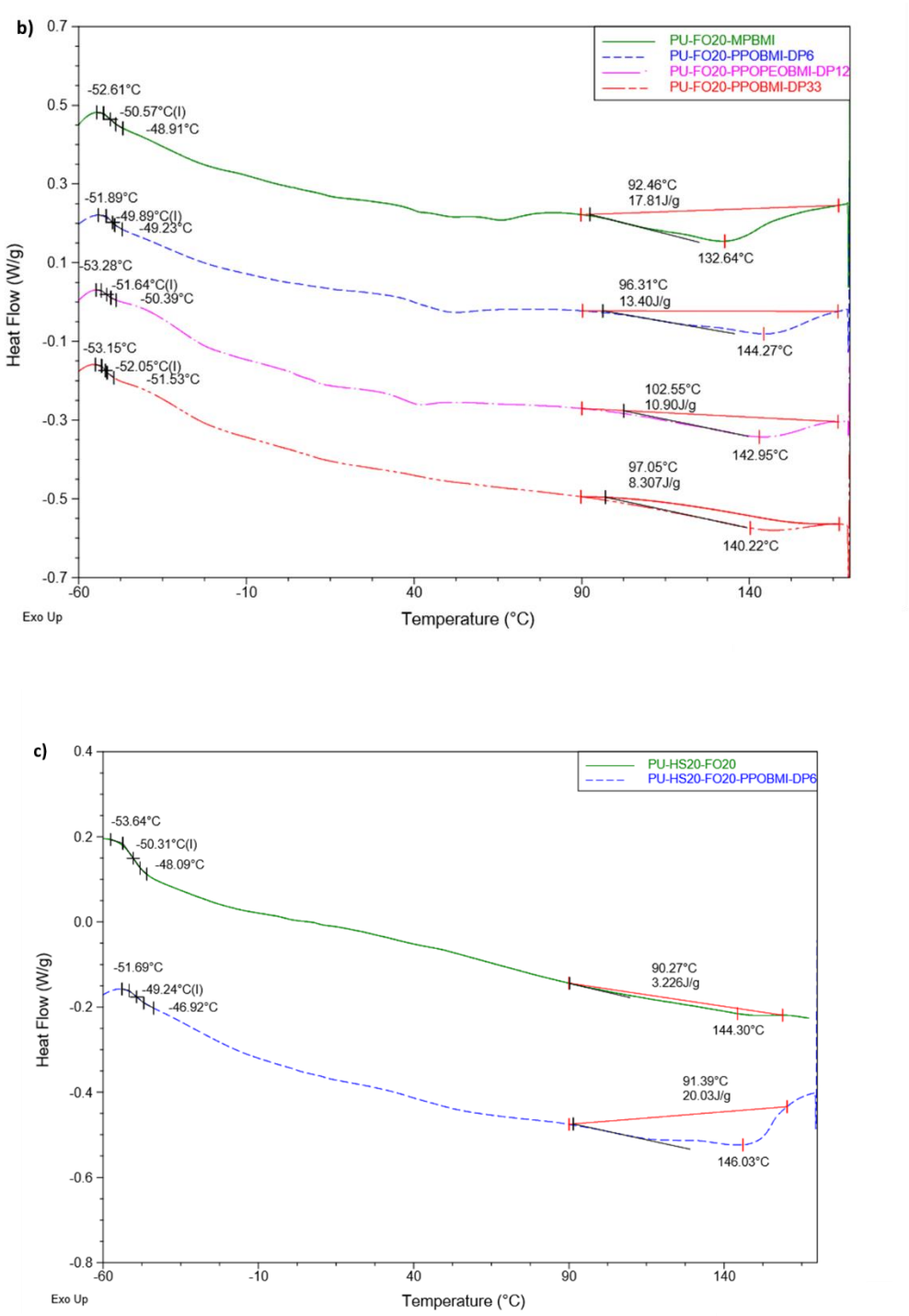

Figure S3.16 – Differential scanning calorimetry (DSC) thermograms of materials (a) PU-FO10-MPBMI (green, sold), PU-FO20-MPBMI (blue, dashed), PU-FO30-MPBMI (pink, dash-dot), (b) PU-FO20-MPBMI (green, sold), PU-FO20-PPOBMI-DP6 (blue, dashed), PU-FO20-PPOPEOBMI-DP13 (blue, dash-dot), PU-FO20-PPOBMI-DP6 (pink, dash-dot), PU-FO20-PPOBMI-DP33 (red, line-dash), (c) PU-HS20-FO20 (green, sold), PU-HS20-FO20-PPOBMI-DP6 (blue, dashed).

Table S3.5 – Summary of T_g and mechanical properties data of all PUs materials: original, reprocessed, original exposed to 120 °C heating and control.

PU system	Processing step	DSC T_g (°C)	Young's modulus (MPa)	$\sigma^{[a]}$ (MPa)	$\varepsilon^{[b]}$ (%)
PU-FO10-MPBMI	Original	-51	1.86 ± 0.12	0.95 ± 0.08	265 ± 27
	Reprocessing 1	-51	2.09 ± 0.14	1.02 ± 0.07	208 ± 32
	Reprocessing 2	-51	1.03 ± 0.06	1.02 ± 0.13	193 ± 24
	120 °C Heating	-	1.44	0.53	222
PU-FO20-MPBMI	Original	-51	2.40 ± 0.22	1.10 ± 0.04	120 ± 5
	Reprocessing 1	-51	1.86 ± 0.04	1.01 ± 0.03	119 ± 11
	Reprocessing 2	-50	1.22 ± 0.08	0.91 ± 0.11	121 ± 14
	120 °C Heating	-	0.95	0.62	95
PU-FO30-MPBMI	Original	-51	2.22 ± 0.19	1.58 ± 0.16	118 ± 10
	Reprocessing 1	-52	1.74 ± 0.21	1.42 ± 0.07	101 ± 6
	Reprocessing 2	-52	1.21 ± 0.09	1.00 ± 0.04	84 ± 5
	120 °C Heating	-	0.80	0.61	106
PU-FO20-PPOBMI-DP6	Original	-50	1.65 ± 0.15	1.10 ± 0.03	129 ± 8
	Reprocessing 1	-48	1.36 ± 0.09	0.901 ± 0.02	119 ± 9
	Reprocessing 2	-51	1.03 ± 0.11	0.63 ± 0.03	108 ± 10
	120 °C Heating	-	0.82	0.44	84
PU-FO20-PPOPEOBMI-DP13	Original	-52	1.57 ± 0.21	0.86 ± 0.01	131 ± 5
	Reprocessing 1	-50	1.21 ± 0.05	0.75 ± 0.06	128 ± 9
	Reprocessing 2	-52	0.76 ± 0.02	0.44 ± 0.08	84 ± 15
	120 °C Heating	-	0.40	0.34	104
PU-FO20-PPOBMI-DP33	Original	-52	1.22 ± 0.10	0.80 ± 0.07	120 ± 7
	Reprocessing 1	-52	0.70 ± 0.07	0.45 ± 0.04	91 ± 7
	Reprocessing 2	-51	0.59 ± 0.01	0.36 ± 0.04	88 ± 9
	120 °C Heating	-	0.63	0.34	115
PU-HS20-FO20-PPOBMI-DP6	Original	-49	14.47 ± 3.50	1.74 ± 0.20	24 ± 10
	Reprocessing 1	-49	13.81 ± 1.83	2.12 ± 0.08	39 ± 6
	Reprocessing 2	-51	12.44 ± 1.16	1.62 ± 0.34	33 ± 8
	120 °C Heating	-	12.12	1.42	34
	Control	-50	11.84 ± 1.16	1.15 ± 0.11	30 ± 9

[a] Tensile strength. [b] Elongation.

Two tailed paired student t-test were used to determine whether the means of mechanical properties of initial materials were significantly different to those of reprocessed materials. It was found that statistically similar means include : the mechanical properties of the initial PU-FO10-

MPBMI and PU-FO10-MPBMI-RP1 (reprocessed 1), the tensile strength (TS) elongation of PU-FO10-MPBMI and PU-FO10-MPBMI-RP2, tensile strength and elongation of PU-FO20-MPBMI and that of PU-FO20-MPBMI-RP1 and PU-FO20-MPBMI-RP2, the Young's modulus and elongation of PU-FO20-PPOBMI-DP6 and PU-FO20-PPOBMI-DP6-RP1, the elongation of PU-FO20-PPOPEOBMI-DP13 and PU-FO20-PPOPEOBMI-DP13-RP1 and lastly the initial mechanical properties of PU-FO20-HS20-PPOBMI-DP6 and FO20-HS20-PPOBMI-DP6-RP1 and PU-FO20-HS20-PPOBMI-DP6-RP2. All reprocessed mechanical properties data were found to have statically different means when compared to the mechanical properties of initial material.

Table S3.6 – Summary of mechanical properties data of original and healed samples of PU materials.

PU System	Sample	Young's Modulus (MPa)	$\sigma^{[a]}$ (MPa)	$\varepsilon^{[b]}$ (%)
PU-FO10-MPBMI	Original	1.86 ± 0.12	0.95 ± 0.08	265 ± 27
	Healed 1	1.19	0.39	125
	% Recovery (%)	64	41	47
PU-FO20-MPBMI	Original	2.40 ± 0.22	1.10 ± 0.04	120 ± 5
	Healed 1	0.80	0.40	70
	% Recovery	33	36	58
PU-FO30-MPBMI	Original	2.22 ± 0.19	1.58 ± 0.16	118 ± 10
	Healed 1	0.94	0.56	66
	% Recovery	43	35	44
PU-FO20-PPOBMI-DP6	Original	1.65 ± 0.15	1.10 ± 0.03	129 ± 8
	Healed 1	0.63	0.31	75
	% Recovery	38	28	58
PU-FO20-PPOPEOBMI-DP12	Original	1.57 ± 0.21	0.86 ± 0.01	131 ± 5
	Healed 1	0.63	0.25	42
	% Recovery	40	29	32
PU-FO20-PPOBMI-DP33	Original	1.22 ± 0.10	0.80 ± 0.07	120 ± 7
	Healed 1	0.52	0.25	61
	% Recovery	43	31	51

[a] Tensile strength. [b] Elongation.

Conclusion of Chapter 3

The aim of this study was to further expand on the proof of concept established in the previous chapter. The previous chapter presented a thorough characterization of the furan oligomer (FO) and proof concept of thermoreversible biobased cross-linked polyurethanes (PUs) via the Diels-Alder reaction, using a short poly(propylene-oxide) (PPO) based bismaleimide (BMI) with a degree of polymerization (DP) = 3 as a cross-linker. Chapter 3 explored the effect of various BMIs which varied in length and structure and the incorporate of hard segments (by adding 1,4 - butanediol to increase the prevalence of hydrogen bonding) on the polymer properties, thermal recyclability and heated induced healing of biobased cross-linked responsive PU networks. Four different bismaleimides where used: 1,1'-(Methylenedi-4,1-phenylene)bismaleimide (MPBMI), PPO-based BMI with DP = 6 (PPOBMI-DP6), PPO-poly(ethylene-oxide)-based BMI with an overall DP = 13 (PPOPEOBMI-DP13) and PPO-based BMI with a DP = 33 (PPOBMI-DP33).

It was generally observed that PUs cross-linked by the different BMIs showed that cross-linking by MPBMI would yield superior mechanical properties compared to aliphatic counterparts. The distinguishment of PU networks cross-linked by the different BMIs was evidenced in the swelling, thermal recyclability and healing ability of PU networks. The introduction of further phase segregation in PU materials by the addition of hard segments would yield cross-linked materials with superior mechanical properties (when compared to linear control counterpart), good thermal recyclability and adhesion. Future efforts should be dedicated to further developing systems containing varying amounts of hard segments for the material applications such as adhesives and coatings.

Chapter 4. Renewable and responsive cross-linked systems based on polyurethane backbones, from clickable biobased bismaleimide architecture

Chapter 1: State of the art – Click chemistry and vegetable oils

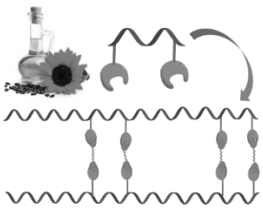

Chapter 2: Synthesis of Furan Oligomer and biobased PU CANs

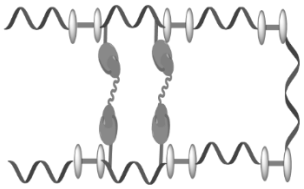

Chapter 3: Further elaboration of biobased PU CANs containing FO

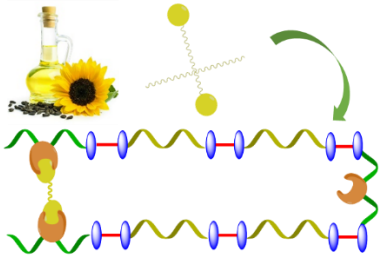

Chapter 4: Synthesis of Methyl oleate bismaleimide and biobased PU CANs

Introduction of Chapter 4

In the previous experimental chapters, we examined and characterized the synthesis of the Furan Oligomer and its incorporation into biobased polyurethane (PU) backbones. The effects of cross-linking these PUs with different bismaleimides (BMIs) as well as incorporating hard segments (HS) in these architectures were also investigated.

In this experimental chapter, we continue along the same strategy of exploring different aspects of biobased PUs cross-linked by Diels-Alder via furan and maleimides moieties. Similarly, biobased PUs are synthesized using a polyester polyol derived from rapeseed oil and hexamethylene diisocyanate, however furan moieties are incorporated into PU backbone via the use of Furan-2,5-diyl-dimethanol (FDM) as a chain extender. FDM is a short and largely available diol, containing a di-substituted furan-ring. The furan moiety can be reacted with maleimide groups via the Diels-Alder reaction. Different PU materials and macromolecular architectures were synthesized by varying the HS content, and cross-linking via different synthesized and conventional bismaleimides was also accomplished. As the HS consists of the chain extender and the diisocyanate, varying the HS content ultimately varies the cross-linking density. Two conventional aromatic and aliphatic BMIs were used with 1'-(Methylene-di-4,1-phenylene) bismaleimide and poly(propylene oxide)-based BMI with a degree of polymerization of 3. In the frame of this study, an additional and original biobased bismaleimide derived from methyl oleate, denoted methyl oleate bismaleimide (MOBMI) was fully synthesized and then used. Corresponding properties were compared to the conventional BMIs. MOBMI was synthesized via a three-step reaction pathway. MO was first epoxidized, followed by a ring-opening reaction by 1, 4-butanediol and lastly 6-maleimidohexanoic acid was used in the esterification reaction of two newly accessible hydroxyl groups. Contrary to the previous studies presented in the last chapters, we particularly examined the reversible cross-linking taking place in the HS of PUs. Different behaviors such as the physical, mechanical and self-repair properties of these different materials were studied.

Renewable and responsive cross-linked systems based on polyurethane backbones, from clickable biobased bismaleimide architecture.

Khantutta-Kim Tremblay-Parrado[1], Clement Bordin[1], Samuel Nicholls[1], Luc Avérous*,[1]

(1) BioTeam/ICPEES-ECPM, UMR CNRS 7515, Université de Strasbourg, 25 rue Becquerel, 67087 Strasbourg Cedex 2, France

(*) Corresponding author: luc.averous@unistra.fr

1. Abstract

A new biobased bismaleimide architecture from methyl oleate, consisting of an aliphatic branched structure, denoted methyl oleate bismaleimide (MOBMI), was synthesized and fully characterized. MOBMI was used as a cross-linking agent to obtain networks using linear biobased furan bearing PUs via the Diels-Alder reaction, and compared with more conventional aromatic or aliphatic bismaleimides (BMIs). These networks can be defined as dissociative covalent adaptable networks (CANs). Different linear biobased PUs were synthesized using rapeseed-based polyol, hexamethylene diisocyanate and furan-2,5-diyl-dimethanol as a chain extender. Furan content was controlled by varying the hard segment content. Compared to conventional BMIs, MOBMI as biobased cross-linker impacts particularly the materials performance and the mechanical properties, with e.g. an increase of the elasticity. MOBMI also yields most consistent advanced properties in terms of thermal recyclability and self-healing.

Keywords: Renewable Resources, Methyl Oleate, Biobased polymers, Polyurethane, Diels-Alder-Cycloaddition, Reversible network

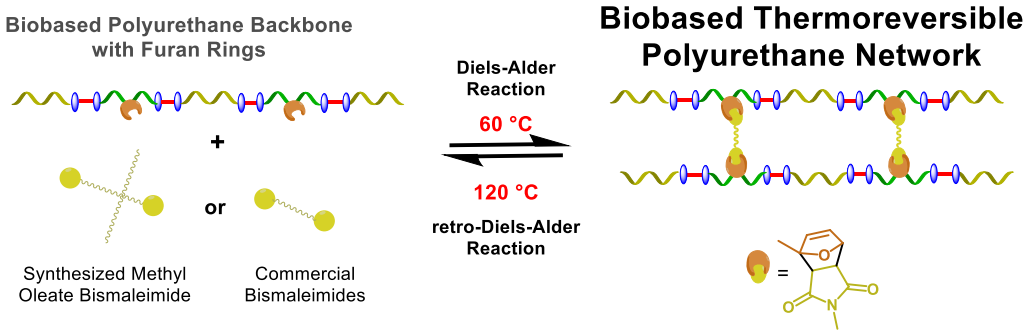

2. Introduction

Polymer science has been established as a distinct field of organic chemistry for over 100 years (Staudinger 1920; Frey and Johann 2020). Since that era, the invention of plastics has drastically changed our daily lives. However, most plastics are based on synthetic macromolecules that originate from non-renewable petroleum resources (Bioplastics 2019). Recently, the worldwide polymer industry has performed considerable progress to ensure the development of sustainable polymers with lower environmental impact, using renewable feed-stocks. Nevertheless, continued progress for these materials to contain advanced materials with properties such as a controlled end-of–life to improved waste management is still required.

Renewable feed-stocks are very diverse such as vegetable oils, woods, sugars and polysaccharides from annual cultures. Plant oils are of particular interest as their innate chemical architectures allow for a vast panel of potential chemical modifications (Ronda et al. 2011). They are also of interest from an industrial perspective, as they highly accessible at rather low production cost with low toxicity (Lligadas et al. 2013). Vegetable oils as well as their fatty acid derivatives have been widely used for the synthesis of polymers such as polyesters (Pan, Sengupta, and Webster 2011; Duarte et al. 2020), polyamides (Hablot et al. 2010; Türünç et al. 2012), epoxy resins (Tan and Chow 2010) and quite prominently polyurethanes (PUs) (Hablot et al. 2008; Bueno-Ferrer, Hablot, Perrin-Sarazin, et al. 2012; Desroches et al. 2012; Pfister, Xia, and Larock 2011).

PUs are a leading polymer family, with their production ranked 6th amongst all polymers (Carré et al. 2019). Due to their wide structural variability, PUs are used for applications such as e.g., the building, transportation and furniture industries (Haponiuk and Formela 2017). Although, the use of plant oils for the synthesis biobased PUs is on the raise (Miao et al. 2014), limited research has exploited these biobased structures to develop advanced materials, with for instance, dynamic and adaptable materials with high recyclability and extended lifetimes.

In the last 20 years, the introduction of dynamic cross-links in polymers has developed a new generation of polymer materials, which can be reprocessed like thermoplastics, all the while maintaining the benefits of thermosets. This incorporated feature allows for the possibility of advanced properties such as healing, reprocessability and then extended material lifetimes, can

reduce the consumption of energy and resources, as well as reduce waste (Fortman et al. 2018). These networks have been defined as covalent adaptable networks (CANs) (Kloxin et al. 2010) based on dynamic covalent bonds that can assemble and disassemble by “dissociative” or “associative” means when exposed to specific stimuli (Denissen, Winne, and Du Prez 2016). In associative CANs, dynamicity occurs by a substitution reaction between an existing cross-link and a pending reactive group, whereas in dissociative CANs, cross-links are cleaved back into their individual reactive moieties before reforming again. Dissociative CANs have been predominately studied (Gandini et al. 2018; Bergman and Wudl 2008; Sun et al. 2019), more specifically those cross-linked via Diels-Alder (DA) adducts formed between furan and maleimide moieties. The DA reaction between furan and maleimide functions is defined as a click cycloaddition reaction and occurs at modest temperatures (below 90 °C), whereas the retro-DA (r-DA) reaction, occurs between 110 and 130 °C (Chen et al. 2002). Although there have been increasing reports of biobased CANs, associative (Dhers, Vantomme, and Avérous 2019) and dissociative alike (Duval et al. 2015; Buono et al. 2017; Duval et al. 2017; García-Astrain and Avérous 2018; Yoshie, Yoshida, and Matsuoka 2019; Gandini et al. 2018), limited research has explored the use of the thermoreversible DA in biobased cross-linked PUs (Tremblay-Parrado and Avérous 2019; Hu, Chen, and Torkelson 2019; Zhang, Michel Jr, and Co 2019).

The aim of this study is to explore reversible cross-linked PUs based on vegetable oils using thermal reversible furan-maleimide DA reaction, with a particular interest in studying the changeability of cross-links localised on hard segments and the use of original and biobased bismaleimide. As depicted in Scheme 4.1, furan-2,5-diyl-dimethanol (FDM) is used as furan bearing chain extender incorporated into the linear polymer backbone and further cross-linked with the use of different bismaleimides (BMIs). In this frame, we report the synthesis of a new methyl oleate based BMI which is compared to aromatic and aliphatic fossil-based BMIs. The corresponding materials were synthesized with varying furan contents and different cross-linkers. They are studied for advanced properties such as thermal reprocessability and self-healing ability.

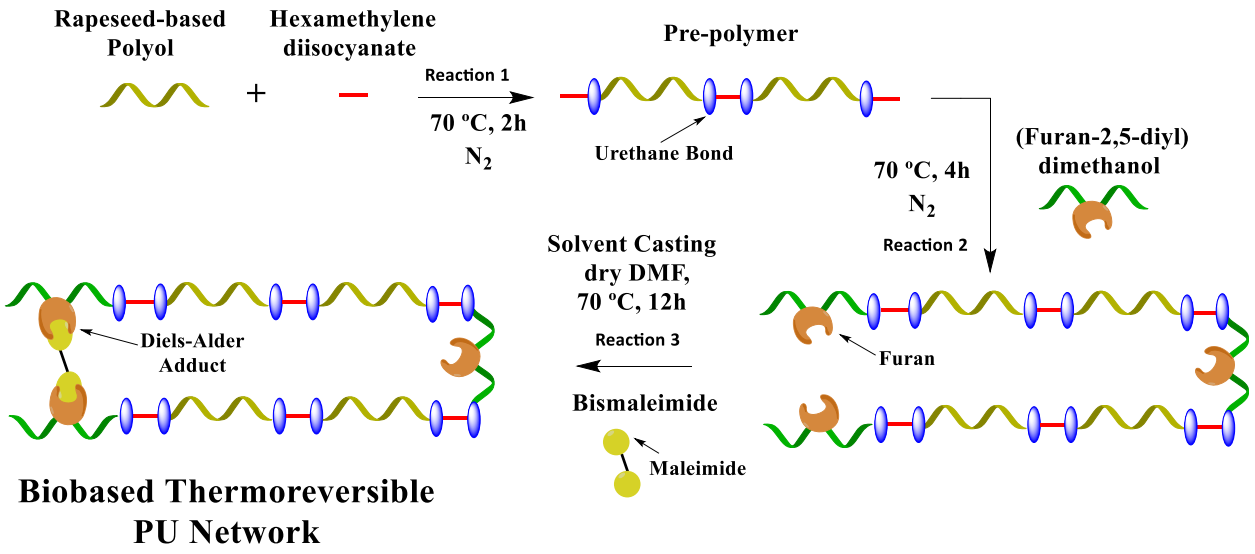

Scheme 4.1 – Illustration of the general synthesis of biobased thermoreversible PU-based systems using furan-2, 5-diyl- dimethanol and different BMIs.

3. Experimental Section

3.1. Reagents and materials

Methyl Oleate (MO) from sunflower oil was kindly supplied by ITERG (France). It is a fatty acid with an acid value of 0.34 mg KOH/g and iodine value of 77 g I_2 / 100 g. Biobased polyester polyol (purchased from Oleon-France) was derived from dimeric fatty acids from rapeseed oil with purity greater than 98% and weight average molar mass (M_w) around 3 000 g/mol. Hydroxyl and acid values were 33.7 and 0.253 mg/g KOH, respectively. 2-chloro-4,4,5,5-tetramethyl-1,3,2-dioxaphospholane (CL-TDP, 95%), and 6-maleimidohexanoic acid (6-MHA, 95%), hydrogen peroxide (H_2O_2, 30% *w/v* aqueous solution), chromium (III) acetylacetonate (99.99%), [D_6]dimethyl sulfoxide (DMSO, 100%, 99.96% atom D), chloroform-d ($CDCl_3$, 100%, 99.96% atom D), amberlyst 15, 1,4-butanediol (BDO, 98%), oxalyl chloride (99%) and cholesterol (>99%) were purchased from Sigma Aldrich. 1,1'-(Methylene di-4,1-phenylene)bismaleimide (95%, MPBMI) were purchased from Alfa Aesar. N,N-dimethylformamide (DMF, 99.8%), chloroform (99.8% stabilized with amylene), glacial acetic acid (GAA, >99%), and ethyl acetate (EA, 95%) were purchased from Fisher Scientific. Amberlite IR-120 H from Fluka Chemicals. Poly(propylene oxide)-based bismaleimide (PPO BMI) with DP_n = 3 was obtained from Specific Polymers (Castries, France). 2,3,4,5,6-pentafluorobenzaldehyde (PFB, 98%) and (Furan-2,5-diyl)dimethanol (FDM,

97%) was purchased from fluorochem. Reagents and solvents from commercial suppliers were used without additional purification.

3.2. Syntheses and material preparations

3.2.1. Epoxidation of methyl-oleate from sunflower oil

The epoxidation of methyl oleate (MO) was conducted by the in-situ formation of peracetic acid from glacial acetic acid and H_2O_2, and was adapted from Arbenz *et al* (Arbenz, Perrin, and Avérous 2017). In a two-necked round bottom flask, equipped with a magnetic stirrer and a dropping funnel, MO (1 mol eq of unsaturations), amberlite IR-120 H (25 wt% of MO), glacial acetic acid (0.5 mol eq) was inserted into the flask and dissolved at 0.5 ml/g of MO in toluene. The solution was stirred to 70 °C and then 1.5 mol eq. of H_2O_2 was added dropwise. The mixture was stirred at 70°C for 7 hours. The solution was diluted in ethyl acetate. The amberlite IR-120 H was filtered off and the solution was washed with distilled water until a neutral pH was attained. The organic phase was dried with anhydrous sodium sulphate and then filtered. The solvent was evaporated under reduced pressure. Methyl 8-(3-octyloxiran-2-yl)octanoate (MOO) was dried under vacuum overnight, at 50 °C. The reaction product, Methyl 8-(3-octyloxiran-2-yl)octanoate (MOO), was a clear light yellow oil.

Methyl 8-(3-octyloxiran-2-yl)octanoate (MOO) - ^{1}H NMR (400 MHz, $CDCl_3$): δ = 3.63 (s, 3H, (C=O)OC*H*$_3$), 2.9 (m, 2H, C*H*OC*H*), 2.3 (t, 2H, C*H*$_2$C(=O)), 1.6 (m, 2H, C*H*$_2$CH$_2$C(=O)), 1.3-1.0 (m, 24H, aliphatic CH_2), 0.9 (t, 3H, C*H*$_3$). ^{13}C NMR (400 MHz, $CDCl_3$): δ: 174 (*C*=O), 57.2(O*C*H$_3$), 57.2 (H*C*-O-*C*H), 51.4 (O*C*H$_3$), 34.0 (*C*H$_2$–C(=O)), 31.9-22.7 (aliphatic *C*H$_2$), 14.1 (*C*H$_3$)

3.2.2. Ring-opening by butane-1, 4-diol of methyl 8-(3-octyloxiran-2-yl)octanoate

In a round bottom flask, equipped with a magnetic stirrer, MOO (1 mol eq of epoxy), amberlyst 15 (4 wt% of MOO), butane-1,4-diol (10 mol eq) was introduced. The mixture was stirred at 75°C for 10 hours. The solution was diluted in ethyl acetate and the amberlyst 15 was filtered off. The solution was washed with distilled water until a neutral pH was attained and the excess of BDO was removed. The organic phase was dried with anhydrous sodium sulphate, and then filtered. The solvent was evaporated under reduced pressure. Methyl 10-hydroxy-9-(4-

hydroxybutoxy)octadecanoate (MO-Diol) was dried under vacuum overnight, at 50 °C. The reaction product, MO-Diol, was a clear light yellow oil.

Methyl 10-hydroxy-9-(4-hydroxybutoxy)octadecanoate (MO Diol) - ^{1}H NMR (400 MHz, $CDCl_3$) δ: 3.63 (s, 3H, (C=O)OC*H*$_3$), 3.65 – 3.45 (m, 1H, C*H*OH) and (m, 2H, C*H*$_2$OH), 3.47 (t, 2H, C*H*$_2$OCH), 3.10 (q, 1H, CH_2OCH), 2.3 (t, 2H, C*H*$_2$C(=O)), 1.6 (m, 2H, C*H*$_2$CH$_2$C(=O)), 1.3-1.0 (m, 28H, aliphatic C*H*$_2$), 0.9 (t, 3H, C*H*$_3$). ^{13}C NMR (400 MHz, $CDCl_3$) δ: 174 (C=O), 83.0 (CH_2CHOH), 72.7 (*C*HOH), 70.5 (CH_2CHOH), 51.4 (OCH_3), 34.0 (CH_2–C(=O)), 31.9-22.7 (aliphatic CH_2), 14.1 (CH_3).

3.2.3. Chlorination of 6-maleimidoheaxnoic acid

6-MHA (1 mol eq) was placed in a two-necked flame-dried round-bottomed flask flushed with argon and charged with a magnetic stirring bar. Anhydrous ethyl acetate was then added and the solution cooled down to 0°C under a flow of nitrogen. An excess of oxalyl chloride (1.5 mol eq) was then added dropwise at 0°C (15 min) and finally heated at 50°C for 3h. The excess of oxalyl chloride and solvent was evaporated under vacuum. The product, 6-maleimidhexanoyl chloride (6-MHC) was obtained as a low-melting yellow solid and used without any further purification.

6-maleimidohexanoyl chloride (6-MHC) - ^{1}H NMR (400 MHz, $CDCl_3$, δ (ppm)): 6.69 (s, 2H, C*H*-ring), 3.56 (t, 2H, C*H*$_2$-N), 2.89 (t, 2H, C*H*$_2$(C=O)Cl), 1.71 (m, 2H, C*H*$_2$CH$_2$(C=O)Cl), 1.60 (m, 2H, C*H*$_2$CH$_2$-N), 1.3 ppm (m, 2H, C*H*$_2$CH$_2$CH$_2$-N); ^{13}CNMR (400 MHz, $CDCl_3$) δ: 174 ((*C*=O)Cl), 170 (*C*O-ring), 135 (*C*H-ring), 46.7 (CH_2(C=O)Cl), 39.0 (CH_2N), 29.3–25.0 (aliphatic chain carbons).

3.2.4. Synthesis of MOBMI

MO Diol was esterified with 1.2 equivalents of 6-MHC with respect to the amount of total hydroxy groups. In agreement with different green chemistry principles, the reaction was catalyst-free at 65°C. $CHCl_3$ was added to homogenize the reaction mixture. At the end of the reaction, a brown viscous product was obtained. Methanol was added to quench the unreacted 6-MHC, and the mixture was left stirring for an additional 30 min. The solvents were then evaporated under vacuum and the resultant MOBMI products finally dried under high vacuum for 24 h

Methyl Oleate Bismaleimide (MOBMI) - ^{1}H NMR ($CDCl_3$, 400MHz) δ : 6.69 (s, 4H, C*H*-ring), 4.61 (m, 1H, C*H*O(C=O)), 4.06 (t, 2H, (C=O)OC*H*$_2$), 3.63 (s, 3H, (C=O)OC*H*$_3$), 3.56 (t, 4H, C*H*$_2$-N), 3.47 (t,

2H, C*H*$_2$OCH),), 3.25 (q, 1H, CH$_2$OC*H*), 2.30 (m, 6H, CH$_2$(C=O)O), 1.20-1.80 (multi, 40H, CH$_2$), 0.9 (t, 3H,CH$_3$); ^{13}CNMR (400 MHz, CDCl$_3$) δ: 174 (CH$_2$(*C*=O)), 171 (*C*O-ring), 134 (*C*H-ring), 51.4 (OCH$_3$), 39.0 (*C*H$_2$N), 34.0 (*C*H$_2$–C(=O)), 31.9-22.7 (aliphatic CH$_2$), 14.1 (*C*H$_3$).

3.2.5. Study of the DA reaction between MOBMI and FDM

MOBMI (200 mg) was dissolved in [D$_6$]DMSO (2 mL) in a 10 mL round bottom flask. Furan-2,5-diyl-dimethanol (FDM) was added to obtain a furan / maleimide ratio of 1:1 (mol/mol). The solution was placed in an oil bath regulated to 65 °C and samples (200 µL) were taken at regular intervals over 4 days. The samples were further diluted to 650 µL and analyzed by ^{1}H NMR to determine the reaction conversion and *endo/exo* ratio of the DA adducts.

3.2.6. Synthesis of PUs based on FDM

All glassware and reactants were previously dried. PUs were synthesized by a two-step polymerization process. Three different kinds of PUs films were prepared by a two-step synthesis process by varying the content of hard segments (HS) in wt%, based on di-isocyanate and FDM, by 5, 10, and 20%. First, for the pre-polymerization step, in a three-necked round bottom flask flushed with nitrogen, the biobased rapeseed polyester polyol was added to hexamethylene di-isocyanate (HDI) and the mixture was mechanically stirred at 70 °C for approximately 2h, until appropriate NCO value was attained.

During the synthesis, aliquots were extracted to determine the NCO content to control and follow the NCO consumption during the reaction. A specific method has been performed to determine isocyanate content by reaction with on equivalent of *N*-dibutylamine, to give NCO content (in wt%). Prepolymer sample (≈ 1.2 g) was diluted in a standard solution (20 mL) of dibutylamine 0.2M in THF for the reaction with the unreacted diisocyanate. The amine excess was back-titrated with a 0.5 aqueous solution of HCl. NCO content (wt%) was determined using Equation (1):

$$\%NCO = \frac{(V_{blank} - V_s) * 42 * 0.1}{m_s} \quad (1)$$

in which V_{blank} (mL) is the HCl solution volume required for a blank titration of the dibutylamine solution, while V_s is the volume required for the prepolymer titration and m_s is the prepolymer weight. This result was used for the addition for the precise amount of FDM. The appropriate

amount of FDM is dissolved in anhydrous DMF (1 ml/g FDM) and added to the above mentioned reaction system and stirred for 3 h. The ratio –NCO/-OH functional groups were fixed to 1.05 in all cases.

3.2.7. Cross-linking of PUs by each BMI

The PU was dissolved in anhydrous DMF. The respective amount of each bismaleimide was added in a 1:1 furan to maleimide ratio (mol/mol). The reaction mixture was stirred at 70 °C for 12 h to allow for the DA adducts to form. The solution was poured into a polytetrafluoroethylene mold and put into the oven to evaporate the solvent (70 °C, 48 h). Solvent traces were removed under vacuum at 70 °C for 24h. Cross-linked PU systems using MOBMI were labelled PU-HS5-MOBMI, PU-HS10, PU-HS20-MOBMI, respectively. Two additional cross-linked PUs were obtained using linear PU-HS20 with cross-linked with a reference and conventional BMI: MPBMI or PPO BMI, and denoted as PU-HS20-MPBMI or PU-HS20-PPOBMI, respectively.

3.2.8. Study of the reprocessability behavior of PUs

PU films were reprocessed by compression molded in tile mold (10 cm x 10 cm x 1 mm) at 140 °C in LabTech Scientific press hot press. First, the films were cut in several small pieces and placed in the center of the tile and left to undergo a 10 min preheating cycle to soften the material. This was followed by several venting steps and the material was pressed with a constant applied force of 16 MPa between both plates for 15 min. The square materials were then cured at 60 °C in the oven for 48 h and post cured for 24 h at room temperature.

3.2.9. Study of self-healing behavior

The macroscopic self-healing ability of material was analyzed on a dumbbell-shaped sample cut in half and then healed. The dumbbell was cut in the middle and subsequently healed by placing the halves in contact for 1 hour at 120 °C, followed by 60 °C overnight, and then 24 h at room temperature and 50% RH, and then tested by uniaxial tensile tests in order to evaluate the recovery of the integrity of the self-healed dumbbells.

3.3. Methods

3.3.1. Iodine Value

Iodine value (IV) was determined using the Wijs method to quantify the double bond content according to ISO 3961:2018(E)

3.3.2. Hydroxyl Value

Hydroxyl Value (HV) was determined by esterification method using a 1 M solution of phthalic anhydride in pyridine (ASTM 4274-99) for the MO Diol and the biobased polyester polyol. The appropriate mass of sample was dissolved (1.25 g for MO Diol and 7.5 g for the polyester polyol) in 20 mL of phthalic anhydride solution and was heated to 130 °C under reflux for 45 minutes and cooled at room temperature. Pyridine were added (10 ml) from the top of the reflux to collect all reactions products, lastly 20 mL of pyridine and 30 mL of water was added. The solution was titrated with 1 M potassium hydroxide (KOH) solution phenolphthalein solution as indicator. Hydroxyl Value (HV) was determined in mg of KOH.g^{-1}, as described in Equation 2.

$$HV = \frac{((V_{blank} - V_S) * C * 56.1)}{W_S} \quad (2)$$

Where V_{blank} (mL) and V_S (mL) are the volumes of KOH solution required for blank and polyol sample titrations, respectively. C (mol.L^{-1}) is the KOH solution concentration and W_S (g) is the polyol weight.

3.3.3. NMR Spectroscopy

All NMR spectra were recorded on a Bruker Ascend 400 or 500 MHz spectrometer. Sample were dissolved in deuterated chloroform ($CDCl_3$) or deuterated dimethyl sulfoxide ([D_6]DMSO) with contents between 8-10 and 20-30 mg/mL for ^{1}H-NMR and ^{13}C-NMR spectroscopy, respectively. The calibration of ^{1}H- and ^{13}C-NMR spectra was performed using the chloroform peaks at δ = 7.26 and 77.16 ppm, respectively and DMSO peak at δ = 2.50 ppm as references.

^{31}P NMR analysis was performed by 2-chloro-4,4,5,5-tetramethyl-1,3,2-dioxaphospholane as phosphytilating agent. Scans (128) were recorded with a 15 s delay and a spectral width of 80

ppm (180-100 ppm). Cholesterol was used as an internal standard, as described in standard protocols (Spyros 2002).

In the case of quantitative ^{1}H NMR spectroscopic analysis, 20 mg was dissolved in [D_6]DMSO (0.5 mL) for each sample before the addition of a standard solution (100 µL) of pentafluorobenzaldehyde in [D_6]DMSO. 32 scans were collected 10 s delay.

3.3.4. Fourier Transform Spectroscopy (FTIR)

For FTIR spectroscopy of experimental samples, a blank background was performed prior to examining samples (32 scans, resolution 4 cm^{-1}) on a Nicolet 380 spectrometer equipped with an ATR diamond module (FTIR-ATR) in reflection mode.

3.3.5. Thermal Gravimetric Analysis (TGA)

Sample weighing between 1-3 mg were evaluated by TGA (TA Instrument Hi-Res TGA Q5000) at a heating rate of 10 °C min^{-1} from 25 to 700 °C, without oxidative atmosphere, under nitrogen flow rate atmosphere at 25 mL min^{-1}.

3.3.6. Differential Scanning Calorimetry (DSC)

In standard aluminum pans, samples between 1 to 3 mg by weight were examined by DSC (TA Instrument Q200) under nitrogen flow at 50 mL min^{-1}. For cross-linked PUs, a single heating ramp of 10 °C min^{-1} over the same aforementioned temperature range. Non-cross-linked materials were evaluated using a cyclical heating ramp.

3.3.7. Uniaxial Tensile Tests

Uniaxial tensile testing was performed on an Instron model 5567 H, USA at strain rate of 20 mm min^{-1} on dumbbell specimens of approximately 30 X 5 X 1 mm^3. For each synthesized or reprocessed PU, five dumbbell samples were tested.

3.3.8. Swelling and Index and Gel Content Determination

The swelling ratio (SR) for each PU was determined between dried (m_i) and swollen samples (m_s) in DMF according to Equation 3:

$$SR = \frac{m_s - m_i}{m_i} * 100 \ (3)$$

PU samples of approximately 10-20 mg were swollen in 15 mL of solvent over an entire day. Three repetitions were examined for each PU formulation. The insoluble fraction (IF) was determined by drying the swollen sample (m_f) according to Equation 4:

$$IF = \frac{m_f}{m_i} * 100 \ (4)$$

4. Results and Discussion

Analysis of synthesis of MOBMI

The alkene moiety of methyl oleate (MO) was used as the reaction site to yield a MO based BMI as depicted in Scheme 4.2. First, MO underwent an *in-situ* epoxidation with peroxyacetic acid as the oxidizing agent to yield MOO. This type of epoxidation is routinely used on vegetable oils (Petrović et al. 2002). Other pathways for epoxidations using e.g., pre-synthesized oxidizing agents such as meta-chloroperoxybenzoic acid (mCPBA) require large quantities of solvents. Thus, the *in situ* epoxidation method abides more precisely the principles of green chemistry. The FTIR spectrum of MOO (Figure 4.1-b) shows the disappearance of the double bonds at $\tilde{\nu}$ = 3009 cm^{-1} and the appearance of the C-H bending associated to appearance of epoxides at $\tilde{\nu}$ = 825 cm^{-1}. By ^{1}H NMR spectroscopic analysis (Figure 4.2-b) the structure is confirmed with the disappearance of the vinyl and allyl protons at δ = 5.35 and 2.0 ppm respectively, and by the appearance of the epoxide and protons alpha to the epoxides at δ = 2.90 and 1.45 ppm respectively. The results of the ^{13}C NMR spectroscopic analysis of MOO agreed with the assigned structure as depicted in Figure S4.9 in supporting information (SI).

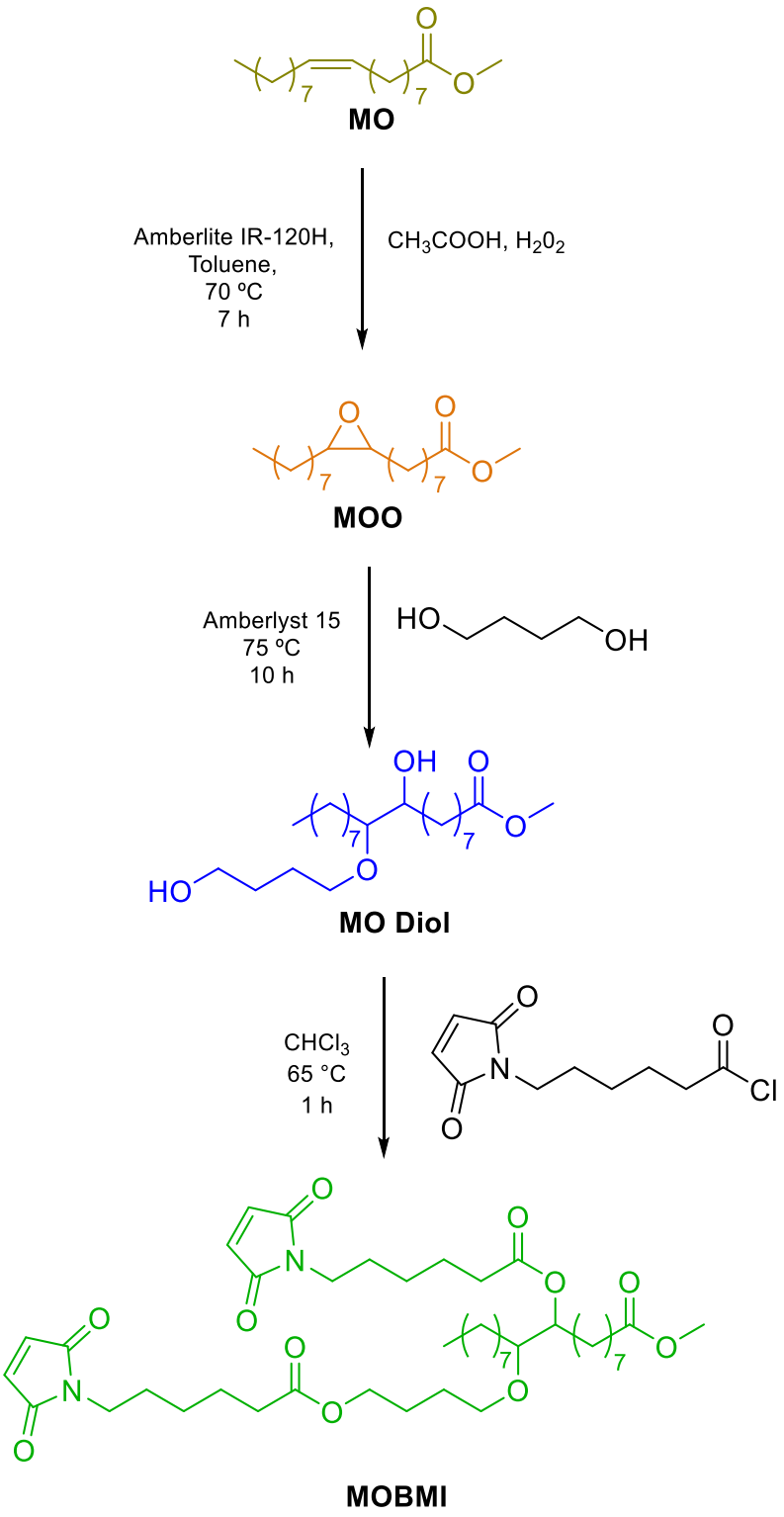

Scheme 4.2 – Global reaction pathway of MOBMI.

Thereafter, MOO underwent a ring opening reaction with BDO to give MO Diol as the main product along with a diester diol as a side product (chemical structure in Figure S4.10 in SI). This diester as a side product is apparent by size exclusion chromatograms (SEC) as depicted in Figure S4.11 in SI. The protocol developed by Palaskar *et al*. was slightly altered and improved (Palaskar et al. 2012). The reaction was for instance limited to 10 h compared to 20 h, since the transesterication between the ester moiety and BDO largely took place after 10 h**.** Figure S4.12 illustrates in SI that at 10 h, all epoxy moieties have been opened by BDO and the transesterication reaction begins to take place. Furthermore, the purification step for the removal of BDO consisted solely of water-based washing as oppose to vacuum distillation to avoid further side reactions. The HV was determined by two methods: a chemical esterification titration method using phthalic anhydride and quantitative ^{31}P NMR which gave similar and reproducible results (Figure S4.13 and Table S4.3). HV of MO Diol is 223 mg KOH/ g. This is relatively close to the theoretical value of 258 mg KOH/g if only the MO Diol product was achieved without diester side product. The FTIR spectrum of MO Diol (Figure 4.1-c) shows the disappearance of C-H bending associated to the epoxides at $\tilde{\nu}$ = 825 cm^{-1}, the appearance of a broad band between $\tilde{\nu}$ = 3600 to 3100 cm^{-1} corresponding to the hydroxyl groups, as well as the appearance of C-O stretch of newly formed alcohols. The ^{1}H NMR spectrum of MO Diol along with proton assignments is presented Figure 4.2-c. The chemical structure of MO-Diol is confirmed by the appearance of peaks at δ = 3.65 ppm (e) (CH_2OH), 3.60 ppm (h) (CH-OH), 3.47 ppm (f) (CH_2OCH) and at 3.10 ppm (g) the proton adjacent to ether bond. The results of the analysis of ^{13}C NMR of MO Diol agreed with the assigned chemical structure as depicted in Figure S4.9 in SI.

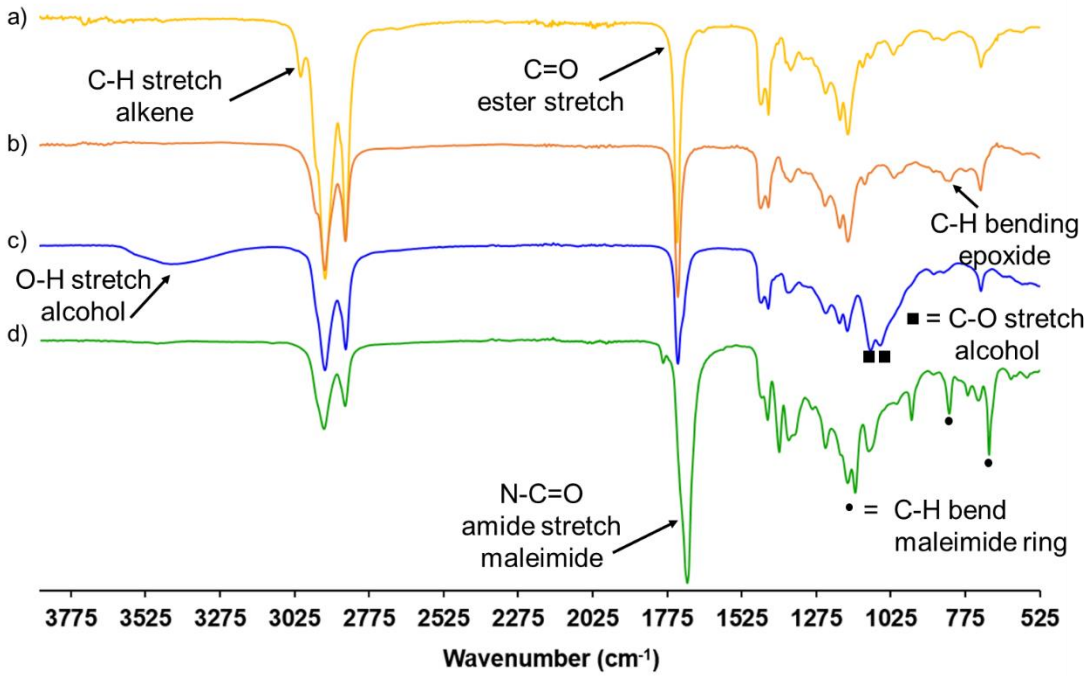

Figure 4.1 – FTIR spectra (a) MO, (b) MOO, (c) MO Diol, and (d) MOBMI with the assignations of the main peaks.

MOBMI was finally synthesized by the esterification of the hydroxyl groups of MO Diol by 6-MHA. Similarly to previously reported work (Buono et al. 2017; Duval et al. 2015), 6-MHA was transformed into an acyl chloride derivative, 6-MHC, to increase the reactivity of the reaction (Scheme S4.3 in SI). The success of this transformation reaction is attested by the ^{1}H NMR spectra of 6-MHA and 6-MHC and corresponding proton assignments found in Figure S4.14 in SI. The derivatization of MO Diol was then conducted by using 1.2 of 6-MHC under catalyst free conditions to yield MOBMI products. The success of the reaction is evidenced by FTIR (Figure 4.1-d), ^{1}H NMR (Figure 4.2-d), ^{13}C NMR (Figure S4.9 in SI) and quantitative ^{1}H NMR (Figure S4.15 in SI) to determine the maleimide content of MOBMI reported to be 1.83 mmol/g. The FTIR spectrum of MOBMI evidences the disappearance of a broad band between $\tilde{\nu}$ = 3600 to 3100 cm^{-1} corresponding to the hydroxyl groups and C-O stretch of alcohols. Furthermore, the N-C=O amide stretch of the maleimide ring is detected at $\tilde{\nu}$ = 1701 cm^{-1}, as well as the C-H bend associated to the maleimide ring at $\tilde{\nu}$ = 826 cm^{-1} and 696 cm^{-1}. The ^{1}H NMR spectrum of MOBMI was analyzed and evidenced by appearance a strong signal at δ = 6.7 ppm belonging to the maleimide ring double bond protons. Quantitative ^{1}H NMR (in [D_6]DMSO) was used to determine the maleimide content using the C-H bending signal at δ = 7.1 ppm as this signal is free from

overlap from other MO Diol signals. This calculation is further depicted by Figure S4.15 and Table S4.4 in SI. The SECs for the raw material and all reactions steps are presented in Figure S4.11 in SI. The molar mass distribution are progressively shifted towards higher molar masses as a result of success reaction pathway.

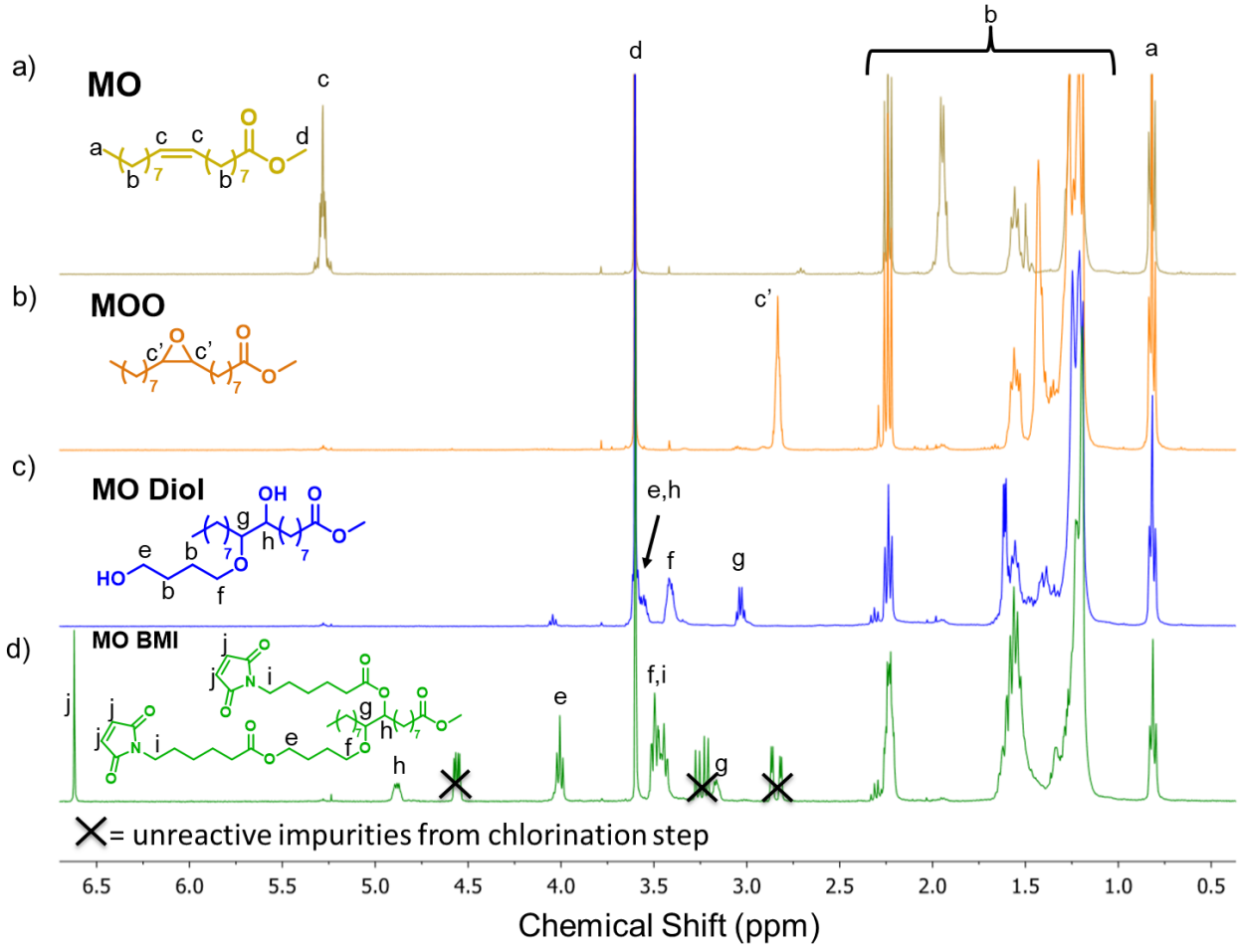

Figure 4.2 – ^{1}H NMR spectra of (a) MO, (b) MOO, (c) MO Diol, and (d) MOBMI, with the assignations of the main signals and the corresponding chemical structures.

In order to confirm and study the DA adduct formation by ^{1}H NMR of MOBMI when exposed to furan moieties, MOBMI was reacted with FDM in DMSO at 65 °C (Figure 4.3-a). As depicted in Figure 4.3-b, the ^{1}H NMR spectrum and proton assignment confirms the formation of the DA adduct. Proton assignment was confirmed using the ^{1}H NMR of initial reactional entities and compared to the literature (Froidevaux et al. 2015). To quantify the conversion, proton signals, f_1 (in the furan) and f_1' (in the adduct) were used as they are free from overlap with other signals

(Figure 4.3-b). The conversion was calculated by Equation 5 for proton set f_1 and f_1' as follows; where Int_{f1} and $Int_{f1'}$ represent the integral values of their respective protons:

$$X\ (\%) = \frac{Int_{f_1'}}{Int_{f_1} + Int_{f_1'}} * 100 \quad (5)$$

In Figure 4.3-c, the trend of the conversion with respect to time at 65 °C is shown. As similarly reported in literature, an equilibrium conversion of 88% was obtained after 78 hours of reaction time. Moreover, proton signals, $f_{1'}$ were used to assess the presence of the two diastereomers of the DA adduct (endo and exo) with respect to time (Figure 4.3-b), as the chemical shift differs for each diastereomer. The kinetically favored endo adduct is first formed at 80%. An equilibrium between the two diastereomers starts after 78 hours (50 w.t. %)

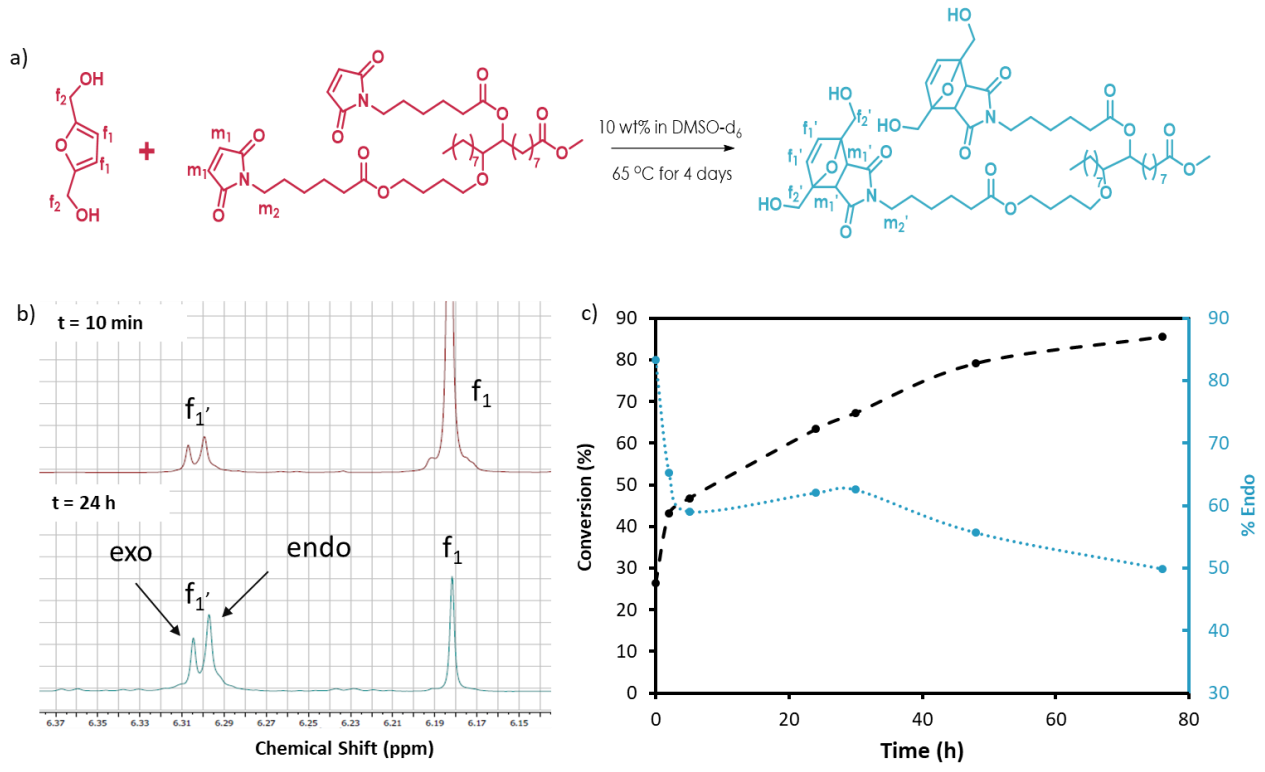

Figure 4.3 – (a) Reaction scheme between FDM and MOBMI, (b) ^{1}H NMR of spectra of mixture of FDM and MOBMI after 10 min and 24 h, and (c) conversion and percentage of endo structure with respect to time and 65 °C.

Cross-linked biobased PUs containing thermoreversible DA adducts were synthesized. Scheme 4.1 depicts the synthesis of (i) the control systems (linear PUs – reaction 1 and 2) and (ii) the cross-linked PUs (reactions 1 to 3). Different PUs were obtained by varying the HS % in the PU structure.

The HS % is the mass of HDI and FDM, with respect to the mass of the global structure. The HS % in the PU systems was varied either as 5,10 or 20%. The nomenclature of all PU systems prepared is summarized in Table 4.1. The chemical structure of these both BMIs are illustrated in Figure 4.4

Table 4.1 – Linear PU (control) and cross-linked systems: nomenclature and corresponding formulations.

PU system	Type of system	HS content [%]	Type of BMI cross-linker
PU-HS5	linear	5	N/A
PU-HS10	linear	10	N/A
PU-HS20	linear	20	N/A
PU-HS5-MOBMI	cross-link	5	MO BMI
PU-HS10-MOBMI	cross-link	10	MO BMI
PU-HS20-MOBMI	cross-link	20	MO BMI
PU-HS20-MPBMI	cross-link	20	MP BMI
PU-HS20-PPOBMI	cross-link	20	PPO BMI (DP=3)

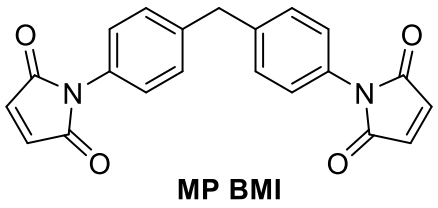

MP BMI

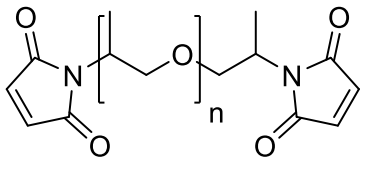

n = 3

PPO BMI

Figure 4.4 – Chemical structure of both conventional maleimide-terminated BMIs used as cross-linkers.

All PU networks after post curing (linear and cross-linked) were insoluble in conventional solvents ($CHCl_3$, DMSO, THF, DMF) and were thus examined by FTIR. In Figure 4.5, a comparison of the FTIR spectra of PU-HS5, PU-HS10, PU-HS20, polyester polyol and FDM is presented. In the spectra of the three linear control PUs (Figure 4.5 a to c), no peak was found at $\tilde{\nu}$ = 2270 cm^{-1} (NCO stretching band) and the disappearance the hydroxyl stretches (approximately at $\tilde{\nu}$ = 3600 to 3025 cm^{-1}) associated to the hydroxyls of polyester polyol and FDM is observed. Furthermore, the FTIR spectra of PU-HS5, PU-HS10, and PU-HS20 could be used to highlight the main structural differences between them. As expected, the main variations are related to the increasing content of HS %, leading to higher concentration urethane groups (-NH-C=O-O-). This is highlighted by the increasing vibrations of –NH stretching and bending ($\tilde{\nu}$ = 3335 and 1550 cm^{-1}, respectively) as well as the C=O stretching from the urethane group ($\tilde{\nu}$ = 1680 cm^{-1}) from PU-HS5 to PU-HS20.

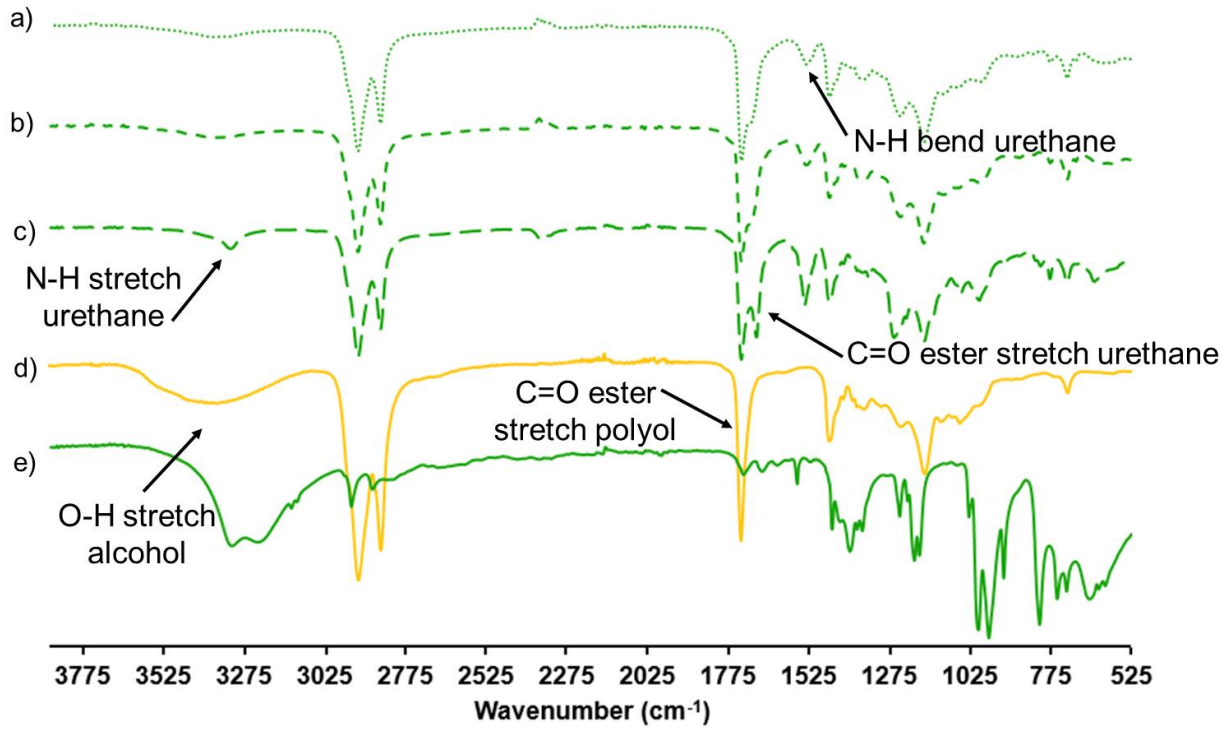

Figure 4.5 – FTIR spectra of, from top to bottom, (a) PU-HS5, (b) PU-HS10, (c) PU-HS20, (d) rapeseed-based polyol, and (e) FDM.

The FTIR spectra of all cross-linked PU networks compared to their control PU and bismaleimides is displayed in Figure 4.6 and Figure S4.16. Figure 4.6 displays the FTIR spectra of PU-HS20 (Figure 4.6-a) compared the cross-linked PU networks: PU-HS20-PPOBMI (Figure 4.6-b), PU-HS20-MPBMI

(Figure 4.6-d) and PU-HS20-MOBMI (Figure 4.6-f) with their respective BMIs, PPO BMI (Figure 4.6-c), MP BMI (Figure 4.6-e) and MOBMI (Figure 4.6-g). The FTIR spectrum of MP BMI distinguishes itself by the C-C stretches of the aromatic ring at $\tilde{\nu}$ = 1500 cm^{-1} (Figure 4.6-e). It is observed that in PS-HS20-PPOBMI and PU-HS20-MPBMI lose the prevalence of the peaks associated to the HS concentration (N-H stretch, bend and urethane C=O ($\tilde{\nu}$ = 1550 cm^{-1}). In Figure S4.16 it can be observed that for each PU network cross-linked with MOBMI, PU-HS5-MOBMI (Figure S4.16-b), PU-HS10-MOBMI (Figure S4.16-d) and PU-HS20-MOBMI (Figure S4.16-f) the carbonyl stretch corresponding to the urethane of the control PU-HS5 (Figure S4.16-a), PU-HS10 (Figure S4.16-c) and PU-HS20 (Figure S4.16-e) becomes masked by the carbonyl stretch of the amide of the maleimide. Furthermore, the N-H stretch of the urethane at ($\tilde{\nu}$ = 3335 cm^{-1}) becomes slightly less prevalent, most specifically in the case PU-HS20-MOBMI. Moreover, as all PU cross-linked networks are cross-linked via DA reaction, the disappearance of the C-H bending of maleimide ring ($\tilde{\nu}$ = 826 and 692 cm^{-1}) is observed.

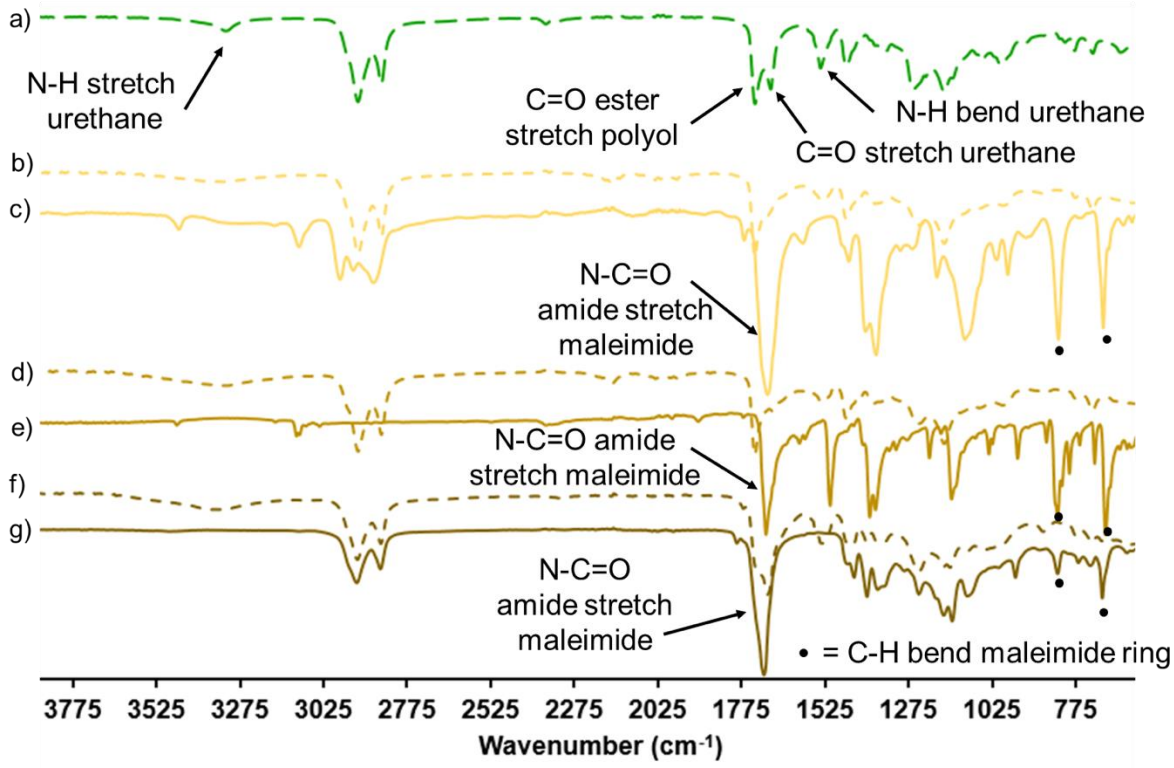

Figure 4.6 – FTIR spectra of, from top to bottom, (a) PU-HS20, (b) PU-HS20-PPOBMI, (c) PPOBMI, (d) PU-HS20-MPBMI, (e) MPBMI, (f) PU-HS20-MOBMI, and (g) MOBMI.

TGA was used to evaluate the thermal stability of PU materials. Detailed TGA results can be found in Figure S4.18 in SI. In Table 4.2, the initial thermal degradation ($T_{5\%}$) is reported. The $T_{5\%}$ for all materials is considerably above the r-DA reaction of approximately 120 °C, allowing for the r-DA reaction to take place without any significant thermal degradation of materials. Control PUs (PU-HS5, PU-HS10 and PU-HS20) exhibit decreased $T_{5\%}$ with increasing HS ratio. As described in a previous study of our group, for equivalent biobased PU materials (Bueno-Ferrer, Hablot, Garrigós, et al. 2012), initial degradation takes place in the HS domain and the thermal degradation is directly linked to the HS content. When comparing control PUs with their respective cross-linked materials, the $T_{5\%}$ decreased for cross-linked entities. Furthermore, when comparing $T_{5\%}$ of control PU-HS20 to cross-linked PU materials, the lowest $T_{5\%}$ reported is that of PU-HS20-MOBMI whereas PU-HS20-PPOBMI and PU-HS20-MPBMI were observed to be 30 °C higher. This can be linked to the long-chain aliphatic nature of MOBMI as well as traces of reagents from synthesis of MOBMI. In contrast, PU material PU-HS20-MPBMI exhibits the highest $T_{5\%}$ in comparison to other cross-linked PU-HS20 materials and this could be related to the aromaticity of the cross-linker.

The glass transition temperatures (T_g) were determined by DSC. To avoid degradation, the T_g of cross-linked PU materials were recorded using a single heating ramp from -80 to 175 °C as reported in Table 4.2. Detailed DSC thermograms can be found in SI, Figure S4.19. The T_g of all PU materials were observed in a very small window, from -51 to -48 °C. As a general trend, the T_g of cross-linked materials increased (due to cross-linking) when compared to their control counterpart with the exception of PU-HS5-MOBMI. Endothermic peaks corresponding to the r-DA reaction did not seem to appear clearly in any cross-linked PU due the consequently predominant T_g related to the HS domains and could not be studied.

Table 4.2 – Main characterizations of synthesized biobased PUs.

PU system	TGA $T_{5\%}$ [° C]	DSC T_g [° C]	Young's modulus [MPa]	σ[a] [MPa]	ε[b] [%]	SR[c] in DMF [%]	IF[d] [%]
PU-HS5	348	-50	2.33 ± 0.21	0.55 ±0.01	91 ± 14	40 ± 3	97.6 ± 0.1
PU-HS10	322	-50	2.73 ± 0.15	0.88 ± 0.01	155 ± 4	167 ± 18	97.5 ± 4.4
PU-HS20	281	-49	5.64 ±1.12	1.73 ± 0.08	74 ± 8	137 ± 6	93.5 ± 1.0
PU-HS5-MOBMI	339	-51	1.80 ± 0.12	0.57 ± 0.02	102 ± 13	42 ± 1	96.4 ± 0.1
PU-HS10-MOBMI	298	-48	3.80 ±0.05	0.35 ± 0.01	299 ± 15	105 ± 2	91.2 ± 1.6
PU-HS20-MOBMI	230	-49	0.17 ±0.01	0.15 ± 0.01	114 ± 9	116 ± 5	84.8 ± 3.0
PU-HS20-PPOBMI	261	-48	6.20 ±1.03	2.28 ± 0.21	114 ± 9	70 ± 11	97.1 ± 1.3
PU-HS20-MPBMI	268	-49	13.4 ±1.81	2.07 ± 0.06	97 ± 12	69 ± 2	96.1 ± 0.6

[a] Tensile strength. [b] Elongation. [c] SR=swelling ratio. [d] IF=insoluble fraction.

The mechanical properties of all PUs were evaluated at room temperature by uniaxial tensile tests. They were reported in Table 4.2 and Figure S4.17. For control PUs, results indicated that increased HS content led to increased tensile strength and decreased elongation, with the exception of PU-HS5, which exhibited a predictable lower tensile strength but also surprisingly lower elongation at break. As expected, the Young's modulus increased due the increasing HS content of the control PUs materials. For PU materials which are cross-linked by MOBMI (Figure S4.17-a), the building block MOBMI tends to have a softening effect compared to the others systems. These PU materials presents an increased elongation break and a strong decrease in Young's Modulus and tensile strength. This behavior was most apparent in PU-HS10-MOBMI and PU-HS20-MOBMI. This can be explained by the aliphatic and branched long chains of MOBMI. Furthermore, as MOBMI was synthesized with an excess of 6-MHC, the neutralized 6-MHC by methanol gave the corresponding methyl ester, which certainly impacts on the softness of the materials. Nevertheless, the cross-linking does not counter this softening effect due to MOBMI architecture, nor that of remnant reagents. In contrast, PU-HS20 cross-linked by conventional BMIs, PPOBMI and MPBMI, led to the expected increase in Young's modulus and tensile strength, but surprisingly similar with some elevated elongation at break (Figure S4.17-b). Other research groups have used FDM as part of synthesis of polymer backbones, such as polyesters (Zhang et al. 2017) and PUs (Gu and Wu 2018), both cross-linked by varying amounts of MPBMI, where the

PU study exhibited similar behavior. This could perhaps be explained by the fact that the cross-linking took place in the HS domain. This could be further developed in studying PU networks with constant HS content and cross-linked by varying amount of BMI. Given that the cross-linking takes places in the HS, there is an interplay between the phase segregation of the materials and the DA reaction, especially evident with short BMIs. Nevertheless, it is apparent the structure of the BMIs played an evident role in improving the material properties, as PU-HS20-MPBMI reported higher Young's modulus than PU-HS20-PPOBMI. However, the PUs cross-linked with different conventional BMIs reported similar tensile strength.

Lastly, all PUs were characterized by swelling tests in DMF. Results are reported in Table 4.2. The PUs cross-linked by MOBMI appear to have decreased swelling ratios (SRs) with respect to the linear counterpart, but as well experienced a decrease in insolubility fraction (IF). This is highly likely due to remnants reagents and by-products carried over from the MOBMI synthesis, as depicted in the ^{1}H NMR and ^{13}C NMR spectroscopic analyses (Figure 4.2 and Figure S4.9). Some questions stay open and at this level, it is difficult to fully conclude whether the decreasing in swelling is solely due to cross-linking or rather soluble mass transferred to the organic solvent phase. Additional investigations could be needed on this point. In contrast, a significant decrease in SRs and increase in IFs is evidently apparent in PUs cross-linked by the conventional BMIs.

As an advanced property, reprocessability was studied using PU materials cross-linked by conventional BMIs and PU-HS10-MOBMI and reported in Figure 4.7 and Table S4.5. The reprocessability of these PUs was evaluated by comparing the mechanical properties of original materials processed by solvent casting, to materials reprocessed by compression molding. Of all materials evaluated, PU-HS10-MOBMI seem to best preserve its static mechanical properties over two hot press reprocessing cycles, with only experiencing a loss in Young's modulus after a second reprocessing cycle. PU-HS20-PPOBMI seems to preserve its Young's modulus over all processing cycles whereas PU-HS20-MPBMI evidenced an apparent decrease over reprocessing cycles. Although the aromatic nature for the MPBMI yields superior mechanical properties, it can affect the reprocessing ability of the material by compression molding. The high melting temperature of MPBMI (approximately 150 °C), can be effecting the reprocessing ability of materials, specifically during the curing step (DA reaction) of the procedure as this limits the local mobility

of MPBMI in the material. Nevertheless, PU-HS20-MPBMI loss in Young's modulus and tensile strength remains quantitatively superior than PU-HS20-PPOBMI for the respective reprocessing step. The notable lack of preservation of material properties over processing cycles can be attributed to the inability of the material to maintain its cross-linking density when exposed to this thermal treatment. As previously mentioned, dissociative CANs often exhibit varying cross-link densities after reprocessing, which in turn effect the mechanical properties due to chain rearrangement, vitrification and cross-link ruin (Kloxin et al. 2010). Furthermore, since there is an interplay between the hydrogen bonding due to the phase segregation of the materials and the DA reaction, exposing the material to different reprocessing procedures could enhance reprocessability. For example, higher curing temperatures than 60 °C but lower than 90 °C, for the DA reaction to take place, could increase the kinetics of the DA reaction in the material but as well enhance local mobility.

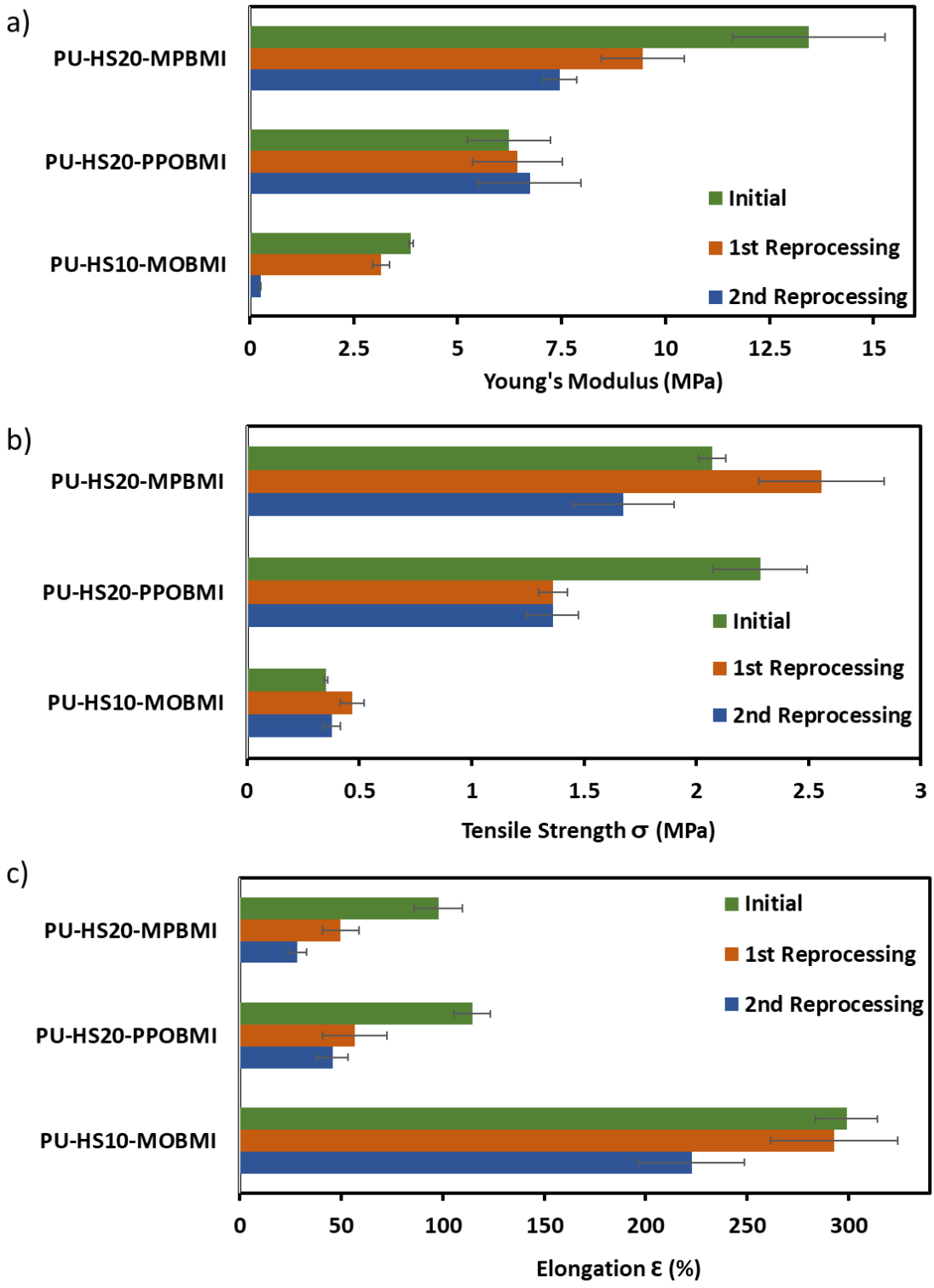

Figure 4.7 – Uniaxial tensile tests to compare the mechanical results of initial and reprocessed materials: PU-HS20-MPBMI, PU-HS20-PPOBMI, PU-HS10-MOBMI, (a) Young's modulus, (b) tensile strength (σ), and (c) elongation (ε).

As an advanced property, the self-healing ability of PU-HS10-MOBMI was also evaluated. The initial 120 °C heating allows the r-DA to take place but as well as promotes adhesion, whereas the 60 °C heating cycle allows for the network to be reformed by the DA reaction. After thermal treatment, the cut dumbbells have recovered their integrities. As depicted in the stress-strain curved of the initial and healed sampled displayed in Figure 4.8, the healed sample seems to almost fully recover in Young's modulus and attain about 50% of the initial tensile strength. Due to their toughness, PU-HS20-PPOBMI and PU-HS20-MPBMI samples could not be easily tested for self-healing. In contrast, an adhesion test could be further developed to further characterize these stiffer materials by examining the adhesion between two pieces of these material on larger surfaces areas.

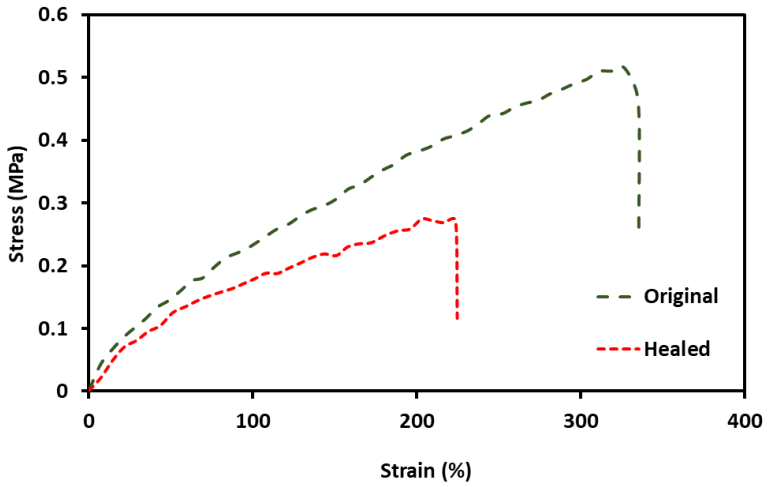

Figure 4.8 – Uniaxial tensile tests: Stress-strain curves of healed samples PU-HS10-MOBMI.

5. Conclusion

A new approach of producing cross-linked vegetable oil based PUs via the thermoreversible furan-maleimide DA reaction was studied and successfully developed. Linear PUs were synthesized using rapeseed-based polyol, HDI and FDM, a furan containing chain extender. By using FDM as chain extender, the cross-linking of PUs in the HS domain can be explored. The furan content was varied in PUs by varying the HS content (5, 10 and 20 %). Furthermore, to ultimately avoid the use of fossil-based BMIs and provide a new branched BMI, an original biobased methyl oleate BMI

derived from sunflower oil was synthesized and fully characterized. The PUs were cross-linked by MOBMI as well as two conventional and fossil-based BMIs: 1,1'-(Methylenedi-4,1-phenylene)bismaleimide and PPO-based BMI. Control PUs (without BMI cross-linking) generally exhibited increase Young's modulus and tensile strength and decreased elongation with increasing HS content. However, when these PUs were cross-linked by MOBMI, MOBMI tends to have a softening effect on the material, with increased elasticity. The long branched aliphatic chains of MOBMI as well of short-comings of its synthesis process can be attributed to the reported behaviour. In contrast, PUs cross-linked with shorter linear BMIs would yield increased Young's modulus, tensile strength, T_g, IF and decreased SR. PUs cross-linked by MOBMI exhibited the most consistent thermal recyclability and heat-induced self-healing. Nevertheless, PUs cross-linked by conventional BMIs showed promising thermal recyclability that requires further optimization by modified thermal treatments. Future efforts consist of further examining the temperature-dependent viscoelastic behaviour of these CANs to further improve thermal recyclable behaviour

These PU networks are reported for the first time with such a high biobased content (90 wt%). Synthesizing such networks provides a holistic approach to sustainable material design by incorporating sustainable raw materials but as well as attempting to control the end-life of materials, as a means to reduce energy and waste. This innovative work contributes to the development of biobased intrinsically dynamic architectures for a wide range of material domains.

6. References

Arbenz, Alice, Rémi Perrin, and Luc Avérous. 2017. 'Elaboration and Properties of Innovative Biobased PUIR Foams from Microalgae', *Journal of Polymers and the Environment*, 26: 254-62.

Bergman, Sheba D, and Fred Wudl. 2008. 'Mendable polymers', *Journal of Materials Chemistry*, 18: 41-62.

Bueno-Ferrer, Carmen, Elodie Hablot, María del Carmen Garrigós, Sergio Bocchini, Luc Averous, and Alfonso Jiménez. 2012. 'Relationship between morphology, properties and degradation parameters of novative biobased thermoplastic polyurethanes obtained from dimer fatty acids', *Polymer Degradation and Stability*, 97: 1964-69.

Bueno-Ferrer, Carmen, Elodie Hablot, Florence Perrin-Sarazin, M. Carmen Garrigós, Alfonso Jiménez, and Luc Averous. 2012. 'Structure and Morphology of New Bio-Based Thermoplastic Polyurethanes Obtained From Dimeric Fatty Acids', *Macromolecular Materials and Engineering*, 297: 777-84.

Buono, Pietro, Antoine Duval, Luc Averous, and Youssef Habibi. 2017. 'Thermally healable and remendable lignin-based materials through Diels – Alder click polymerization', *Polymer*, 133: 78-88.

Carré, Camille, Yvan Ecochard, Sylvain Caillol, and Luc Averous. 2019. 'From the synthesis of biobased cyclic carbonate to polyhydroxyurethanes: a promising route towards renewable non-isocyanate polyurethanes', *Chemsuschem*, 12: 3410.

Chen, Xiangxu, Matheus A. Dam, Kanji Ono, Ajit Mal, Hongbin Shen, Steven R. Nutt, Kevin Sheran, and Fred Wudl. 2002. 'A Thermally Re-mendable Cross-Linked Polymeric Material', *Science*, 295: 1698-702.

Denissen, Wim, Johan M. Winne, and Filip E. Du Prez. 2016. 'Vitrimers: permanent organic networks with glass-like fluidity', *Chemical Science*, 7: 30-38.

Desroches, M., M. Escouvois, R. Auvergne, S. Caillol, and B. Boutevin. 2012. 'From Vegetable Oils to Polyurethanes: Synthetic Routes to Polyols and Main Industrial Products', *Polymer Reviews*, 52: 38-79.

Dhers, Sébastien, Ghislaine Vantomme, and Luc Avérous. 2019. 'A fully bio-based polyimine vitrimer derived from fructose', *Green Chemistry*, 21: 1596-601.

Duarte, Martín E., Birgit Huber, Patrick Theato, and Hatice Mutlu. 2020. 'The unrevealed potential of elemental sulfur for the synthesis of high sulfur content bio-based aliphatic polyesters', *Polymer Chemistry*, 11: 241-48.

Duval, A., G. Couture, S. Caillol, and L. Averous. 2017. 'Biobased and Aromatic Reversible Thermoset Networks from Condensed Tannins via the Diels-Alder Reaction', *ACS Sustainable Chemistry & Engineering*, 5: 1199-207.

Duval, Antoine, Heiko Lange, Martin Lawoko, and Claudia Crestini. 2015. 'Reversible crosslinking of lignin via the furan-maleimide Diels-Alder reaction', *Green Chemistry*, 17: 4991-5000.

Fortman, D. J., J. P. Brutman, G. X. De Hoe, R. L. Snyder, W. R. Dichtel, and M. A. Hillmyer. 2018. 'Approaches to Sustainable and Continually Recyclable Cross-Linked Polymers', *ACS Sustainable Chemistry & Engineering*, 6: 11145-59.

Froidevaux, V, M Borne, E Laborbe, R Auvergne, A Gandini, and B Boutevin. 2015. 'Study of the Diels–Alder and retro-Diels–Alder reaction between furan derivatives and maleimide for the creation of new materials', *RSC Advances*, 5: 37742-54.

Gandini, Alessandro, Antonio J. F. Carvalho, Eliane Trovatti, Ricardo K. Kramer, and Talita M. Lacerda. 2018. 'Macromolecular materials based on the application of the Diels–Alder reaction to natural polymers and plant oils', *European Journal of Lipid Science and Technology*, 120: 1700091.

García-Astrain, Clara, and Luc Avérous. 2018. 'Synthesis and evaluation of functional alginate hydrogels based on click chemistry for drug delivery applications', *Carbohydrate Polymers*, 190: 271-80.

Gu, Lin, and Qing-Yun Wu. 2018. 'Recyclable bio-based crosslinked polyurethanes with self-healing ability', *Journal of Applied Polymer Science*, 135: 46272.

Hablot, Elodie, Bertrand Donnio, Michel Bouquey, and Luc Avérous. 2010. 'Dimer acid-based thermoplastic bio-polyamides: Reaction kinetics, properties and structure', *Polymer*, 51: 5895-902.

Hablot, Elodie, Dan Zheng, Michel Bouquey, and Luc Avérous. 2008. 'Polyurethanes Based on Castor Oil: Kinetics, Chemical, Mechanical and Thermal Properties', *Macromolecular Materials and Engineering*, 293: 922-29.

Haponiuk, Józef T., and Krzysztof Formela. 2017. 'Chapter 1 - PU Polymers, Their Composites, and Nanocomposites: State of the Art and New Challenges.' in Sabu Thomas, Janusz Datta, Józef T. Haponiuk and Arunima Reghunadhan (eds.), *Polyurethane Polymers* (Elsevier: Amsterdam).

Hu, Sumeng, Xi Chen, and John M. Torkelson. 2019. 'Biobased Reprocessable Polyhydroxyurethane Networks: Full Recovery of Crosslink Density with Three Concurrent Dynamic Chemistries', *ACS Sustainable Chemistry & Engineering*, 7: 10025-34.

Kloxin, Christopher J., Timothy F. Scott, Brian J. Adzima, and Christopher N. Bowman. 2010. 'Covalent Adaptable Networks (CANs): A Unique Paradigm in Cross-Linked Polymers', *Macromolecules*, 43: 2643-53.

Lligadas, G., J. C. Ronda, M. Galia, and V. Cadiz. 2013. 'Renewable polymeric materials from vegetable oils: a perspective', *Materials Today*, 16: 337-43.

Miao, Shida, Ping Wang, Zhiguo Su, and Songping Zhang. 2014. 'Vegetable-oil-based polymers as future polymeric biomaterials', *Acta Biomaterialia*, 10: 1692-704.

Palaskar, Dnyaneshwar V., Aurélie Boyer, Eric Cloutet, Jean-François Le Meins, Benoit Gadenne, Carine Alfos, Céline Farcet, and Henri Cramail. 2012. 'Original diols from sunflower and ricin oils: Synthesis, characterization, and use as polyurethane building blocks', *Journal of Polymer Science Part A: Polymer Chemistry*, 50: 1766-82.

Pan, Xiao, Partha Sengupta, and Dean C. Webster. 2011. 'High Biobased Content Epoxy–Anhydride Thermosets from Epoxidized Sucrose Esters of Fatty Acids', *Biomacromolecules*, 12: 2416-28.

Petrović, Zoran S, Alisa Zlatanić, Charlene C Lava, and Snežana Sinadinović-Fišer. 2002. 'Epoxidation of soybean oil in toluene with peroxoacetic and peroxoformic acids—kinetics and side reactions', *European Journal of Lipid Science and Technology*, 104: 293-99.

Pfister, D. P., Y. Xia, and R. C. Larock. 2011. 'Recent Advances in Vegetable Oil-Based Polyurethanes', *Chemsuschem*, 4: 703-17.

Ronda, Juan Carlos, Gerard Lligadas, Marina Galià, and Virgínia Cádiz. 2011. 'Vegetable oils as platform chemicals for polymer synthesis', European Journal of Lipid Science and Technology, 113: 46-58.

Spyros, A. 2002. 'Quantitative determination of the distribution of free hydroxylic and carboxylic groups in unsaturated polyester and alkyd resins by 31P-NMR spectroscopy', *Journal of Applied Polymer Science*, 83: 1635-42.

Sun, Hao, Christopher P. Kabb, Michael B. Sims, and Brent S. Sumerlin. 2019. 'Architecture-transformable polymers: Reshaping the future of stimuli-responsive polymers', *Progress in Polymer Science*, 89: 61-75.

Tan, S. G., and W. S. Chow. 2010. 'Biobased Epoxidized Vegetable Oils and Its Greener Epoxy Blends: A Review', *Polymer-Plastics Technology and Engineering*, 49: 1581-90.

Tremblay-Parrado, Khantutta-Kim, and Luc Avérous. 2019. 'Renewable Responsive Systems Based on Original Click and Polyurethane Cross-Linked Architectures with Advanced Properties', *Chemsuschem*, 13: 238.

Türünç, Oğuz, Maulidan Firdaus, Gregor Klein, and Michael A. R. Meier. 2012. 'Fatty acid derived renewable polyamides via thiol–ene additions', *Green Chemistry*, 14: 2577-83.

Yoshie, Naoko, Shoma Yoshida, and Koji Matsuoka. 2019. 'Self-healing of biobased furan polymers: Recovery of high mechanical strength by mild heating', *Polymer Degradation and Stability*, 161: 13-18.

Zhang, Lu, Frederick C. Michel Jr, and Anne C. Co. 2019. 'Nonisocyanate route to 2,5-bis(hydroxymethyl)furan-based polyurethanes crosslinked by reversible diels–alder reactions', *Journal of Polymer Science Part A: Polymer Chemistry*, 57: 1495-99.

Zhang, Yang, Zehui Dai, Jiarui Han, Ting Li, Jun Xu, and Baohua Guo. 2017. 'Interplay between crystallization and the Diels–Alder reaction in biobased multiblock copolyesters possessing dynamic covalent bonds', *Polymer Chemistry*, 8: 4280-89.

7. Supporting Information

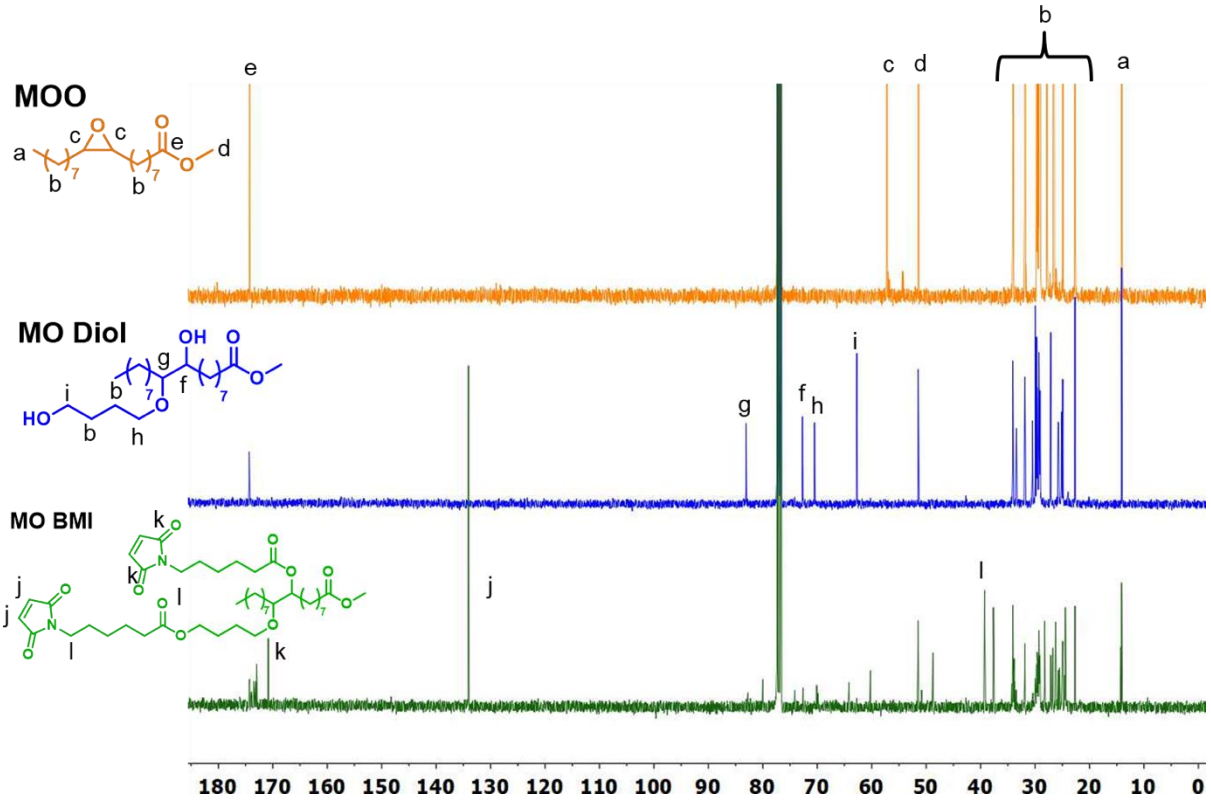

Figure S4.9 – ^{13}C NMR spectrum of MOO, MO Diol, and MOBMI.

MO Diol-Diester

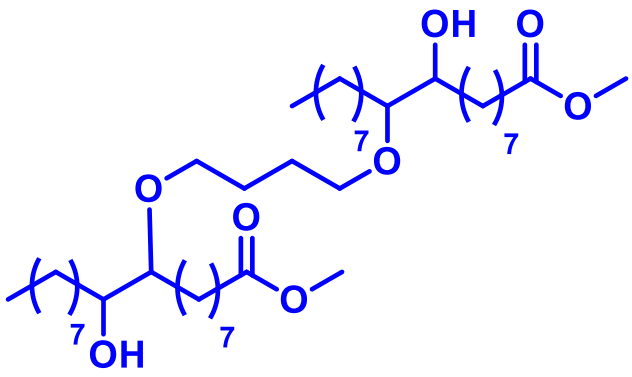

Figure S4.10 – Chemical structure of MO Diol-diester formed during MO Diol synthesis.

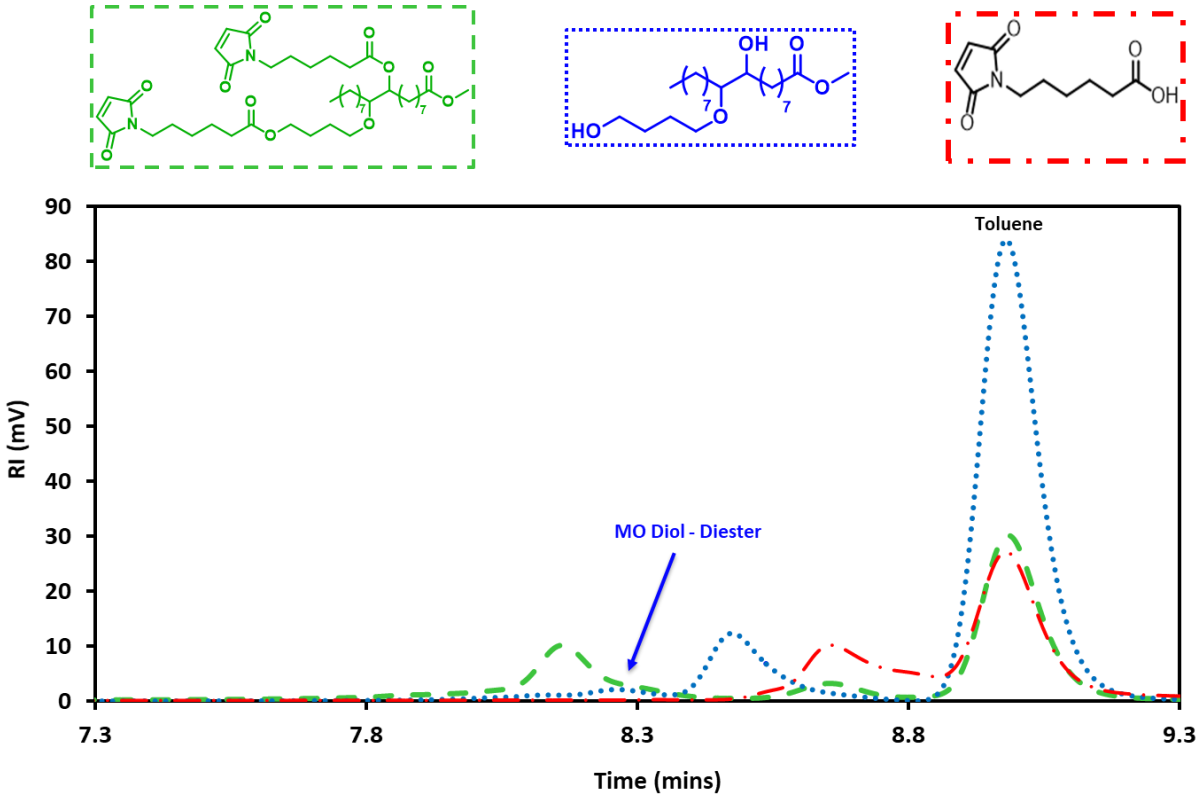

Figure S4.11 – SECs of 6-MHA, MO Diol and MOBMI.

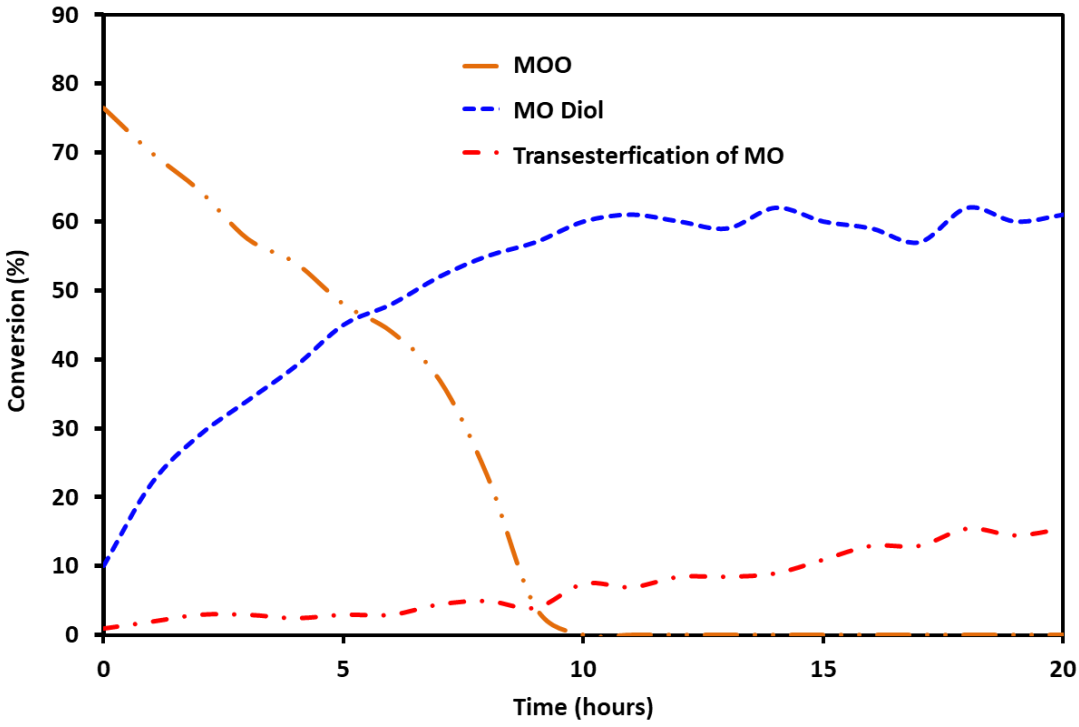

Figure S4.12 – Evolution of the conversion of different entities formed during synthesis of MO Diol over 20 h.

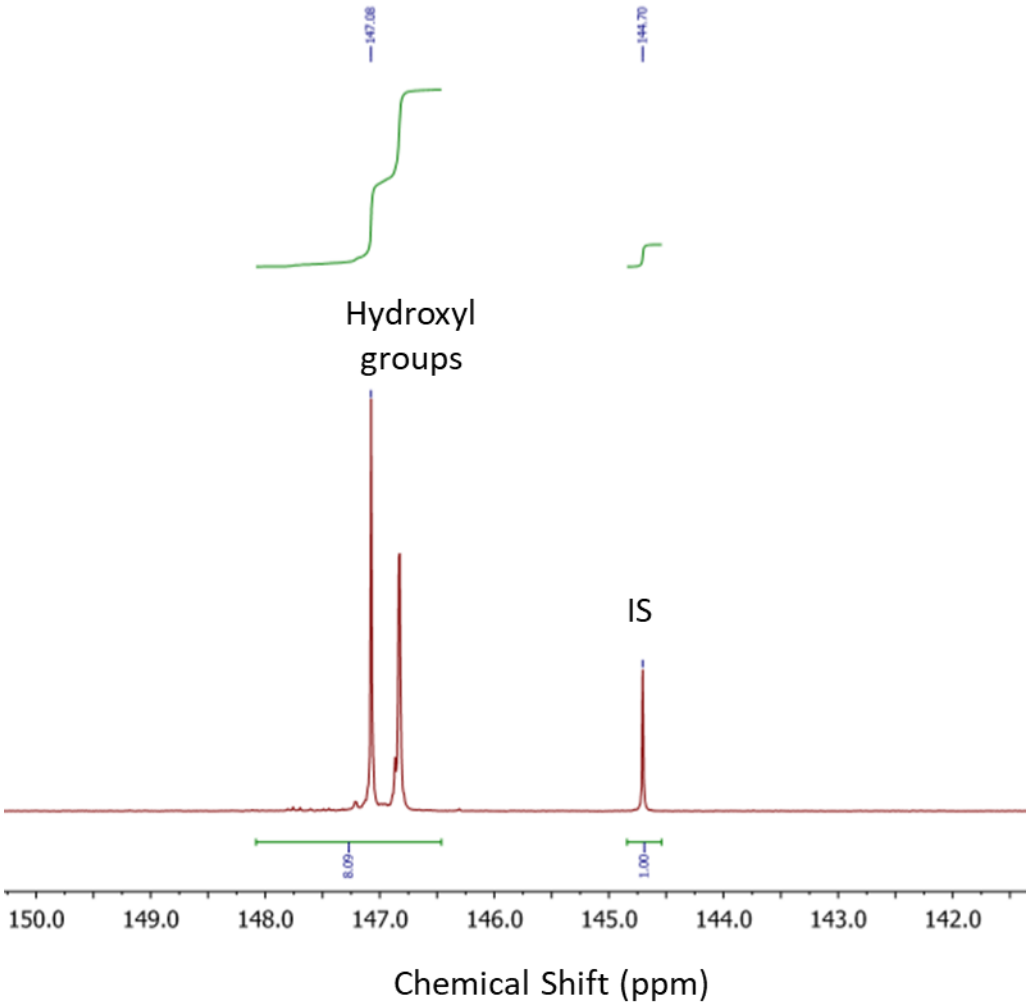

Figure S4.13 – ^{31}P NMR of MO Diol with integrations. IS = internal standard (cholesterol). ^{31}P-NMR was performed with Cl-TDP as phospholane reagent. Phospilated product clearly indicated signals linked to the OH area (146 -148 ppm) of primary and secondary hydroxyl groups.

Table S4.3 – HV of MO Diol determined by ^{31}P NMR (mg KOH/g) from Figure S4.13 and chemical titration.

Sample	Mass [mg]	Primary & Secondary Hydroxyl δ [ppm]	Area	mmol/g	HV [mg KOH/g]	HV [mg KOH/g] Chemical Titration
MO Diol	22.4	146 - 148	8.09	3.97	223	220

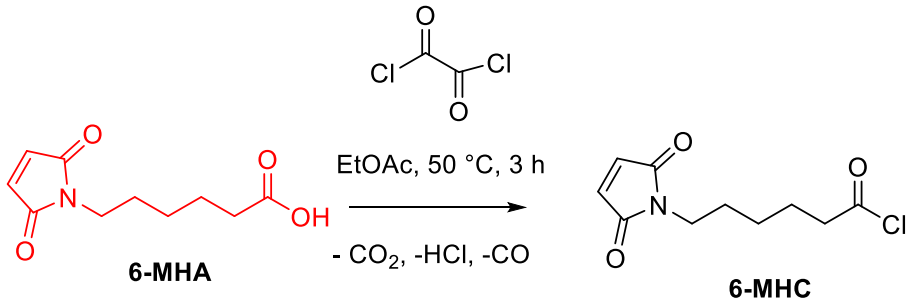

Scheme S4.3 – General reaction scheme of 6-MHC.

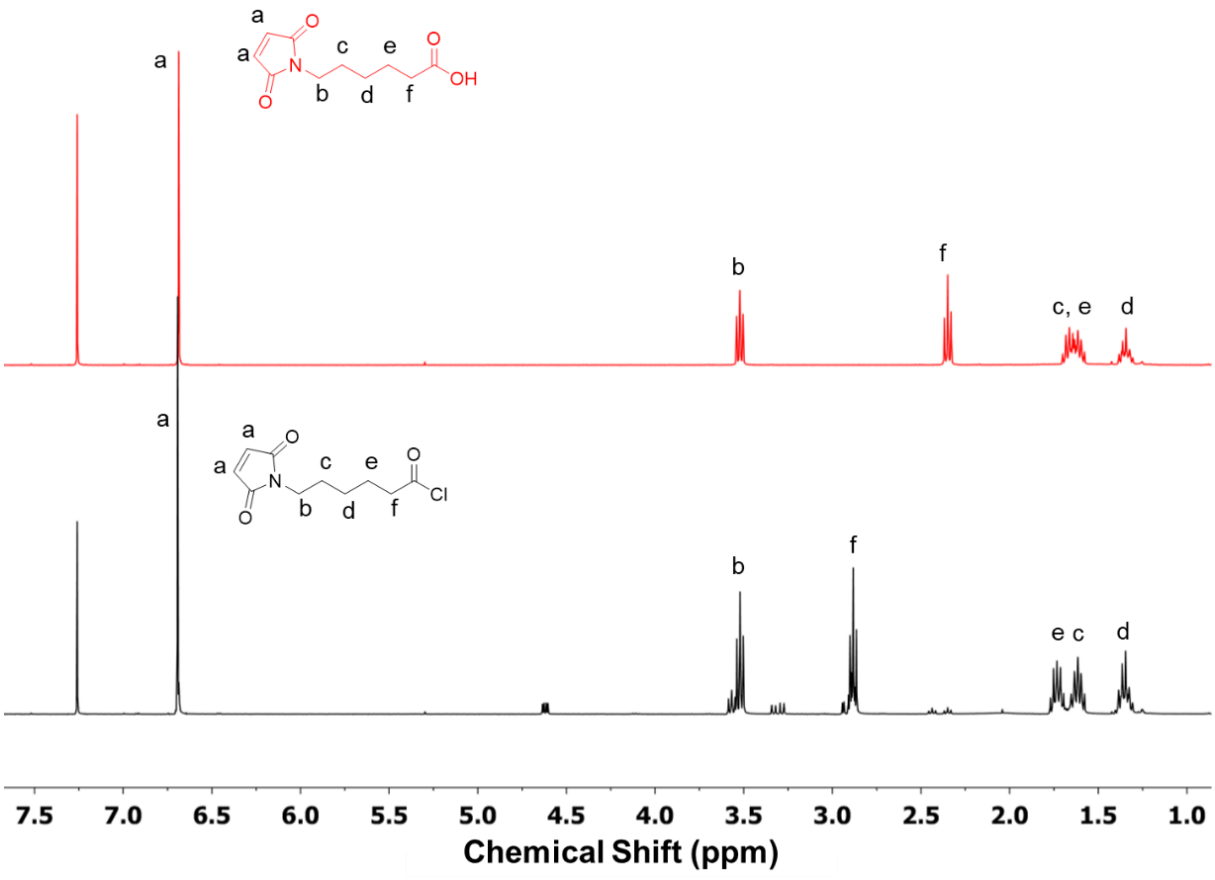

Figure S4.14 – ^{1}H NMR spectra of 6-MHA and 6-MHC.

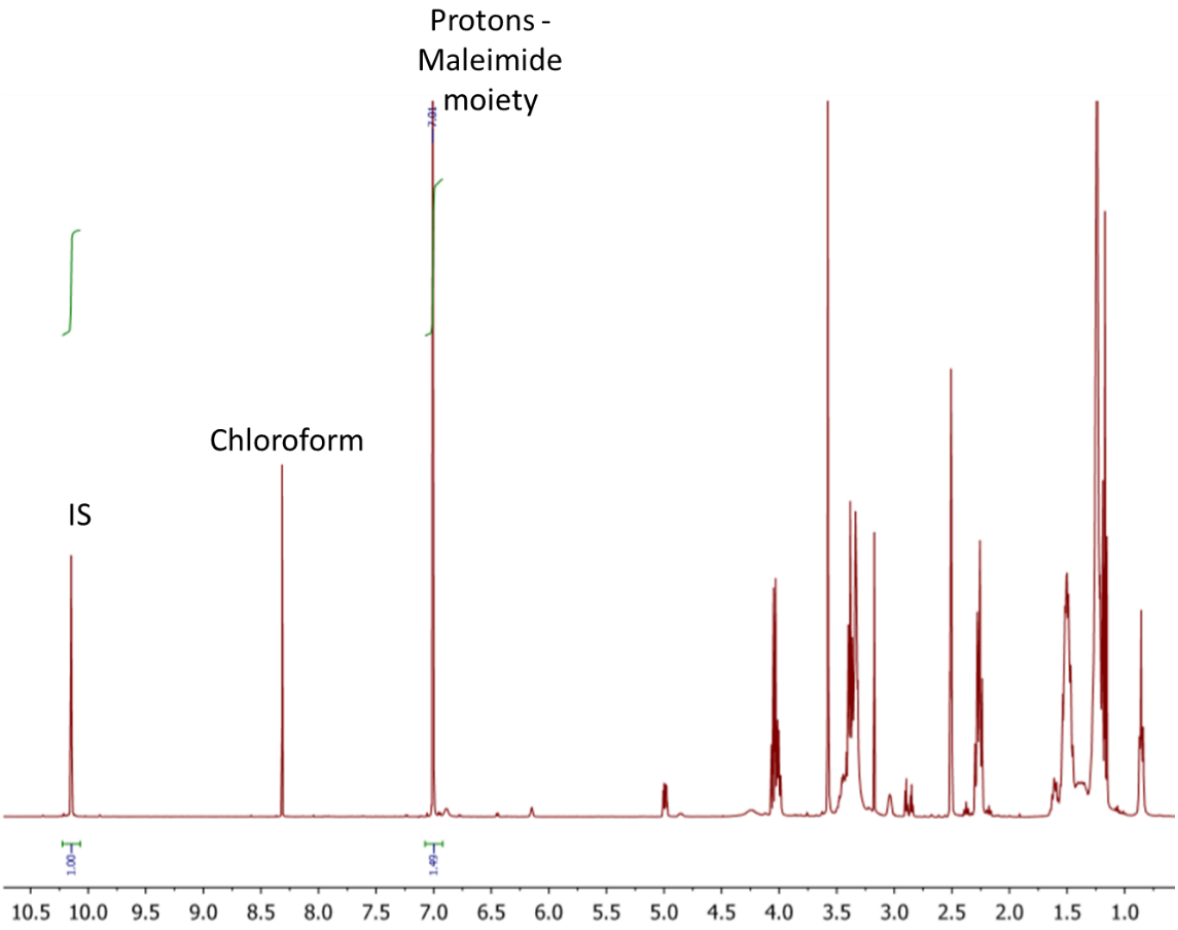

Figure S4.15 – Quantitative ^{1}H NMR of MOBMI with the integrations, internal standard PFB in DMSO.

Table S4.4 – Maleimide content in mmol/g of MOBMI determined by quantitative ^{1}H NMR from Figure S4.16

Sample	Mass [mg]	δ [ppm]	Area	mmol/g
MOBMI	20.1	7.01	1.49	1.83

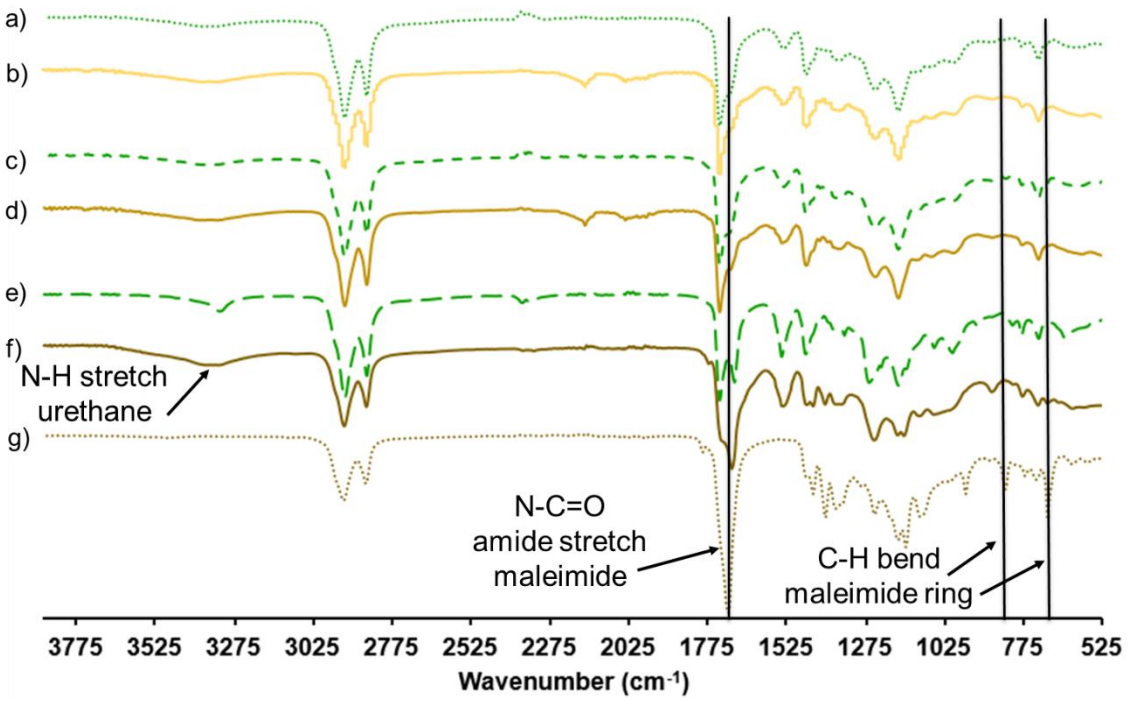

Figure S4.16 – FTIR spectra of (a) PU-HS5, (b) PU-HS5-MOBMI, (c) PU-HS10, (d) PU-HS10-MOBMI, (e) PU-HS20, (f) PU-HS20-MOBMI, and (g) MOBMI.

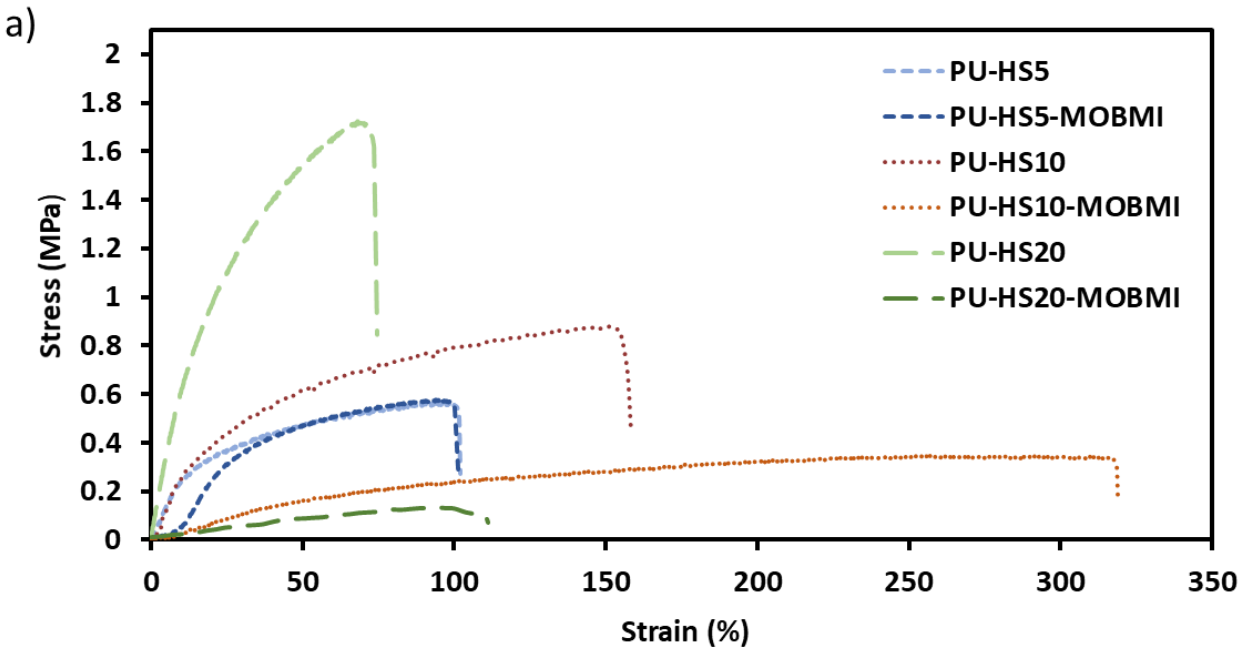

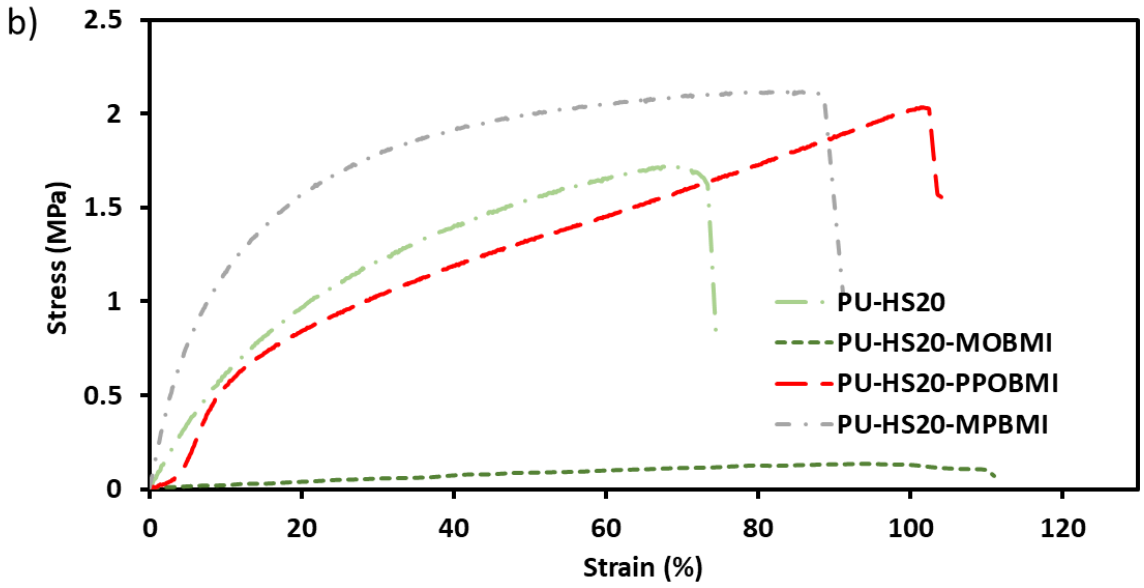

Figure S4.17 – (a) Stress-strain curves of control and cross-linked PUs by MOBMI, (b) stress-strain curves of PU-HS20, PU-HS20-MOBMI, PU-HS20-PPOBMI, and PU-HS20-MPBMI.

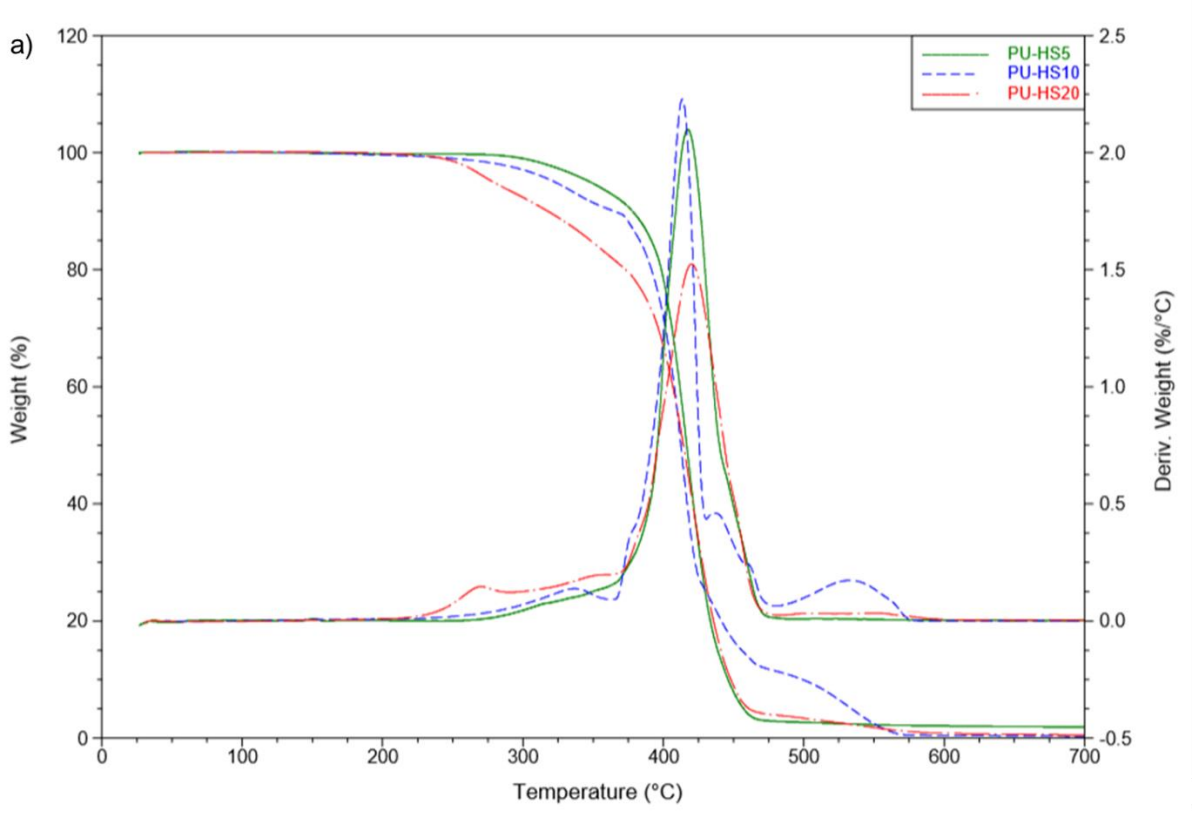

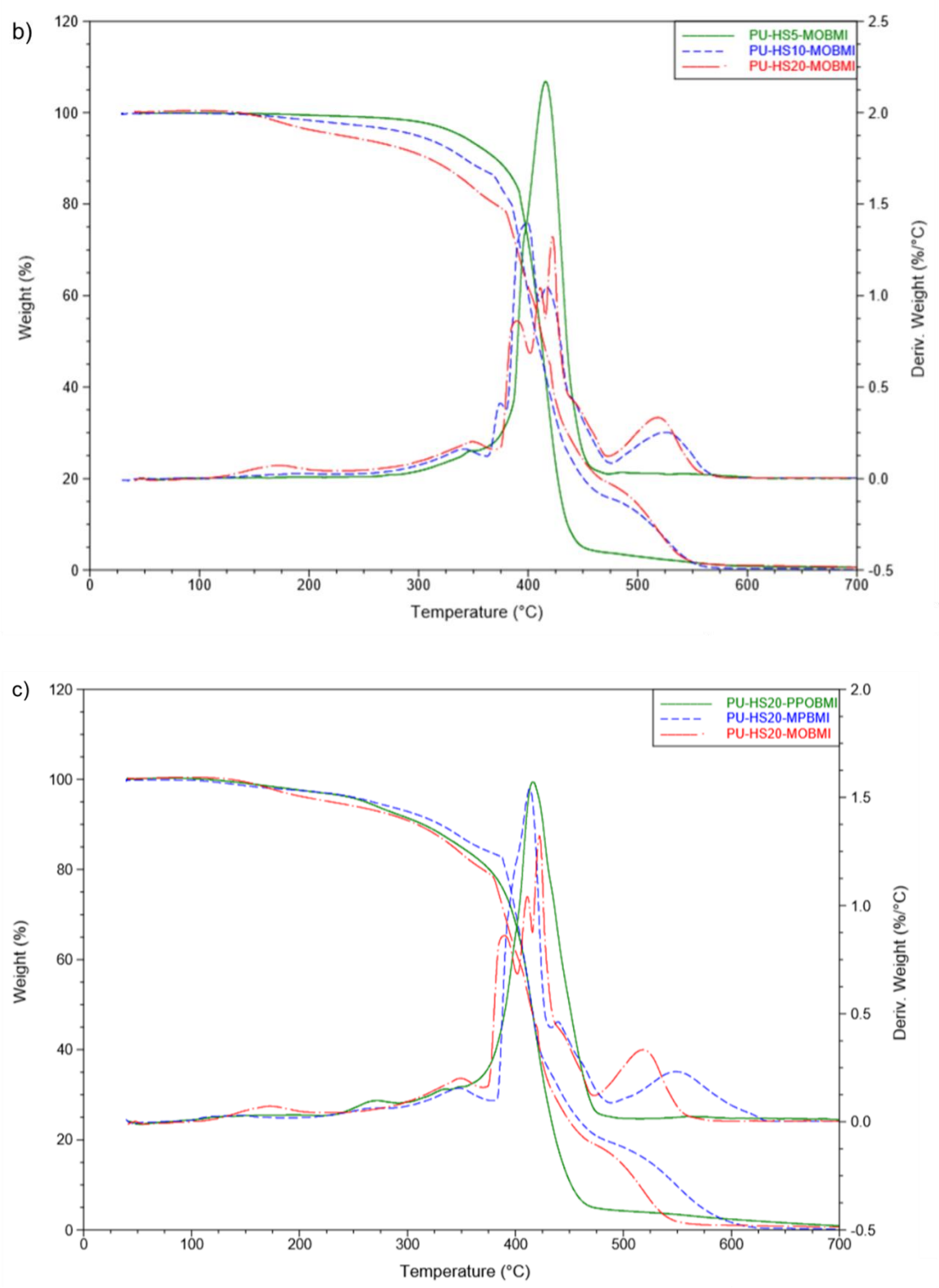

Figure S4.18 - Thermogravimetric analysis curves (TGA) and derivative thermogravimetric analysis curve (DTG) of materials (a) PU-HS5 (green, solid), PU-HS10 (blue, dashed), and PU-HS20 (red, dash dot), (b) PU-HS5-MOBMI (green, solid), PU-HS10-MOBMI (blue, dashed), and PU-HS20-MOBMI (red, dashed dot), and (c) PU-HS20-PPOBMI (green, solid), PU-HS20-MPBMI (blue, dashed), and PU-HS20-MOBMI (red, dash dot).

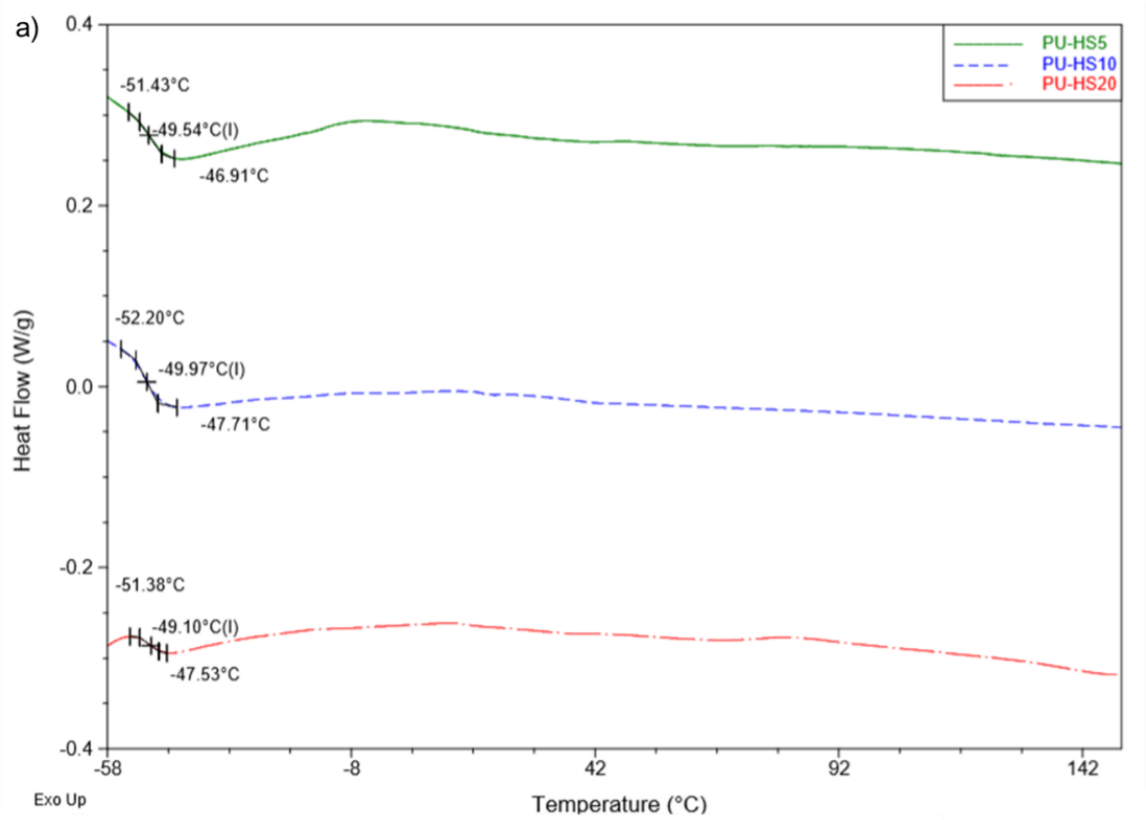
a)
PU-HS5
PU-HS10
PU-HS20
-51.43°C
-49.54°C(I)
-46.91°C
-52.20°C
-49.97°C(I)
-47.71°C
-51.38°C
-49.10°C(I)
-47.53°C
Heat Flow (W/g)
0.4
0.2
0.0
-0.2
-0.4
-58
-8
42
92
142
Exo Up
Temperature (°C)

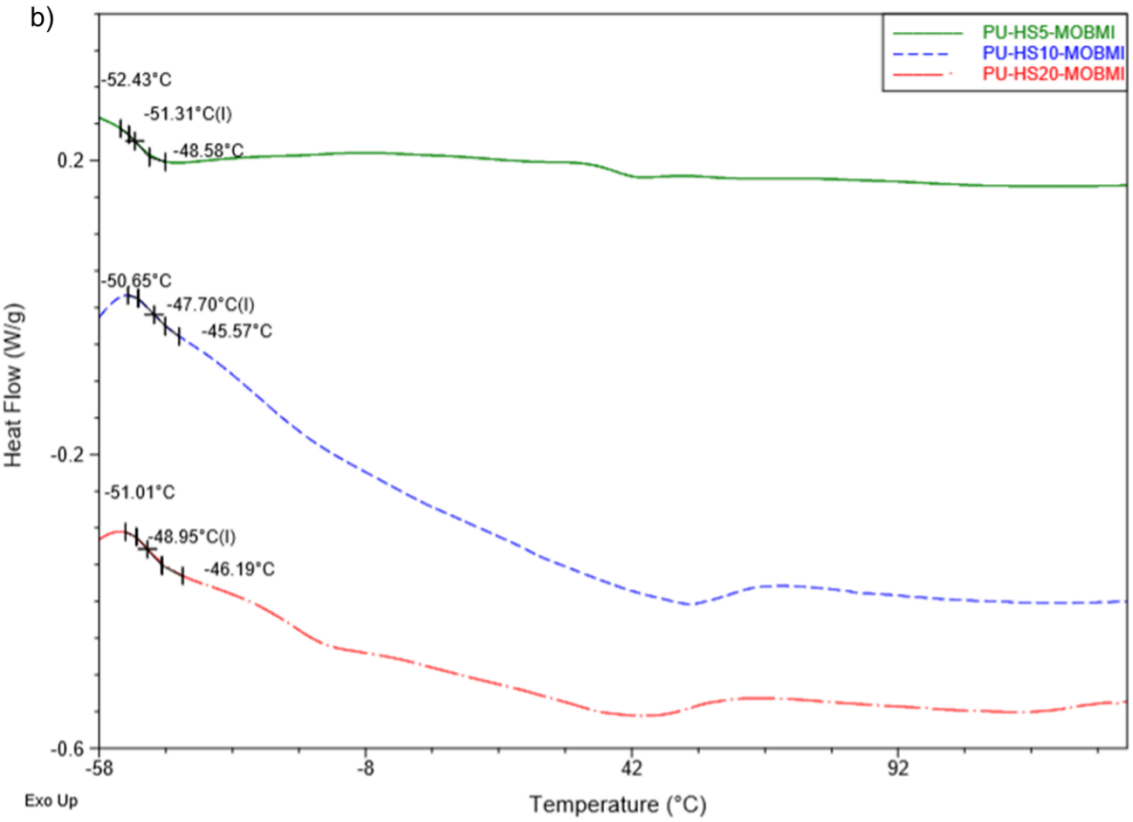
b)
PU-HS5-MOBMI
PU-HS10-MOBMI
PU-HS20-MOBMI
-52.43°C
-51.31°C(I)
-48.58°C
-50.65°C
-47.70°C(I)
-45.57°C
-51.01°C
-48.95°C(I)
-46.19°C
Heat Flow (W/g)
0.2
-0.2
-0.6
-58
-8
42
92
Exo Up
Temperature (°C)

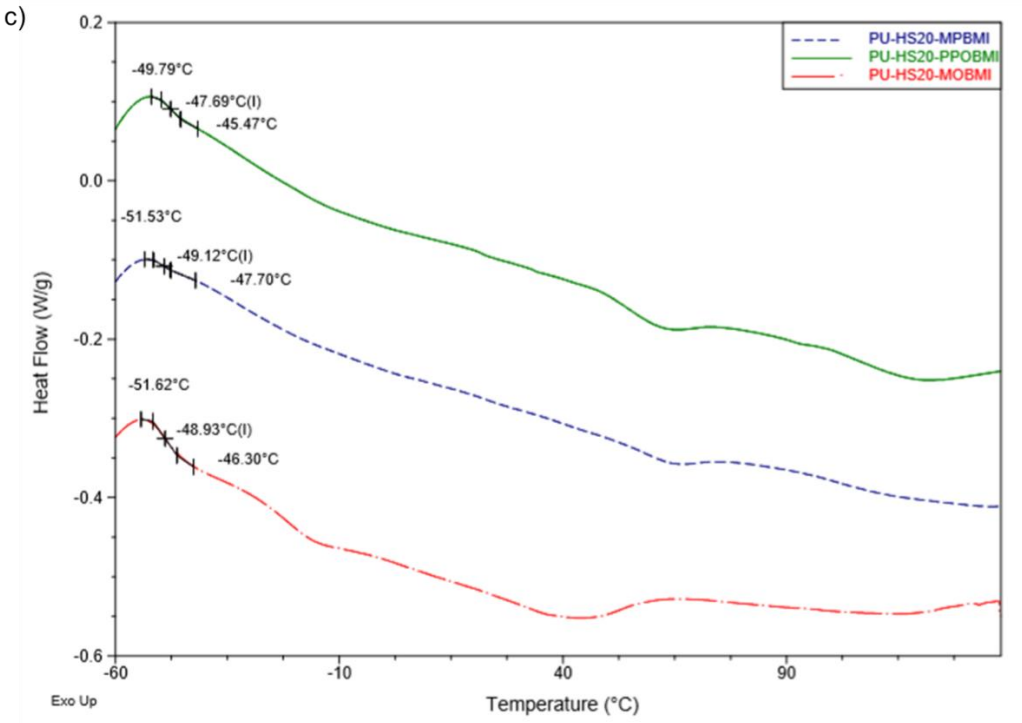

Figure S4.19 – Differential scanning calorimetry (DSC) thermograms of materials (a) PU-HS5 (green, solid), PU-HS10, (blue dashed),and PU-HS20 (red, dash dot), (b) PU-HS5-MOBMI (green, solid), PU-HS10-MOBMI (blue, dashed), and PU-HS20-MOBMI (red, dashed dot), and (c) PU-HS20-MPBMI (green, solid) PU-HS20-PPOBMI (blue, dashed) and PU-HS20-MOBMI (red, dashed dot).

To reprocess material by compression molding, initial materials are cut into several small pieces and placed in the center of square tile mold. In a hot press, the material is left to preheat at 150 °C for 15 mins, followed by 10 mins under compression at 150 °C. The material is then left at 60 °C for 48 h in order for DA cross-links to be reformed

Table S4.5 – Summary of mechanical properties data (initial and reprocessed) of PU-HS20-MPBMI, PU-HS-MPBMI, and PU-HS10-MOBMI PUs materials.

PU system	Processing step	Young's modulus [MPa]	$\sigma^{[a]}$ [MPa]	$\varepsilon^{[b]}$ [%]
PU-HS20-MPBMI	Initial	3.88 ± 0.05	0.35 ±0.01	300 ± 15
	Reprocessing 1	3.16 ± 0.20	0.47 ± 0.05	293 ± 31
	Reprocessing 2	0.26 ± 0.02	0.38 ± 0.04	222 ± 26
PU-HS20-PPOBMI	Initial	6.23 ± 1.00	2.28 ± 0.21	114 ± 9
	Reprocessing 1	6.45 ± 1.08	1.36 ± 0.06	57 ± 16
	Reprocessing 2	6.73 ± 1.23	1.36 ± 0.11	46 ± 8
PU-HS10-MOBMI	Initial	13.44 ± 1.83	2.07 ± 0.06	98 ± 12
	Reprocessing 1	9.45 ±1.00	2.55 ±0.28	50 ± 9
	Reprocessing 2	7.46 ± 1.23	1.67 ± 0.22	28 ± 5

[a] Tensile strength. [b] Elongation.

Conclusion of Chapter 4

The aim of this last experimental chapter was to explore another strategy to obtain cross-linking biobased PUs by the DA reaction. This chapter uses FDM as chain extender in PU synthesis, to explore the cross-linking in the HS domains of PUs. Furthermore, to ultimately avoid the use of fossil-based BMIs and provide a new branched BMI, an original biobased methyl oleate BMI derived from sunflower oil was synthesized and fully characterized. The furan content of PU backbone was controlled by varying the HS content (5, 10 and 20 %). The PUs were cross-linked by MOBMI as well as two conventional and fossil-based BMIs: 1,1'-(Methylenedi-4,1-phenylene)bismaleimide and PPO-based BMI.

It was generally observed that MOBMI brings a softening effect when used as a PU cross-linker. When compared to control PUs counterparts, PU cross-linked with MOBMI has considerably increased the elasticity materials. This is hypothesized to be due the long-chain branched nature of MOBMI but as well as shortcomings of the MOBMI synthesis in which remnant reagents could have played a role in softening the materials. Perspectives include further improving the MOBMI synthesis. Nevertheless, PUs cross-linked by the conventional BMIs would yield increased Young's modulus, tensile strength, T_g, IF and decreased SR. Although, PUs cross-linked by conventional BMIs showed promising thermal recyclability that require further optimization by modified thermal treatments, PUs cross-linked by MOBMI exhibited the most consistent thermal recyclability and heat-induced self-healing.

General Conclusion & Perspectives

This PhD thesis took place within the BioTeam group directed by Pr. Luc Avérous, at the Institut of Chemistry and Processes for Energy, Environment and Health (Institut de Chimie et Procédés pour l'Energie, l'Environnement et la Santé, ICPEES), a joint research unit (UMR 7515) between University of Strasbourg and CNRS. Moreover, this work also involved in the frame of Mutaxio, a joint research entity between the BioTeam and the R&D of Soprema France. Soprema is world recognized leader in the construction industry. In the context of this thesis, Soprema and the BioTeam took part in the Trans'alg consortium funded by BPI-France, with the aim of developing advanced water proof membranes and insulation from biosourced molecules. In the context of this project, Soprema did not impose materials specifications or specific objectives. This PhD had the liberty of creative freedom in context of research and innovations for the development of new adaptive biobased PUs derived from vegetable oils.

This PhD thesis situates itself within a historical research thematic of the BioTeam – developing polyurethanes (PUs) with innovative renewable macromolecular architectures from diverse biomass such as vegetable oils. As this research thematic evolved in time, a reflection around sustainable polymer design concluded that although materials should increasingly integrate renewable raw materials, they should also be designed with advanced properties to facilitate recyclability and a controlled end-of-life. Covalent adaptable networks (CANs) have been shown to display such properties. They contain dynamic cross-links which allows them to be reprocessed like thermoplastics, as well as maintain the benefits of thermosets. CANs networks can subdivided into two categories: associative and dissociative. In associative CANs, dynamicity occurs by a substitution reaction between an existing cross-link and a pending reactive group, whereas in dissociative CANs, cross-links are cleaved back into their individual reactive moieties before reforming again. Combining the emergence of CANs with our historically acquired knowledge in biobased PUs; the objective of this work was to develop reversibly cross-linked PUs based on vegetable oils. The synthesized and achieved biobased networks were studied for their physico-chemical properties and for their advanced performances such as thermal recyclability and self-healing ability.

The manuscript is structured with chapters and publications. Each publication acts as the backbone of each chapter. This thesis is built under publications format for the submission of

three scientific articles as well as a bibliographic review to peer-reviewed journals. One publication linked to the second chapter has already been fully published in *ChemSusChem (2020, Vol. 13, p. 238).*

Following a general introduction, the manuscript consists of four chapters. In **the first chapter,** an exhaustive bibliographic review of the use of 'green' click chemistry for the synthesis of polymers and networks derived from vegetable oils was accomplished. This allowed us to explore the most prevalent chemical modifications on vegetable oils as well as comprehend the importance of click chemistry reactions as a powerful tool for the synthesis of innovative architectures. Furthermore, the analysis of the literature allowed us to apprehend the main problematics associated with this means of synthesis, most notably the use of the DA reaction by the furan maleimide coupling. The use of the furan-maleimide DA reaction for the synthesis vegetable oil-based networks is in its infancy, when compared to a more established reaction such as thiol-ene addition. Nevertheless, the furan-maleimide DA reaction is a thermally reversible click chemistry reaction that instills itself well in the ideals of green chemistry and is an established reaction for the synthesis of dissociative CANs. Thus, the development of reversibly cross-linked PUs based on vegetable oils would be achieved by utilizing the thermally reversible furan-maleimide DA click reaction. Vegetable oil-based building blocks, containing furan and maleimide moieties were synthesized and could readily integrated to precedently established biobased PUs of our group. The review highlights emergence of the DA reaction and triazolinedione chemistry for the synthesis of sustainable polymers with advanced properties and the potential of click chemistry for the synthesis of vegetable oil-based polymers for a wide range of applications.

Chapters 2, 3 and 4 consist of the experimental part of this manuscript. In the **second chapter,** a new biobased furan bearing building block derived from sunflower oil, denoted the Furan Oligomer (FO), was synthesized for the first time, according our knowledge, and fully characterized. This original FO consists of diol structure with pendant furan rings. Due to its structure, the FO can integrate PU backbones. The FO alongside a conventional bismaleimide (BMI) was used in the synthesis of thermoreversible cross-links in PUs. The dynamicity solely between the FO and BMI was first studied and proved by different means. Then, the FO and BMI

were integrated in to the synthesis of PUs, which led to advanced dynamic architectures with advanced properties such as thermal recyclability and self-healing.

In a follow-up study of this work, **the third chapter** studies the dynamicity of the FO with other conventional linear BMIs that varied in the length and structure, as well as the integration of these different BMIs in renewable biobased PU structures. It was concluded that aromatic BMIs would yield superior mechanical properties in comparison to their linear aliphatic counterparts. Nevertheless, varying the length of linear aliphatic BMIs did not yield a significant effect on the mechanical properties, but rather on the ability of the materials to be thermally recycled. Increasing the length of BMIs led to a decreased ability of materials to be thermally recycled. Furthermore, the introduction of hard segments in the linear backbone of the PUs showed that these PUs could have enhanced mechanical properties by DA cross-links and showed promising thermal recyclability and adhesion.

Lastly, the **fourth chapter** put forth the synthesis and characterization of fatty acid BMI, methyl oleate BMI (MOBMI) and its use as a cross-linker in PU architectures. In chapter two and three, the dynamic cross-links were introduced in the soft segments of PU architectures. In chapter four, dynamic cross-links were introduced in the hard segments (HS) of biobased PU architectures and was explored for its effect on physico-chemical properties polymers and on advanced properties such as thermal recyclability and self-healing. It was concluded that the MOBMI had a softening effect when used as cross-linker, most probably due to its long aliphatic branched nature. Cross-linking PUs with conventional BMIs led to improved mechanical properties.

Finally, it has been made clear that there is interest in developing CAN networks using the furan-maleimide DA reaction for the synthesis of advanced biobased PU architectures. This work allows for the valorization of vegetable oils and the thermoreversible DA reaction for synthesis of complex biobased PUs. We have acquired numerous scientific findings on the development of biobased building blocks containing furan and maleimide moieties, as well as understanding their effect once integrated into PU architectures. Further understanding on the temperature dependent visco-elastic behavior of these biobased PU architectures during thermal reprocessing opens a path to future developments.

The experimental work in this manuscript provides a stepping stone in the development of innovative, biobased and dynamic architecture for a wide range of applications. The PU-based thermo-reversible networks derived from vegetable oils are the first of their kind to be examined. The interesting and promising results obtained in the framework of this study has allowed for the potential of numerous perspectives for the synthesis of advanced biobased CANs.

Firstly, significant work remains to be accomplished to acquire more refined knowledge on the different materials synthesized to answer the still open scientific questions. For instance, dynamic mechanical testing must be carried out to further understand the temperature-dependent visco-elastic behavior of the materials and better interpret the thermal recyclability is required. Furthermore, climate ageing analyses (UV, temperature, humidity) as well as life cycle analyses are necessary to complete our studies before preparing the transfer to industry facilities through a long scaling-up step. In order to adhere to societal ambitions and facilitate a transfer to industry, the syntheses involved would require a more stringent application of green chemistry principles, such as eliminating the use of solvents and greener modifications (such as e.g., chemo-enzymatic reactions).

Secondly, throughout this study we examined two main strategies of cross-linking biobased PUs; (i) introducing pedant furan rings into soft segments of PU backbones and cross-linking with a BMI and (ii) introducing furan rings in line with the PU backbone in the HS and cross-linking with a BMI. Nevertheless, many different perspective strategies for cross-linking and can also be envisioned and have yet to be explored. For example, (i) synthesizing a building block containing both furan and maleimide moieties for a one pot cross-linking process (Figure C.1-a), (ii) synthesizing maleimide containing building block that can be integrated in to PU backbones and cross-linked by bis-furan or multi-furan linkers (Figure C.1-b), and (iii) synthesizing PU prepolymers terminated by furan or maleimide moieties to be cross-linked via multi-maleimide or multi furan linkers (Figure C.1-c), respectively. Cross-linking by different strategies ensues a multitude of characterization and studies to determine how these different strategies impact the physico-chemical properties of polymers as well as thermal recyclability and heat induced self-healing.

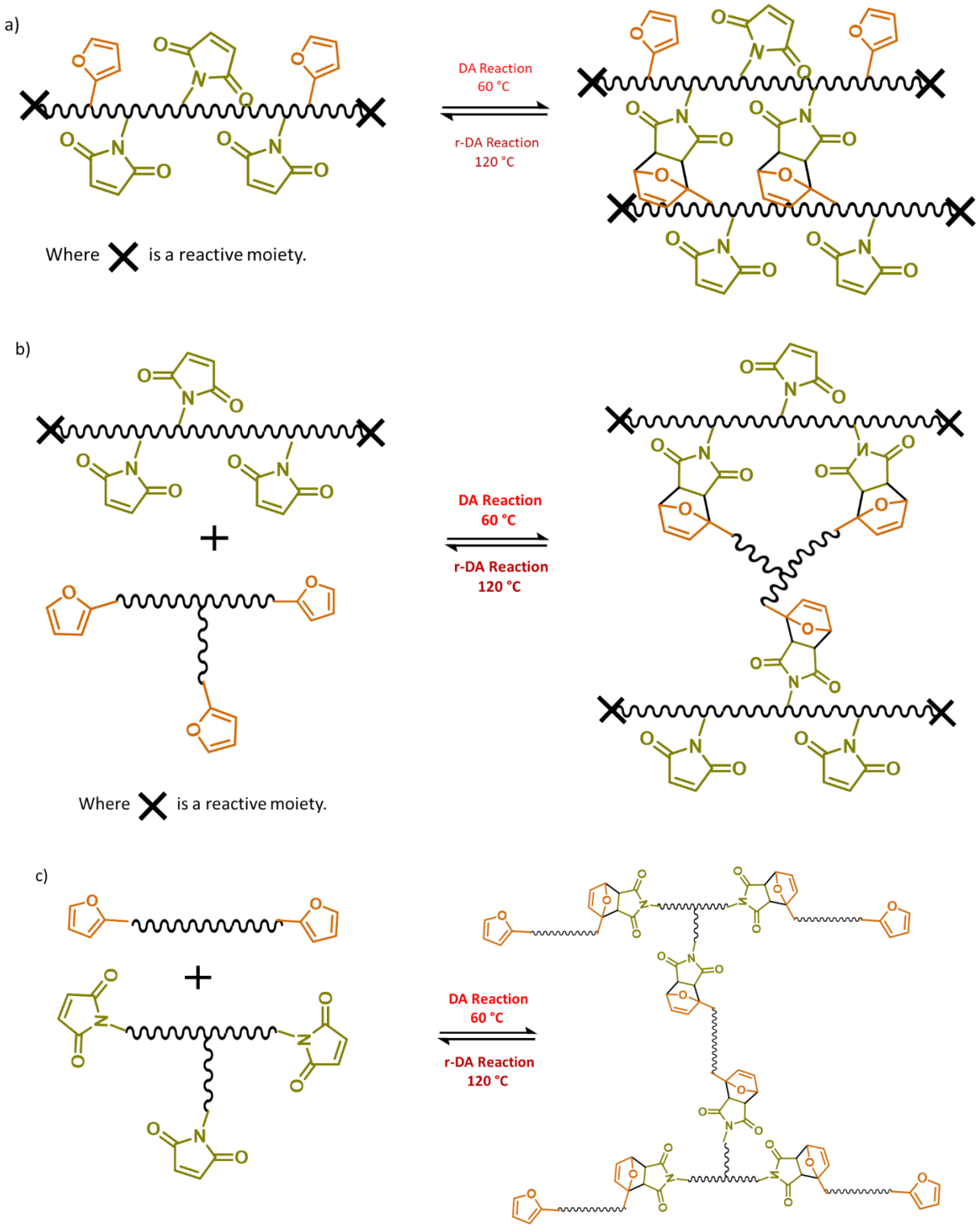

Figure C.1—Alternative cross-linking strategies (a) building block containing furan and maleimide moieties, (b) building block containing maleimide moieties cross-linked with multi-furan linkers, (c) prepolymer terminated furan cross-linked with multi-maleimide linkers.

During the course of this work, we developed new biobased building blocks, such as FO and MOBMI. As the FO consist of diol structure with furan pendant rings, the architecture could be integrated into other polymer backbones such as polyesters and polyethers for the cross-linking of other polymer architectures. Furthermore, the synthesis of FO and MOBMI could be adapted to other readily accessible vegetable oils such soybean rapeseed oil. Moreover, fatty acids derived from micro-algae are becoming an increasing and appealing renewable resources. Microalgae can be grown in bioreactors under controlled environments without competing with land or food uses. The synthesis of MOBMI can be readily adapted to eicosapentaenoic acid (C20:5) or docosahexaenoic acid (C22:6) which are main constituents of fatty acids derived from microalgae oil. These fatty acids contain carbon chains that are 20 to 22 carbons long and high level of unsaturations (5 to 6 double bonds) which can readily be used for the synthesis of multi-maleimide linker by the same route to attaining MOBMI.

Lastly, this work utilized the thermoreversible furan-maleimide DA reaction for the synthesis of biobased PU dissociative CANs. Nevertheless, there exists a panel of reversible chemical reactions that can be integrated for the synthesis of associative and dissociative biobased PU CANs and more largely biobased CANs. Several thermoreversible cross-linking chemistries for synthesis of CANs have also been explored such as triazolinedione Alder-ene reactions, hindered urea exchange, oxime-enabled transcarbamoylation, transesterification, transamination of vinylogous urethanes and many more. These reactions should be studied and integrated in the synthesis of biobased PU CANs as well as biobased CANs for a holistic approach to sustainable polymer design.

Complete list of bibliographic references

Adzima, Brian J., H. Alan Aguirre, Christopher J. Kloxin, Timothy F. Scott, and Christopher N. Bowman. 2008. 'Rheological and Chemical Analysis of Reverse Gelation in a Covalently Cross-Linked Diels−Alder Polymer Network', *Macromolecules*, 41: 9112-17.

Akindoyo, John, Mohammad Beg, Suriati Ghazali, Muhammad Islam, Nitthiyah Jeyaratnam, and Yuvaraj Ar. 2016. 'Polyurethane types, synthesis and applications-a review', *RSC Advances*, 6: 114453-82.

Alagi, Prakash, Ye Jin Choi, Joonil Seog, and Sung Chul Hong. 2016. 'Efficient and quantitative chemical transformation of vegetable oils to polyols through a thiol-ene reaction for thermoplastic polyurethanes', *Industrial Crops and Products*, 87: 78-88.

Anastas, Paul T., and John Charles Warner. 1998. Green chemistry : theory and practice (Oxford University Press: Oxford [England]; New York).

Arbenz, Alice, Rémi Perrin, and Luc Avérous. 2017. 'Elaboration and Properties of Innovative Biobased PUIR Foams from Microalgae', *Journal of Polymers and the Environment*, 26: 254-62.

Ates, Zeliha, Paul D Thornton, and Andreas Heise. 2011. 'Side-chain functionalisation of unsaturated polyesters from ring-opening polymerisation of macrolactones by thiol–ene click chemistry', *Polymer Chemistry*, 2: 309-12.

Bakhshi, Hadi, Hamid Yeganeh, Shahram Mehdipour-Ataei, Atefeh Solouk, and Shiva Irani. 2013. 'Polyurethane Coatings Derived from 1,2,3-Triazole-Functionalized Soybean Oil-Based Polyols: Studying their Physical, Mechanical, Thermal, and Biological Properties', *Macromolecules*, 46: 7777-88.

Behr, A., A. Westfechtel, and J. Pérez Gomes. 2008. 'Catalytic Processes for the Technical Use of Natural Fats and Oils', *Chemical Engineering and Technology*, 31: 700-14.

Belgacem, Naceur, and Alessandro Gandini. 2008. Monomers, Polymers and Composites From Renewable Resources (Elsevier: Amsterdam).

Bergman, Sheba D, and Fred Wudl. 2008. 'Mendable polymers', *Journal of Materials Chemistry*, 18: 41-62.

Bétron, Cyrille, Philippe Cassagnau, and Véronique Bounor-Legaré. 2018. 'EPDM crosslinking from bio-based vegetable oil and Diels–Alder reactions', *Materials Chemistry and Physics*, 211: 361-74.

Beyazkilic, Zeynep, Gerard Lligadas, Juan Carlos Ronda, Marina Galià, and Virginia Cádiz. 2014. 'Vinylsulfide-Containing Polyesters and Copolyesters from Fatty Acids: Thiol-yne Monomer Synthesis and Thiol-ene Functionalization', *Macromol. Chem, Phys*., 215: 2248-59.

Beyazkilic, Zeynep, Gerard Lligadas, Juan Carlos Ronda, Marina Galià, and Virginia Cádiz. 2015. 'Synthesis and functionalization of vinylsulfide and ketone-containing aliphatic copolyesters from fatty acids', Polymer, 79: 290-98.

Biermann, Ursula, Wolfgang Friedt, Siegmund Lang, Wilfried Lühs, Guido Machmüller, Juergen O Metzger, Mark Ruesch gen. Klaas, Hans J Schäfer, and Manfred P Schneider. 2000. 'New syntheses

with oils and fats as renewable raw materials for the chemical industry', *Angew. Chem. Int. Ed.*, 39: 2206-24.

Billiet, Stijn, Kevin De Bruycker, Frank Driessen, Hannelore Goossens, Veronique Van Speybroeck, Johan M. Winne, and Filip E. Du Prez. 2014. 'Triazolinediones enable ultrafast and reversible click chemistry for the design of dynamic polymer systems', *Nat Chem*, 6: 815-21.

Biswas, Atanu, H. N. Cheng, Sanghoon Kim, and Zengshe Liu. 2014. 'Modified Triglyceride Oil Through Reactions with Phenyltriazolinedione', *Journal of the American Oil Chemists' Society*, 91: 125-31.

Biswas, Atanu, Brajendra K. Sharma, J. L. Willett, Atanu Advaryu, S. Z. Erhan, and H. N. Cheng. 2008. 'Azide Derivatives of Soybean Oil and Fatty Esters', *Journal of Agricultural and Food Chemistry*, 56: 5611-16.

Boutelle, Robert C., and Brian H. Northrop. 2011. 'Substituent Effects on the Reversibility of Furan–Maleimide Cycloadditions', *Journal of Organic Chemistry*, 76: 7994-8002.

Bueno-Ferrer, Carmen, Elodie Hablot, María del Carmen Garrigós, Sergio Bocchini, Luc Averous, and Alfonso Jiménez. 2012. 'Relationship between morphology, properties and degradation parameters of novative biobased thermoplastic polyurethanes obtained from dimer fatty acids', *Polymer Degradation and Stability*, 97: 1964-69.

Bueno-Ferrer, Carmen, Elodie Hablot, Florence Perrin-Sarazin, M. Carmen Garrigós, Alfonso Jiménez, and Luc Averous. 2012. 'Structure and Morphology of New Bio-Based Thermoplastic Polyurethanes Obtained From Dimeric Fatty Acids', *Macromolecular Materials and Engineering*, 297: 777-84.

Buono, Pietro, Antoine Duval, Luc Averous, and Youssef Habibi. 2017. 'Thermally healable and remendable lignin-based materials through Diels – Alder click polymerization', *Polymer*, 133: 78-88.

Buono, Pietro, Antoine Duval, Luc Avérous, and Youssef Habibi. 2018. 'Clicking Biobased Polyphenols: A Sustainable Platform for Aromatic Polymeric Materials', *Chemsuschem*, 11: 2472-91.

Calle, Mariola, Gerard Lligadas, Juan Ronda, Marina Galià, and Virginia Cadiz. 2016. 'Non-Isocyanate Route to Biobased Polyurethanes and Polyureas via AB-type Self-Polycondensation', *European Polymer Journal*, 84: 837-48.

Canary, Stephen A., and Malcolm P. Stevens. 1992. 'Thermally reversible crosslinking of polystyrene via the furan–maleimide Diels–Alder reaction', *Journal of Polymer Science Part A: Polymer Chemistry,* 30: 1755-60.

Cardoso, Priscilla B., Thiago O. Machado, Paulo E. Feuser, Claudia Sayer, Michael A. R. Meier, and Pedro H. H. Araújo. 2018. 'Biocompatible Polymeric Nanoparticles From Castor Oil Derivatives via Thiol-Ene Miniemulsion Polymerization', *Eur. J. Lipid Sci. Technol*., 120: 1700212.

Carré, Camille, Yvan Ecochard, Sylvain Caillol, and Luc Averous. 2019. 'From the synthesis of biobased cyclic carbonate to polyhydroxyurethanes: a promising route towards renewable non-isocyanate polyurethanes', *Chemsuschem*, 12: 3410.

Charlon, M., B. Heinrich, Y. Matter, E. Couzigné, B. Donnio, and L. Avérous. 2014. 'Synthesis, structure and properties of fully biobased thermoplastic polyurethanes, obtained from a diisocyanate based on modified dimer fatty acids, and different renewable diols', *European Polymer Journal*, 61: 197-205.

Chattopadhyay, Subrata, and Filip Du Prez. 2016. 'Simple design of chemically crosslinked plant oil nanoparticles by triazolinedione-ene chemistry', *European Polymer Journal*, 81: 77-85.

Chen, Xiangxu, Matheus A. Dam, Kanji Ono, Ajit Mal, Hongbin Shen, Steven R. Nutt, Kevin Sheran, and Fred Wudl. 2002. 'A Thermally Re-mendable Cross-Linked Polymeric Material', *Science*, 295: 1698-702.

Claudino, Mauro. 2011. 'Thiol–ene Coupling of Renewable Monomers: at the forefront of bio-based polymeric materials'.

Comi, M., G. Lligadas, J. C. Ronda, M. Galia, and V. Cadiz. 2016. 'Synthesis of castor-oil based polyurethanes bearing alkene/alkyne groups and subsequent thiol-ene/yne post-modification', *Polymer*, 103: 163-70.

Cookson, R. C., S. S. H. Gilani, and I. D. R. Stevens. 1962. '4-Phenyl-1,2,4-triazolin-3,5-dione: a powerful dienophile', *Tetrahedron Letters*, 3: 615-18.

Cookson, R. C., S. S. H. Gilani, and I. D. R. Stevens. 1967. 'Diels–Alder reactions of 4-phenyl-1,2,4-triazoline-3,5-dione', *J. Chem. Soc. C*, 0: 1905-09.

Corma, Avelino, Sara Iborra, and Alexandra Velty. 2007. 'Chemical Routes for the Transformation of Biomass into Chemicals'*, Chemical Reviews*, 107: 2411-502.

Cornille, Adrien, Rémi Auvergne, Oleg Figovsky, Bernard Boutevin, and Sylvain Caillol. 2017. 'A perspective approach to sustainable routes for non-isocyanate polyurethanes', *European Polymer Journal*, 87: 535-52.

Cornille, Adrien, Vincent Froidevaux, Claire Negrell, Sylvain Caillol, and Bernard Boutevin. 2014. 'Thiol-ene coupling: An efficient tool for the synthesis of new biobased aliphatic amines for epoxy curing', *Polymer*, 55: 5561-70.

Council, American Chemistry. 2017. 'U.S. Resin Production and Sales', Accessed 19/11/2019. https://plastics.americanchemistry.com/PlasticsStatistics/ACC-PIPS-Year-End-2017-Resin-Stats-vs-2016.pdf.

Dannecker, Patrick-Kurt, Ursula Biermann, Alexandra Sink, Fabian R. Bloesser, Jürgen O. Metzger, and Michael A. R. Meier. 2019. 'Fatty Acid–Derived Aliphatic Long Chain Polyethers by a Combination of Catalytic Ester Reduction and ADMET or Thiol-Ene Polymerization', *Macromol. Chem, Phys.*, 220: 1800440.

Das, Sudipto, David F. Cox, Garth L. Wilkes, Derek B. Klinedinst, Iskender Yilgor, Emel Yilgor, and Frederick L. Beyer. 2007. 'Effect of Symmetry and H-bond Strength of Hard Segments on the Structure-Property Relationships of Segmented, Nonchain Extended Polyurethanes and Polyureas', *Journal of Macromolecular Science, Part B*, 46: 853-75.

De Bruycker, Kevin, Stijn Billiet, Hannes A. Houck, Subrata Chattopadhyay, Johan M. Winne, and Filip E. Du Prez. 2016. 'Triazolinediones as Highly Enabling Synthetic Tools', Chemical *Reviews*, 116: 3919-74.

de Espinosa, L. M., and M. A. R. Meier. 2011. 'Plant oils: The perfect renewable resource for polymer science?!', *European Polymer Journal*, 47: 837-52.

Denissen, Wim, Johan M. Winne, and Filip E. Du Prez. 2016. 'Vitrimers: permanent organic networks with glass-like fluidity', *Chemical Science*, 7: 30-38.

Desroches, M., S. Caillol, R. Auvergne, and B. Boutevin. 2012. 'Synthesis of pseudo-telechelic diols by transesterification and thiol-ene coupling', *European Journal of Lipid Science and Technology*, 114: 84-91.

Desroches, M., M. Escouvois, R. Auvergne, S. Caillol, and B. Boutevin. 2012. 'From Vegetable Oils to Polyurethanes: Synthetic Routes to Polyols and Main Industrial Products', *Polymer Reviews*, 52: 38-79.

Dhers, Sébastien, Ghislaine Vantomme, and Luc Avérous. 2019. 'A fully bio-based polyimine vitrimer derived from fructose', *Green Chemistry*, 21: 1596-601.

Diels, Otto, and Kurt Alder. 1931. 'Synthesen in der hydroaromatischen Reihe. VIII. Mitteilung: Dien-Synthesen des Anthracens. Anthracen-Formel', *Justus Liebigs Annalen der Chemie*, 486: 191-202.

Diels, Otto, Jacob Hansen Blom, and Werner Koll. 1925. 'Über das aus Cyclopentadien und Azoester entstehende Endomethylen-piperidazin und seine Überführung in 1,3-Diamino-cyclopentan', *Justus Liebigs Annalen der Chemie*, 443: 242-62.

Dolci, E., V. Froidevaux, G. Michaud, F. Simon, R. Auvergne, S. Fouquay, and S. Caillol. 2017. 'Thermoresponsive crosslinked isocyanate-free polyurethanes by Diels-Alder polymerization', *Journal of Applied Polymer Science*, 134: 44408.

Dolci, Elena, Guillaume Michaud, Frédéric Simon, Bernard Boutevin, Stéphane Fouquay, and Sylvain Caillol. 2015. 'Remendable thermosetting polymers for isocyanate-free adhesives: a preliminary study', *Polymer Chemistry*, 6: 7851-61.

Du, P. F., H. Y. Jia, Q. H. Chen, Z. Zheng, X. L. Wang, and D. L. Chen. 2016. 'Slightly crosslinked polyurethane with Diels-Alder adducts from trimethylolpropane', *Journal of Applied Polymer Science*, 43971.

Duarte, Martín E., Birgit Huber, Patrick Theato, and Hatice Mutlu. 2020. 'The unrevealed potential of elemental sulfur for the synthesis of high sulfur content bio-based aliphatic polyesters', *Polymer Chemistry*, 11: 241-48.

Dumont, Marie-Josée. 2016. 'Polymeric Products Derived From Industrial Oils for Paints, Coatings, and Other Applications', *Industrial Oil Crops*, 3: 895-905.

Durand, Pierre-Luc, Antoine Brège, Guillaume Chollet, Etienne Grau, and Henri Cramail. 2018. 'Simple and Efficient Approach toward Photosensitive Biobased Aliphatic Polycarbonate Materials', *ACS Macro Letters*, 7: 250-54.

Durand, Pierre-Luc, Guillaume Chollet, Etienne Grau, and Henri Cramail. 2019. 'Versatile cross-linked fatty acid-based polycarbonate networks obtained by thiol–ene coupling reaction', *RSC Advances*, 9: 145-50.

Duval, A., G. Couture, S. Caillol, and L. Averous. 2017. 'Biobased and Aromatic Reversible Thermoset Networks from Condensed Tannins via the Diels-Alder Reaction', *ACS Sustainable Chemistry & Engineering*, 5: 1199-207.

Duval, Antoine, Heiko Lange, Martin Lawoko, and Claudia Crestini. 2015. 'Reversible crosslinking of lignin via the furan-maleimide Diels-Alder reaction', *Green Chemistry*, 17: 4991-5000.

Espinosa, Juan P., Vivina Hanazumi, Pablo M. Stefani, and Roxana A. Ruseckaite. 2020. 'Curing behavior and properties of high biosourced epoxy resin blends based on a triepoxy monomer and a tricarboxylic acid hardener from 10-undecenoic acid', *Polymer Testing*, 81: 106208.

Fairbanks, Benjamin D., Timothy F. Scott, Christopher J. Kloxin, Kristi S. Anseth, and Christopher N. Bowman. 2009. 'Thiol-Yne Photopolymerizations: Novel Mechanism, Kinetics, and Step-Growth Formation of Highly Cross-Linked Networks', *Macromolecules*, 42: 211-17.

Feng, Yechang, Haiyan Liang, Ziming Yang, Teng Yuan, Ying Luo, Puwang Li, Zhuohong Yang, and Chaoqun Zhang. 2017. 'A Solvent-Free and Scalable Method To Prepare Soybean-Oil-Based Polyols by Thiol–Ene Photo-Click Reaction and Biobased Polyurethanes Therefrom', *ACS Sustainable Chemistry & Engineering*, 5: 7365-73.

Feng, Zhanbin, Jing Hu, Bing Yu, Hongchi Tian, Hongli Zuo, Nanying Ning, Ming Tian, and Liqun Zhang. 2019. 'Environmentally Friendly Method To Prepare Thermo-Reversible, Self-Healable Biobased Elastomers by One-Step Melt Processing', *ACS Applied Polymer Materials*, 1: 169-77.

Finnveden, Maja, Sara Brännström, Mats Johansson, Eva Malmström, and Mats Martinelle. 2018. 'Novel sustainable synthesis of vinyl ether ester building blocks, directly from carboxylic acids and the corresponding hydroxyl vinyl ether, and their photopolymerization', *RSC Advances*, 8: 24716-23.

Finnveden, Maja, Peter Hendil-Forssell, Mauro Claudino, Mats Johansson, and Mats Martinelle. 2019. 'Lipase-Catalyzed Synthesis of Renewable Plant Oil-Based Polyamides', *Polymers*, 11: 1730.

Floros, Michael C., Alcides Lopes Leão, and Suresh S. Narine. 2014. 'Vegetable oil derived solvent, and catalyst free "click chemistry" thermoplastic polytriazoles', *BioMed Research International*, 2014: 792901.

Fortman, D. J., J. P. Brutman, G. X. De Hoe, R. L. Snyder, W. R. Dichtel, and M. A. Hillmyer. 2018. 'Approaches to Sustainable and Continually Recyclable Cross-Linked Polymers', *ACS Sustainable Chemistry & Engineering*, 6: 11145-59.

Frias, Célia F., Ana C. Fonseca, Jorge F. J. Coelho, and Arménio C. Serra. 2015. 'Straightforward functionalization of acrylated soybean oil by Michael-addition and Diels–Alder reactions', *Industrial Crops and Products*, 64: 33-38.

Froidevaux, V, M Borne, E Laborbe, R Auvergne, A Gandini, and B Boutevin. 2015. 'Study of the Diels–Alder and retro-Diels–Alder reaction between furan derivatives and maleimide for the creation of new materials', *RSC Advances*, 5: 37742-54.

Fu, Changqing, Jiancheng Liu, Hongying Xia, and Liang Shen. 2015. 'Effect of structure on the properties of polyurethanes based on aromatic cardanol-based polyols prepared by thiol-ene coupling', Progress in Organic Coatings, 83: 19-25.

Fu, Changqing, Jiahui Wang, Lie Chen, and Liang Shen. 2019. 'Synthesis of a Fully Biobased Polyfunctional Vinyl Oligomer and Their UV Cured Films Prepared via Thiol-ene Coupling', *Journal of Renewable Materials*, 7: 795-805.

Fu, Changqing, Zhe Yang, Zitong Zheng, and Liang Shen. 2014. 'Properties of alkoxysilane castor oil synthesized via thiol-ene and its polyurethane/siloxane hybrid coating films', *Progress in Organic Coatings*, 77: 1241-48.

Fu, Changqing, Zitong Zheng, Zhe Yang, Yiwang Chen, and Liang Shen. 2014. 'A fully bio-based waterborne polyurethane dispersion from vegetable oils: From synthesis of precursors by thiol-ene reaction to study of final material', *Progress in Organic Coatings*, 77: 53-60.

Gallart-Sirvent, Pau, Anlong Li, Kaichang Li, Gemma Villorbina, and Ramon Canela-Garayoa. 2017. 'Preparation of pressure-sensitive adhesives from tung oil via Diels-Alder reaction', *International Journal of Adhesion and Adhesives*, 78: 67-73.

Gandini, A., D. Coelho, and A. J. D. Silvestre. 2008. 'Reversible click chemistry at the service of macromolecular materials. Part 1: Kinetics of the Diels-Alder reaction applied to furan-maleimide model compounds and linear polymerizations', *European Polymer Journal*, 44: 4029-36.

Gandini, A., A. J. D. Silvestre, and D. Coelho. 2011. 'Reversible click chemistry at the service of macromolecular materials', *Polymer Chemistry*, 2: 1713-19.

Gandini, Alessandro. 2013. 'The furan/maleimide Diels–Alder reaction: A versatile click–unclick tool in macromolecular synthesis', *Progress in Polymer Science*, 38: 1-29.

Gandini, Alessandro, Antonio J. F. Carvalho, Eliane Trovatti, Ricardo K. Kramer, and Talita M. Lacerda. 2018. 'Macromolecular materials based on the application of the Diels–Alder reaction to natural polymers and plant oils', *European Journal of Lipid Science and Technology*, 120: 1700091.

Gandini, Alessandro, and Talita Lacerda. 2018. Polymers from Plant Oils (Scrivener Publishing: Beverly, MA, USA).

Gandini, Alessandro, Talita M Lacerda, and Antonio JF Carvalho. 2013. 'A straightforward double coupling of furan moieties onto epoxidized triglycerides: synthesis of monomers based on two renewable resources', *Green Chemistry*, 15: 1514-19.

Gandini, Alessandro, Talita M. Lacerda, Antonio J. F. Carvalho, and Eliane Trovatti. 2016. 'Progress of Polymers from Renewable Resources: Furans, Vegetable Oils, and Polysaccharides', *Chemical Reviews*, 116: 1637-69.

Gandini, Alessandro, Armando J. D. Silvestre, and Dora Coelho. 2010. 'Reversible click chemistry at the service of macromolecular materials. 2. Thermoreversible polymers based on the Diels-Alder reaction of an A-B furan/maleimide monomer', *Journal of Polymer Science Part A: Polymer Chemistry*, 48: 2053-56.

García-Astrain, C., A. Gandini, D. Coelho, I. Mondragon, A. Retegi, A. Eceiza, M. A. Corcuera, and N. Gabilondo. 2013. 'Green chemistry for the synthesis of methacrylate-based hydrogels crosslinked through Diels–Alder reaction', *European Polymer Journal*, 49: 3998-4007.

García-Astrain, Clara, and Luc Avérous. 2018. 'Synthesis and evaluation of functional alginate hydrogels based on click chemistry for drug delivery applications', *Carbohydrate Polymers*, 190: 271-80.

García-Astrain, Clara, and Luc Avérous. 2019. 'Synthesis and behavior of click cross-linked alginate hydrogels: Effect of cross-linker length and functionality', *International Journal of Biological Macromolecules,* 137: 612-19.

García Astrain, Clara, Rebeca Hernandez, Olatz Guaresti, Ljiljana Fruk, Carmen Mijangos, Arantxa Eceiza, and Nagore Gabilondo. 2016. 'Click Crosslinked Chitosan/Gold Nanocomposite Hydrogels', *Macromol. Mater. Eng.,* 301: 1295-1300

Gerpen, Jon Van. 2005. 'Biodiesel processing and production', *Fuel Processing Technolog*y, 86: 1097-107.

Gheneim, R., C. Perez-Berumen, and A. Gandini. 2002. 'Diels-Alder reactions with novel polymeric dienes and dienophiles: Synthesis of reversibly cross-linked elastomers', Macromolecules, 35: 7246-53.

Gholami, Hoshyar, Hamid Yeganeh, Saeed Beigi Burujeny, Marziyeh Sorayya, and Elias Shams. 2018. 'Vegetable Oil Based Polyurethane Containing 1,2,3-Triazolium Functional Groups as Antimicrobial Wound Dressing', *Journal of Polymers and the Environment,* 26: 462-73.

Gholami, Hoshyar, Hamid Yeganeh, Reza Gharibi, Mehrdad Jalilian, and Marziyeh Sorayya. 2015. 'Catalyst free-click polymerization: A versatile method for the preparation of soybean oil based poly1,2,3-triazoles as coatings with efficient biocidal activity and excellent cytocompatibility', *Polymer*, 62: 94-108.

Goethals, Fabienne, Steven Martens, Pieter Espeel, Otto van den Berg, and Filip E. Du Prez. 2014. 'Diversely Substituted Polyamide Structures through Thiol–Ene Polymerization of Renewable Thiolactone Building Blocks', *Macromolecules*, 47: 61-69.

Gonzalez-Paz, R. J., G. Lligadas, J. C. Ronda, M. Galia, and V. Cadiz. 2013. 'Thiol-yne Reaction of Alkyne-derivatized Fatty Acids: Thiol-Reactive Linear Polyurethane', *Journal of Renewable Materials,* 1: 187-94.

González-Paz, Rodolfo J., Gerard Lligadas, Juan C. Ronda, Marina Galià, and Virginia Cádiz. 2012. 'Thiol–yne reaction of alkyne-derivatized fatty acids: biobased polyols and cytocompatibility of derived polyurethanes', *Polymer Chemistry*, 3: 2471-78.

González-Paz, Rodolfo J., Gerard Lligadas, Juan C. Ronda, Marina Galià, Ana M. Ferreira, Francesca Boccafoschi, Gianluca Ciardelli, and Virginia Cádiz. 2012. 'Enhancement of Fatty Acid-based Polyurethanes Cytocompatibility by Non-covalent Anchoring of Chondroitin Sulfate', *Macromolecular Bioscience*, 12: 1697-705.

González, Kizkitza, Clara García-Astrain, Arantzazu Santamaria-Echart, Lorena Ugarte, Luc Avérous, Arantxa Eceiza, and Nagore Gabilondo. 2018. 'Starch/graphene hydrogels via click chemistry with relevant electrical and antibacterial properties'*, Carbohydrate Polymers*, 202: 372-81.

Gousse, C., A. Gandini, and P. Hodge. 1998. 'Application of the Diels-Alder reaction to polymers bearing furan moieties. 2. Diels-Alder and retro-Diels-Alder reactions involving furan rings in some styrene copolymers', *Macromolecules*, 31: 314-21.

Gu, Lin, and Qing-Yun Wu. 2018. 'Recyclable bio-based crosslinked polyurethanes with self-healing ability', *Journal of Applied Polymer Science*, 135: 46272.

Guaresti, O., C. García–Astrain, R. H. Aguirresarobe, A. Eceiza, and N. Gabilondo. 2018. 'Synthesis of stimuli–responsive chitosan–based hydrogels by Diels–Alder cross–linking `click´ reaction as potential carriers for drug administration', *Carbohydrate Polymers*, 183: 278-86.

Guaresti, Olatz, Clara García Astrain, Leire Urbina, Arantxa Eceiza, and Nagore Gabilondo. 2018. 'Reversible swelling behaviour of Diels-Alder clicked chitosan hydrogels in response to pH changes', *Express Polymer Letters*, 13: 27-36.

Hablot, Elodie, Bertrand Donnio, Michel Bouquey, and Luc Avérous. 2010. 'Dimer acid-based thermoplastic bio-polyamides: Reaction kinetics, properties and structure', *Polymer*, 51: 5895-902.

Hablot, Elodie, Dan Zheng, Michel Bouquey, and Luc Avérous. 2008. 'Polyurethanes Based on Castor Oil: Kinetics, Chemical, Mechanical and Thermal Properties', *Macromolecular Materials and Engineering*, 293: 922-29.

Haponiuk, Józef T., and Krzysztof Formela. 2017. 'Chapter 1 - PU Polymers, Their Composites, and Nanocomposites: State of the Art and New Challenges.' in Sabu Thomas, Janusz Datta, Józef T. Haponiuk and Arunima Reghunadhan (eds.), Polyurethane Polymers (Elsevier: Amsterdam).

Hazer, Baki. 2015. 'Simple synthesis of amphiphilic poly(3-hydroxy alkanoate)s with pendant hydroxyl and carboxylic groups via thiol-ene photo click reactions', *Polymer Degradation and Stability*, 119: 159-66.

He, Minghui, Shun Jiang, Ruixin Xu, Jianwen Yang, Zhaohua Zeng, and Guangxue Chen. 2014. 'Facile functionalization of soybean oil by thiol-ene photo-click reaction for the synthesis of polyfunctional acrylate', *Progress in Organic Coatings,* 77: 868-71.

Heo, Yunseon, and Henry A. Sodano. 2014. 'Self-Healing Polyurethanes with Shape Recovery', *Advanced Functional Materials*, 24: 5261-68.

Hong, Jian, Qiang Luo, and Bipin K. Shah. 2010. 'Catalyst- and Solvent-Free “Click” Chemistry: A Facile Approach to Obtain Cross-Linked Biopolymers from Soybean Oil', *Biomacromolecules*, 11: 2960-65.

Hong, Jian, Qiang Luo, Xianmei Wan, Zoran S. Petrović, and Bipin K. Shah. 2012. 'Biopolymers from Vegetable Oils via Catalyst- and Solvent-Free “Click” Chemistry: Effects of Cross-Linking Density', *Biomacromolecules*, 13: 261-66.

Hong, Jian, Dragana Radojčić, Djavan Hairabedian, Xianmei Wan, and Zoran S. Petrović. 2015. 'Alkynated and azidated octadecane as model compounds for kinetic studies of Huisgen 1,3-dipolar cycloaddition in vegetable oils', *European Journal of Lipid Science and Technology*, 117: 266-70.

Hoogenboom, Richard. 2010. 'Thiol–Yne Chemistry: A Powerful Tool for Creating Highly Functional Materials', *Angewandte Chemie International Edition*, 49: 3415-17.

Hoyle, Charles E., and Christopher N. Bowman. 2010. 'Thiol–Ene Click Chemistry', *Angewandte Chemie International Edition*, 49: 1540-73.

Hu, Jianqing, Kaimei Peng, Jinshan Guo, Dingying Shan, Gloria B. Kim, Qiyao Li, Ethan Gerhard, Liang Zhu, Weiping Tu, Weizhong Lv, Michael A. Hickner, and Jian Yang. 2016. 'Click Cross-Linking-Improved Waterborne Polymers for Environment-Friendly Coatings and Adhesives', *ACS Applied Materials & Interfaces,* 8: 17499-510.

Hu, Sumeng, Xi Chen, and John M. Torkelson. 2019. 'Biobased Reprocessable Polyhydroxyurethane Networks: Full Recovery of Crosslink Density with Three Concurrent Dynamic Chemistries', *ACS Sustainable Chemistry & Engineering*, 7: 10025-34.

Huang, Kun, Zengshe Liu, Jinwen Zhang, Shouhai Li, Mei Li, Jianling Xia, and Yonghong Zhou. 2014. 'Epoxy Monomers Derived from Tung Oil Fatty Acids and Its Regulable Thermosets Cured in Two Synergistic Ways', *Biomacromolecules*, 15: 837-43.

Huang, Kun, Zengshe Liu, Jinwen Zhang, Shouhai Li, Mei Li, Jianling Xia, and Yonghong Zhou. 2015. 'A self-crosslinking thermosetting monomer with both epoxy and anhydride groups derived from tung oil fatty acids: Synthesis and properties', *European Polymer Journal*, 70: 45-54.

Huang, Kun, Pei Zhang, Jinwen Zhang, Shouhai Li, Mei Li, Jianling Xia, and Yonghong Zhou. 2013. 'Preparation of biobased epoxies using tung oil fatty acid-derived C21 diacid and C22 triacid and study of epoxy properties', *Green Chemistry*, 15: 2466-66.

Huang, Yugang, Laixing Pang, Hongliang Wang, Rong Zhong, Zhaohua Zeng, and Jianwen Yang. 2013. 'Synthesis and properties of UV-curable tung oil based resins via modification of Diels–Alder reaction, nonisocyanate polyurethane and acrylates', *Progress in Organic Coatings*, 76: 654-61.

Ionescu, M. 2005. Chemistry and Technology of Polyols for Polyurethanes. Milhail Ionescu. Rapra Technology, Shrewsbury, UK. Polym. Int.

Ionescu, Mihail, Dragana Radojčić, Xianmei Wan, Zoran S. Petrović, and Thomas A. Upshaw. 2015. 'Functionalized vegetable oils as precursors for polymers by thiol-ene reaction', *European Polymer Journal*, 67: 439-48.

Iqbal, Muhammad, Remco Knigge, Hero Heeres, Antonius Broekhuis, and Francesco Picchioni. 2018. 'Diels–Alder-Crosslinked Polymers Derived from Jatropha Oil', *Polymers*, 10: 1177-77.

Irusta, L., M. J. Fernandez-Berridi, and J. Aizpurua. 2017. 'Polyurethanes based on isophorone diisocyanate trimer and polypropylene glycol crosslinked by thermal reversible diels alder reactions', *Journal of Applied Polymer Science*, 134: 44543.

Jeppesen, Jacob Benjamin, Jean-Francois Devaux, and Jean-Luc Dubois. 2015. "Five Novel Bio Based Diesels Tested in a Light-Duty Road Going Engine." In.: SAE International.

Jia, Puyou, Yufeng Ma, Haoyu Xia, Minrui Zheng, Guodong Feng, Lihong Hu, Meng Zhang, and Yonghong Zhou. 2018. 'Clean Synthesis of Epoxidized Tung Oil Derivatives via Phase Transfer Catalyst and Thiol–ene Reaction: A Detailed Study', ACS Sustainable Chemistry & Engineering, 6: 13983-94.

Kade, Matthew J., Daniel J. Burke, and Craig J. Hawker. 2010. 'The power of thiol-ene chemistry', *Journal of Polymer Science Part A: Polymer Chemistry*, 48: 743-50.

Kim, Cheal, Teddy G. Traylor, and Charles L. Perrin. 1998. 'MCPBA Epoxidation of Alkenes: Reinvestigation of Correlation between Rate and Ionization Potential', *Journal of the American Chemical Society*, 120: 9513-16.

Kloxin, Christopher J., Timothy F. Scott, Brian J. Adzima, and Christopher N. Bowman. 2010. 'Covalent Adaptable Networks (CANs): A Unique Paradigm in Cross-Linked Polymers', *Macromolecules*, 43: 2643-53.

Koenig, N. H., and Daniel Swern. 1957. 'Organic Sulfur Derivatives. I. Addition of Mercaptoacetic Acid to Long-chain Monounsaturated Compounds', Journal of the American Chemical Society, 79: 362-65.

Kolb, Hartmuth C., M. G. Finn, and K. Barry Sharpless. 2001. 'Click Chemistry: Diverse Chemical Function from a Few Good Reactions', *Angewandte Chemie International Edition*, 40: 2004-21.

Konkolewicz, Dominik, Angus Gray-Weale, and Sébastien Perrier. 2009. 'Hyperbranched Polymers by Thiol−Yne Chemistry: From Small Molecules to Functional Polymers', *Journal of the American Chemical Society*, 131: 18075-77.

Korntner, Philipp, Ivan Sumerskii, Markus Bacher, Thomas Rosenau, and Antje Potthast. 2015. 'Characterization of technical lignins by NMR spectroscopy: optimization of functional group analysis by 31P NMR spectroscopy', *Holzforschung*, 69: 807-14.

Kwart, Harold, and Isabel Burchuk. 1952. 'Isomerism and Adduct Stability in the Diels—Alder Reaction.1a I. The Adducts of Furan and Maleimide', *Journal of the American Chemical Society*, 74: 3094-97.

Lacerda, T. M., A. J. F. Carvalho, and A. Gandini. 2014. 'Two alternative approaches to the Diels-Alder polymerization of tung oil', *RSC Advances*, 4: 26829-37.

Lacerda, T. M., and A. Gandini. 2014. 'Marriage of Furans and Vegetable Oils through Click Chemistry for the Preparation of Macromolecular Materials: A Succinct Review', *Journal of Renewable Materials,* 2: 2-12.

Lacerda, Talita M., Antonio J. F. Carvalho, and Alessandro Gandini. 2016. 'A minimalist furan–maleimide AB-type monomer and its thermally reversible Diels–Alder polymerization', *RSC Advances*, 6: 45696-700.

Lakatos, C., K. Czifrak, J. Karger-Kocsis, L. Daroczi, M. Zsuga, and S. Keki. 2016. 'Shape memory crosslinked polyurethanes containing thermoreversible Diels-Alder couplings', Journal of Applied Polymer Science, 133: 44145.

Lamarzelle, Océane, Geoffrey Hibert, Sébastien Lecommandoux, Etienne Grau, and Henri Cramail. 2017. 'A thioglycerol route to bio-based bis-cyclic carbonates: poly(hydroxyurethane) preparation and post-functionalization'*, Polymer Chemistry*, 8: 3438-47.

Laurichesse, Stéphanie, and Luc Avérous. 2014. 'Chemical modification of lignins: Towards biobased polymers', *Progress in Polymer Science,* 39: 1266-90.

Ligthelm, S. P., E. von Rudloff, and Donald A. Sutton. 1950. '622. Preparation of unsaturated long-chain alcohols by means of lithium aluminium hydride: some typical members of the series', *Journal of the Chemical Society (Resumed):* 3187-90.

Liu, Chengguo, Wen Lei, Zhengchun Cai, Jianqiang Chen, Lihong Hu, Yan Dai, and Yonghong Zhou. 2013. 'Use of tung oil as a reactive toughening agent in dicyclopentadiene-terminated unsaturated polyester resins', *Industrial Crops and Products*, 49: 412-18.

Liu, Chengguo, Zengshe Liu, Brent H. Tisserat, Rongpeng Wang, Thomas P. Schuman, Yonghong Zhou, and Lihong Hu. 2015. 'Microwave-assisted maleation of tung oil for bio-based products with versatile applications', Industrial Crops and Products, 71: 185-96.

Lligadas, G. 2013. 'Renewable Polyols for Polyurethane Synthesis via Thiol-ene/yne Couplings of Plant Oils', Macromolecular Chemistry and Physics, 214: 415-22.

Lligadas, G., J. C. Ronda, M. Galià, U. Biermann, and J. O. Metzger. 2006. 'Synthesis and characterization of polyurethanes from epoxidized methyl oleate based polyether polyols as renewable resources', *Journal of Polymer Science Part A: Polymer Chemistry,* 44: 634-45.

Lligadas, G., J. C. Ronda, M. Galia, and V. Cadiz. 2013. 'Renewable polymeric materials from vegetable oils: a perspective', *Materials Today,* 16: 337-43.

Lligadas, Gerard, Joan C. Ronda, Marina Galià, and Virginia Cádiz. 2007. 'Polyurethane Networks from Fatty-Acid-Based Aromatic Triols: Synthesis and Characterization', *Biomacromolecules*, 8: 1858-64.

Lligadas, Gerard, Juan C. Ronda, Marina Galià, and Virginia Cádiz. 2013. 'Monomers and polymers from plant oils via click chemistry reactions', *Journal of Polymer Science Part A: Polymer Chemistry*, 51: 2111-24.

Lluch, Cristina, Braulio Esteve-Zarzoso, Albert Bordons, Gerard Lligadas, Juan C. Ronda, Marina Galià, and Virginia Cádiz. 2014. 'Antimicrobial Polyurethane Thermosets Based on Undecylenic Acid: Synthesis and Evaluation'*, Macromolecular Bioscience*, 14: 1170-80.

Lu, Yongshang, and Richard C. Larock. 2009. 'Novel Polymeric Materials from Vegetable Oils and Vinyl Monomers: Preparation, Properties, and Applications', *Chemsuschem*, 2: 136-47.

Ma, Guozhang, Tong Zhang, Jianbing Wu, Caiying Hou, Lixia Ling, and Baojun Wang. 2013. 'Preparation and properties of glycerin ester of tung oil modified rosin'*, Journal of Applied Polymer Science*, 130: 1700-06.

Machado, Thiago O., Priscilla B. Cardoso, Paulo Emilio Feuser, Claudia Sayer, and Pedro H. H. Araújo. 2017. 'Thiol-ene miniemulsion polymerization of a biobased monomer for biomedical applications', *Colloids and Surfaces B: Biointerfaces*, 159: 509-17.

Maisonneuve, Lise, Anne-Laure Wirotius, Carine Alfos, Etienne Grau, and Henri Cramail. 2014. 'Fatty acid-based (bis) 6-membered cyclic carbonates as efficient isocyanate free poly(hydroxyurethane) precursors', *Polymer Chemistry*, 5: 6142-47.

Maiti, Binoy, Sonu Kumar, and Priyadarsi De. 2014. 'Controlled RAFT synthesis of side-chain oleic acid containing polymers and their post-polymerization functionalization', *RSC Advances*, 4: 56415-23.

Mangeon, Carine, France Thevenieau, Estelle Renard, and Valérie Langlois. 2017. 'Straightforward Route To Design Biorenewable Networks Based on Terpenes and Sunflower Oil', *ACS Sustainable Chemistry & Engineering*, 5: 6707-15.

Meier, Michael A. R., Jurgen O. Metzger, and Ulrich S. Schubert. 2007. 'Plant oil renewable resources as green alternatives in polymer science', *Chemical Society Reviews,* 36: 1788-802.

Miao, Shida, Ping Wang, Zhiguo Su, and Songping Zhang. 2014. 'Vegetable-oil-based polymers as future polymeric biomaterials', *Acta Biomaterialia*, 10: 1692-704.

Montarnal, D., M. Capelot, F. Tournilhac, and L. Leibler. 2011. 'Silica-Like Malleable Materials from Permanent Organic Networks', *Science*, 334: 965-68.

Montero de Espinosa, L., J. C. Ronda, M. Galià, and V. Cádiz. 2008. 'A new enone-containing triglyceride derivative as precursor of thermosets from renewable resources', *Journal of Polymer Science Part A: Polymer Chemistry,* 46: 6843-50.

Montero de Espinosa, Lucas, Andreas Gevers, Benjamin Woldt, Michael Graß, and Michael A. R. Meier. 2014. 'Sulfur-containing fatty acid-based plasticizers via thiol–ene addition and oxidation: synthesis and evaluation in PVC formulations', *Green Chemistry*, 16: 1883-96.

Moreno, Maryluz, Gerard Lligadas, Juan C. Ronda, Marina Galià, and Virginia Cádiz. 2014. 'Polyketoesters from oleic acid. Synthesis and functionalization', *Green Chemistry,* 16: 1847-53.

Moser, Bryan R., Kenneth M. Doll, and Steven C. Peterson. 2019. 'Renewable Poly(Thioether-Ester)s from Fatty Acid Derivatives via Thiol-Ene Photopolymerization', *Journal of the American Oil Chemists' Society*, 96: 825-37.

Moses, John E., and Adam D. Moorhouse. 2007. 'The growing applications of click chemistry', *Chemical Society Reviews,* 36: 1249-62.

Mubofu, Egid B. 2016. 'Castor oil as a potential renewable resource for the production of functional materials', *Sustainable Chemical Processes,* 4: 11.

Muthusamy, Kumarasamy, Krishnamoorthy Lalitha, Yadavali Siva Prasad, Ayyapillai Thamizhanban, Vellaisamy Sridharan, C. Uma Maheswari, and Subbiah Nagarajan. 2018. 'Lipase-Catalyzed Synthesis of Furan-Based Oligoesters and their Self-Assembly-Assisted Polymerization', *ChemSusChem*, 11: 2453-63.

Nalawade, Priyanka P., Brinda Mehta, Coleen Pugh, and Mark D. Soucek. 2014. 'Modified soybean oil as a reactive diluent: Synthesis and characterization', *Journal of Polymer Science Part A: Polymer Chemistry,* 52: 3045-59.

Nguyen, Phan Huy, Steven Spoljaric, and Jukka Seppälä. 2018. 'Renewable polyamides via thiol-ene ‘click’ chemistry and long-chain aliphatic segments', *Polymer,* 153: 183-92.

Obadia, Mona M., Antoine Jourdain, Philippe Cassagnau, Damien Montarnal, and Eric Drockenmuller. 2017. 'Tuning the Viscosity Profile of Ionic Vitrimers Incorporating 1,2,3-Triazolium Cross-Links', *Advanced Functional Materials*, 27: 1703258.

Omrani, Ismail, Abdolreza Farhadian, Niloofar Babanejad, Hasan Kashef Shendi, Abbas Ahmadi, and Mohammad Reza Nabid. 2016. 'Synthesis of novel high primary hydroxyl functionality polyol from sunflower oil using thiol-yne reaction and their application in polyurethane coating', *European Polymer Journal,* 82: 220-31.

Otsuka, Hideyuki, Koichiro Aotani, Yuji Higaki, Yoshifumi Amamoto, and Atsushi Takahara. 2007. 'Thermal Reorganization and Molecular Weight Control of Dynamic Covalent Polymers Containing Alkoxyamines in Their Main Chains', *Macromolecules*, 40: 1429-34.

Palaskar, Dnyaneshwar V., Aurélie Boyer, Eric Cloutet, Jean-François Le Meins, Benoit Gadenne, Carine Alfos, Céline Farcet, and Henri Cramail. 2012. 'Original diols from sunflower and ricin oils: Synthesis, characterization, and use as polyurethane building blocks', *Journal of Polymer Science Part A: Polymer Chemistry*, 50: 1766-82.

Pan, Xiao, Partha Sengupta, and Dean C. Webster. 2011. 'High Biobased Content Epoxy–Anhydride Thermosets from Epoxidized Sucrose Esters of Fatty Acids', *Biomacromolecules*, 12: 2416-28.

Pang, Chengcai, Jie Zhang, Guolin Wu, Yinong Wang, Hui Gao, and Jianbiao Ma. 2014. 'Renewable polyesters derived from 10-undecenoic acid and vanillic acid with versatile properties', *Polymer Chemistry*, 5: 2843-53.

Petrovic, Z. S. 2008. 'Polyurethanes from vegetable oils', *Polymer Reviews*, 48: 109-55.

Petrović, Zoran S, Alisa Zlatanić, Charlene C Lava, and Snežana Sinadinović-Fišer. 2002. 'Epoxidation of soybean oil in toluene with peroxoacetic and peroxoformic acids—kinetics and side reactions', *European Journal of Lipid Science and Technology*, 104: 293-99.

Petrović, Zoran S., Ivana Cvetković, DooPyo Hong, Xianmei Wan, Wei Zhang, Tim Abraham, and Jeff Malsam. 2008. 'Polyester polyols and polyurethanes from ricinoleic acid', *Journal of Applied Polymer Science*, 108: 1184-90.

Petrović, Zoran S., Wei Zhang, and Ivan Javni. 2005. 'Structure and Properties of Polyurethanes Prepared from Triglyceride Polyols by Ozonolysis', *Biomacromolecules*, 6: 713-19.

Peyrton, Julien, Clémence Chambaretaud, and Luc Avérous. 2019. 'New Insight on the Study of the Kinetic of Biobased Polyurethanes Synthesis Based on Oleo-Chemistry', *Molecules*, 24: 4332.

Pfister, D. P., Y. Xia, and R. C. Larock. 2011. 'Recent Advances in Vegetable Oil-Based Polyurethanes', *Chemsuschem,* 4: 703-17.

Pham, Phuoc Dien, Vincent Lapinte, Yann Raoul, and Jean-Jacques Robin. 2014. 'Lipidic polyols using thiol-ene/yne strategy for crosslinked polyurethanes', *Journal of Polymer Science Part A: Polymer Chemistry*, 52: 1597-606.

Qin, Anjun, Jacky W. Y. Lam, and Ben Zhong Tang. 2010. 'Click polymerization', *Chemical Society Reviews,* 39: 2522-44.

Rauf, Abdul, and Humaira Parveen. 2004. 'Direct esterification of fatty acids with phenylalkanols by using dicyclohexylcarbodiimide', *European Journal of Lipid Science and Technology*, 106: 97-100.

Reulier, M., R. Matadi Boumbimba, Z. Walsh Korb, R. Vaudemont, and L. Avérous. 2017. 'Thermomechanical and cyclic behavior of biocomposites based on renewable thermoplastics from dimer fatty acids', *Journal of Applied Polymer Science*, 134: 44610.

Reulier, M., R. Perrin, and L. Avérous. 2016. 'Biocomposites based on chemically modified cellulose fibers with renewable fatty-acid-based thermoplastic systems: Effect of different fiber treatments', *Journal of Applied Polymer Science*, 43878.

Reulier, Marie, and Luc Avérous. 2015. 'Elaboration, morphology and properties of renewable thermoplastics blends, based on polyamide and polyurethane synthesized from dimer fatty acids', *European Polymer Journal*, 67: 418-27.

Reulier, Marie, Rodrigue Matadi Boumbimba, Damien Rasselet, and Luc Avérous. 2016. 'Renewable thermoplastic multiphase systems from dimer fatty acids, with mineral microfillers', *Journal of Applied Polymer Science*, 133: 43055.

Rivero, Guadalupe, Le-Thu T. Nguyen, Xander K. D. Hillewaere, and Filip E. Du Prez. 2014. 'One-Pot Thermo-Remendable Shape Memory Polyurethanes', *Macromolecules*, 47: 2010-18.

Romera, Cristian de Oliveira, Débora de Oliveira, Pedro Henrique Hermes de Araújo, and Claudia Sayer. 2019. 'Biobased Ester 2-(10-Undecenoyloxy)ethyl Methacrylate as an Asymmetrical Diene Monomer in Thiol–Ene Polymerization', *Industrial & Engineering Chemistry Research*, 58: 21044-55.

Ronda, J. C., G. Lligadas, M. Galia, and V. Cadiz. 2011. 'Vegetable oils as platform chemicals for polymer synthesis', *European Journal of Lipid Science and Technology*, 113: 46-58.

Rostovtsev, Vsevolod V., Luke G. Green, Valery V. Fokin, and K. Barry Sharpless. 2002. 'A Stepwise Huisgen Cycloaddition Process: Copper(I)-Catalyzed Regioselective "Ligation" of Azides and Terminal Alkynes', *Angew. Chem. Int. Ed*., 41: 2596-99.

Ruiz, L., G. Lligadas, J. C. Ronda, M. Galià, and V. Cádiz. 2019. 'Synthesis of acid degradable oxidation responsive poly(β-thioether ester)s from castor oil', *European Polymer Journal*, 110: 183-91.

Rybak, Anastasiya, Patrice A. Fokou, and Michael A. R. Meier. 2008. 'Metathesis as a versatile tool in oleochemistry', *Eur. J. Lipid Sci. Technol.,* 110: 797-804.

Salehpour, Somaieh, and Marc A. Dubé. 2008. 'Biodiesel: a green polymerization solvent', G*reen Chemistry*, 10: 321-26.

Sanyal, Amitav. 2010. 'Diels–Alder Cycloaddition-Cycloreversion: A Powerful Combo in Materials Design', *Macromolecular Chemistry and Physics*, 211: 1417-25.

Scheltjens, G., M. M. Diaz, Joost Brancart, Guy Van Assche, and Bruno Mele. 2013. 'A self-healing polymer network based on reversible covalent bonding', *Reactive and Functional Polymers*, 73: 413-20.

Scheutz, Georg M., Jacob J. Lessard, Michael B. Sims, and Brent S. Sumerlin. 2019. 'Adaptable Crosslinks in Polymeric Materials: Resolving the Intersection of Thermoplastics and Thermosets', *Journal of the American Chemical Society*, 141: 16181-96.

Sengupta, Avery, Tanmoy Dey, Mahua Ghosh, Jaydip Ghosh, and Santinath Ghosh. 2012. 'Enzymatic Synthesis of Furfuryl Alcohol Ester with Oleic Acid by Candida antarctica Lipase B and Its Kinetic Study', *Journal of The Insitution of Engineers (India),* 93: 31-36.

Shoda, Shin-ichiro, Hiroshi Uyama, Jun-ichi Kadokawa, Shunsaku Kimura, and Shiro Kobayashi. 2016. 'Enzymes as Green Catalysts for Precision Macromolecular Synthesis', *Chemical Reviews*, 116: 2307-413.

Shrestha, Maha L., Mihail Ionescu, Xianmei Wan, Bili, Nikola, Petrovi, Zoran S., and Tom Upshaw. 2018. 'Biobased Aromatic-Aliphatic Polyols from Cardanol by Thermal Thiol-Ene Reaction', *Journal of Renewable Materials*, 6: 87-101.

Silbert, Leonard S. 1984. 'Facile dehydrobromination of vic-dibromo fatty acids: A one-vessel bromination-dehydrobromination of oleic acid to stearolic acid', *Journal of the American Chemical Society*, 61: 1090-92.

Song, Lingzhi, Tianyu Zhu, Liang Yuan, Jiangjun Zhou, Yaqiong Zhang, Zhongkai Wang, and Chuanbing Tang. 2019. 'Ultra-strong long-chain polyamide elastomers with programmable supramolecular interactions and oriented crystalline microstructures', *Nature Communications*, 10: 1315.

Spyros, A. 2002. 'Quantitative determination of the distribution of free hydroxylic and carboxylic groups in unsaturated polyester and alkyd resins by 31P-NMR spectroscopy', *Journal of Applied Polymer Science*, 83: 1635-42.

Stemmelen, Mylène, Vincent Lapinte, Jean-Pierre Habas, and Jean-Jacques Robin. 2015. 'Plant oil-based epoxy resins from fatty diamines and epoxidized vegetable oil', *European Polymer Journal*, 68: 536-45.

Sun, Hao, Christopher P. Kabb, Michael B. Sims, and Brent S. Sumerlin. 2019. 'Architecture-transformable polymers: Reshaping the future of stimuli-responsive polymers', *Progress in Polymer Science*, 89: 61-75.

Tan, S. G., and W. S. Chow. 2010. 'Biobased Epoxidized Vegetable Oils and Its Greener Epoxy Blends: A Review', *Polymer-Plastics Technology and Engineering,* 49: 1581-90.

Thompson, Richard C., Charles J. Moore, Frederick S. vom Saal, and Shanna H. Swan. 2009. 'Plastics, the environment and human health: current consensus and future trends', *Philosophical transactions of the Royal Society of London. Series B, Biological Sciences*, 364: 2153-66.

Tornøe, Christian W., Caspar Christensen, and Morten Meldal. 2002. 'Peptidotriazoles on Solid Phase: [1,2,3]-Triazoles by Regiospecific Copper(I)-Catalyzed 1,3-Dipolar Cycloadditions of Terminal Alkynes to Azides', *The Journal of Organic Chemistry,* 67: 3057-64.

Tremblay-Parrado, Khantutta-Kim, and Luc Avérous. 2019. 'Renewable Responsive Systems Based on Original Click and Polyurethane Cross-Linked Architectures with Advanced Properties', *Chemsuschem*, 13: 238.

Truong, Thuy Thu, Ha Tran Nguyen, Man Ngoc Phan, and Le-Thu T. Nguyen. 2018. 'Study of Diels–Alder reactions between furan and maleimide model compounds and the preparation of a healable thermo-reversible polyurethane', *Journal of Polymer Science Part A: Polymer Chemistry,* 56: 1806-14.

Truong, Thuy Thu, Son Hong Thai, Ha Tran Nguyen, Dung Thuy Thi Phung, Loc Tan Nguyen, Hung Quang Pham, and Le-Thu T. Nguyen. 2019. 'Tailoring the Hard–Soft Interface with Dynamic Diels–Alder Linkages in Polyurethanes: Toward Superior Mechanical Properties and Healability at Mild Temperature', Chemistry of *Materials*, 31: 2347-57.

Türünç, Oğuz, Stijn Billiet, Kevin De Bruycker, Samira Ouardad, Johan Winne, and Filip E. Du Prez. 2015. 'From plant oils to plant foils: Straightforward functionalization and crosslinking of natural plant oils with triazolinediones', *European Polymer Journal,* 65: 286-97.

Türünç, Oğuz, Maulidan Firdaus, Gregor Klein, and Michael A. R. Meier. 2012. 'Fatty acid derived renewable polyamides via thiol–ene additions', *Green Chemistry*, 14: 2577-83.

Türünç, Oğuz, and Michael A. R. Meier. 2012. 'A novel polymerization approach via thiol-yne addition', *Journal of Polymer Science Part A: Polymer Chemistry*, 50: 1689-95.

Türünç, Oğuz, and Michael A. R. Meier. 2013. 'The thiol-ene (click) reaction for the synthesis of plant oil derived polymers', *Eur. J. Lipid Sci. Technol*., 115: 41-54.

Unverferth, Maike, and Michael A. R. Meier. 2016. 'Selective formation of C36-dimer fatty acids via thiol-ene addition for copolyamide synthesis', *European Journal of Lipid Science and Technology*, 118: 1470-74.

Ursula, Biermann, Bornscheuer Uwe, Meier Michael A. R., Metzger Jürgen O., and Schäfer Hans J. 2011. 'Oils and Fats as Renewable Raw Materials in Chemistry', *Angewandte Chemie International Edition*, 50: 3854-71.

Uysal, Naci, Gokhan Acik, and Mehmet Atilla Tasdelen. 2017. 'Soybean oil based thermoset networks via photoinduced CuAAC click chemistry', *Polymer International*, 66: 999-1004.

Vilela, Carla, Letizia Cruciani, Armando J. D. Silvestre, and Alessandro Gandini. 2011. 'A Double Click Strategy Applied to the Reversible Polymerization of Furan/Vegetable Oil Monomers', *Macromolecular Rapid Communications*, 32: 1319-23.

Vilela, Carla, Letizia Cruciani, Armando J. D. Silvestre, and Alessandro Gandini. 2012. 'Reversible polymerization of novel monomers bearing furan and plant oil moieties: a double click exploitation of renewable resources', *RSC Advances*, 2: 2966-74.

Vilela, Carla, Armando J. D. Silvestre, and Alessandro Gandini. 2013. 'Thermoreversible nonlinear diels-alder polymerization of furan/plant oil monomers'*, Journal of Polymer Science Part A: Polymer Chemistry,* 51: 2260-70.

Wang, Haoran, and Qixin Zhou. 2018. 'Synthesis of Cardanol-Based Polyols via Thiol-ene/Thiol-epoxy Dual Click-Reactions and Thermosetting Polyurethanes Therefrom', *ACS Sustainable Chemistry & Engineering,* 6: 12088-95.

Wang, Qing, Guangxue Chen, Yanyan Cui, Junfei Tian, Minghui He, and Jian-Wen Yang. 2017. 'Castor Oil Based Biothiol as a Highly Stable and Self-Initiated Oligomer for Photoinitiator-Free UV Coatings', *ACS Sustainable Chemistry & Engineering,* 5: 376-81.

Wang, Tiansheng, Liping Li, Yongjian Cao, Qingwen Wang, and Chuigen Guo. 2019. 'Preparation and flame retardancy of castor oil based UV-cured flame retardant coating containing P/Si/S on wood surface'*, Industrial Crops and Products*, 130: 562-70.

Wang, Tiansheng, Liping Li, Qingwen Wang, Guijun Xie, and Chuigen Guo. 2019. 'Castor oil based UV-cured coatings using thiol-ene click reaction for thermal degradation with flame retardance', *Industrial Crops and Products*, 141: 111798.

Wang, Z. K., Y. Q. Zhang, L. Yuan, J. Hayat, N. M. Trenor, M. E. Lamm, L. Vlaminck, S. Billiet, F. E. Du Prez, Z. G. Wang, and C. B. Tang. 2016. 'Biomass Approach toward Robust, Sustainable, Multiple-Shape-Memory Materials', *ACS Macro Letters,* 5: 602-06.

Willocq, B., F. Khelifa, J. Brancart, G. Van Assche, Ph Dubois, and J. M. Raquez. 2017. 'One-component Diels-Alder based polyurethanes: a unique way to self-heal', *RSC Advances*, 7: 48047-53.

Wilson, Jedediah F., and Eugene Y. X. Chen. 2019. 'Difuranic Diols for Renewable Polymers with Pendent Furan Rings', *ACS Sustainable Chemistry & Engineering,* 7: 7035-46.

Wool, R. P., and X. Sun. 2005. Bio-Based Polymers and Composites (Elsevier).

Wu, Wan-Xia, Jun Li, Xian-Ling Yang, Na Wang, and Xiao-Qi Yu. 2019. 'Lipase-catalyzed synthesis of renewable acid-degradable poly(β-thioether ester) and poly(β-thioether ester-co-ricinoleic acid) copolymers derived from castor oil', *European Polymer Journal*, 121: 109315.

Xia, Ying, and Richard C. Larock. 2010. 'Vegetable oil-based polymeric materials: synthesis, properties, and applications', *Green Chemistry*, 12: 1893-909.

Xu, Dongdong, Zhiyuan Cao, Tong Wang, Jiang Zhong, Jinze Zhao, Fei Gao, Xuyang Luo, Zhaoli Fang, Jinsong Cao, Suzhen Xu, and Liang Shen. 2019. 'An ambient-cured coating film obtained via a Knoevenagel and Michael addition reactions based on modified acetoacetylated castor oil prepared by a thiol-ene coupling reaction', *Progress in Organic Coatings*, 135: 510-16.

Xu, Y. J., Z. Petrovic, S. Das, and G. L. Wilkes. 2008. 'Morphology and properties of thermoplastic polyurethanes with dangling chains in ricinoleate-based soft segments', Polymer, 49: 4248-58.

Yang, Xuejuan, Shouhai Li, Jianling Xia, Jian Song, Kun Huang, and Mei Li. 2015. 'Novel renewable resource-based UV-curable copolymers derived from myrcene and tung oil: Preparation, characterization and properties', *Industrial Crops and Products*, 63: 17-25.

Yang, Xuejuan, Chunpeng Wang, Shouhai Li, Kun Huang, Mei Li, Wei Mao, Shan Cao, and Jianling Xia. 2017. 'Study on the synthesis of bio-based epoxy curing agent derived from myrcene and castor oil and the properties of the cured products', *RSC Advances,* 7: 238-47.

Ying, Hanze, Yanfeng Zhang, and Jianjun Cheng. 2014. 'Dynamic urea bond for the design of reversible and self-healing polymers', *Nature Communications,* 5: 3218.

Yoshie, Naoko, Shoma Yoshida, and Koji Matsuoka. 2019. 'Self-healing of biobased furan polymers: Recovery of high mechanical strength by mild heating', *Polymer Degradation and Stability,* 161: 13-18.

Zhang, Dandan, Hongbo Liang, Jiang Bu, Lei Xiong, Shengmei Huang, D. D. Zhang, H. B. Liang, J. Bu, L. Xiong, and S. M. Huang. 2015. 'UV curable soybean-oil hybrid systems based on thiol-acrylate and thiol-ene-acrylate chemistry', *Journal of Applied Polymer Science*, 132: 42095.

Zhang, Lu, Frederick C. Michel Jr, and Anne C. Co. 2019. 'Nonisocyanate route to 2,5-bis(hydroxymethyl)furan-based polyurethanes crosslinked by reversible diels–alder reactions', *Journal of Polymer Science Part A: Polymer Chemistry,* 57: 1495-99.

Zhang, Yang, Zehui Dai, Jiarui Han, Ting Li, Jun Xu, and Baohua Guo. 2017. 'Interplay between crystallization and the Diels–Alder reaction in biobased multiblock copolyesters possessing dynamic covalent bonds', *Polymer Chemistry*, 8: 4280-89.

Zheng, Kaiwen, Yazhou Tian, Mengjin Fan, Junying Zhang, and Jue Cheng. 2018. 'Recyclable, shape-memory, and self-healing soy oil-based polyurethane crosslinked by a thermoreversible Diels-Alder reaction', *Journal of Applied Polymer Science*, 135: 46049-49.

Zlatanic, Alisa, Charlene Lava, Wei Zhang, and Zoran Petrović. 2004. 'Effect of Structure on Properties of Polyols and Polyurethanes Based on Different Vegetable Oils', *Journal of Polymer Science Part B: Polymer Physics*, 42: 809-19.

Zuo, Hanqi, Zhiyuan Cao, Jinbing Shu, Dongdong Xu, Jiang Zhong, Jinze Zhao, Tong Wang, Yongming Chen, Fei Gao, and Liang Shen. 2019. 'Effect of structure on the properties of ambient-cured coating films prepared via a Michael addition reaction based on an acetoacetate-modified castor oil prepared by thiol-ene coupling', *Progress in Organic Coatings,* 135: 27-33.

Khantutta-Kim TREMBLAY-PARRADO

Synthèse par chimie click de réseaux biosourcées de polyuréthanes performants aux propriétés avancées.

Résumé

Notre époque a connu une révolution avec l'émergence des matières plastiques qui ont désormais une importance inégalée dans notre vie quotidienne. Cependant, ce fort développement entraine de trop nombreux déchets dans l'environnement avec de forts impacts environnementaux et ceci de façon croissante. Pour répondre à cela, l'élaboration de polymères durables avec l'utilisation de ressources renouvelables et des propriétés avancées pour gérer la fin de vie des matériaux est attendue. Le développement de réseaux covalents adaptables (RCA) est apparu comme une alternative intéressante pour répondre à ces attentes en développant des applications dans le domaine des polyuréthanes (PUs) biosourcées. Dans ces travaux, nous utilisons la réaction de Diels-Alder thermoréversible avec un couplage furanne-maléimide pour la synthèse de PUs dérivés d'huiles végétales et des points de réticulation thermoréversibles. Deux nouveaux synthons dérivés de l'huile de tournesol, portant des groupes furane et maléimide, ont été obtenus et incorporés dans des réseaux PU biosourcées. Les réseaux obtenus donnent des résultats prometteurs en termes de propriétés, de recyclabilité thermique et d'autoréparation thermo-induite. Les réseaux PU synthétisés et analysés constituent un tremplin dans le développement de RCA biosourcées à plus faible impact environnemental.

Mots-clés : Polymères biosourcées, polyuréthane, réaction de Diels-Alder, huiles végétales

Abstract

The modern era was revolutionized by the invention of plastics and as such have gained prevalence in most aspects of our daily lives, causing an increasing appearance in landfills and oceans. For this reason, sustainable polymer design should not only require the use of renewable resources, but also factor in advanced properties to manage the end-of-life materials for the reduction of energy use, resources and waste. Developing covalent adaptable networks (CANs) has emerged as an interesting alternative to address this problematic, but with little to no application in the domain of biobased polyurethanes. In this work, we utilize the thermoreversible Diels-Alder reaction of the furan-maleimide coupling for the synthesis of vegetable oil derived polyurethanes (PUs) with thermo-reversible cross-linking points. Two new building blocks derived from sunflower oil, bearing furan and maleimide moieties, were obtained and incorporated into the synthesis of biobased PU networks. The obtained PU networks yield promising results in terms of polymer properties, thermal recyclability and heat-induced self-healing. The synthesized PU networks provide a stepping-stone in the development of biobased CANs.

Keywords: Biobased Polymers, Polyurethane, Diels-Alder Reaction, Vegetable oils